Development of novel resin modified glass ionomer cements (RMGICs) with reduced water uptake for use in cementing fixed prosthodontics

Amani Agha

Thesis submitted in fulfillment of the requirement for the Degree of Doctor of Philosophy in The Institute of Dentistry, Barts and The London School of Medicine and Dentistry, Queen Mary University of London

April 2016

Statement of Originality

I, Amani Agha, confirm that the research included within this thesis is my own work or that where it has been carried out in collaboration with, or supported by others, that this is duly acknowledged below and my contribution indicated. Previously published material is also acknowledged below.

I attest that I have exercised reasonable care to ensure that the work is original, and does not to the best of my knowledge break any UK law, infringe any third party's copyright or other Intellectual Property Right, or contain any confidential material.

I accept that the College has the right to use plagiarism detection software to check the electronic version of the thesis.

I confirm that this thesis has not been previously submitted for the award of a degree by this or any other university.

The copyright of this thesis rests with the author and no quotation from it or information derived from it may be published without the prior written consent of the author.

Signature: Amani Agha

Date: 26/05/2016

Abstract:

Resin modified glass ionomer cements (RMGICs) comprise GIC and a polymerisable resin monomer, commonly 2-hydroxyethyl methacrylate (HEMA). Therefore, they have the advantages of a resin (e.g. improved strength), together with those of GICs (e.g. fluoride release). However, RMGICs possess some limitations, these being a high water uptake thus leading to expansion, due to the incorporation of the resin, which has subsequently led to fractures of some all-ceramic crowns. Moreover, release of unconverted monomers (HEMA) from RMGICs was associated with decreasing their biocompatibility.

The goals of this study were i) to develop novel cements with lower water uptake and dimensional changes compared to commercial RMGICs through incorporating alternative monomers (resin) that are known for their lower water uptake compared to HEMA, ii) to develop control materials that mimic the compositions of commercial materials, iii) to assess the physical, mechanical and biological properties of the new cements and compare them with the commercial and home material counterparts.

To achieve the above goals, two commercial materials (Fuji Plus, GC and RelyX Luting, 3M-ESPE) were included in this study. Two control liquids were prepared based on the composition of the two commercial materials (using the materials MSDS and FT-IR). Eight novel liquid compositions were also developed replacing HEMA (partially or fully) with THFM and/or HPM, where the powder used was the same powder as their commercial counterparts. All materials underwent various experiments and investigations. These included water absorption, dimensional

changes, polymerisation shrinkage and exotherm, working and setting times, FT-IR analyses, HPLC for detecting leachants, mechanical properties and cell viability studies.

All novel materials demonstrated lower water uptake and dimensional changes compared to their commercial and home counterparts. They showed comparable properties with respect to the other properties investigated (e.g. polymerisation shrinkage and handling properties). Two compositions (F3 and F4, based on Fuji Plus formulation) showed improved biocompatibility.

This study improved some of the main limitations associated with RMGICs (high water uptake and dimensional change), which will widen the applications of these products.

Acknowledgments:

My deepest gratitude and appreciation for the help and support are extended to my primary supervisor, Dr Mangala P Patel, whose expertise, guidance and understanding made this thesis a reality. I also take this opportunity to thank my second supervisor Dr Sandra Parker for her help and guidance on this project.

I would like to convey my utmost gratefulness to Dr Garry JP Fleming for giving me the opportunity to perform the flexural testing in the Materials Science Unit, Dublin Dental University Hospital, also for his continuous support and invaluable encouragement. I would also like to thank Professor Ken Parkinson for his help in performing the cell culture study, Dr Lingzhi Gong, for his guidance and advice on HPLC.

My gratitude also goes to Professor Joy Hinson, Professor Rob Allaker, Professor Robert Hill and Ms Jacqui Frith for their help and support during my time at QMUL.

I am extremely grateful to Alessia D'Onofrio for her priceless friendship and to all my fellow PhD students for the good times.

I would like to acknowledge the University of Damascus, Syria for their support.

Special thanks to my parents and my brothers for their continuous support and love.

Most importantly, this work would not have been possible without the love and support of the most important people in my life, my dear husband, Mazen, my handsome boy, Hazem, and my unborn baby who shared the last few months with me.

Table of contents

List of Figures

List of Tables

List of Abbreviations

- RMGICs - Resin modified glass ionomer cements
- GICs - Glass ionomer cements
- Fuji Plus - FP
- RelyX Luting - RX
- FT-IR - Fourier transform infrared spectroscopy
- HEMA - Hydroxyethyl methacrylate
- UDMA - Urethane dimethacrylate
- THFM - Tetrahydrofurfuryl methacrylate
- HPM - Hydroxypropyl methacrylate
- HPLC - High performance liquid chromatography
- Bis-GMA - Bisphenol-A-glycidyldimethacrylate
- TEGDMA - Triethylenglycol-dimethacrylate
- 4-META - 4-methacryloxyethyl trimellitate anhydride
- DMAEMA - N,N-dimethylaminoethyl methacrylate
- MAA - Methacrylic acid
- ROS - Reactive oxygen species
- GSH - Glutathion
- PEM - Poly (ethyl methacrylate)
- MMA - Methyl-methacrylate
- PMMA - Poly(methyl methacrylate)
- MM - Methyl methacrylate
- nBM - N-butyl methacrylate
- MSDS - Material's safety data sheet
- g - Gram
- CAS number - Chemical Abstract Service number
- rpm - Revolutions per minute
- F1, F2, F3 and F4 - Novel cement formulated based on Fuji Plus composition
- R1, R2, R3 and R4 - Novel cements formulated based on RelyX Luting composition
- DW - Deionised water
- AS - Artificial saliva
- ACN - Acetonitrile
- PTFE - Polytetrafluoroethylene
- ISO - International standardisation organisation
- ATR - Attenuated total reflectance
- LVDT - Linear variable displacement transducer
- µm - Micrometre
- mV - Millivolt
- mAU - Milli absorbant unit
- UV-vis spectroscopy - Ultraviolet-visible spectroscopy

- ppm - Parts per million
- NHDF - Normal human dermal fibroblasts
- FBS - Fetal bovine serum
- DMEM - Dulbecco Modified Eagle's Medium
- MTT - 3-(4, 5-dimethylthiazolyl-2)-2, 5-diphenyltetrazolium bromide
- DMSO - Dimethyl sulfoxide
- OD - Optical density
- SD - Standard deviation

1 INTRODUCTION

Introduction:

Luting cements play an important role in determining the long-term clinical success of fixed prosthodontic restorations (Ladha and Verma, 2010). A good and durable bond between the tooth (enamel/dentine) and the restoration is essential in order to achieve high quality outcomes (Diaz-Arnold *et al*., 1999). Selecting a luting cement appropriately is very difficult due to the availability of a wide range of products, resulting from recent improvements in this field (Pameijer, 2012). An ideal luting agent should be able to maintain retention and have adequate and reliable bonding of the restoration to natural tooth tissue. This is dependent on particular biological, physico-mechanical and handling properties of the cement (Rosenstiel *et al*., 1998).

The biological requirements include: biocompatibility in the oral environment and perfect sealing at the interface between the tooth and restoration to avoid plaque accumulation, microbial ingress and subsequently secondary caries (de la Macorra and Pradies, 2002). Moreover, luting materials should sustain adequate mechanical properties, present physical or chemical bonds with the tooth and prosthesis, be 'stable', and radio-opaque (de la Macorra and Pradies, 2002).

Currently, due to the improvements in adhesive dentistry, different types of luting cements are available on the market. The clinicians choice should be based on understanding the advantages, disadvantages, biological and mechanical properties of each cement so that they can select the most suitable material for each individual dental case (Pameijer, 2012).

Conventional glass ionomer cements (GICs) are examples of dental cement that offer many advantages, including chemical adhesion to tooth substance (Wilson and

McLean, 1988), fluoride release and thus caries inhibition (Mount, 1994). They moreover do not have a reaction exotherm nor undergo polymerisation shrinkage (Sidhu and Watson, 1995; Brook and Hatton, 1998). However, These cements are more susceptible to wear and abrasion, they possess low strength and are sensitive to moisture (Cho and Cheng, 1999). To improve these limitations, resin modified glass ionomers (RMGICs) were developed.

RMGICs contain the original GIC cement along with a resin system commonly used, hydroxyethyl methacrylate (HEMA), to provide a material that incorporates the advantages of a resin (e.g. improved strength), with the improved properties of GICs (Mathis and Ferracane, 1989). These cements undergo two setting reactions: the conventional acid-base reaction (the same as of the GICs) and polymerisation of the resin monomer where the polymerisation can be either light or chemically activated (Wilson and Nicholson, 2005).

Despite the advantages and superior properties of RMGICs compared to GICs (e.g. improved strength), these cements demonstrate some limitations and disadvantages that include:

1- Polymerisation exotherm: due to the fact that RMGICs contain HEMA and undergo polymerisation (light and/or chemically), a rise in temperature is commonly associated with this type of cement.
2- RMGIC's demonstrate lower biocompatibility compared to GICs. This occurs as a result of residual (unconverted) monomer (HEMA) being released from the cement. This monomer possesses a low molecular weight and is of hydrophilic nature, which renders it easy to diffuse through the dentinal

tubules to the pulpal tissues and cause inflammation (Gerzina and Hume, 1996; Hamid *et al*., 1998).

3- Water uptake is a common problem of RMGICs following placement in the oral environment. This occurs as a result of the hydrophilic nature of HEMA (Nicholson and Anstice, 1994). Therefore, HEMA in RMGICs is responsible for the water uptake of the material (Yap and Lee, 1997). Various problems occur as a result of the water uptake, including weakening of the cement and plasticising the matrix, which in turn could affect the materials' strength (Malacarne *et al*., 2006; Pastila *et al*., 2007).

4- Swelling of the resin matrix is another problem associated with the water uptake, which occurs to provide a space for the diffused water through the matrix (Braden *et al*., 1976) as well as filling the microvoids in the cement (Oysaed and Ruyter, 1986). This hygroscopic expansion increases the incidence of the all-ceramic fracture when cemented with RMGIC (Sindel *et al*., 1999; Federlin *et al*., 2004; Mese *et al*., 2008).

All the above limitations are mainly attributed to the incorporation of HEMA monomer in the liquid composition of RMGICs, which increases the materials water uptake. Therefore, the purpose of this study is to improve these limitations by replacing HEMA partially, or fully, with two alternative monomers, tetrahydrofurfuryl methacrylate (THFM) and hydroxylpropyl methacrylate (HPM). THFM has been reported to have unique water absorption properties and, with poly(ethyl methacrylate), it has been shown to have a low shrinkage (%) and exotherm, as well as being biocompatible in bone and dental pulp (Patel *et al*. 1987; Pearson *et al*. 1986). HPM has been reported in the literature with respect to

polymerisation shrinkage where it showed lower shrinkage strain rate compared to dimethacrylate monomers (e.g. urethane dimethacrylate, UDMA) (Atai *et al*., 2005) and it appears less reactive than HEMA (Patel *et al*., 2001), thus it will produce a lower exotherm.

Therefore, a summary of this project includes: i) the development of novel RMGICs [replacing HEMA partially or fully with two alternative monomers (THFM and/or HPM)] in order to reduce their water uptake, dimensional change and exotherm compared to commercially available products; ii) to investigate and compare their handling and mechanical properties, iii) to measure the release of HEMA and other monomers from the cements, and iv) to compare the biocompatibility of commercial and novel RMGICs. These are fully described in the Aims and Objectives chapter.

Hence, with the incorporation of these alternative monomers, the resulting RMGICs will present with improved properties (e.g. lower water uptake, dimensional changes) compared to commercial products, thus indicating their suitability for taking them forward for potential commercialisation.

2 LITERATURE REVIEW

2.1 *Classification of Dental Cements:*

Dental cements can be classified into three categories according to their clinical usage: liners and bases, temporary and permanent cements (de la Macorra and Pradies, 2002; Pameijer, 2012). Dental cements, which can also be referred to as luting agents, are also classified according to their bonding durability:

1. Low, represented by zinc phosphate cements
2. Medium, such as polycarboxylate cements
3. High, represented by glass ionomer cement (GIC), resin-modified glass ionomer cements (RMGICs) and resin composites (Pameijer, 2012).

These cements are discussed further below.

2.1.1 Zinc Phosphate Cement:

Zinc phosphate cement was introduced more than a century ago and has undergone several improvements throughout the years; it is not commonly used nowadays. This cement sets via an acid-base reaction and contains a mix of a powder and a liquid (Diaz-Arnold *et al*., 1999). The powder mainly contains zinc oxide and magnesium oxide and the liquid is a mixture of phosphoric acid, aluminum phosphate (and sometimes zinc phosphate), and ~33% water (Anusavice and Phillips, 2003). This cement was used to lute crowns and long-span bridges (Lad *et al*., 2014). Due to its initial low pH, this cement bonds mechanically to teeth, through penetrating dentinal tubules, after dissolution of the smear layer. This low pH value and, also heat generated during the setting reaction, can irritate the pulp and subsequently the teeth may need to be treated endodontically (Pameijer, 2012). Attempts have been made to prevent phosphoric acid from penetrating the dentinal tubes by using a varnish (e.g.

Copalite) prior to using the cement, but this procedure can compromise retention of the restoration (Felton *et al*., 1987).

2.1.2 Zinc Polycarboxylate Cement:

Polycarboxylate cement also sets via an acid-base reaction. The powder contains a mix of zinc oxide, magnesium oxide, bismuth salts and aluminum oxide; the liquid is either an aqueous solution of poly(acrylic acid) or a copolymer of acrylic acid and another unsaturated carboxylic acid. The acid weight concentration ranges from 32% to 42% (Pameijer, 2012). This cement doesn't irritate the pulp, despite its low pH level, as the latter increases faster than that of zinc phosphate cements. Moreover, polycarboxylate ions do not penetrate the dentinal tubes due to their higher molecular weight (Charlton *et al*., 1991; Anusavice and Phillips, 2003). Although polycarboxylate cement can chemically bond to teeth through Ca^{+2} ions in enamel and dentine, it fails at the cement-restoration interface, when bonding precious alloys (like gold) due to their 'highly inert nature'. This cement cannot form a chemical bond with ceramics and thus their bonding failure is also at the cement-restoration interface. However, it can be used to bond non-precious alloys (e.g. nickel chromium alloy) through the oxide layer on the surface of the alloy (Ladha and Verma, 2010). This cement is not recommended for luting long-span restorations, and also cannot bear high occlusal loads due to its high plastic deformation (Oilo, 1991). As a result, polycarboxylate cement is only recommended for temporary cementation or for single units (crowns) with low occlusal loads (Diaz-Arnold *et al*., 1999; Pameijer, 2012).

2.1.3 Resin Cement:

Resin cements were introduced in the 1960s. They consist of resin matrix, filler and coupling agent. Commonly, the monomer (resin) used is bisphenol-A-glycidyldimethacrylate (Bis-GMA) and triethylenglycol-dimethacrylate (TEGDMA) is added to reduce the materials viscosity. Silicone dioxide, boron silicates, lithium aluminium silicates and quartz represent the filler part of resin composites. Metal ions (e.g. barium, strontium, zinc, aluminium or zirconium) can be used for partial substitution of the quartz in order to increase radio-opacity of the cement (Reis *et al*., 2012). A silane coupling agent is used to bond the two components, the organic and the in-organic matrix in the set material (Zimmerli *et al*., 2010). They set through polymerisation, instead of an acid-base reaction, and can be chemical, light or dual-cured. Resin cements bond to etched enamel through micromechanical interlocking of the resin into the enamel rods (Buonocore, 1955). Bonding to enamel involves etching with phosphoric acid and rinsing, which is considered as the 'gold standard'. The role of phosphoric acid is to remove the pellicle layer and surface enamel in order to increase its surface roughness. This roughness can then be penetrated by the unfilled resin by 'capillary attraction' (Kanca, 1992) leading to micromechanical interlocking through the resin tags (Milia *et al*., 2012).

Their bonding with dentine involves conditioning of the dentine surface to remove the smear layer, open the dentinal tubes and dissolve the minerals around collagen fibres, in order to produce channels. Then, a priming agent (e.g. Scotchbond, 3M-ESPE, containing a bifunctional monomer, like hydroxyethyl methacrylate, HEMA) is applied in order to wet the surface of dentine and replace water by penetrating the

tubules via its hydrophilic end; its hydrophobic end then chemically bonds to the adhesive resin (Tay *et al*., 1996).

Resin cements are used to bond restorations made of resin composite (as described above) or silanated porcelain (Diaz-Arnold *et al*., 1999). Moreover, adhesive resin cements that contain 4-methacryloxyethyl trimellitate anhydride (4-META) or phosphonated resin (e.g. Panavia EX, Kuraray), can be used to bond metal alloys through a chemical reaction with the oxide layer on the restoration surface through the phosphate ends of the phosphonate and carboxyl groups from 4-META (Watanabe *et al*., 1988; Aquilino *et al*., 1990).

Resin cements are recommended for restorations lacking retention, such as Maryland bridges, and also for aesthetic restorations, due to the availability of different resin cement shades that can match the restoration and enhance the appearance of the clinical treatment (e.g. when bonding veneers) (Diaz-Arnold *et al*., 1999). However, bonding resin cements to noble metals and zirconia is still problematic (Diaz-Arnold *et al*., 1999; Duarte *et al*., 2009). Moreover, care should be taken during the bonding procedure as it's considered technique-sensitive and it requires multiple steps (Diaz-Arnold *et al*., 1999).

2.1.4 Conventional Glass-ionomer Cements (GIC):

2.1.4.1 History:

The reason for adding 'conventional' to glass ionomers is to differentiate this cement from two new modifications of this particular type. These two modifications include: metal reinforced GIC, which contains the same GIC components but with additional incorporation of a metal alloy (silver) for enforcement (improving the strength). The

other type is resin modified GIC (RMGIC) that contains a monomer in the liquid, to improve the conventional cement properties (this type will be discussed later in this chapter) (Wilson and McLean, 1988). Glass ionomer Cements (GICs) were introduced by Wilson and Kent in 1972 (Wilson and Kent, 1972). They were first prepared in 1969 at the Laboratory of the Government Chemist in London, United Kingdom. The early (conventional) GICs were first called 'Glass Polyalkenoate Cements' as described by the International Standard Organization (ISO) (1991), and contained a degradable glass and a polymeric acid (poly alkenoic acid, e.g. polyacrylic acid) (McLean, 1994). The term GIC was more adopted by clinicians although it does not describe accurately the chemical composition of these cements (McLean, 1994). GIC is best defined by McLean *et al*. (1994), as 'a cement that consists of basic glass and an acidic polymer, which sets by an acid-base reaction that occurs between these components'.

2.1.4.2 Composition:

GICs are mainly presented as powder and liquid cements, which can also be in encapsulated form.

Powder composition:

The GIC powder composition is generally a calcium fluoro-alumino-silicate glass, first introduced by Wilson and Kent in 1972 (Wilson *et al*., 1980). Calcium oxide (CaO) in the original compositions was replaced with CaF_2, which improved the cements setting time (faster setting) and mechanical properties. The GICs glass is prepared through melting its components (silicone dioxide - SiO_2, aluminium oxide - Al_2O_3, calcium fluoride - CaF_2, sodium fluoride - NaF, sodium hexafluoroaluminate

- Na_3AlF_6 and aluminium phosphate - $AlPO_4$), at 1100 to 1500°C, in a furnace. Then, the glass is cooled rapidly by quenching in cold water to form a frit. Finally, the frit is ground in a rotary ball mill and sieved to a particle size of < 45 μm for restorative GIC, and 15-20 μm for use in luting cements (Nicholson *et al*., 1988). Some glasses have been prepared as aluminosilicates or aluminoborates, in place of fluoride (Anstice *et al*., 1992; Nicholson *et al*., 1992). Strontium and lanthanum oxide can be used to replace calcium in the glass composition to increase radio-opacity of the cement (Wilson and McLean, 1988). Aluminuborate glasses showed improved compressive fracture strength (CFS) and diametral tensile strength (DTS) compared to aluminosilicate glasses (Neve *et al*., 1992; Neve *et al*., 1992; Neve *et al*., 1993); but they showed higher solubility compared to the aluminosilicate glasses (Neve *et al*., 1992). Another composition of GIC powder included the incorporation of zinc, where alumino-zinc-silicate glasses were 'hydrolytically stable', but their CFS was lower than that recommended by the ISO standards (100 MPa). Therefore, zinc and borate based glasses could not be used as alternatives for aluminosilicate glasses in GICs.

Liquid Composition:

The first GIC described by Wilson and Kent included polyacrylic acid in the liquid formulation (Wilson and Kent, 1972). A 50% solution of the acid in water was used in order to produce optimum mechanical properties (Crisp *et al*., 1980). This formulation showed limitations, due to gelation on storage, thus making it difficult to manipulate (mixing of the cement; (Crisp *et al*., 1980). To reduce the gelation problem associated with the poly(acrylic acid) (a homopolymer), copolymers have been used (Figure 2.1), such as acrylic acid with itaconic, maleic (Crisp *et al*., 1980)

or 3-butene-1,2,3-tricarboxylic acids (Hashiguchi *et al*., 1976). Poly(acrylic) acid molecules are known to be mobile and flexible, which allows the formation of hydrogen bonding between these molecules and then gelation of liquid occurs. Therefore, the copolymerisation helped to reduce the flexibility of the acrylic acid molecules and solved the gelation problems occurring in the bottle (Crisp *et al*., 1980).

Acrylic Acid

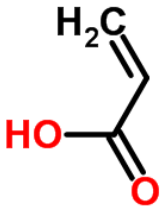

Maleic acid

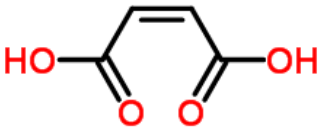

Itaconic acid

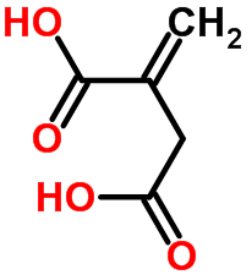

3-Butene-1, 2, 3-tricarboxylic Acid

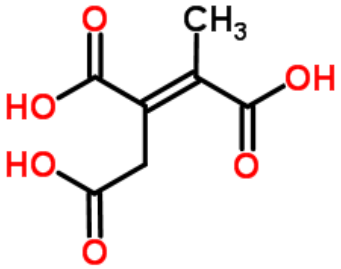

Figure 2.1 Chemical structures of monomer acids, which are polymerised and then used in GIC liquid.

The GIC liquid also contains water and 5-10% tartaric acid. Tartaric acid plays an important role as a reaction controller; it decreases the setting time but increases the working time of the cement (by holding the cement forming ions), as well as 'sharpening' the set (the cement forming ions are released giving the sharp set)

(Crisp and Wilson, 1976; Nicholson *et al*., 1988). Although, the role of tartaric acid in the setting reaction of the GIC is not completely identified, it is known to enhance the 'extraction' of the aluminium ions from the glass after mixing, and it assists their (aluminium ions) matrix binding by increasing their reaction with poly(acrylic acid); this results in increasing the rate of forming aluminium polyacrylate (Crisp and Wilson, 1976; Nicholson *et al*., 1988).

Water also plays an important role in the setting reaction of GIC. It is required for both transportation of metal ions during the setting reaction between the glass and the liquid, and hydrating the metal ions and siliceous gel (around glass particles) during the setting process. Water is included in sufficient amounts so that the setting reaction and maturation (an increase in the ratio of bound to unbound water) can proceed (Croll and Nicholson, 2002).

GICs are also presented in water mixable format. These cements contain freeze-dried polymeric acid in the powder component. They are then mixed with either i) only distilled water (in this case, the tartaric acid is incorporated in the cement powder), or ii) an aqueous solution of tartaric acid. These compositions improved the cement handling properties, due to their low viscosity, and were therefore popular as luting cements (McLean *et al*., 1984). However, it was reported that these products increased post-operative sensitivity compared to conventional GICs (McLean, 1988).

2.1.4.3 Setting reaction of GIC:

GIC sets through an acid-base reaction. It contains glasses that are degradable in the presence of polyacids and water. The latter ionises the polyacid and then the hydrogen ions react with the glass. This results in the glass releasing mainly

aluminium, calcium, sodium, strontium cations and fluoride ions. Subsequently, calcium and aluminium ions form a polysalt through replacing hydrogen in the carboxylic group of the polyacrylic acid; then the salts hydrate to form a silica hydrogel (Wilson and Nicholson, 1993). The acid anion chains chelate to form salt bridges with the released cations resulting in a cross-linked cement. This setting reaction occurs in four different stages. The first stage occurs following mixing of the powder and liquid, the liquid comes into contact with the glass particles. The polyacids attack the glass surface in the second phase causing release of metal ions in the aqueous solution surrounding the glass particles (metal ions 'in soluble form' represented by red dots in Figure 2.2). At this stage glass particles contain an ion depleted surface consisting mainly of silica gel. 'Gelation' and 'hardening' of the cement represent the third and fourth (final) phases, where the metal ions that are liberated from the glass, react with the carboxyl group on the poly(acrylic acid); this procedure occurs throughout the setting time and continues to the point where all the metal ions become insoluble (''bound to the poly-acid chain'' represented by the blue dots in Figure 2.2) (Wilson and McLean, 1988).

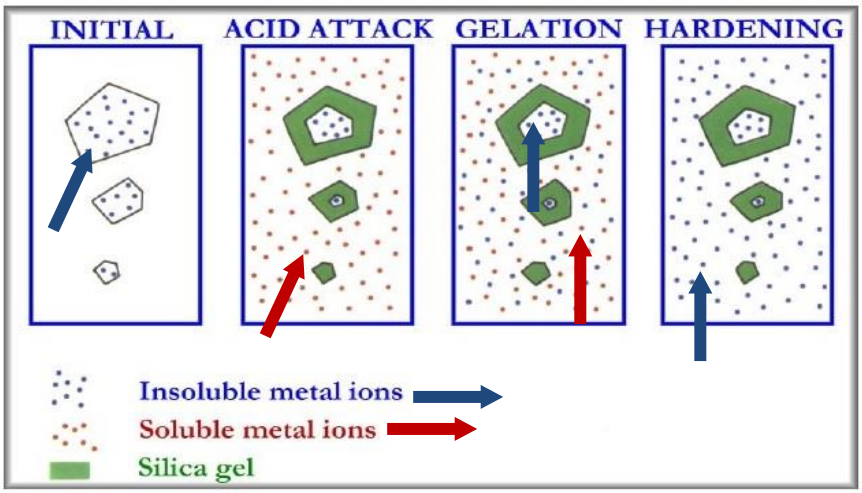

Figure 2.2 Setting reaction stages of GIC (Wilson and McLean, 1988).

Theoretically, during the setting process, water from the liquid is integrated completely in the cement matrix, but this is rarely the case. These cements are water-sensitive, and any additional water during the setting process can jeopardise the procedure through dissolving the reactive metal cations (required for crosslinking). Following setting, the GIC structure contains both bound and unbound water. The maturation process of the GIC continues after mixing and during this process, more water becomes bound to the matrix, hence the mechanical properties improves over time during the maturation phase (Wilson and Nicholson, 1993). Through this maturation phase, GICs should be protected from water loss, as this can cause cracking in the cement structure and forms a chalky appearance (Nicholson and Wilson, 2000). Since the acid attacks only the surface of the glass, the core powder stays un-reacted and is held by the salt bridges that are formed between the metal ions and the carboxyl groups in the cement matrix (Wilson *et al*., 1979).

Throughout the acid-base reaction, fluoride ions move freely from the cement, into the teeth and vice versa. Fluoride loss from the cement is not problematic, since it is not one of the cement forming elements (Wilson *et al*., 1985; Mount, 1994). GICs are widely accepted by clinicians because of their fluoride release and their ability to increase fluoride levels in saliva (Rezk-Lega *et al*., 1991) and in adjacent enamel (Scoville *et al*., 1990). Thus, this type of cement can play an important role in caries inhibition (ten Cate and van Duinen, 1995).

Another important feature of GICs is their chemical adhesion to tooth tissues. This adhesion occurs as a result of exchanging ions between the cement matrix and the tooth structure as described by Wilson in 1978. The bonding procedure is not fully understood and can be explained by two theories; the first is the chemical bond

between the tooth structure and the cement. This procedure includes a reaction between the COO- group in the cement and Ca^{+2} from enamel or dentine. The second theory includes the dissolution of the apatite from the surface of the teeth in contact with acid, and then the reprecipitated calcium phosphate is accumulated on the surface and can bond to the polyacid chain of the cement. In dentine, there is further bonding between the carboxyl group of the cement and 'reactive groups' present in the collagen (McCabe and Walls, 2009; Khoroushi and Keshani, 2013).

2.1.4.4 Limitation of conventional GIC:

Conventional GICs possess many advantages, such as chemical adhesion to tooth substance (Wilson and McLean, 1988), fluoride release and thus caries inhibition (Mount, 1994). GICs do not undergo polymerisation shrinkage and have a 'very low to non-existent reaction exotherm' (Sidhu and Watson, 1995; Brook and Hatton, 1998). However, a number of limitations are associated with GICs. These type of cements are more susceptible to wear and abrasion, and their low flexural strength and low modulus of elasticity, results in them being brittle and more 'prone to fracture' (Cho and Cheng, 1999).

Another disadvantage of GICs is their moisture sensitivity, especially during the early stages of the setting reaction and, more importantly, within the first 24 hours of application (maturation phase) (Nicholson and Czarnecka, 2008). This happens as a result of the water in the cement matrix becoming more bound in the cement. The ratio of bound to unbound water increases during the maturation process, but if more water is evaporated (lost) from the cement, then the setting reaction will be

disrupted, and this will subsequently affect the material's aesthetic quality and physical and mechanical properties (Nicholson and Czarnecka, 2007).

Different approaches have been suggested and tested to overcome GIC's weaknesses. One proposal included preparation of novel glasses with the addition of 'dispersed-phases of crystallites'. These materials included adding large amounts of reinforcing crystals e.g., carborundum (Al_2O_3), rutile (TiO_2), baddeleyite (ZrO_2) and tielite (Al_2TiO_5) (Prosser *et al*., 1986). These modifications showed improved flexural strength compared to conventional GIC, but the problem of sensitivity to moisture remained the same (Moshaverinia *et al*., 2011).

A second suggestion was incorporation of different fibres (alumina, glass, carbon and silica) in the cement powder to enhance the flexural strength. However, in order to enhance the strength efficiently, the fibres needed to be added in large quantities, which adversely affected the cements handling properties (Moshaverinia *et al*., 2011).

Addition of metal fibres to conventional GIC was patented by Sced and Wilson in 1980. The benefit of this material was the increased flexural strength of the set cement (Sced and Wilson, 1980). Simmons (1983) introduced the 'miracle mixture' in 1983, which involved the addition of amalgam alloy powder to the cement. Although these new compositions resulted in a set cement with improved flexural strength and abrasion resistance, they lacked aesthetics and they had lower bond strengths to enamel and dentine (Thornton *et al*., 1986) than conventional GICs, which led to more micro-leakage (Robbins and Cooley, 1988). Moreover, GIC compositions with modified particle size and distribution of the powder led to an

improvement in the mechanical properties and reduced the early sensitivity to moisture, but with a compromise in the aesthetics and translucency of the set cement (Croll, 1998; Leirskar *et al*., 2003).

All the above compositions and improvements did not solve two important problems associated with conventional GIC: sensitivity to moisture and 'lack of command cure' (Rao, 2008). In order to solve these problems, the incorporation of a resin system into the GIC cement was introduced, to provide a material that incorporates the advantages of a resin (e.g. improved strength), with the improved properties of GICs (Mathis and Ferracane, 1989). This was first mentioned in a patent application in 1988 (Antonucci *et al*., 1988), and it was introduced as a new development by Mitra in 1989 (Mitra, 1992). Since then they have been further developed into a range, of what we now know, as resin modified glass ionomers (RMGICs), which are the focus of this research, and will be discussed in the next section.

2.1.4.5 Classification of materials containing GIC:

Materials that contain one or more components of a conventional GIC set through either an acid-base reaction and/or polymerisation and these can be classified into three categories (McCabe, 1998):

'Modified composites': These materials set merely by a polymerisation reaction whilst containing an 'ion-leachable glass', in order to maintain the fluoride release characteristic of GIC. Examples of these products include Variglass (Dentsply).

Hybrid Materials: This applies to all materials that set through both acid-base reaction and polymerisation; this type includes RMGIC. Hybrid materials can set

without even initiating the polymerisation reaction. They are cements that contain a GIC component in addition to the composite resins. Vitremer (3M-ESPE, USA) and Fuji II LC from GC (Japan) are examples of such products.

Compomers: Water is the only component that is excluded from the paste of compomers, which contain all glass ionomer ingredients in addition to the resin composites. The reason for removing the water is to prevent the occurrence of the setting reaction without initiating the polymerisation process. Later, after polymerisation, water absorption by the cement activates the acid-base reaction, but this late reaction is believed to happen only on a limited scale. Compomers are supplied as one paste and the setting is light initiated. Dyract (Dentsply, Germany) and Compoglass (Vivadent, Schaan, Liechtenstein) are compomer examples present on the market. Different materials called 'Giomer' can be classified as compomers but differ in the addition of 'pre-reacted glass ionomer' in order to maintain the properties of fluoride release. These cements set by light irradiation similar to resin composites (Jyothi *et al*., 2011).

RMGIC can be classified as 'hybrid material', but the term RMGIC is more commonly used.

2.1.5 Resin Modified Glass Ionomer Cements (RMGICs):

This type of cement incorporates two setting mechanisms: the conventional acid-base reaction and polymerisation of the resin monomer where the polymerisation can be either light or chemically activated (Wilson and Nicholson, 2005). These materials have the same composition as conventional GICs, with the incorporation of poly(acrylic acid) or co-polymer of acrylic acid and other alkenoic acids. But the

difference in composition of RMGIC is the addition of a polymerisable resin monomer, commonly 2-hydroxyethyl methacrylate (HEMA) (Figure 2.3). HEMA also works as a 'co-solvent' in order to keep all the components in one phase (Mathis and Ferracane, 1989; Nicholson and Anstice, 1994). This will be discussed further in section 2.2.1.

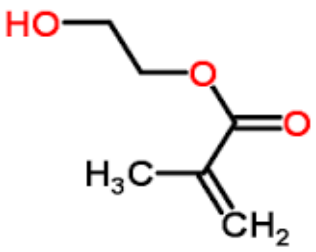

Figure 2.3 HEMA chemical formulation.

2.1.5.1 Composition of RMGICs:

As mentioned earlier, RMGICs comprise the basic ingredients of GIC, containing ion leachable glass, poly(acrylic acid) and water. A proportion of water was replaced with a resin monomer HEMA (Antonucci *et al*., 1988) and other methacrylates, like bisphenol A dimethacrylate (Bis-GMA) (Mitra, 1992). RMGIC moreover contains initiators and activators in order to start the polymerisation reaction. Benzoyl peroxide is an example of an initiator used in these cements, which reacts with a tertiary amine to start the polymerisation reaction; another example is ascorbic acid, which is used particularly with sulphates (e.g. potassium persulfates) to initiate the reaction. These components are used in the chemically (or auto) cured materials, whilst the light cured ones include camphoroquinone as a photo initiator and a

tertiary amine, such as N,N-dimethylaminoethyl methacrylate (DMAEMA) as an activator (Lim *et al*., 2009) (Andrzejewska *et al*., 2003).

The exact formulation is not identical in all commercial products and different manufacturers claim different compositions. RMGIC is supplied as powder/liquid (both hand mixed or capsulated) and paste-paste formulations. The first commercial material produced was Vitrabond, known later as Vitrebond (3M-ESPE), and was developed by Mitra (1988), as a lining material (e.g. Baseline, Dentsply). Following their wide acceptance by clinicians, they were later introduced as a restorative material (Fuji Ⅱ LC-GC, Photac-Fil-ESPE, Vitremer-3M-ESPE) (Nicholson and Croll, 1997). RMGIC luting cements also had huge success and acceptance due to their easy handling, strength and fluoride release. They included chemically cured materials. Examples of luting products include, Fuji Plus (GC), Vitremer luting (later called RelyX luting, 3M-ESPE) and Advance (Dentsply).

2.1.5.2 Setting Reaction:

RMGIC cements set by an acid-base reaction and polymerisation of the resin monomer. In light cured materials, the acid-base reaction is initiated first following mixing, whilst the free radical polymerisation will occur when irradiated with visible light. Following setting, the cement consists of an 'interpenetrating' network, polyHEMA and polyacrylate salts (Sidhu and Watson, 1995). The setting reaction was described by Yelamanchili and Darvell in (2008) as a 'competition network' formation between the acid-base reaction and polymerisation of the monomer (Yelamanchili and Darvell, 2008) (Figure 2.4). According to this, any delay in the GIC reaction will make the polymerisation of the monomer more complete and vice

versa since these two reactions compete with each other in the same matrix. Consequently, no reaction will be fully completed.

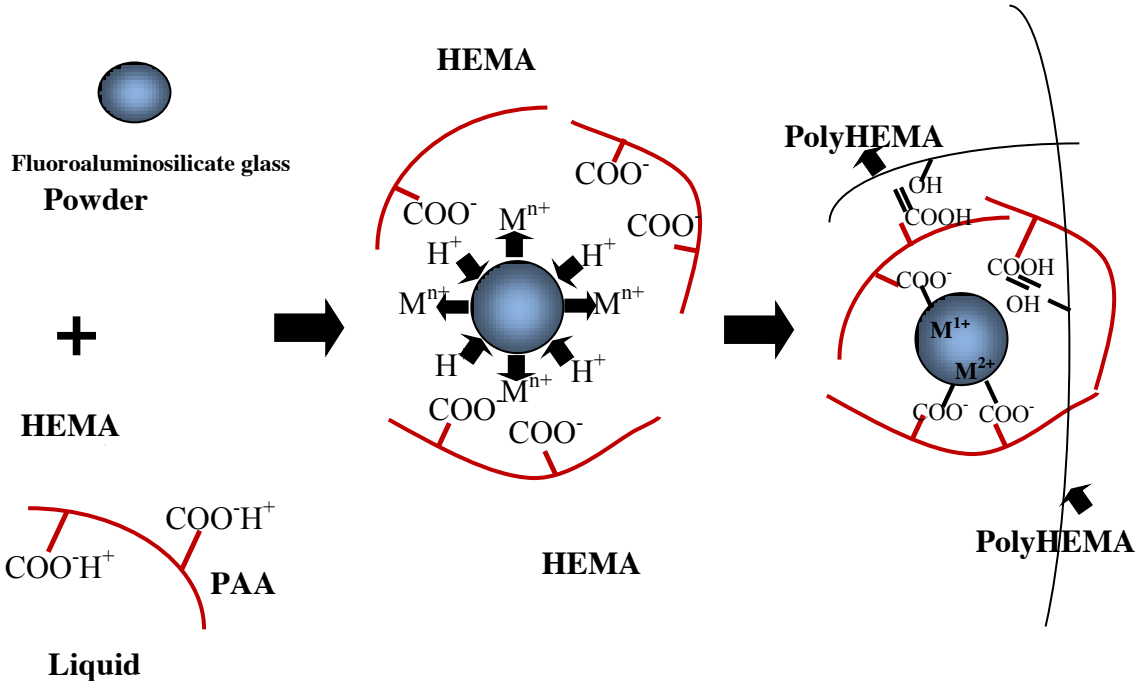

Figure 2.4 Mixing and setting reaction of RMGIC, re-drawn and modified from Lohbauer (2009) (Lohbauer, 2009).

The resin polymerisation can be activated either chemically or through light irradiation. Chemical activation involves either heating (not appropriate for RMGIC which is used at the chairside), or through chemical activator and initiator in order to form free radicals. Initiators in general are molecules that can be decomposed through their weak bond to form two reactive molecules with unpaired electrons. An example of an initiator used in chemically activated dental resins is benzoyl peroxide which reacts with an aromatic amine activator, which makes it possible for the reaction to occur at room temperature. In the light-cured materials, ketones or benzoin methyl ether can be decomposed with a tertiary amine in the presence of

light irradiation to form free radicals. The whole reaction can be simplified in four stages (McCabe and Walls, 2013):

1. Activation: in this stage, free-radicals are produced from the peroxide initiator following either heating, light irradiation (causes the photo initiator to react with a tertiary amine) or chemically (tertiary amine reacts with benzoyl peroxide) (Powers, 2006).
2. Initiation: this occurs when the free radicals attack the monomer molecules at their double bond sites (Powers, 2006; McCabe and Walls, 2013).
3. Propagation: following initiation, further free radicals attack more monomer molecules and the polymer chains begin to grow; this process continues until termination, which represents the last stage of this mechanism.
4. Termination: Theoretically, the propagation should continue for all monomer molecules. However, this does not happen normally for all the molecules, since propagation (chain growth) could stop at different stages, due to different factors, such as, when 'radicals of two growing chains are combined to form one dead chain (by forming a covalent bond between the chains), or when the activated initiator reacts with the chain and forms a 'dead polymer' (McCabe and Walls, 2013). This may lead to un-converted monomers and oligomers that can be released and thus decrease the material's biocompatibility.

In addition to the polymerisation reaction of the resin, RMGICs setting reaction includes the acid-base reaction similar to the GIC. This setting reaction is fully described in section 2.1.4.3 and can be simplified in three stages:

1- Ionisation: Polyacrylic acid ionises in water to produce H+ ions, and these subsequently attack the glass surface, leading to the release of metal cations.

2- Gelation phase: This stage involves increased release of metallic cations and the formation of metal ion cross-linking the polyacrylate chains.

3- Maturation: The reaction mentioned above continues beyond the setting time with an increase in the ratio of bound to unbound water (Nicholson, 1998).

Although the polymerisation reaction occurs in the first 10 minutes, evidence has shown that the acid-base reaction in RMGIC continues over 24 hours (Feilzer *et al*., 1988; Palmer *et al*., 1999). The set cement has been found to include a matrix of poly salt and polymers with 'embeded' glass particles (Palmer *et al*., 1999).

A study conducted by Kakaboura *et al*. (1996) on the setting mechanism of RMGIC showed that initiating the polymerisation of the monomer slows down and reduces the acid-base reaction, when compared to a conventional GIC. One of the materials used in their study (Variglass, Dentsply) did not show any acid-base reaction. Although Variglass is marketed as a RMGIC, this product contains only a small amount of water, which does not support the acid-base reaction and the cement will not be able to set in the dark. Therefore, this product cannot be classified as RMGIC and should be under the group 'modified composites', polyacid or fluoride releasing composites (compomers) (Wilson, 1990), as described in 2.1.4.5, rather than RMGIC as the company claims.

There are products classified as RMGICs which are claimed to have a 'tri-cure' reaction, where the setting reaction involves the acid-base reaction together with

photo and chemically initiated polymerisation. Therefore, even in the absence of light, these materials undergo an acid-base reaction and polymerisation of the resin monomer (McCabe, 1998). The 'third' chemical reaction occurs as a result of adding potassium persulfate and ascorbic acid to the cement ingredients, as a water activated redox system. These two components, in the presence of water, can initiate free radical polymerisation (Mitra and Mitra, 1992; Mitra, 1992). The advantage of this type of cement (the tri-cure) is mainly for large restorations where the material is placed in bulk, and due to the additional chemical cure occurring in these cements, the 'incremental' build-up of the cavities will not be necessary. An example of these materials is Vitremer (3M-ESPE) which is used as a core build-up or a restorative material (McCabe, 1998).

2.1.5.3 Review of the Literature on RMGIC:

The aim of this section is to review existing literature on RMGICs and their properties, and to critically appraise the evidence available on their use, advantages, disadvantages, their strengths and weakness. Electronic databases have been searched for any evidence in the literature regarding RMGICs and their properties. RMGICs have been in use for a long time (more than 20 years), therefore numerous literature were found regarding their performance, both in in-vitro and in-vivo studies, so priorities in reporting (where applicable) were given for the highest level of evidence beginning with systematic reviews, clinical trials, clinical studies and then in vitro studies.

2.1.5.3.1 Mechanical properties:

RMGICs were introduced to enhance the properties of conventional GICs. They demonstrate improved setting properties with longer working times and sharper set. They moreover show improved early development of strength and resistance to early moisture sensitivity (Uno *et al*., 1996). However, RMGICs physical and mechanical properties should be evaluated in order to identify their advantages and disadvantages in their properties, and any limitations in their clinical use.

Table 2.1 summarises the main articles used in this section with regards to strength and fracture toughness of RMGICs and compare it with other types of materials (e.g. GICs, resin composites and compomers).

Table 2.1 Main studies on strength and fracture toughness of RMGICs and different materials (including GICs, resin composites and compomers).

Article	Mechanical property	Material tested	Value
(Mallmann *et al*., 2007)	Compressive strength	GIC RMGIC	46-54 MPa 91-105 MPa
(Ilie and Hickel, 2007)	Flexural strength Diametrical tensile strength Compressive strength	GIC RMGICs GIC RMGICs GIC RMGICs	14.9-34.4 MPa 39.1-78.2 MPa 9.4-12 MPa 14.3-20.7 MPa 78.8-99.0 MPa 116.0-165.4 MPa
(Yamazaki *et al*., 2006)	Flexural strength Diametrical tensile strength Compressive strength	GIC RMGICs GIC RMGICs GIC RMGICs	The exact values were not clear, but it was reported that RMGICs demonstrated higher flexural and diametrical tensile strength.
(Xie *et al*., 2000)	Flexural strength Diametrical tensile strength Compressive strength	GIC RMGICs GIC RMGICs GIC RMGICs	11.1-31.4 MPa 71.1-82.1 MPa 18.2-25.5 MPa 37.9-47.5 MPa 176.0-301.3 MPa 243.5-306.2 MPa
(Uno *et al*., 1996)	Diametrical tensile strength	GIC RMGICs Resin composite	7.5-12.5 MPa 11.4-48.4 MPa 44.4-62.6 MPa
(Braem *et al*., 1995)	Young's modulus Restrained fracture strength Flexural fatigue limit	GIC RMGICs Resin composite	Table and values are not clear but it was stated that Young's modulus for resin are inferior to that of GIC and RMGICs
(Ilie *et al*., 2012)	Fracture toughness	GIC RMGICs Resin composite Compomers	0.45 MPa√m 1.12 MPa√m 1.02-1.84 MPa√m 1.29-1.44 MPa√m
(Ryan *et al*., 2002)	Fracture toughness	GIC RMGICs Polyacid modified resin composite	0.26-0.27 $MN/m^{3/2}$ 0.67-0.72 $MN/m^{3/2}$ 0.45-0.48 $MN/m^{3/2}$

Strength:

In general, improved results were associated with RMGIC compared to GIC when testing compressive strength (Mallmann *et al*., 2007). According to Ilie and Hickel (2007), RMGIC demonstrated improved mechanical properties (macroscopic flexural strength and modulus of elasticity, diametrical indirect tensile and compressive strengths) than GIC. The higher compressive strength of RMGIC compared to GIC was also confirmed by Mallmann *et al*. (2007). Both Xie *et al*. (2000) and Yamazaki *et al*. (2006) agreed that RMGIC had higher flexural strength and diametrical tensile strength values compared to GIC (Xie *et al*., 2000; Yamazaki *et al*., 2006). However, some authors reported resin composites to have higher compressive strength and diametrical tensile strength than RMGIC (Attin *et al*., 1996; Uno *et al*., 1996; Piwowarczyk and Lauer, 2003). Moreover, RMGIC were reported to present with lower elastic modulus than composite resins (Braem *et al*., 1995). So generally RMGIC have improved strength and modulus compared to GIC but inferior strength and modulus to resin composites.

Fracture toughness:

As reported in the literature, restoration failure is mainly attributed to fracture in the restorative material (van Dijken, 2000; Brunthaler *et al*., 2003; Van Nieuwenhuysen *et al*., 2003). Fracture toughness is used to measure the material's ability to resist fracture (Ilie *et al*., 2012). Ilie *et al*. (2012) measured the fracture toughness of various materials, including GIC, RMGIC, resin composites and others. They reported that there was a statistically significant difference in the fracture toughness between GIC and RMGIC, the latter showed higher values, but with similar results between RMGIC and resin composites. Agreement with these results was also

reported by Yamazaki *et al*. (2006) and Mitsuhashi *et al*. (2003). RMGIC presented greater resistance to fracture compared to GIC.

Mitsuhashi *et al*. (2003) tested different powder to liquid ratios, powder particle size and their effect on the fracture resistance of the material (RMGIC). They reported higher fracture toughness values when using a small particle size of up to 10 μm, and the importance of the resin used in RMGICs to improve the fracture toughness, compared to conventional GICs. According to Ryan *et al*. (2001), their in-vitro study results showed no correlation between the different ratios used and the material's ability to withstand fracture. In comparison, the use of a smaller particle size (not smaller than 10μm) powder in RMGICs was reported to increase the materials fracture toughness, in agreement with Mitsuhashi *et al*. (2003). The fracture toughness was also measured as a toughness of the interface between the cement and dentine. The authors reported that the strength of the interface between dentine and the dental material was dependent on the fracture behaviour of this material. According to their study, RMGIC showed higher fracture toughness than GIC (Ryan *et al*., 2002). The dentine-cement interface played an important role in decreasing the fracture toughness levels of all materials tested. It was proposed that the transfer of water from, and into, the cement or dentine, could affect the fracture and crack propagation. Despite this, RMGIC obtained improved results in withstanding fracture than GIC, when measured both as a material (Ryan *et al*., 2001), or at the dentine-cement interface (Ryan *et al*., 2002).

Bonding:

Bonding to tooth structure:

Bonding between tooth tissue and dental materials through ion exchange was first described by Smith in 1968; it was proposed following the use of polyalkenoic acid in these cements (Smith, 1968). Improved bonding occurred with GIC and RMGIC compared to resin composites, especially when bonding to dentine. This occurs through the ion exchange between poly(acrylic acid) from GIC and 'reactive groups' in the collagen fibres in dentine (McLean, 1992). It is hypothesised that in addition to the ion exchange in GIC and RMGIC, due to the presence of HEMA, this cement can bond to dentine mechanically, through hygroscopic expansion, and also chemically through the reaction between the ester group in HEMA and amino groups in collagen, following the polymerisation of the monomer (Xu *et al*., 1997). As a result of the inorganic nature of enamel, bonding to it can be more efficient mechanically with resin composites through mechanical interlocking, compared to chemical bonding with GIC (Buonocore, 1955). The bonding of GIC to enamel includes chemical ionic bonding between calcium ions from enamel and carboxyl groups from the polyacrylic acid in the GIC (Wilson *et al*., 1983; Zhang *et al*., 2013).

When bonding to dentine, RMGICs are better than resin composites, but this is not the case when bonding to enamel, due to the differences in dentine and enamel structure. When bonding to dentine, products containing glass ionomer can bond to the ions inside and surrounding the collagen fibres, through poly(acrylic acid) molecules where the carboxyl groups from poly(acrylic acid) bond to the amino groups of the collagen. Moreover, the monomers in RMGIC will then crosslink with

poly(acrylic acid) that is already connected to the collagen fibres. When bonding to enamel, due to the low organic nature of this tissue, the bonding achieved is mainly by monomer polymerisation inside its microporosities, following the etching procedure, in addition to the chemical reaction between Ca^{+2} from enamel and carboxyl group from poly(acrylic acid) (Gordan *et al*., 1998). However, RMGIC has demonstrated improved bonding to enamel compared to GIC, through the mechanical bonding of the resin matrix with the enamel. In the same study it was recommended to etch the enamel surface before applying GIC or RMGIC, in order to increase the microporosities in the enamel, and hence, increase the tensile bond strength (Imbery *et al*., 2013; Zhang *et al*., 2013).

In a clinical study involving bonding of orthodontic brackets with different adhesive materials, the authors suggested that RMGIC could be used efficiently to bond orthodontic brackets, even in areas where there are high occlusal forces. Despite this, it was confirmed that resin adhesives possessed higher bond strengths to enamel than RMGIC (Shammaa *et al*., 1999). Restoring class V cavities with RMGIC or resin composites was also evaluated in a clinical study where RMGIC showed better retention results than composites, after 24 months (Brackett *et al*., 2003). Ermis (2002) in a clinical study demonstrated higher retention rates of class V RMGIC restorations compared to polyacid resin composites (compomers) after two years. Moreover, Franco *et al*. (2006) reported on the superiority of the retention of RMGIC class V restorations compared to resin composites after 5 years (Franco *et al*., 2006).

Care should be taken when extrapolating results from in-vitro studies to clinical situations and, it is not possible to compare results from different studies, due to

variations in the test methodologies and materials used. Also, the reported clinical studies included bias due to their small sample size (n=30 - Shammaa *et al*., 1999; n=38 - Brackett *et al*., 2003), lack of appropriate reporting on the randomisation process and if there was any blinding throughout the study.

An attempt to correlate the in-vitro results with clinical studies regarding retention of class V restorations restored by different materials were the subject of a systematic review (Heintze *et al*., 2011). These authors tried to link tensile bond strength results to a systematic review (Heintze *et al*., 2011) on the retention of RMGICs and different resin composites, but not surprisingly without success. This may be due to the different variables between the clinical studies, for example, cavities with different dentine thicknesses and pre- preparation performed, thus biasing the analyses of the clinical studies. Whilst tensile bond strength results favoured the resin composites, the clinical studies showed better retention of restorations restored with RMGIC, after 12 and 36 months of application, so no correlation was made.

Bond strength to restorative materials:

This is highly important when considering RMGIC as a base or liner under composite restorations. Reports on the physical properties of RMGIC suggest the superiority of RMGIC bonding to composite compared to GIC (Chadwick and Woolford, 1993; Li *et al*., 1996; Pamir *et al*., 2012; Babannavar and Shenoy, 2013). Kerby and Knobloch (1992) tested the bond between resin composites, light-cured RMGICs and chemically cured GICs. The authors explained that the stronger bond between the light-cured RMGIC and composites, when compared to other reinforced GICs (e.g. silver reinforced GIC, Fuji Miracle Mix, GC), was a result of unconverted monomers after curing, which increased ‘wetting’ of the bonding agent and resin

composite during the bonding procedure. Moreover, the authors suggested that there was formation of 'covalent' bonds between the resin bonding agent and the unconverted methacrylate groups in the RMGIC (Kerby and Knobloch, 1992). Improved adhesion was reported for RMGIC when luted to precious and non-precious alloys, compared to GIC and zinc phosphate cements (Ergin and Gemalmaz, 2002).

No statistically significant difference was found between RMGIC and resin composites when bonding zirconia crowns (Ernst *et al*., 2005; Palacios *et al*., 2006). There are contradictions in the literature on bonding all-ceramic crowns made of feldspathic porcelain or low-strength ceramics with RMGICs. Different articles have reported incidences of fracture of ceramic restorations, following cementation with RMGIC, and therefore their authors have recommended not to use this type of cement to bond low-strength ceramics (Sindel *et al*., 1999; Behr *et al*., 2003; Federlin *et al*., 2004; Federlin *et al*., 2005). This is in agreement with clinical observations and also companies recommendations, contraindicating the use of RMGIC to bond low-strength all-ceramic restorations. This is a result of the higher water uptake of RMGIC, which subsequently leads to hygroscopic expansion (swelling) following application (Leevailoj *et al*., 1998; Federlin *et al*., 2005). The polyHEMA in RMGIC will contribute to the higher expansion rate of RMGIC, since it is more hydrophilic than the resins used in resin composites (Leevailoj *et al*., 1998).

On the contrary, different studies regarding the use of RMGIC to bond ceramics did not correlate the incidence of fracture with the type of luting cement tested (RMGIC) (Leevailoj *et al*., 1998; Snyder *et al*., 2003).

2.1.5.3.2 Release of fluoride:

Sustained fluoride release is one of the main advantages of GICs and it was reported that restorative RMGIC release it to the same extent as conventional GICs (Mitra, 1991; Tam *et al*., 1991; Forsten, 1995). The mechanism of fluoride release is described as an ion exchange procedure or 'wash out' from the restoration. If the fluoride release occurs as a 'wash out', other ions, mainly calcium, will also be released and this will result in 'gradual disintegration' of the cement (Tam *et al*., 1991). Clinical reports suggested decreasing the light irradiation time of the RMGIC in order to increase the fluoride release, but this will negatively affect its physical properties. Application of topical fluoride can recharge the fluoride in both GIC and RMGIC materials and hence increase the fluoride release (Forsten, 1995).

2.1.5.3.3 Exothermic setting reaction:

Temperature rise in the tooth during, or following, some dental procedures can cause irreversible damage to the pulpal tissue (Zach and Cohen, 1965). Zack and Cohen (1965) demonstrated that a temperature rise of 5.5°C could harm the pulp in deep cavities following their experiments on Macaca Rhesus monkeys, where 15% of the examined pulp failed to recover. In the same experiment, 60% of the pulp tissues showed permanent damage when the temperature was raised to 11.2°C. The temperature rise was associated with necrosis and permanent damage of the pulp tissues (Zach and Cohen, 1965). Various authors contradicted the work of Zach and Cohen, as Lloyd *et al*. (1986) argued the reliability of the method used to determine the effect on the pulp, since the teeth were heated using a soldering iron rather than the heat produced from dental materials. Baldissara *et al*. (1997) demonstrated that a temperature rise of 11.2°C did not show harmful effects on pulp tissues (Lloyd *et al*.,

1986; Baldissara *et al*., 1997). As a conclusion, it appears that there is no conclusive evidence in the literature with regards to the actual temperature that can induce permanent damage to the pulp, and therefore, reducing the exotherm on setting of dental materials is highly desirable.

Polymerisation of resin materials is exothermic and, in the case of light activated products, there can be extra heat generated from the light curing device (McCabe, 1985). Due to the fact that RMGICs contain HEMA and undergo polymerisation (light and/or chemically), a rise in temperature is commonly associated with this type of cement. Kanchanavasita *et al* (1996) reported a rise in temperature of RMGICs that reached 20.2ºC when tested at 37ºC.The higher the HEMA monomer content in the material, the higher exotherm is observed, as the conversion of HEMA to polyHEMA includes the conversion of the double bonds to single bonds in the molecule, and this is associated with rise in temperature. Although, decreasing the conversion rate can reduce the exotherm, this will leave more unconverted HEMA within the material that may leach out and reduce the biocompatibility of the material due to HEMA's cytotoxicity (Kanchanavasita *et al*., 1996).

In theory, RMGICs produce more heat than resin composites, as the composition contains HEMA, which polymerises to polyHEMA and is reported to have a high exotherm on setting (Kanchanavasita *et al*., 1996); co-polymerisation between HEMA and 'unsaturated groups' of the poly(acrylic acid), and a further cross-linking of the poly(acrylic acid), takes place to increase the strength of the material. Kanchanavasita *et al*. (1996) agreed with the theory presented and demonstrated higher exotherm values for RMGIC compared to resin composites (20.2ºC for

RMGICs compared to 5°C for resin composites). The authors also agreed the higher temperature rise of RMGIC was due to HEMA, and referred to its low molecular weight, which is generally associated with higher exotherm and shrinkage, compared to higher molecular weight monomers used in resin composites. According to Kim and Watts (2004) and Atai *et al*. (2005), the smaller the molecular weight of the monomer, the more monomers are polymerised for a similar volume, hence a higher exothermic reaction will be taking place (Kim and Watts, 2004; Atai *et al*., 2005). Conversely, RMGICs were found to have similar exotherm results to those reported for resin composites (Al-Qudah *et al*., 2005). There was no explanation in the latter article on why their results differed from what was documented in the literature (Kanchanavasita *et al*. 1996). However, it can be assumed that this could have been due to the two studies using different method for measuring the exotherm, and/or materials (brands).

Other factors were also reported to influence the temperature rise following polymerisation, such as powder: liquid ratio of the material, since a lower ratio will subsequently mean more monomers in the set cement. Therefore, lining and luting cements may demonstrate a higher exotherm compared to restorative materials (Kanchanavasita *et al*., 1996). Specimen's thickness for light-activated materials was reported to influence the temperature rise. For larger samples less exothermic reaction was observed compared to smaller samples, since the light source may have caused less conversion of the monomers, and hence a lower exotherm (Kanchanavasita *et al*., 1996).

2.1.5.3.4 Biocompatibility:

Biocompatibility is defined as 'the ability of a material to perform with an appropriate host response in a particular application' (Williams, 1987). GICs were classified as biocompatible materials due to their reduced setting exotherm compared to other materials (Crisp *et al*., 1978) and, the ions released from the set cement are not cytotoxic, with the exception of aluminium ion. Aluminium is known to have a toxic effect on the human body, but the amount released from GIC in the mouth is very low to cause any cytotoxic effect (Czarnecka *et al*., 2002).

RMGIC, as well as GIC, release small amounts of cytotoxic ions (Al^{+3}, F^{-}, Sr^{+2}) however the cytotoxic effect of RMGIC was associated with the release of unconverted HEMA monomer and its effect on the pulp (Stanislawski *et al*., 1999). HEMA toxicity cannot only damage the pulp cells, but also affect dental patients and dental practitioners, as when in contact with skin, this monomer can cause dermatitis to different degrees (Nicholson and Czarnecka, 2008).

The use of RMGIC as a direct pulp capping material was investigated by Nascimento *et al*. (2000); it was compared with calcium hydroxide, which is often considered as the material of choice for pulp capping, due to its ability to support the formation of dentine bridges and it seals the exposed pulp tissue. According to this study, all teeth restored with RMGIC showed irreversible pulp damage and with no signs of any dentine bridge formation. Moreover, it was reported that HEMA could penetrate the dentinal tubules and subsequently cause inflammation and changes in their 'cell structure' (Bouillaguet *et al*., 1996; Oliva *et al*., 1996; Hashimoto *et al*., 2004). Biocompatibility of HEMA is discussed further in section 2.2.1.

In contrast to these studies, a systematic review on 'pulp capping' comparing calcium hydroxide (material of choice for pulp capping) and RMGIC, concluded that pulp response to both materials were similar, and preferences were drawn (Mickenautsch *et al*., 2010). In the literature, there have always been contradictions regarding the biocompatibility and pulp response to RMGIC (Geurtsen, 2000; Sidhu and Schmalz, 2001; Nicholson and Czarnecka, 2008), which made the above mentioned systematic review necessary. Although the authors attempted to draw a definite conclusion regarding this issue, they failed because of many limitations in their article. First of all, the review included only one randomised clinical trial (RCT), while the other studies were not randomised, and this can lead to a selection bias, especially on how deep the cavity was in which the two materials where applied; this can bias the results of the clinical trials and subsequently of the systematic review. The only RCT included (Marchi *et al*., 2006) was of low quality with a sample size of 27, and lack of adequate reporting on randomisation. Therefore, the interpretation, analysis and consequently the results and conclusion of this systematic review were extremely biased and needed to be interpreted with caution, especially when they disagreed with in-vitro and cell culture studies on RMGIC and HEMA.

2.1.5.3.5 Release of residual HEMA:

RMGIC's low biocompatibility was directly linked to the release of residual unconverted HEMA from the set cement. Due to its low molecular weight and hydrophilicity, the monomer can easily diffuse through the dentinal tubules to the pulp tissue, and subsequently cause irreversible inflammation (Gerzina and Hume, 1996; Hamid *et al*., 1998).

High performance liquid chromatography (HPLC) has been used in dental research studies reporting residual monomer from dental polymers and composites (Beriat and Nalbant, 2009). Using HPLC, Hamid *et al*. (1997) showed that HEMA can move through infected and healthy dentine, though it tends to diffuse in at an increased rate through infected dentine.

Moreover, Hamid and Hume (1997) studied the effect of various dentine thicknesses (ranging from 3.6 to 0.4mm) for HEMA diffusion to the pulp tissues. According to their study, increased dentine thickness did not play a role in preventing HEMA from diffusing through dentine, and all thicknesses studied allowed the monomer to move freely to the pulp. Expectedly, smaller dentine thicknesses were associated with higher diffusion rates towards the pulp (Hamid and Hume, 1997).

Different factors can affect the amount of HEMA released, one of which is light curing time with light-cured RMGIC. In a study by Palmer *et al*. (1999), regarding the release of HEMA from different commercial products with varying irradiation times using HPLC, it was demonstrated that there was a link between the cure time and the release of HEMA, with more release of HEMA occurring at reduced irradiation times. It was also noted that different commercial materials, although of the same generic type (RMGIC), each had a different curing time recommended by the manufacturers, which must be followed in order to reduce the amount of unconverted HEMA (Palmer *et al*., 1999).

2.1.5.3.6 Water uptake and swelling:

RMGIC sets through acid-base and polymerisation reactions. It was observed that the acid-base reaction of such cements progresses at a slower rate than in

conventional GICs. The decrease in the reaction rate is a result of the initiation of the polymerisation of the resin monomer, HEMA in RMGIC, either by light or chemically in the auto cured materials. This also occurs as a result of reduced water content in the RMGIC liquid compared to the GIC liquid, due to the incorporation of HEMA; this reduction leads to a slower reaction as water is an essential part of the acid-base reaction (Sidhu and Watson, 1998). Whilst the two different independent reactions (acid-base and polymerisation of the monomer) happen at the same time in these cements, a 'high degree' of cross-linking occurs between these two 'matrices' (Mount *et al*., 2002). HEMA as a hydrophilic monomer plays an important role in the water uptake of RMGIC from the oral environment and a 'mild hydrogel' behaviour was associated with these cements (Nicholson and Anstice, 1994). According to the literature, hydrogels containing HEMA monomer are linked with high water uptake, which was reported to reach 80% by mass (Pedley *et al*., 1980). Consequently, a higher amount of HEMA in the RMGIC will correlate to higher water sorption (Yap and Lee, 1997). Swelling of the resin matrix occurs to provide a space for the diffused water through the matrix (Braden *et al*., 1976) as well as filling the microvoids in the cement (Oysaed and Ruyter, 1986).

Different problems, e.g. weakening of the cement and plasticising the matrix, have been linked to the water uptake of RMGIC (Malacarne *et al*., 2006; Pastila *et al*., 2007). RMGIC samples immersed in water, or in a humid environment, for 24 hours to three months, tended to show reduced physical properties (flexural strength and hardness) compared to those stored dry. Therefore, the decrease in strength was linked to the water uptake of the RMGIC (Cattani-Lorente *et al*., 1999). A decrease in compressive and flexural strength of RMGIC, following immersion in distilled

water for 24 hours and 150 days was also reported by Piwowarczyk and Lauer (2003). In another study, RMGIC showed higher water uptake after 7 days of immersion in distilled water and higher solubility rates than resin cements. This was as a result of the higher hydrophilic monomer content and lower filler content compared to resin cements (Gerdolle *et al*., 2008). These results were also in agreement with Mese *et al*. (2008). Following immersion in water in the case of *in vitro* tests, or clinically in the oral environment, RMGIC released some components like unconverted monomers; this subsequently led to a loss in weight or volume (Knobloch *et al*., 2000; Toledano *et al*., 2003). This loss of weight and shrinkage was compensated in RMGIC by swelling of the material, due to water uptake. Even with the material's shrinkage, the water uptake of RMGIC was reported in an article to be between 8-14% by weight (Knobloch *et al*., 2000). This hygroscopic expansion following water uptake increases the incidence of the all-ceramic fracture when cemented with RMGIC (Sindel *et al*., 1999; Federlin *et al*., 2004; Mese *et al*., 2008).

The aforementioned weaknesses of RMGIC were attributed to the cement's water uptake and this is reported to be correlated with the HEMA monomer (Yap, 1996; Meyer *et al*., 1998; Karaoglanoglu *et al*., 2009). On the one hand, HEMA in the polymer chain is responsible for electrostatic interactions (hydrogen bonding), and therefore, for improving the materials properties compared to conventional GICs. On the other hand, the material tends to absorb more water due to its hydrophilic nature. With increased water sorption (in a clinical situation, where the restoration is not coated), the polymer matrix tends to be more 'flexible' and, due to the decrease of the electrostatic interaction, the good physical properties of the material are jeopardised (Anstice and Nicholson, 1992).

2.1.5.4 Summary of the literature review on RMGIC:

RMGIC were introduced as a modification to conventional GICs, in order to maintain their good characteristics, like fluoride release and good adhesion to tooth structure, and furthermore to improve their mechanical and handling properties. From the literature review, it can be concluded that RMGICs have enhanced mechanical properties over conventional GICs. They have been shown to release similar amounts of fluoride compared to GICs. However, these cements have been reported to have limitations associated with their poor biocompatibility, high setting exotherm and high water uptake. According to the literature review above, all these limitations and weaknesses were mainly attributed to the incorporation of HEMA monomer in the liquid composition of RMGICs.

The following part of the literature review will focus on HEMA monomer used in commercially available RMGICs, and possible alternative monomers that may potentially be used in RMGICs.

2.2 *Introduction to HEMA monomer used in commercial RMGICs and two proposed monomers for use as novel RMGIC:*

2.2.1 2-hydroxyethyl methacrylate monomer (HEMA):

HEMA is a low molecular weight monomer based on methacrylic acid (MAA), and it is used extensively in commercial dental materials compositions like dental adhesives, resin composites and RMGIC (Yourtee *et al*., 2001). This monomer is moreover used for other biomedical applications, like soft contact lenses (Selby *et al*., 2013). HEMA hydrogels were first developed for the fabrication of contact lenses by Wichterle and Lim in 1960 (Hoffman, 2001). In dentistry, this monomer is highly effective due to being a bifunctional monomer with one end of its structure

being hydrophilic and the other hydrophobic (Bakopoulou *et al*., 2009). Its hydrophilic nature is desirable when bonding to dentine as it increases the wettability of the adhesive material, and as a result, increases the bond strength (Hasegawa *et al*., 1989).

PolyHEMA is a hydrophilic homopolymer and is best known for its ability to swell in a moist environment. When not fully cross-linked, poly HEMA is known to absorb up to 42-80% water per unit mass despite its high molecular weight (Pinchuk *et al*., 1984). Similar to other hydrogels, the poly HEMA network consists of two areas, 'cluster' and 'low cross-linking' areas. The cluster area is very cross-linked with minimal ability to absorb or swell in water, unlike the low cross-linked area where high water absorption and swelling are more likely to occur (Hoffman, 2001). Moreover, hydrogels can uptake water to fill the voids in the structure (Hoffman, 2001).

Following placement of a material containing HEMA in the oral environment, unconverted HEMA can diffuse through the dentine to the pulp tissue (Bakopoulou *et al*., 2009). HEMA can cause cell death either by apoptosis or necrosis (Becher *et al*., 2006). Apoptosis occurs when the membrane of the cell stays intact and damage mainly occurs inside the cell itself. Necrosis, on the other hand, involves damaging of the cell membrane and swelling of the cell, which subsequently leads to its death. Necrosis is associated with an inflammatory response as a result of cell death, which spreads through the bone. Thus necrosis progresses through the pulp to the surrounding tissues (Fouad *et al*., 2008). HEMA monomer has been associated with both apoptosis and necrosis cell death when tested *in vitro*, and the damage was seen in compomer materials tested after only 20 hours (Becher *et al*., 2006).

Studies of the effect of HEMA on cells revealed the cytotoxicity of this monomer and its increased damaging effect compared to other monomers released from dental materials (Yoshii, 1997; Orimoto *et al*., 2013). It has been documented that HEMA can disrupt the function of the fibroblasts in the pulp, and cause severe damage even when it is used in low concentrations (Bouillaguet *et al*., 2000). However, diffusion through dentine to the pulp tissue remains a problem in spite of the reduced concentration of the monomer (Bouillaguet *et al*., 2000). In an attempt to understand the mechanism and the effect of HEMA on cells and hypersensitivity, Schweikl *et al*. (2006) studied HEMA's influence on chromosomes and DNA strands (Schweikl *et al*., 2006). According to their study, HEMA caused serious damage to chromosomes and moreover broke the DNA strands, causing a delay in specific phases in the mammalian cell cycle. The mechanism in which the monomer caused this damage is not fully understood, but it was established that the monomer can reduce the level of cell protection, thus making it more prone to damage. Other monomers (for example, triethylene glycol dimethacrylate, TEGDMA) commonly used in resin composites were also linked to cell death.

The cytotoxicity of HEMA has also been linked to cell damage by the production of reactive oxygen species (ROS), for example free radicals or peroxides (Circu and Aw, 2012). Glutathion (GSH) in cells is considered a key part in protection from damage that can be caused by ROS. HEMA is known to decrease the amount of GSH, and subsequently, resulted in more damage and more induced apoptosis occurred (Gallorini *et al*., 2013).

Genotoxicity is also linked to the increased number of ROS. This was studied *in vitro* and identified through observing an increase in micronucleated cell numbers;

moreover, ROS is known to react with DNA components, such as sugar moieties and chromatin proteins (Krifka *et al*., 2012). HEMA is also linked to the breaking of DNA double strands and genome damage (Gallorini *et al*., 2013).

From the abovementioned problems, it was suggested that it may be beneficial to replace the HEMA in RMGIC with a monomer that is known to have lower water uptake, setting exotherm and improved biocompatibility. Tetrahydrofurfuryl methacrylate (THFM) and/or hydroxpropyl methacrylate (HPM) are two monomers proposed to replace HEMA in this thesis, for the formation of novel RMGIC.

2.2.2 Tetrahydrofurfuryl methacrylate (THFM):

THFM is a heterocyclic reactive hydrophobic monomer with a molecular weight of 170.21 g/mol. Its chemical formula is $C_9H_{14}O_3$. The structure of THFM is shown in Figure 2.5 below.

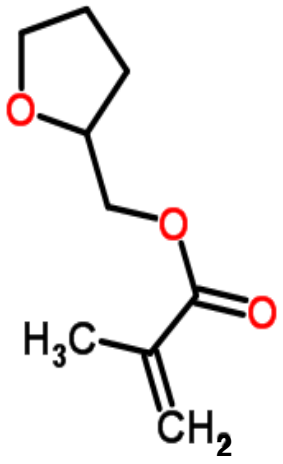

Figure 2.5 THFM chemical structure.

THFM monomer has been patented for different biomedical applications, such as temporary crown and bridge materials (Glace and Ibsen, 1981), fluoride releasing biomaterials (Braden *et al*., 2001) and as a tissue repair material (Braden *et al*.,

1993). This monomer was also mentioned in patents concerning RMGIC (Mitra and Mitra, 1992) (Anstice *et al*., 2001). Mitra (1992) included the monomer in the description and one of different choices to be used for RMGIC, but did not include any example or evidence in utilising or testing the monomer. Anstice *et al*. (2001) included several examples of using THFM in RMGIC but without reporting on water uptake or desorption data. Moreover, they utilised THFM with different percentages of other monomers, and replaced all the HEMA in the cement. This differs from our study as THFM will be used with different percentages of HEMA and/or hydroxypropyl methacrylate (HPM), to develop novel RMGICs.

THFM was studied as a homopolymer and with poly (ethyl methacrylate) (PEM) in order to form a suitable room temperature polymerising system (Patel and Braden, 1991a; Patel and Braden, 1991b). The molar volume of THFM is high compared to methyl-methacrylate (MMA), and this contributes to its low polymerisation shrinkage (Patel *et al*., 1987). This characteristic was advantageous for the construction of hearing aids in order to improve the fit of these appliances (Bhusate and Braden, 1983).

Materials comprising room-temperature polymerising PEM with THFM were tested for their water uptake, mechanical properties and potential clinical uses (Patel and Braden, 1991a; Patel and Braden, 1991b; Patel and Braden, 1991c). A low temperature polymerisation exotherm was associated with this material, with adequate mechanical properties for clinical use (Patel and Braden, 1991b), and low water uptake (about 1.5% by weight) when measured in a different solutions (Sawtell *et al*., 1997).

Although the water uptake results showed that PEM/THFM absorbed water and polyTHFM alone absorbed up to 34% water over two years (Patel and Braden, 1991a) when immersed in distilled water, this value dropped to 2.5% in other solutions like artificial saliva (AS) and phosphate buffered saline (PBS) (Sawtell *et al*., 1997). This indicates that the uptake is osmotically driven where the driving force is the osmotic gradient between the internal clusters/droplets in the material and the external solution. Clusters/droplets are formed at the hydrophilic/water soluble sites. This is more fully explained in section 2.3.1.2.

PEM/THFM was compared with poly(methyl methacrylate) (PMMA)/methyl methacrylate (MM) and PEM/n-butyl methacrylate (nBM) temporary crown material and their biocompatibility/effect on monkey's dental pulp was tested, when placed on 1.0-1.5 mm thickness dentine. PEM/THFM showed no irritation to the pulp tissue after 4 weeks, followed by PEM/nBM, with PMMA/MM showing irritation (Pearson *et al*., 1986).

2.2.3 Hydroxpropyl methacrylate (HPM):

HPM is also a hydrogel, and it is the next member above HEMA in the homologous series, with an extra CH_2 group between the hydroxyl and the methacrylate groups. It has a lower setting exotherm and reduced water uptake compared to HEMA (Patel *et al*., 2001). HPM is a hydrophilic monomer with a molecular weight of 144 g/mol. Its chemical formula is $C_7H_{12}O_3$ (Figure 2.6).

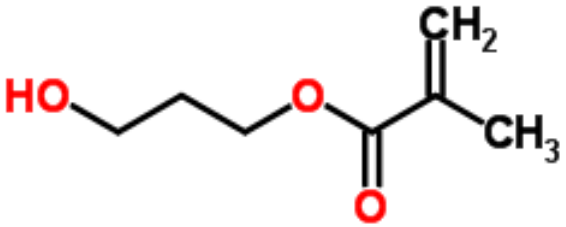

Figure 2.6 HPM chemical structure.

As mentioned in the previous section, PEM/THFM had a high water uptake due to the hydrophilic sites in the polymer matrix. The initial stage of water uptake followed Fickian diffusion, but was preceded by the formation of osmotically active sites (clustering) responsible for the high water uptake. The replacement of THFM with different amounts of HPM decreased the water uptake value through decreasing clustering at hydrophilic sites within the polymer, and the initial diffusion process also followed Fickian diffusion (Patel *et al*., 2001).

Polymerisation exotherm was also studied for the methacrylate systems where THFM was partially replaced with HEMA or HPM. Whilst a high polymerisation exotherm was observed for the systems incorporating HEMA, there was no increase in polymerisation exotherm for systems where HPM was added (Patel *et al*., 2001).

Unfortunately, limited literature was found regarding the use of HPM in the dental applications. One of the articles found on HPM in dentistry is the one mentioned above by Patel *et al*. (2001), the other was by Atai *et al*. (2005), which reported the shrinkage strain rate of dental resin monomers (including HPM). The latter authors confirmed the lower shrinkage rate of HPM compared to the higher molecular weight monomers (e.g. UDMA), but no differences were found compared to HEMA.

As a conclusion, THFM and HPM present as good alternatives to the monomer HEMA in formulating the novel RMGICs, since they both demonstrate lower water uptake compared to HEMA, and it can be assumed that this will lead to lower dimensional changes, which is one of the main aims in this study.

2.3 *Literature review of methods used in this study:*

2.3.1 Water Uptake, Desorption and Solubility:

2.3.1.1 Introduction:

Water uptake and solubility of dental materials are very important characteristics of dental cements as they can be directly linked to the material's dimensional change, biocompatibility and degradation. They can affect marginal integrity, aesthetic properties and survival of the restoration (Yap and Lee, 1997).

The incorporation of a hydrophilic monomer, HEMA in RMGIC, renders these types of cements more vulnerable to water absorption, and subsequently, the increased amount of water absorbed into the polymer matrix can influence the mechanical and physical properties of the cement (Nicholson *et al*., 1992).

2.3.1.2 Mechanisms of water uptake:

Two features can be distinguished for the mechanism of water absorption:

First, the kinetics of the diffusion process. Diffusion can be divided into three categories: Fickian (Case I), Case II and non-Fickian diffusion (anomalous; Crank 1979).

Fickian diffusion is based on the mathematical theory of Fick's first law. The hypothesis of this law is 'the rate of transfer of diffusing substance, through a unit

area of a section, is proportional to the concentration gradient measured normal to the section' (Equation 2.1) (Crank, 1979).

$$F = -D\,\frac{\partial c}{\partial x} \qquad \text{Equation 2.1}$$

Where

F, is the rate of transfer per unit

C, concentration of diffusing substance

x, the space measured normal to section

D, is the diffusion Coefficient.

This law is used when at a specific concentration, the diffusion coefficient is constant. Where this is not the case, Fick's second law is applied. This law is derived from the first one (Equation 2.2).

$$\frac{\partial c}{\partial t} = -D\,\frac{\partial^2 c}{\partial x^2} \qquad \text{Equation 2.2}$$

This formula can be further integrated in terms of distance and time to give the equation of mass uptake (Equation 2.3).

$$\frac{Mt}{M\infty} = 2\left[\frac{Dt}{\pi l^2}\right]^{1/2} \qquad \text{Equation 2.3}$$

Where:

M_t, is the mass uptake at a time t

M_∞, is the uptake at equilibrium

l, half thickness (Crank, 1979).

Diffusion coefficient can be derived from plotting M_t/M_∞ against $t^{1/2}$ where the slope (s), from the initial linear region is used to calculate it, as shown in the Equation 2.4.

$$S = 2\left[\frac{Dt}{\pi l^2}\right]^{1/2} \quad \text{Equation 2.4}$$

Case II diffusion happens as a result of molecular relaxation of the polymer chains and swelling of the glassy polymer. This behavior cannot be described nor calculated using Fick's law (Thomas and Windle, 1982). This can be differentiated from Fickian diffusion as the relationship of the uptake with time is linear, while for Fickian diffusion, the uptake is linear with square root of time (Thomas and Windle, 1982). The kinetics of non-Fickian diffusion can be a mix of Case I and Case II (polymer relaxation) (Crank, 1979).

The second aspect to be considered is the amount of water absorbed until equilibrium is reached. The absorption of water into the polymer matrix may follow one or multiple mechanisms (Kalachandra and Kusy, 1991). Water can be either locked in voids within the polymer matrix or by 'dissolution' of the polymer matrix (Kalachandra and Kusy, 1991). The dissolution is dependent on the hydrophilic species within the matrix and the 'electrostatic' interaction between water and these species. Either clusters or droplets are formed as a result of dissolution (Barrie and Machin, 1969). Clustering occurs as a result of the attraction between water and hydrophilic sites within the polymer matrix. It can be differentiated from droplet formation as clustering is dependent on the molecules in the polymer and it occurs at specific locations in the matrix (Rodríguez *et al*., 2003). Droplets are formed in the polymer matrix as a result of dissolved water soluble additives or impurities (Thomas and Muniandy, 1987). Since THFM is hydrophobic, the water absorption

of PEM/THFM was dependant on the osmotic pressure of the solution in which the material was immersed and, the formation of clusters/droplets in the matrix, which results in an osmotic pressure gradient (Riggs *et al*., 2001); this effect did not occur for the material containing HEMA, since HEMA is a hydrophilic monomer (Sawtell *et al*., 1997).

2.3.1.3 Available literature on water uptake of RMGIC and methodology of testing:

The International Organization for Standardization (ISO) is the organization responsible for developing and publishing international standards. It is well known that ISOs ensure ‘‘that products and services are safe, reliable and of good quality. For business, they are strategic tools that reduce costs by minimizing waste and errors and increasing productivity”. ISO 9917:2010 (1 and 2), which focuses on water-based dental materials, does not contain any requirement or methods for conducting the water uptake experiment. The ISO standards concerning polymer-based restorative materials (ISO, 4049:2009) provide a water uptake experiment, but since RMGIC contain the GIC phase in addition to the resin matrix, there is no agreed method in the literature on how to carry out their water absorption experiments. Beriat and Nalbant (2009) followed the ISO 4049. The samples were prepared and after setting they were transferred immediately to desiccators, where they were stored until an equilibrium weight was reached, they were then transferred to bottles containing water and the water uptake measurements were commenced with weights measured at specific time intervals up to 7 days (Beriat and Nalbant, 2009). This methodology was in agreement with various studies (Mortier *et al*., 2004; Cefaly *et al*., 2006; Gerdolle *et al*., 2008). Other studies did not follow the ISO

based standards and immersed the samples in solutions, or in a humid environment, following the setting time for the chemically cured materials, and irradiation for the light cured ones (Small *et al*., 1998; Mese *et al*., 2008; Percq *et al*., 2008). Articles have adopted the ISO 4049 technique for testing the water absorption of RMGICs since they contain a resin phase. They justify using this standard, which is designed for polymer-based materials since it is agreed internationally. However, this can be contradicted as water in RMGICs forms an essential part of the structure and removing the unbound water can alter the materials characteristics and thus the results will be biased.

As a conclusion, different methods were used in literature to test the water uptake of RMGIC following immersion in different solutions (water, water and ethanol, artificial saliva), or in a humid environment. Despite this, there was agreement in all literature that RMGICs absorbed water following setting, and this uptake was high compared to resin cements (Yap and Lee, 1997; Small *et al*., 1998; Mese *et al*., 2008). However, it was noted that different products responded differently in water uptake studies, as a result of varying HEMA percentages in different formulations and products (Yap and Lee, 1997). There was no conclusive evidence in the literature on the best method for conducting the experiment.

Considering the evidence in the literature regarding the method to be used to test the water uptake of RMGICs, in this project, it would be beneficial to test the materials following the ISO 4049 requirements, which includes desiccation of samples before immersion in solutions. However, an alternative water absorption method for polymeric materials, described by Stafford and Braden (1968) (samples immersed immediately after the setting time), will also be trialled. This would give an

indication of the differences in the results obtained and the best method to use for RMGICs.

2.3.2 Degree of conversion and working and setting times:

2.3.2.1 Introduction:

As a result of the incorporation of HEMA in GICs, in order to improve their mechanical properties, RMGICs cytotoxicity is still a controversial subject, but it is well established that it is higher than that of GICs (Lan *et al*., 2003). In RMGIC, both the acid-base reaction and polymerisation of monomers take place at the same time (Wilson and Prosser, 1982). Not all the monomers convert to polymer, thus residual unconverted monomers can leach out of the cement and into the oral environment thus reducing the materials biocompatibility (Costa *et al*., 2003; dos Santos *et al*., 2012). In contrast, a higher degree of conversion of the monomer to polymer may increase the cements shrinkage and improve the mechanical properties (Stansbury *et al*., 2005). Other studies have also shown that the mechanical, biological and physical properties of the RMGICs can be greatly affected by the degree of conversion of the resin component (Vande Vannet and Hanssens, 2007; Jonke *et al*., 2008). The degree of conversion of monomer to polymer is measured by calculating the percentage of carbon-carbon single bonds resulted from converted double bonds (C=C) in the vinyl group.

2.3.2.2 Methods used to identify the degree of conversion:

Degree of conversion is commonly characterised in resin composites as the percentage of carbon-carbon double bonds converted to single bonds following polymerisation (Anusavice *et al*., 2012). In resin composites, not all carbon double

bonds are converted to single bonds since, as the cross-linking progresses, the viscosity of the resin increases and limits access of radicals to the reactive groups (C=C groups) (Yoon *et al*., 2002). Although, it is favourable to increase the degree of conversion of materials in order to enhance their mechanical and biological properties (Du and Zheng, 2008), a high degree of conversion is less desirable due to the possibility of increasing polymerisation shrinkage and brittleness of the material (Stansbury *et al*., 2005).

Different spectroscopy techniques have been used to identify the degree of conversion for dental materials. These techniques include Fourier transform infrared spectroscopy (FT-IR) and Raman spectroscopy. Earlier techniques included halogenation of residual carbon double bonds (Scheerer *et al*., 1964), differential scanning calorimetry (DSC) (Antonucci and Toth, 1983) and differential thermal analysis (DTA) (Nicholson, 1998; Smith, 1998). These earlier techniques were valuable for identification of materials undergoing one reaction, but with materials like RMGIC, which undergo an acid-base reaction and a free-radical polymerisation at the same time, these techniques did not seem to be useful for the identification of each reaction. However, FT-IR and Raman were able to identify each type of reaction that was occurring (Kakaboura *et al*., 1996; Young *et al*., 2000). FT-IR is considered the most reliable, and straight forward technique to measure the monomer conversion of the resin material (Yoon *et al*., 2002).

The polymerisation process can be characterised by FT-IR as this technique is based on the absorption of radiation, of the molecular vibration in the infrared frequency range, of the functional groups in the polymer chain (Koenig, 1984).

Literature regarding the degree of conversion of resin composites measured the ratio of absorbance intensities of the aliphatic carbon–carbon double bond (C=C), at ~1638 cm^{-1}, and aromatic double bond (C=C) at ~1609 cm^{-1} (Ribeiro *et al*., 2012; Galvão *et al*., 2013; Abed *et al*., 2015). The literature concerning RMGIC focused on the carbon-carbon double bond at 1638 cm^{-1} and the C=O at 1720 cm^{-1} as a reference peak (Kim *et al*., 2015). However, another study showed that the peak at 1638 cm^{-1} could not be used to quantify the degree of conversion as the RMGIC formulation contains water, which absorbs at this wavenumber, thus making it difficult to determine the peak base at this point. Therefore, a different peak was used (at 1320 cm^{-1}) and, the degree of conversion results obtained using this peak, were in agreement with those obtained from Raman studies (Young *et al*., 2002; Young *et al*., 2004). Therefore, in this project, the method described by Young *et al*. (2002) was followed.

2.3.2.3 Methods for measuring working and setting times:

Handling properties of dental cements are one of the factors that can influence the clinician's choice of material. Working and setting times are very important characteristics for handling and ease of use of chairside materials (McCabe and Walls, 2013). RMGIC contains mixing of two components, either powder and liquid or two pastes, and the viscosity of the material increases following the initiation of the setting reaction, until it reaches a point where the material becomes very viscous and difficult to manipulate. This is defined as the working time of the material. The setting time is calculated from the start of mixing to the point the material reaches its final set stage, or reaches a point where the material has obtained adequate properties for its application (McCabe and Walls, 2013). Determination of working and setting

times for RMGIC, and dental materials in general, is highly important as the materials properties could be jeopardised if any manipulation is attempted beyond the working time (Ogawa *et al*., 2001).

Both the American Dental Associations (ADA) review on auto-cured GICs and ISO 9917-1:2007 (for measurement of GICs setting time) described the use of an indentor. A probe tip of known diameter and weight is used to determine the setting time, by measuring the ability of the probe to penetrate the surface of the material; the latter is placed in a chamber of at least 90% humidity at 37°C. According to this method, the setting time is 'the time elapsed between the end of mixing and the time when the needle fails to make a complete circular indentation in the cement'. This method is dependent on the weight and diameter of the probe. The result obtained is a measure of the time required for the material to reach a point when it can resist the stress generated from the probe, rather than the time for complete set of the cement. This method has limitations related to the operator; there is a requirement for a skilled and trained operator in order to obtain results with good reproducibility (in order to avoid variability) (Bovis *et al*., 1971; Ogawa *et al*., 2001).

Measurements of temperature rise, following the exothermic reaction of dental materials, is also used to identify working and setting times (McCabe and Walls, 2013). The temperature rise is measured using a calorimeter. The method described in ISO 4049 to measure the working and setting times also involves the measurement of temperature rise (using thermocouple) during setting. This may be helpful for resin cements as higher temperature rises are associated with these cements compared to GIC or RMGIC. However, this method does not provide actual

'dynamic' evaluation of the setting time, and thus it does not provide a good correlation with the clinical use of the material (Ogawa *et al*., 2001).

Another method used to identify working and setting times of dental materials is by the reciprocating rheometer. This device is mainly used with impression materials. It involves the measurement of reciprocating plate movements. This method demonstrated various problems amongst studies with minimal reproducibility between results and, the amount of materials placed between plates, is not clinically relevant (does not correlate to the amount used clinically) (Leirskar *et al*., 2003). Moreover, due to the movement between the two plates, makes this a problematic method to measure materials like RMGIC that set to a solid state (Bovis *et al*., 1971).

Another method involves the use of an oscillating rheometer, introduced and designed by Bovis *et al* (1971). Although this instrument does not give definite figures for the viscosity of the material, it gives a measurement for the setting and working times, by means of an increase in 'dynamic viscosity' of the material (Ogawa *et al*., 2001). This technique is a simple, reliable and quick method (Bovis *et al*., 1971) for measuring the working and setting times of materials that set at room temperature e.g. two paste resin composites and polycarboxylate cements etc... (Croll, 1998; Xie *et al*., 2004).

2.3.3 Methods for measuring polymerisation shrinkage:

Dimensional stability of dental cements is an important feature that can affect the longevity of the restoration. Shrinkage that occurs following application of the material can lead to marginal gaps and leakage, which could lead to secondary

caries, and could contribute to the failure of the restoration (Qvist, 1993). Hence, it is beneficial to ensure that the newly developed cements demonstrate similar, or more preferably lower, polymerisation shrinkage compared to the commercial cements.

Theoretically, since the monomers that are being studied for use in the novel cements (HPM and THFM), in this project, have higher molecular weights and higher molar volumes compared to HEMA, it can be assumed that they may demonstrate lower shrinkage values (Patel *et al*., 1987). The occurrence of polymerisation shrinkage is a result of the change in the molecular bonds (from the van-der Waals forces to covalent single bonds) and changes in the distances between atoms. Therefore, the larger the molecular volume of the monomer, the less amount of monomers are required to be converted for the same volume of material (Kim and Watts, 2004; Atai *et al*., 2005). Therefore the shrinkage of novel cements should be evaluated using a reliable and valid method, to ensure they do actually present lower or at least similar shrinkage behaviour compared to commercial materials.

Different approaches have been proposed to measure the shrinkage of dental cements (some including RMGICs), for example, linear shrinkage was measured using a light microscope (Munksgaard *et al*., 1987), densitometry (Patel *et al*., 1987) and dilatometry, either water-based (Lai and Johnson, 1993) or mercury-based (Mulder *et al*., 2013). Dilatometry was the most popular method for measuring shrinkage of dental materials amongst the other methods mentioned earlier. However, there were problems associated with this technique, since it is based on measuring the volume change of a liquid (water or mercury) in a reservoir and, factors that can affect this volume, can influence the results, such as i) a change in the ambient temperature can change the volume of the liquid, ii) any increase in the temperature of the material

tested (polymerisation exotherm) can also impact on the data recorded through thermal expansion or contraction of the liquid and, iii) environmental concerns and contamination associated with the mercury-based dilatometry (Kim and Watts, 2004; Lee *et al*., 2006). A different approach to measure the shrinkage of dental materials was used by Cook *et al*. (1999), who used a gas pycnometer, which measures the change in the volume of the specimen in a helium atmosphere (Cook *et al*., 1999). This method was deemed to be precise and more convenient to use, than water or mercury dilatometry, however, it only measures the total shrinkage of the specimen and does not give an overview of the shrinkage kinetics. It is also more suitable to be used with light activated cements where most of the shrinkage and cure occurs following light irradiation (Cook *et al*., 1999).

Another method (the bonded-disk method) has been developed and used to measure the shrinkage strain value and shrinkage kinetics of dental materials (including RMGICs; Bryant and Mahler, 2007). The bonded-disk method's main design and procedure was first mentioned by Walls *et al*. (1988) and Bausch *et al*. (1982), which was further developed by Watts and Cash (1991), and will be fully discussed in the materials and methods chapter. This method has the following advantages (Watts and Cash, 1991):

1. It can measure the total shrinkage and shrinkage kinetics of dental materials. Shrinkage occurs in the axial direction and this corresponds directly to volume shrinkage strain of the specimen.
2. It allows the use of samples with small thicknesses (e.g. 1mm), thus ensuring equal conversion on top and bottom surfaces and throughout the sample.

3. Shrinkage can be measured under controlled temperatures, either ambient or any specified temperature, through a temperature controlled metal plate.
4. The technique is straight forward and gives precise measurements and reliable results.

It can also be used to measure the change in temperature (exotherm, described subsequently) of a sample while setting, in degree Celsius (°C), simultaneously while measuring the shrinkage strain of it. This part of the equipment includes a K type thermocouple that is inserted in the centre of the sample and connected to an output voltage, which is also connected to a digital converter and data acquisition software (Picolog software). This method is deemed to be reliable and relatively easy to use (Alnazzawi and Watts, 2012). The bonded-disk method will be used in this thesis to measure the shrinkage strain of commercial, home and novel RMGICs.

2.3.4 Methods for measuring polymerisation exotherm:

Various biological aspects should be taken into consideration during the clinical procedure. One of the main aspects is the increase in temperature, which can be a result of the cavity preparation, and this can be controlled by the clinician through following good clinical practice guides. The other feature is related to the dental material's property, its polymerisation exotherm during setting (Zach and Cohen, 1965).

Different methods for measuring the polymerisation exotherm of materials has been reported in the literature, for example, the use of thermocouples (Kanchanavasita *et al*., 1996; Hofmann *et al*., 2002; Kim and Watts, 2004), a differential scanning calorimeter (DSC) (McCabe and Wilson, 1980; Antonucci and Toth, 1983),

differential thermal analyser (DTA) (Lloyd, 1984; Adamson *et al*., 1988) and infrared thermography (Hussey *et al*., 1995).

All the methods mentioned above demonstrated reliable information regarding the polymerisation exotherm of dental cements. Moreover, the infrared thermography scanner technique used by Hussey *et al*. (1995) was able to measure the polymerisation exotherm *in vivo*, by using sensors that were sensitive to the wavelength emitted from the surface of the specimen, which could then be digitized in the system controller. However, the equipment used in their technique was expensive and, the authors specify that the sensor should be very sensitive in order to record the small wavelengths emitted from the sample (Hussey *et al*., 1995).

2.3.5 Methods for measuring monomer release:

Luting cements undergo polymerisation, which can be activated chemically, by light, or both. During this process, with cements that contain monomers (e.g. resin composites and RMGICs), the latter result in polymers through conversion of the double bonds (C=C) to single bonds, and crosslinking with other monomers to form a crosslinked matrix. Theoretically, all monomers should be converted to polymers, but this is not the case in all dental cements, and conversion ranges between 50-75%. Therefore some unconverted monomers will leach out from the cement matrix and into the oral environment (Ferracane, 1994). A low degree of conversion can negatively affect the mechanical properties and biocompatibility of dental cements (Geurtsen *et al*., 1998). Since commercial RMGICs contain mainly HEMA as a monomer, different studies reported a measurable amount of this monomer released in solutions (Hamid *et al*., 1998; Palmer *et al*., 1999). As previously discussed in 2.2.1, unconverted HEMA can diffuse through dentine, to the pulpal tissue, or the

oral mucosa, and then it could cause cytotoxic reactions. It should be noted that one of the aims of this study is to replace the HEMA in RMGICs with monomers that are known to be more biocompatible than HEMA. But, it is still necessary to measure the quantified amount of released monomers to ensure that the new cements demonstrate lower monomer release, and moreover to correlate the results with other properties (e.g. solubility, cytotoxicity and mechanical properties).

FT-IR can be used to measure the monomers released from RMGICs, but it is not possible to quantify the amount of each monomer released, as the spectrum obtained does not give information on the specific molecules (Van Landuyt *et al*., 2011). FT-IR was used in this study to measure the degree of conversion.

High performance liquid chromatography (HPLC) is a sophisticated method that can be used to quantify and analyse the monomers released from each cement following immersion in solutions. HPLC includes liquid chromatography (LC), gas chromatography (GC) (in which the component under analysis should be compared with the known amount of standard of the same compound) and mass spectrometer (MS); the latter identifies the molecular weight of each component that is released. This can then be verified using lab database spectra of known compounds. According to the literature, HPLC and GC are mostly used to quantify released monomers compared to FT-IR (Van Landuyt *et al*., 2011). GC can be used for compounds that generally have low molecular weights, that are stable at high temperatures and can be vaporised (Rogalewicz *et al*., 2006). LC can be used for high molecular weight monomers (Michelsen *et al*., 2008). MS can be combined with LC or GC to give the exact composition of materials, but it is more expensive, as it requires the use of more sophisticated and expensive equipment; hence it was

used where identification is required rather than quantification of known elements (Van Landuyt *et al*., 2011).

HPLC was the method of choice in most of the literatures for the quantification and analysis of released monomers from resin cements and RMGICs (Van Landuyt *et al*., 2011), and the method of choice in this study.

2.3.6 Methods for measuring mechanical properties:

Luting cements, in the oral environment, undergo different masticatory stresses. Therefore, they should be 'stable' and able to sustain adequate mechanical properties while they transfer the stresses from the crown or bridges to the teeth (Li and White, 1999). RMGICs were developed in order to overcome the limitations associated with GICs (e.g. early sensitivity to moisture, brittle fracture, strength and wear) while maintaining their fluoride releasing property (E *et al*., 2010). It is well documented that RMGICs possess improved mechanical properties compared to GICs through the addition of the resin matrix to the organic salt matrix of the GICs (McCabe, 1998; Irie and Suzuki, 2000). Therefore, it was essential to test the mechanical properties of newly developed cements and compare these with commercial and home materials to ensure adequate mechanical properties and strength are maintained.

Different *in vitro* tests were proposed as an indication for the clinical performance and strength of RMGICs. However, according to Li *et al*. (2015), compressive fracture strength (CFS) and three point flexure strength (TFS) remain the most clinically relevant tests to determine the strength of these materials (Li *et al*., 2015). Despite this, there was no testing methodology advocated for RMGIC luting

cements, in the published literature; testing was usually performed following the recommended ISO 9917-1:2010 for GICs (CFS) (Huget, 1998; Nicholson *et al*., 2001; Piwowarczyk and Lauer, 2003; Aratani *et al*., 2005; E *et al*., 2010; Jefferies *et al*., 2013; Kanie *et al*., 2013; Li *et al*., 2015; Patil *et al*., 2015) and, ISO 4049, recommended for resin cements and ISO 9917-2 for RMGICs (TFS) (Attar *et al*., 2003; Piwowarczyk and Lauer, 2003; Behr *et al*., 2008; Saskalauskaite *et al*., 2008; Irie *et al*., 2010; Nakamura *et al*., 2010; Li *et al*., 2015).

In this study, mechanical properties were determined following measurement of CFS, compressive modulus (CM), TFS and three-point flexure modulus (TFM) for commercial, home and novel materials.

2.3.6.1 Compressive fracture strength (CFS):

It is essential to test the compressive strength of dental materials especially the brittle ones, since most of the mastication forces in the oral environment tend to be compressive forces (Powers and Sakaguchi, 2006).

The sample under compressive test is subjected to an axial force, applied along one direction, and results in decreasing the sample's length (Powers and Sakaguchi, 2006) (Figure 2.7).

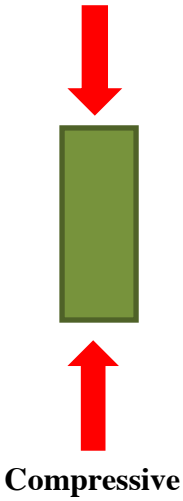

Figure 2.7 Force direction in samples undergoing compressive stress.

ISO 9917-1:2010 standard focuses on examining water-based cements (e.g. GICs) and includes CFS testing, as a strength indicator for these materials. According to ISO 9917-1:2010, the sample under test should have a maximum length: diameter ratio of 2:1, and any increase in this ratio will result in bending of the specimen during the test (Powers and Sakaguchi, 2006). The exact length and diameter, as specified by the ISO standard, is 6 and 4 mm respectively, and it is measured as load to failure per surface area (discussed further in the Materials and Methods section).

Various articles addressed the importance of using the exact powder: liquid ratio that is recommended by the RMGIC's manufacturers, and it was confirmed that any variation in this ratio will affect the material's compressive strength (Aratani *et al*., 2005; E *et al*., 2010). It was reported that using the provided scoops and droppers supplied with the cement, for the measurement of powder: liquid ratio, similar to what would usually happen on the dental clinic, resulted in variations in this ratio (Billington *et al*., 1990; Fleming *et al*., 1999). Therefore, powder and liquid used in

the current study were weighed before mixing to ensure incorporating the exact recommended powder: liquid ratio.

Various articles, after following the ISO 9917-1:2010, compared the compressive strength alone, or with other strength tests, as an indicator of the material's mechanical properties. However, different sample sizes (number of samples) were used in various studies, and the minimum sample size was that recommended in the ISO standard (n=5), according to McCabe and Carrick (1986), a minimum of 20 samples are required to show a significant difference between CFS of brittle materials (McCabe and Carrick, 1986). This sample size was determined using power law statistics (95% power level) where standard deviations were assumed to be similar between groups, and differences between groups were equal to or less than 15% (Fleming *et al*., 2012).

2.3.6.2 Compressive modulus (CM):

Following CFS test, a stress-strain curve can be generated which determines the characteristics of the sample undergoing compressive testing and, it is used to calculate the CM value, as stress divided by strain in the initial linear region of the curve (elastic region) (Wang *et al*., 2003) (described further in the Materials and Methods chapter).

CM is considered as an intrinsic material's property that is not affected by sample's dimensions (Dowling and Fleming, 2008). Despite the importance of CM as an intrinsic mechanical property, most of the literature that evaluated the CFS of RMGICs did not report CM of the same material under investigation.

2.3.6.3 Three point flexure strength (TFS):

Flexure strength of a material is its ability to withstand bending before it breaks (Anusavice, 1993). In a clinical situation, the luting cement should demonstrate an appropriate TFS in order to withstand the biting forces that transfer between the cemented crown or bridge and the tooth tissue without ‘’breaking’’ (Sunico-Segarra and Segarra, 2014).

According to ISO 4049:2009 and ISO 9917-2:2010, the TFS test consists of a rectangular sample measuring (25mm length, 2mm thickness, 2mm width), resting on two supports at each end, with a centrally concentrated load (Figure 2.8 – described further in Materials and Methods chapter).

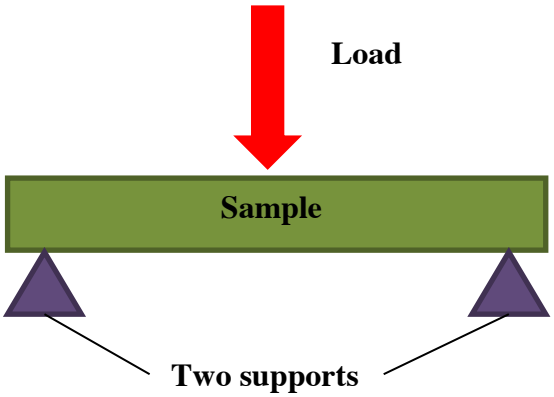

Figure 2.8 Schematic drawing for three point tests (TFS) showing the force direction and the two supports.

Some factors that usually affect the TFS test results include, i) thickness of the sample, or the distance between the two supports, ii) the curing technique. The literature reports that light or dual cured materials performed better than chemically cured ones in the TFS test (Attar *et al*., 2003; Li *et al*., 2015),

2.3.6.4 Tensile flexural modulus (TFM):

A load/deflection curve is generated following TFS test for each sample, which is then used to calculate the TFM, using a specific equation that takes into account the change in load, change in deflection, the distance between the two supports, thickness and width at the centre of each sample. Similar to CM, TFM is considered as an intrinsic material property that can give a good understanding of the physical or mechanical properties of a material, regardless of the specimen's size (Dowling and Fleming, 2008). Although not all researchers calculated TFM, while studying the TFS of RMGICs, various articles reported both (Momoi *et al*., 1995; Attin *et al*., 1996; Irie and Nakai, 1998; Cattani-Lorente *et al*., 1999; Attar *et al*., 2003; Ilie and Hickel, 2007; Nakamura *et al*., 2010; Pameijer *et al*., 2015)

2.3.7 Methods for measuring biocompatibility:

Biocompatibility is one of the main considerations of dental cements in clinical practice, since a cytotoxic material may cause allergic and/or toxic reactions when it comes into contact with the oral soft tissue (e.g. periodontium). Moreover the cytotoxic compound could diffuse through dentinal tubules and cause a cytotoxic reaction in the pulpal tissues (Geurtsen, 2000; Schmid-Schwap *et al*., 2009). Dental resins are considered the main cause of allergic reactions. They can be classified into i) local reaction, and ii) systemic reaction in dental technicians and 12% of dental patients, according to a national survey in the UK that addressed the adverse reactions of dental materials (Scott *et al*., 2004). GICs are considered as biocompatible materials, whereas the biocompatibility of RMGICs is questionable (Stanislawski *et al*., 1999), due to the addition of HEMA to the conventional composition of GICs. HEMA poses a cytotoxic effect as described earlier (in section

2.2.1). Therefore, one of the objectives of this study was to replace HEMA with other monomers that are known to have better biocompatibility. In order to demonstrate this, an appropriate method should be used for the assessment of cytotoxicity of all materials.

Compared to *in vivo* and animal studies, *in vitro* studies offer the advantage of complete control over the experiment variables that sometimes cannot be managed in vivo; they are less expensive and do not possess ethical difficulties compared to animal testing (Schmalz, 1994). Local adverse reactions of dental materials can be classified into two categories, i) mucosal reactions, where the material comes into contact with the oral mucosa (e.g. luting cements and restorative materials), and ii) pulpal reactions, where components leached out of the material travel through the dentinal tubules to the pulpal tissues (Moharamzadeh *et al*., 2009).

Different cells and tests have been used to evaluate the biocompatibility and cytotoxicity of dental materials [References included in Table 2.1(a and b)]. Electronic database have been searched for evidence on the method to be used to test the biocompatibility and cytotoxicity of RMGICs (luting, restorative or lining material). The terms used were: (Cytotoxicity OR biocompatibility) AND (resin modified glass ionomer OR hybrid glass ionomer OR RMGIC OR resin glass ionomer). The search identified 148 articles, which were screened through to check if they could be included. The criteria for inclusion were: *in vitro* study that included testing of RMGICs for cytotoxicity or biocompatibility. These studies are summarised in Tables 2.1(a and b), including the study authors, cells used and the biological endpoint. Table 2.1b is a continuation of Table 2.1a.

Table 2.2a In vitro studies on the biocompatibility and cytotoxicity of RMGICs including the cells used and the biological endpoints.

Study	Cells	Biological end point
(Valanezhad *et al*., 2016)	Osteogenic cell line	MTT assay
(da Fonseca Roberti Garcia *et al*., 2015)	Immortalized odontoblast-like MDPC-23 cells, obtained from rats' dental papillae and human dental pulp cells	[(3-(4,5-dmethylthiazol-2-yl)-2,5-diphenyltetrazolium bromide] MTT assay
(Mohd Zainal Abidin *et al*., 2015)	Stem cells from human exfoliated deciduous teeth (SHED).	MTT assay
(Trumpaite-Vanagiene *et al*., 2015)	Human gingival fibroblast	MTT assay
(Pontes *et al*., 2014)	Odontoblast-like MDPC-23 cells or human dental pulp cells (HDPCs)	MTT assay
(Wanachottrakul *et al*., 2014)	Normal human pulp tissues	MTT assay, flow cytometry and Von Kossa staining
(Botsali *et al*., 2014)	L929 fibroblast cells	MTT assay
(Rodriguez *et al*., 2013)	Human gingival fibroblasts	Phase contrast microscopy, lactate dehydrogenase (LDH) release, and quantitative x-ray microanalysis (EPXMA)
(Selimovic-Dragas *et al*., 2013)	UMR-106 osteoblast cell-line and NIH3T3 mouse fibroblast cell line	MTT assay
(de Castilho *et al*., 2013)	Immortalized cells of an odontoblast-like cell line (MDPC-23)	MTT assay and analysis of cell morphology by scanning electron microscopy
(dos Santos *et al*., 2012)	Fibroblastic L929 cells	Modification of the dye-uptake technique
(de Castilho *et al*., 2012)	MDPC-23 odontoblast-like cells	MTT assay and SEM evaluation
(Mendonça *et al*., 2012)	MDPC-23 odontoblast-like cells	MTT assay
(Malkoc *et al*., 2010)	L929 cells	MTT assay
(Imazato *et al*., 2010)	pluripotent mesenchymal precursor cell line	alkaline phosphatase (ALP) activity
(Hebling *et al*., 2009)	Pulp cells	MTT assay and SEM evaluation

Table 2.2b In vitro studies on the biocompatibility and cytotoxicity of RMGICs including the cells used and the biological endpoints.

Study	Cells	Biological end point
(Schmid-Schwap *et al*., 2009)	L929-fibroblast	Flow cytometry
(Bakopoulou *et al*., 2009)	Normal cultured human lymphocytes	Sister chromatid exchange SCE assay, Chromosomal aberrations (CAs) assay and Assessment of proliferation rate index (PRI)
(Milhem *et al*., 2008)	Brine Shrimp Larvae	Brine Shrimp Larvae Assay
(Melo de Mendonça *et al*., 2007)	odontoblastlike cells MDPC-23	MTT assay
(Aranha *et al*., 2006)	Immortalized odontoblast-cell line	Cell metabolism (MTT assay) and cell morphology
(Souza *et al*., 2006)	MDPC-23 cells	MTT assay
(Uzzaman *et al*., 2005)	Monkey teeth	Hematoxylin and Eosin staining or Brown and Brenn gram stain
(Galler *et al*., 2005)	Three-dimensional cultures of pulp-derived cells	MTT assay
(Lan *et al*., 2003)	Pulp cells	MTT assay
(Lonnroth and Dahl, 2003)	Mouse fibroblasts (L-929)	(MTT) and neutral red (NR)
(Huang and Chang, 2002)	Human pulp cells	MTT assay
(Chen *et al*., 2002)	Deciduous teeth pulpal fibroblasts	MTT assay
(Huang *et al*., 2002)	Human-gingival fibroblast	MTT assay
(do Nascimento *et al*., 2000)	Normal human teeth	Hematoxylin and eosin, Masson's trichrome, or Brown and Brenn technique for bacterial observation
(Kan *et al*., 1997)	3T3 mouse fibroblasts	MTT assay
(Gaintantzopoulou *et al*., 1994)	Dog teeth	Hematoxylin and eosin staining

As can be seen from Table 2.1(a and b), the biological system used to test the biocompatibility of RMGICs varied between studies. Some studies tested the biocompatibility of RMGICs on the pulp tissues, using odontoblasts cells, since they are the first cells that dental materials will come into contact with following leaching out of the dentinal tubules. The tests also included measuring the reaction of materials on fibroblasts, which represents mucosal toxicity assessment. The cells were either human or mouse tissues, and although mouse tissues can be easily obtained and can grow fast, human cells are deemed to be more clinically relevant for testing toxicity of dental materials (Moharamzadeh *et al*., 2009; Sun *et al*., 2011). Human fibroblasts are more favourable for testing since they can be easily obtained from patients, and moreover, they grow faster in culture medium (Moharamzadeh *et al*., 2009). These cells are the cells of choice for the cytotoxicity testing of commercial, home and novel RMGICs in this study.

The biological endpoint of toxicity testing on mucosal tissues can be assessed by measuring the metabolic rate and proliferation status of the cells exposed to dental materials. Various assays were used in literature to measure cells viability, including MTT assay, alamar blue assay, neutral red assay, propidium iodide assay, lactate dehydrogenase (LDH) assay, bromodeoxyuridine incorporation assay, 3H-thymidine incorporation assay, DNA content measurement and protein content measurement (Moharamzadeh *et al*., 2009). Other assays were able to measure the cells function and include the inflammatory mediators measurement, that measures the amount of pro-inflammation mediator in test's supernatant, following exposure to resin materials, Glutathione determination, Heat-Shock Protein and Apoptosis assays (Moharamzadeh *et al*., 2009). Although all mentioned tests provide a valid method

for the determination of cytotoxicity of dental materials, the MTT assay provides rapid results and it is a less expensive assay compared to other assays; it is considered as a sensitive test that has been widely used to measure the cytotoxicity of RMGICs (Table 2.1; it was the assay chosen in this study). This colorimetric assay, developed by Mossman (1983), is based on the measurement of cell viability through assessing mitochondrial dehydrogenase activities. In the viable cells, the methylthiazole tetrazolium is converted to a purple formazan, which can be solubilised using dimethyl sulphoxide (DMSO) and the concentration of the colour is then measured spectrophotometrically. This assay is not expensive, fast and reliable (Mosmann, 1983).

After perusal of the literature it is clear that although RMGICs have many advantages, they do have limitations. Furthermore, after reviewing the methods that have been used for carrying out physical, mechanical or biological testing, there appears to be no ISO standards for RMGICs; researchers have used ISO methods described for GICs or resin cements, which are not appropriate. Therefore, in this project some of the limitations of RMGICs have been addressed, as well as the identification of suitable methods for carrying out some of the testing.

3 AIMS AND OBJECTIVES

3.1 *Aims:*

The aims of this project can be summarised as follows:

1. To develop novel RMGICs, with lower water uptake and dimensional changes compared to commercial products, by fully or partially replacing the monomer HEMA with different percentages of HPM and/or THFM,
2. To find an appropriate method for measuring the water uptake of RMGICs by comparing the ISO 4049:2009 (that includes desiccation of samples before commencing the water uptake) with a method that does not require desiccation of samples. (Currently there is no standard method for measuring the water uptake of RMGICs).
3. To compare the biocompatibility (via cell viability studies) of commercial RMGICs with the novel cements.

3.2 *Objectives:*

The specific objectives of this project were as follows:

1. To develop two control liquids, based on Fuji Plus (FP, GC Corporation, Tokyo, Japan) and RelyX Luting (RX, 3M ESPE, St Paul, MN, USA) formulations where the powder will be kept the same as the commercial counterpart. The formulation and identification of commercial liquids will be performed using FT-IR and pilot studies will be conducted to ensure suitability and similarity of the control liquids compared to commercial materials.

2. To investigate and compare the water uptake, desorption, solubility, diffusion coefficients and dimensional changes of commercial and home RMGICs in DW and AS following two methods: modified ISO 4049:2009 and the method without desiccation, in order to choose the most efficient method for testing the uptake of the novel cements.
3. To develop and analyse different liquid compositions where HEMA is replaced partially, or fully, with different percentages of THFM and/or HPM.
4. To select a range of novel liquid compositions from the above objective, based on each of the commercial materials (Fuji Plus or RelyX Luting). The novel materials will consist of the same corresponding powders while replacing HEMA (partially or fully) in the liquid composition with THFM, HPM and various ratios of THFM/HPM. The selection criteria were that the liquids did not phase separate and that they formed a cement with acceptable handling characteristics resembling the commercial materials.
5. To study the water uptake, desorption, diffusion coefficients, solubility and dimensional changes of the novel cements, in DW and AS, using the selected method, and compare the results with commercial and home materials.
6. To analyse the composition and setting reactions (acid-base and monomer polymerisation) for all RMGICs (commercial, home and novel) using FT-IR, and moreover to measure and compare the degree of monomer(s) conversion.

7. To investigate and compare the handling properties (working and setting times) of RMGICs (commercial, home and novel), and to confirm the clinical suitability of the novel cements.
8. To determine the polymerisation shrinkage and exotherm simultaneously for all materials (commercial, home and novel), using the bonded-disk method, at 23°C and 37°C.
9. To develop two new HPLC methods for the identification and quantification of residuals (e.g. monomers released; individual and cumulative) from all materials immersed in DW, AS and 75:25% ethanol:DW.
10. To determine and compare the compressive fracture strength (CFS) following ISO 9917-1:2003, and three-point flexure strength (TFS) following ISO 4049:2009, between all materials. Compressive modulus (CM) and tensile flexural modulus (TFM) will also be calculated for all materials (commercial, home and novel) to ensure that replacement of HEMA did not jeopardise the materials mechanical properties and strength.
11. To study the cytotoxicity of RMGICs (commercial, home and novel) *in vitro* on fibroblasts, and to highlight improvements in biocompatibility of THFM cements (THFM is known to be biocompatible) compared to those with 100% HEMA.

The above studies and investigations will highlight the various properties of novel RMGICs in relation to commercial and home materials, which will then be useful in determining the effectiveness of the new developed systems. The way forward for meriting further research and investigations prior to commercialisation will be based on the promising results attained for the novel cements.

4 MATERIALS AND METHODS

4.1 *Introduction:*

This study investigates the effect of incorporating novel monomers in RMGICs in order to improve their physico-mechanical properties, for example decrease the water uptake, and swelling compared to commercial products. In order to carry out such investigations, it is essential to know the exact components of the RMGICs, so that the resulting properties could be argued critically with respect to the incorporated ingredients. However, it proved difficult to find out the exact compositions of commercial RMGICs, since manufacturers do not supply such information in detail. Therefore, two controls were used in this study, one being the commercial material itself, and the other being the home-made control, where the powder was kept the same (commercial), the liquid was made in-house with a known concentration of each component. The components used were the same as those listed in the MSDS for the commercial liquids.

4.2 *Materials:*

4.2.1 Commercial and home-made materials compositions:

Two commercial chemically cured resin modified glass-ionomer cements (RMGICs) were included in this study, namely Fuji Plus (FP, GC Corporation, Tokyo, Japan) and RelyX Luting (RX, 3M ESPE, St Paul, MN, USA). The two cements were supplied as separate powder and liquid components. The manufacturer of RelyX Luting recommended a powder: liquid mixing ratio of 1.6:1 g:g, while for Fuji Plus the manufacturer's recommended powder: liquid mixing ratio was 2:1 g:g (Table 4.1). The powder in both cements contained a fluoroalumino silicate glass. The liquid in the two materials consisted mainly of water, poly(acrylic acid), 2-hydroxyethyl methacrylate (HEMA) and tartaric acid as detailed in Table 4.1,

according to the manufacturers material safety data sheet (MSDS). Although, not mentioned in the latter, the powder additionally contains a redox system consisting of potassium persulfate and ascorbic acid, for initiating polymerisation chemically. The components and amounts of the two commercial materials investigated with their corresponding CAS number and manufacturers recommended powder: liquid mixing ratios are presented in Table 4.1.

Table 4.1 The components and amounts of the two commercial materials investigated with their corresponding CAS number and manufacturers recommended powder: liquid mixing ratio.

RMGIC	Composition	CAS	% by weight	Mixing ratio (g)
***FP powder**	Fluoroalumino-silicate glass	Not listed	95-100	2
FP liquid	Distilled water	7732-18-5	20-30	1
	Poly(acrylic acid)	9003-01-4	20-30	
	HEMA	868-77-9	25-35	
	Urethanedimethacrylate (UDMA)	72869-86-4	<10	
	Tartaric acid	87-69-4	5-7	
***RX powder**	Fluoroalumino-silicate glass	Not listed	>98	1.6
	Potassium persulfate	7727-21-1	≤0.2	
RX liquid	Water	7732-18-5	30-40	1
	Copolymer of acrylic and itaconic acids	25948-33-8	30-40	
	HEMA	868-77-9	25-35	
	Ethyl acetate	141-78-6	<2	
	Tartaric acid	Not listed	Not listed	

*Note both powders contain a redox system to initiate polymerisation chemically.

Two additional control (home) liquids were prepared in-house, based on the manufacturer's material safety data sheets. The liquids were prepared in plastic polypropylene amber bottles, which were washed with 10% hydrochloric acid (HCl), rinsed three times with deionised water (DW) and dried with acetone prior to use, to ensure complete evaporation of the water used during washing. Since it was not possible to determine the exact amounts of each product from the manufacturer, different percentages were tried and tested to match the commercial liquids. For the RX group, the acid used was poly(acrylic acid) instead of a copolymer of acrylic and itaconic acids, in order to match the FP group compositions, so that the only difference between the home and novel liquids was the replacement of the monomer HEMA in the two groups. Home liquids were formulated and characterised using Fourier Transform Infrared Spectroscopy (FTIR) and compared with the corresponding commercial liquid formulations; this will be fully discussed in section 5.4.1.

The final compositions of home liquids are presented in Table 4.2. All components were weighed on an electronic balance accurate to 0.0001 g (Explorer, Ohaus Europe GmbH, Nänikon, Switzerland). The liquid was stirred using a magnetic stirrer at room temperature (22 ± 1°C) at 200 rpm (revolutions per minute), for 2 hours. Commercial and homemade liquids were stored in a fridge at 4-6°C.

Table 4.2 Home liquid components and amounts with their corresponding CAS number.

RMGIC	Composition	CAS	%
FP in-house liquid	Distilled water	7732-18-5	30
	Poly(acrylic acid)	9003-01-4	30
	HEMA	868-77-9	31
	Urethanedimethacrylate (UDMA)	72869-86-4	4
	Tartaric acid	87-69-4	5
RX in-house liquid	Water	7732-18-5	35
	Poly (acrylic acid)	9003-01-4	30
	HEMA	868-77-9	29
	Ethyl acetate	141-78-6	1
	Tartaric acid	87-69-4	5

4.2.2 Novel RMGIC liquid compositions:

The procedure mentioned in 4.2.1 was followed to prepare the plastic bottles prior to formulating the liquids. The commercial materials compositions, described in Table 4.1, were used as a guide to produce new formulations, in order to correlate the differences in properties to the change in monomers. The two novel liquids contained two new monomers tetrahydrofurfuryl methacrylate (THFM) and hydroxypropyl methacryate (HPM).

All components required to produce the novel liquids are presented in Tables 4.3 and 4.4, and were supplied by Sigma-Aldrich, St Louis, Missouri, USA. A pilot study was initially conducted where twenty-four liquid compositions based on both

commercial materials were initially screened (Appendix 1). HEMA in commercial materials was replaced with different percentages of HPM and THFM, either completely, when using HPM as a replacement, or in part with THFM. When THFM, as a hydrophobic monomer, replaced HEMA completely, it showed phase separation when mixed with water. Thus there was a need for the THFM to be combined with either HPM or HEMA to avoid this separation. Sixteen compositions showed phase separation during liquid preparations and so these were excluded from both RX and FP groups, but are presented in Appendix 1. Furthermore, as shown in Appendix 1, formulations containing 5% UDMA in FP group formulations also exhibited phase separation, with most of the compositions tested, and so it was necessary to decrease the percentage of this monomer. 4% UDMA was the highest amount that could be added to the RMGIC liquid composition without causing phase separation.

Eight liquid formulations were selected and prepared for further studies, four based on each of the commercial products (RX, FP), where HEMA was replaced with either 100% HPM, 70%/30% HPM/THFM, 50%/50% THFM/HEMA and 30%/70% THFM/HEMA (Tables 4.3 and 4.4).

Table 4.3 FP based novel liquid compositions with the percentage (by weight) of each component.

Components	F1%	F2%	F3%	F4%
Distilled water	30	30	30	30
Poly(acrylic acid)	30	30	30	30
HPM	31	21.7	0	0
THFM	0	9.3	15.5	9.3
HEMA	0	0	15.5	21.7
Urethanedimethacrylate (UDMA)	4	4	4	4
Tartaric acid	5	5	5	5

Table 4.4 RX based novel liquid compositions with the percentage (by weight) of each component.

Components	R1%	R2%	R3%	R4%
Water	35	35	35	35
Poly(acrylic acid)	30	30	30	30
HPM	29	20.3	0	0
THFM	0	8.7	14.5	8.7
HEMA	0	0	14.5	20.3
Ethyl acetate	1	1	1	1
Tartaric acid	5	5	5	5

Note that through the rest of this project labelling of materials will be as follows:

FP and RX = commercial materials, Fuji Plus and RelyX Luting, respectively.

FP home and RX home = home made liquids with commercial powders.

F1, F2, F3 and F4 = novel materials where the liquid was prepared according to Fuji Plus formulation and mixed with the corresponding commercial powder.

R1, R2, R3 and R4 = novel materials where the liquid was prepared according to RelyX Luting formulation and mixed with the corresponding commercial powder.

4.2.3 Immersion media:

DW and artificial saliva (AS) were used as immersion media respectively in the water uptake studies. AS was Orthana Saliva supplied by A.S. Pharma Ltd., UK. Its components are given in Table 4.5. This AS is commonly used to treat dry mouth patients. DW and 75:25% ethanol:DW were used as immersion media in the HPLC experiment.

Table 4.5 AS (Orthana) components and their amount as acquired from the manufacturer's MSDS.

Each 50 mL of AS solutions contains:	
Component	**Amount**
Mucin Gastric	1.75g
Xylitol	1.0g
Methyl Parahydroxybenzoate	50mg
E.D.T.A.-disodium	25mg
Peppermint oil	2.5mg
Spearmint oil	2.5mg
Benzalkonium chloride	1.0mg
Potassium fluoride	0.21mg

4.2.4 HPLC solvents:

Acetonitrile (AC), HPLC grade (Merck Millipore, MA, USA) and DW were used as solvents in the HPLC study.

4.3 *Methods:*

4.3.1 Sample preparation for water uptake/desorption experiment:

Twelve discs were prepared for each material, six discs for immersion in DW and six in AS. Mixing and preparing the materials was performed according to the manufacturer's instructions and the recommended powder: liquid ratio by weight (2:1 g:g for Fuji Plus and Fuji Plus novel compositions group, 1.6:1 g:g for RelyX Luting and RelyX Luting novel compositions group) (Table 4.1). The powder used with all the liquids were the corresponding commercial powders for each group. The powder was weighed on a balance (model SI-403, Denver Instrument, Colorado,

USA) and the liquid was weighed on a glass slab using the same balance, which was accurate to 0.001 g. The components were mixed on the glass slab with a stainless-steel spatula at room temperature (23 ± 1°C) by dividing the powder into approximately two halves. The first half was mixed with the whole liquid for 20 seconds before incorporating the rest of the powder into the mix and mixing for an additional 20 seconds, to a total mixing time of 40 seconds. Two discs were prepared at a time using polytetrafluoroethylene (PTFE) moulds with internal dimensions of 16 mm ± 0.1 mm in diameter and 1.0 ± 0.1 mm depth (Figure 4.1). The moulds were placed on a glass microscope slide covered with an acetate sheet and were slightly over filled with the mixed material; another acetate sheet and glass microscope slide was placed on top of the material while applying hand pressure to remove excess cement (Figure 4.1). This assembly was clamped together with a bulldog clip in order to secure the mould/samples and to eliminate entrapment of air bubbles; note the acetate sheets were in close contact with the sample from both sides. 2g of powder and 1g of liquid of FP were required to fabricate two discs compared to 1.6g powder and 1g liquid of RelyX Luting.

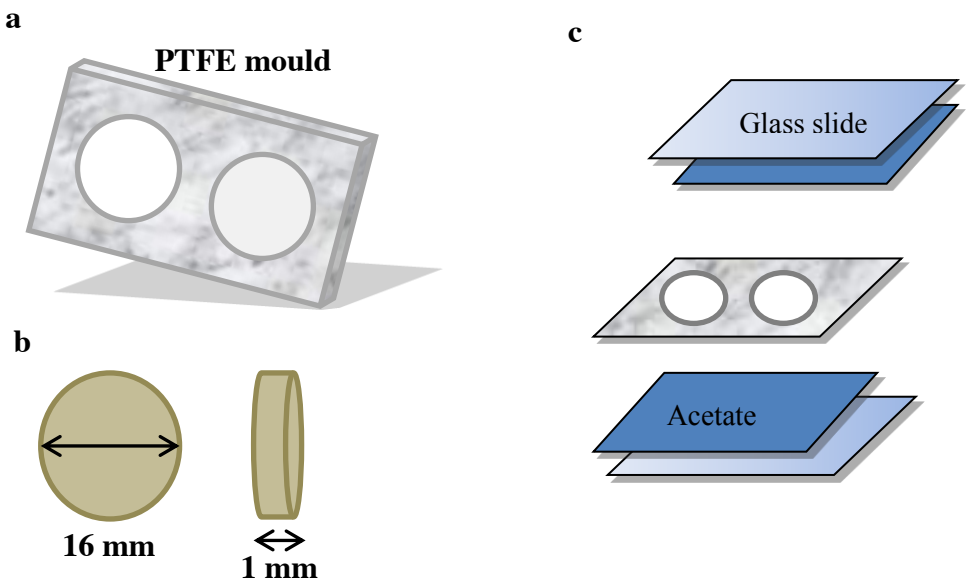

Figure 4.1 Schematic drawing of a: PTFE mould, b: the specimens dimension, c: The whole assembly used to fabricate the specimens.

Samples were left to set in an incubator (Carbolite, Camlab, Cambridge, UK) at 37±1°C for 60 minutes. Pilot studies were conducted in order to find the best storage method to store the samples for the first hour after mixing and before commencing the water-uptake experiment. This included i) allowing the samples to set, then de-moulding and storing them in sealed bags with wet filter paper, in order to maintain humid conditions during the setting of the sample, ii) keeping the discs between the glass slides/acetate sheets in the oven, iii) applying varnish or petroleum jelly (Vaseline) to the surfaces of the discs and leave to set in the oven for 60 minutes, the latter in order to mimic the clinical situation where the material is covered with varnish or petroleum jelly. The lowest change in weight was observed for the method that included applying petroleum jelly, but there were difficulties in removing the petroleum jelly from the sample surfaces before putting in water; this also caused problems during the water uptake experiment with high variations in the uptake

values for samples within the same group. As a result of this, method ii) was followed where samples were left to set in an incubator at 37±1°C for 60 minutes without de-moulding, to protect them from water evaporation; this was deemed to be the second best method for storage compared with Vaseline coverage. Following removal from the incubator and moulds, each specimen was examined with the naked eye under ambient light to check for internal porosities or defects. Samples were processed as quickly as possible (~30 seconds, to avoid dehydration) by hand-lapping using dry silicon carbide abrasive paper P600 (Buehler, IL, USA), to remove any irregularities on the periphery of each disc and the debris was blown away with a dust blower. Any samples with porosities or imperfections were discarded.

4.3.2 Water Uptake/desorption, dimensional change, solubility and diffusion coefficient experiment:

Two methods were used for the water uptake and desorption experiments. One method followed ISO 4049:2009 used for resin cements, which included desiccation of samples before immersion in solutions, and the other method did not include desiccation, but is a well-established method developed in the department by Stafford and Braden (1968).

4.3.2.1 Water uptake, desorption, solubility, diffusion coefficient and dimensional change experiment following modified ISO 4049:2009:

Sample preparation:

Samples were prepared following the same steps as described in 4.3.1. but instead of immersing in solutions immediately, following de-moulding and finishing, they were then transferred to desiccators maintained in an oven (Carbolite, Camlab,

Cambridge, UK) at 37±1°C for 22 hours; then they were transferred to desiccators in an oven (Carbolite, Camlab, Cambridge, UK) at 23±1°C. They were weighed daily using a balance (Explorer, Ohaus Europe GmbH, Nänikon, Switzerland) to an accuracy of +/-0.0001g. This cycle was repeated each day until a constant mass was reached (~ one week).

Water Uptake:

It should be noted that ISO 4049:2009 does not include i) immersion in AS, ii) measuring the uptake of the specimen for more than 7 days and iii) measuring water uptake at regular time intervals (Table 4.6) instead of measuring only after 7 days. However, in this study weight changes were recorded in both AS and DW up to 24 weeks. This was in order to compare the results with the alternative method (without desiccation) so that a suitable method could be identified to use for water uptake of the commercial and novel RMGICs, and to compare the water uptake results, at the same time points.

After desiccation, samples were weighed using a balance to an accuracy of ±0.0001g. Each sample was then immersed in individual labelled screw top bottles filled with 100 ml of DW or AS. The bottles were placed in a thermostatically controlled oven (Heratherm incubator, Thermo Fisher scientific, Massachusetts, USA) at 37±1°C, for at least 24 hours, before immersing the samples. Following immersion, samples were removed from the bottles using tweezers, blotted on filter paper (Fisher Scientific, New Hampshire, USA) to remove excess fluid and weighed at pre-determined regular time intervals. Samples were processed as fast as possible

to avoid dehydration (~30 seconds). Several readings were taken on the first day and then at regular time intervals thereafter up to 24 weeks, as shown in Table 4.6.

Table 4.6 Time intervals and cumulative time in minutes for the water uptake experiment up to 24 weeks.

Day	Time interval (min), t	Cumulative time (min)
1	0	0
	5	5
	10	15
	20	35
	40	75
	60	135
	60	195
	60	255
	60	315
	60	375
	60	435
2	3 x day	
3	2 x day	
4	1 x day	
5	1 x day	
Week 2 **= 3 readings at 3 different days**		
Week 4 **= 1 reading**		
One reading every two weeks to 24 weeks		

At time 't', the percentage weight change was calculated for each specimen (using Equation 4.1)

$$\text{Weight change (\%)} = (W_t - W_0/W_0) \times 100 \qquad \text{Equation 4.1}$$

where W_t is weight at a time and W_0 is the original specimen weight.

The mean weight change (%) and standard deviation (SD) were calculated for the commercial materials and the home-made liquids with commercial powders, and these were plotted against time$^{1/2}$ (seconds), in order to create the weight change profile for each material.

Desorption, solubility and diffusion coefficient:

After 24 weeks, samples were removed from the solutions, blotted, weighed and then transferred to a desorption oven (Carbolite, Camlab, Cambridge, UK) at 37±1°C. Again, several readings were taken on the first day, followed by readings at regular time intervals thereafter until a constant minimum weight was reached (W_d) following the time intervals given in Table 4.6 again.

Similar to the water uptake data, the mean weight change (%) was calculated and plotted against time$^{1/2}$ for the samples following desorption. The solubility of the material was calculated by subtracting the weight after desorption (W_d) from the initial specimen weight (W_0) and dividing by W_0 (Equation 4.2). This is equivalent to the total mass of the components leached from the material.

$$\text{Solubility (\%)} = (W_0 - W_d/W_0) \times 100 \qquad \text{Equation 4.2}$$

The rate of transfer of water entering and leaving the polymer during water uptake and desorption is measured by calculating the diffusion coefficient. Diffusion coefficients were calculated for the uptake and desorption processes where the plots

were linear to time$^{1/2}$ and equilibrium was reached. The equation used is the one derived from Fick's second law for the initial stages of diffusion mentioned in Literature Review chapter (Equation 2.4)

Dimensional changes:

Prior to immersion in media, two measurements were taken of the diameter of each specimen, at right angles to each other, using a digital micrometre (Mitutoyo, RS Components Ltd., Corby, Northants, UK) to an accuracy of 0.001 mm. Thickness was measured at the centre and at four equally spaced points on the circumference. These measurements were repeated after one week, three weeks and at the final reading time (after 24 weeks) in order to calculate the volume changes of the specimens using the following Equation 4.3

$$\text{Volume} = \pi r^2 h \qquad \text{Equation 4.3}$$

where r is the radius and h is the mean thickness of each specimen (Kanchanavasita *et al*., 1997).

4.3.2.2 Water uptake, desorption and dimensional changes experiment without desiccation:

The same method described in 4.3.2.1 was followed for the water uptake and desorption experiments, except that samples were immersed in solutions after allowing setting, 1 hour from the start of mixing.

This method was selected for the water uptake/desorption of novel materials as it was deemed to be more suitable and clinically relevant for the water uptake and

desorption experiments compared to the ISO 4049:2009 method. This will be discussed in the Results and Discussion chapters.

4.3.3 Working and setting times:

An oscillating rheometer was used to measure working and setting times of commercial, home and novel RMGICs, similar to that used by Bovis *et al*. (1971), consisting of a lower platen with a diameter of 10 mm, and a distance of 1.5 mm between the two platens. The lower platen rotated in an oscillatory movement driven by an electric motor with a speed of 10 rpm. The motor was connected to an eccentric wheel, which was attached to a rod by 2 springs 'in tension'. Amplitude was recorded as displacement of the rod in relation to the centre of the lower platen using a 'differential transformer'. The full amplitude corresponded to 0.6 mm movement, at ~ 0.5 degrees torsional angle, for the material placed between the two platens. The upper platen temperature was controlled using a temperature controlled water bath, which was switched on and left to equilibrate for 1 hour prior to commencing this experiment (Figure 4.2).

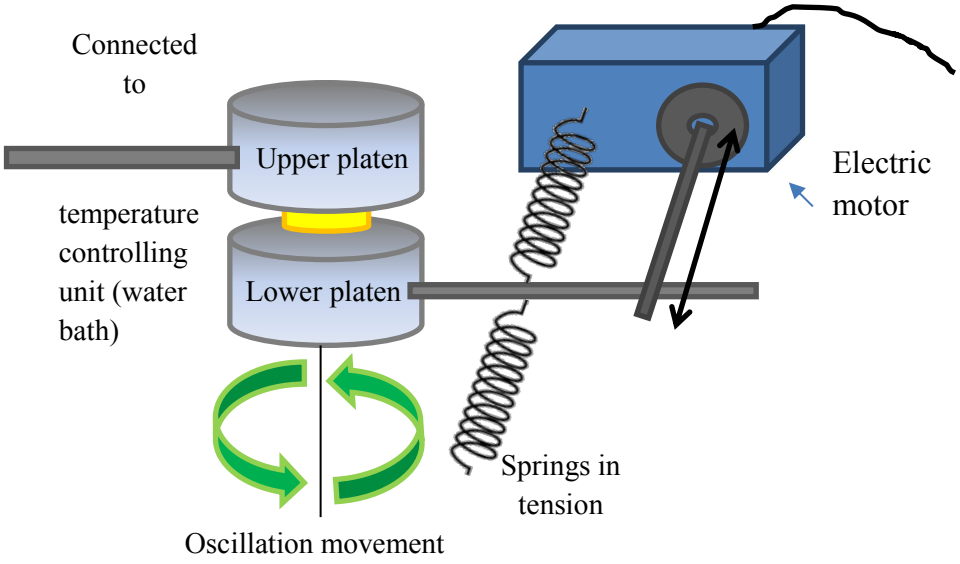

Figure 4.2 Schematic drawing of the principles of oscillating rheometer function.

The materials tested were: commercial FP and RX, FP home, RX home, novel compositions F1, 2, 3, 4 and novel compositions R1, 2, 3 and R4 with six repetitions (n=6) for each material. The materials were mixed at room temperature (23 ± 1°C) according to the manufacturers powder: liquid mixing ratio (2:1 g:g for FP and 1.6:1 g:g for RX) using the same method as described in 4.3.1. 0.5g of powder and 0.25g liquid was required for FP, and 0.4g powder and 0.25g liquid for RX, to produce a disc of 10mm diameter and 1.5mm thickness. Immediately following mixing (~ 40 seconds), the mixture was placed on the lower platen and, the upper platen, which had a controlled temperature of 37°C, was fixed in place with a 1.5 mm gap from the lower platen; this procedure was completed within 55 seconds from the start of mixing (Ogawa *et al*., 2001). The oscillations were recorded from the start of mixing, until the amplitude was zero, using a chart recorder (L200E, Linseis GmbH, Selb, Germany). The rheometer trace decreased with increasing viscosity and with

time, which was translated into working time when the amplitude reached a 5% decrease in the trace and, setting time, with 95% decrease in the first recorded amplitude trace. Figure 4.3 is a schematic drawing of an amplitude trace obtained using the oscillating rheometer, which shows the working and setting times (highlighting decreases by 5% and by 95% respectively) (Pearson and Atkinson, 1987; Ogawa *et al*., 2001).

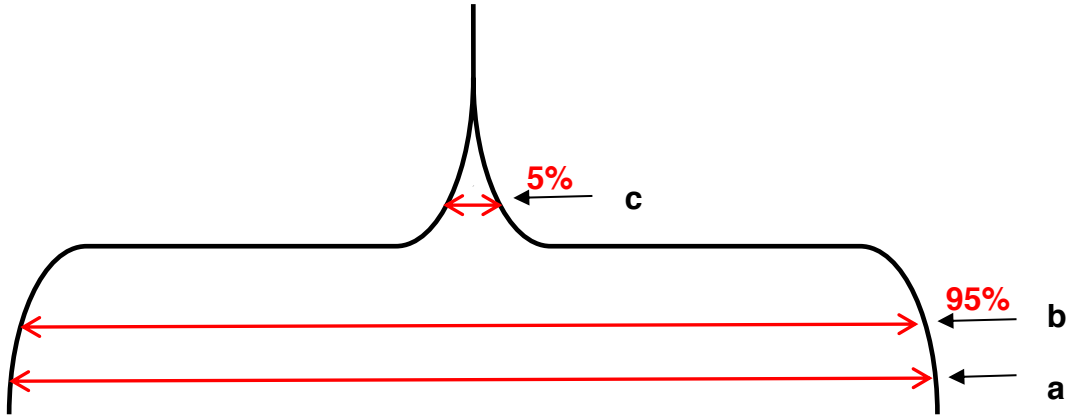

Figure 4.3 Schematic drawing of amplitude trace of oscillating rheometer which includes, a: start of trace, b: decrease of the trace by 5% corresponding to the working time of the material, c: amplitude decrease by 95% corresponding to setting time of material. Redrawn from Ogawa *et al*. (2001).

4.3.4 Degree of conversion using FT-IR:

The polymerisation process can be characterised by FT-IR. This is based on the absorption of infrared radiation passing through a sample and changes in molecular bonds vibrations, in the infrared frequency range of the functional groups, in the polymer chain (Koenig, 1984).

The FT-IR system consists mainly of an IR radiation source, Michelson's interferometer and IR detector. Michelson's interferometer was developed by the

Nobel Prize winner Albert Michelson in 1892. It consists mainly of two mirrors in a position perpendicular to each other; one of these mirrors is fixed while the other one is movable. The infrared beam originates from the IR source, passes to a beam splitter that splits the radiation into two beams perpendicular to each other to the fixed and movable mirrors, and then the beams reflect from the mirror and go back to the beam splitter, which combines them before passing to the detector. As the movable mirror moves, this creates a difference between the two beams of light, called the optical path difference, which is monitored by the detector. The variation of the beam intensities is then calculated versus the optical path difference in the computer, in order to produce a spectrum (Figure 4.4) (Griffiths and De Haseth, 2007). The detector can measure the intensity of radiation transmitted through the sample, in old FT-IR generations, or reflected from a sample when using special accessories, such as attenuated total reflectance (ATR), which was used in this study. In this case the sample did not require further preparation and could be tested using the ATR accessory crystal (Moraes *et al*., 2008).

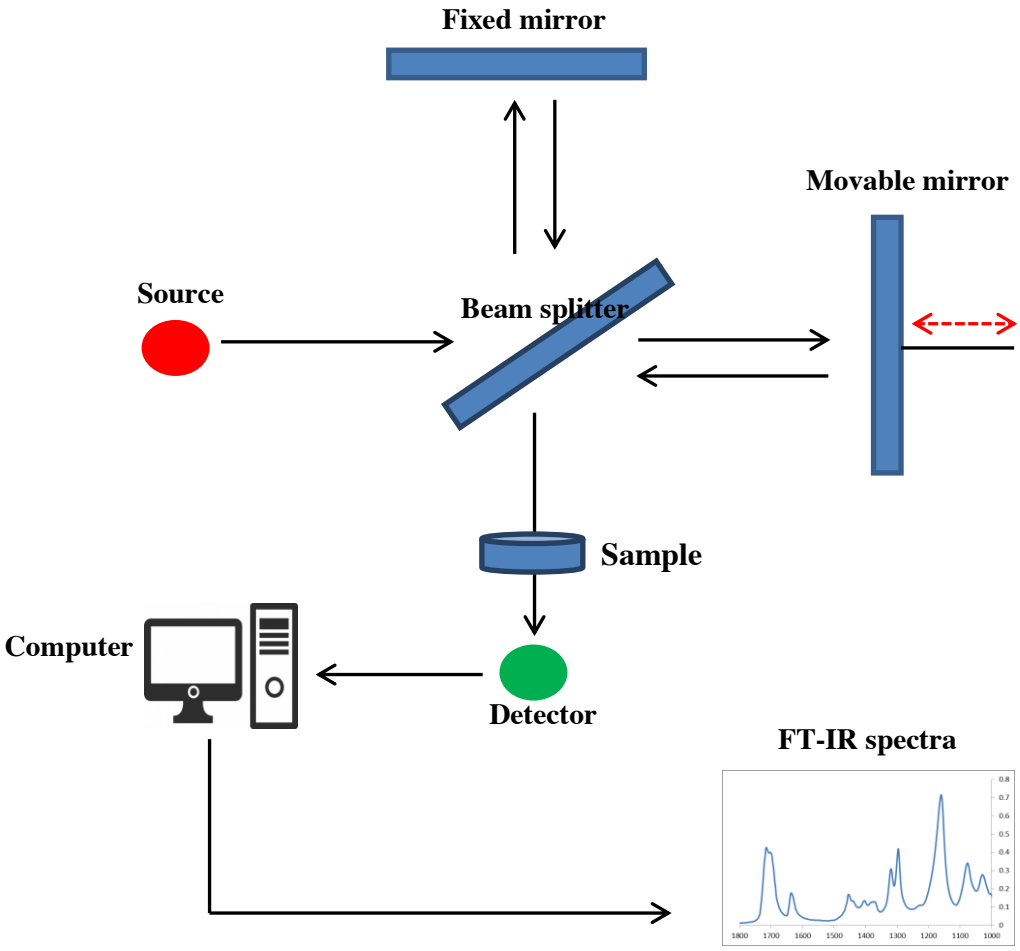

Figure 4.4 Schematic drawing of the theory of FT-IR spectra.

4.3.4.1 Degree of conversion experimental procedure using FT-IR:

All commercial, home and novel materials (unset liquids and set materials) were tested using FT-IR spectrometer (Perkin Elmer series 880) supplied with a Golden Gate Single Reflection Diamond attenuated total reflectance (ATR) accessory (Graseby Specac Ltd, Kent, UK). A total of 180 FT-IR spectra were obtained divided as four spectra taken at four times (at 0, 5, 10 and 30 minutes) from the start of mixing for three samples per material (n=3).

Spectra of absorbance versus wavenumber were obtained at a resolution of 4 cm^{-1} and, 10 scans in the range of 4000-500 cm^{-1}, were used to determine the absorbance peaks of the materials before and after curing. In order to identify the composition of the liquids, spectra of liquids were compared with those of individual RMGIC components, namely HEMA, THFM, HPM, UDMA, tartaric acid, water and poly(acrylic acid). A drop of the liquid was placed on the ATR crystal and scanned immediately. Three repetitions were performed for each liquid (n=3).

For identification of degree of polymerisation, materials were mixed at room temperature (23 ± 1°C) according to the manufacturers recommended powder: liquid mixing ratio (2:1 g:g for FP group and 1.6:1 g:g for RX group). In order to standardise the amount of RMGIC investigated, a wax ring of 8mm diameter and 1.5mm thickness was prepared using a profile wax stick (Berg Dental, Engen, Germany) and placed on the ATR accessory with the ATR crystal in the middle of the wax ring. The mixture then placed inside the wax ring within fifty seconds from the start of mixing; the top surface was covered with an acetate sheet and a scan was run as zero time. After 10 minutes from the start of mixing, pressure was applied to the top surface of the sample using the compression head anvil in the ATR in order to maintain good contact with the crystal. Subsequent spectra were generated at 0, 5, 15 and 30 minutes from the start of mixing thereafter.

Literature regarding the degree of conversion of resin composites measured the ratio of absorbance intensities of the aliphatic carbon–carbon double bond (C=C), at ~1638 cm^{-1}, and aromatic double bond (C=C) at 1609 cm^{-1} (Ribeiro *et al*., 2012; Galvão *et al*., 2013; Abed *et al*., 2015). The literature concerning RMGIC focused on the carbon-carbon double bond at 1638 cm^{-1} and the C=O at 1720 cm^{-1} as a

reference peak (Kim *et al*., 2015). However, another study showed that the peak at 1638 cm^{-1} could not be used to quantify the degree of conversion as the RMGIC formulation contains water, which absorbs at this wavenumber, thus making it difficult to determine the peak base at this point (Figure 4.5). Therefore, a different peak was used (at 1320 cm^{-1}) and, the degree of conversion results obtained using this peak, were in agreement with those obtained from Raman studies (Young, 2002; Young et al., 2004). Hence the degree of monomer conversion in this project was determined from the C-O peak at 1320 cm^{-1}.

Figure 4.5 shows spectra of commercial Fuji Plus plotted as wavenumber (cm^{-1}) versus absorbance, the absence of the peak at 1638 cm^{-1} (red circle), and also a shift in the peaks at 1320 and 1301 (black circle) cm^{-1} to 1276 and 1252, as polymerisation occurred. It moreover highlights the formation of GIC salt peaks at 1409, 1485 and 1550 cm^{-1}

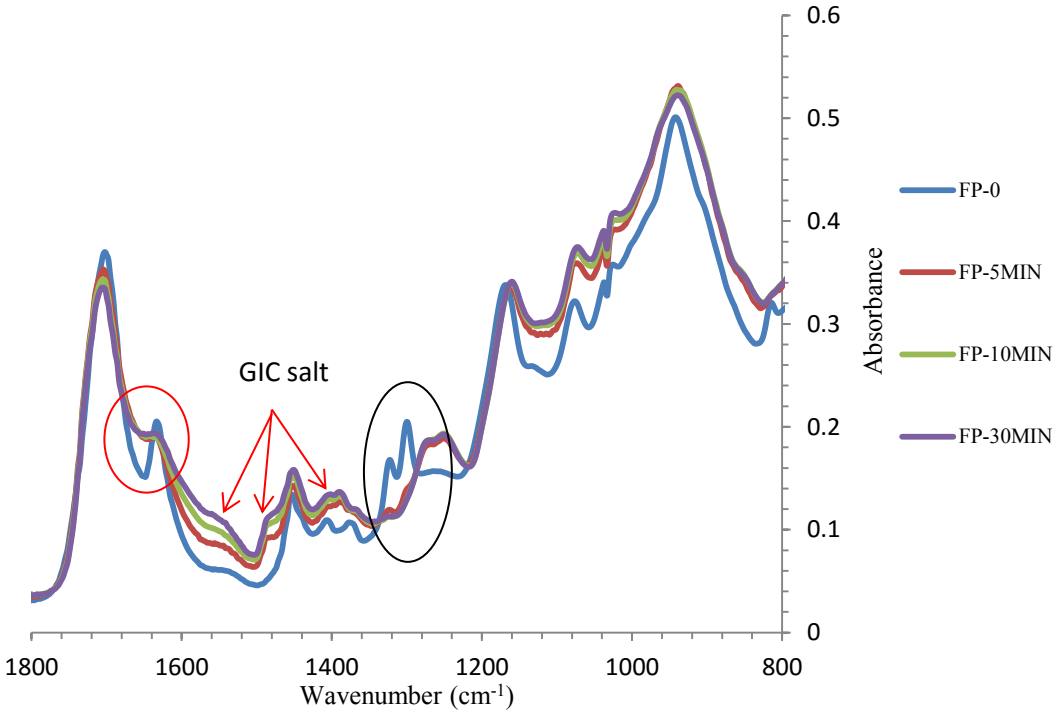

Figure 4.5 Spectra of Fuji Plus RMGIC following mixing representing the polymerisation reaction at 0, 5, 10 and 30 minutes after mixing with the peak used to quantify the degree of conversion of the monomer (black circle), the absence of the peak at 1638cm^{-1} (red circle) and the formation of GIC salts as the polymerisation occurred.

4.3.4.2 Treatment of FT-IR data:

As mentioned earlier in this study, the peak at 1320 cm^{-1} was used to quantify the degree of conversion (DC) of the monomer by measuring the net peak height difference between the absorption from 50 seconds after the start of mixing (A_0), to 30 minutes later (A_t). The formula below (Equation 4.3) was used to calculate the degree of polymerisation.

$$DC\ (\%) = \frac{(A_0 - A_t)}{A_0} * 100 \qquad \text{(Equation 4.3)}$$

Degree of conversion values calculated at each time point (5, 10 and 30 minutes) were compared between all materials for a significant difference using one-way ANOVA followed by post-hoc Tukey test at significance level of p=0.05.

4.3.5 Polymerisation shrinkage strain:

The bonded-disk method's main design and procedure was first mentioned by Walls *et al*. (1988) and Bausch *et al*. (1982), which was further developed by Watts and Cash (1991). This technique was subsequently improved and modified by Watts and Hindi (1999). The shrinkage strain of the material under investigation was measured using the bonded-disk technique after applying the mixed material onto a rigid glass plate (3mm thickness); this material consequently bonded to one surface of the glass maintaining a constant dimension of the circumference at 8mm diameter (Watts and Marouf, 2000). Watts and Cash (1991) demonstrated that no change occurred in the circumference of the tested material as a result of bonding to the glass plate; hence shrinkage occurred only in the vertical plane, in the unbounded surface. Therefore, the measurement of the strain (ε) in the axial plane corresponds to a close approximation, to the volumetric strain of the material, and was calculated using Equation 4.4.

$$\varepsilon = \frac{\Delta L}{L_0} \approx \frac{\Delta V}{V_0} \qquad \text{(Equation 4.4)}$$

where L_0 and V_0 represent the original height and volume of the specimen respectively.

4.3.5.1 Bonded-disk instrument design:

The bonded-disk instrument consisted of a linear variable displacement transducer (LVDT), with sensitivity greater than 0.1 μm, and was fixed to an aluminium stand above a brass anvil (40mm diameter; Figure 4.6).

The experimental assembly in which the material under investigation was placed consisted of 16 ± 0.1mm diameter and 1 ± 0.1mm thickness brass ring (square cross sectioned), bonded centrally on a glass slide (74mm length, 25mm width and 3mm thickness). This glass slide and the brass ring were then covered with a square microscope cover slip (22x22mm and 0.13mm thickness; Number 0, VWR International, Radnor, PA, USA). This assembly was placed centrally on a temperature controlled metal plate and the LVDT was lightly in contact with the centre of the flexible cover slip (Figure 4.6). The movement of the cover slip was detected by the LVDT (where, when the LVDT moved downwards onto the attached cover slip and experimental material = shrinkage, or alternatively, it moves upwards = expansion). The LVDT was connected to a signal-controlling unit (E309, RDP Electronics, Wolverhampton, UK) that transferred the data to a computer through a data logging system hardware and software (ADC-20 multichannel unit and Pico-log software, Picotech, Cambridge, UK).

In order to measure the polymerisation exotherm and shrinkage simultaneously, a thermocouple was passed through a carefully drilled groove in the centre of the glass slide reaching the centre of the brass ring. The end of the thermocouple was placed centrally in the test material. This thermocouple was attached to a type-K

thermocouple amplifier (TCK-4, Audon Electronics, Nottingham, UK), which transferred the exotherm data to the ADC-20 unit.

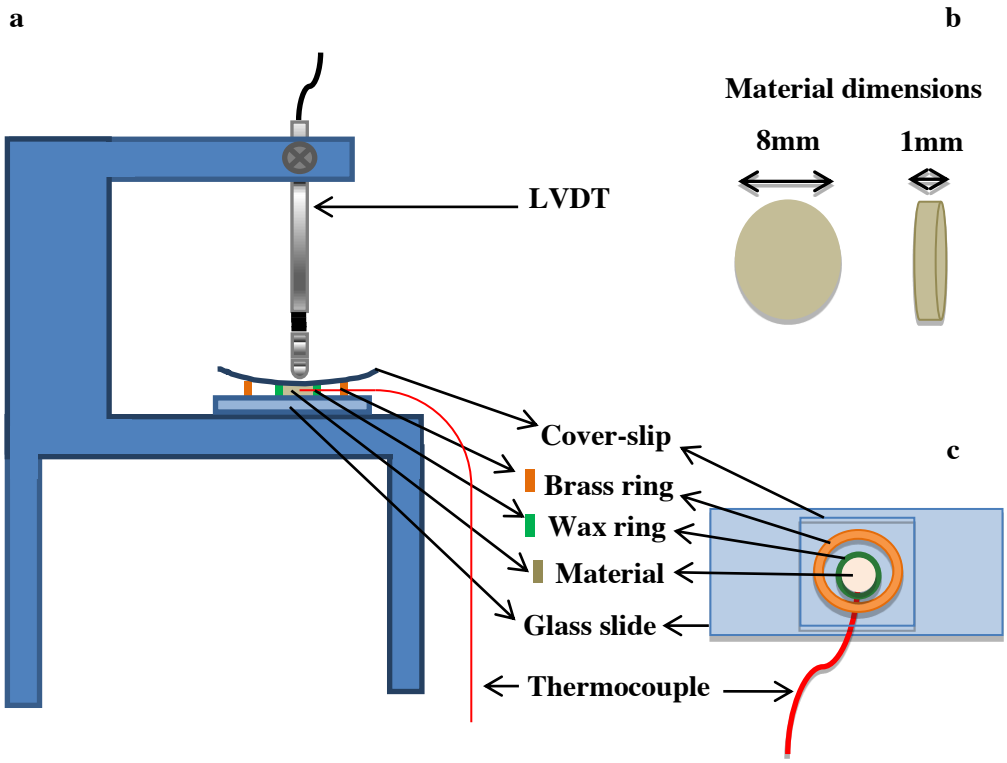

Figure 4.6 Schematic drawing of a: bonded-disk instrument, b: final material dimensions and the c: glass slide assembly design.

4.3.5.2 Calibration of the LVDT:

The LVDT probe was calibrated prior to starting the shrinkage experiment using a modified and calibrated micrometre (Mitutoyo, RS Components Ltd., Corby, Northants, UK) accurate to 1µm, by clamping it horizontally so that it was opposing and touching the anvil of the micrometre. The LVDT probe was displaced through changing the micrometre armature and recording the displacement in the micrometre

display (µm) and the output displacement as recorded using the Pico-log software in mV (Figure 4.7).

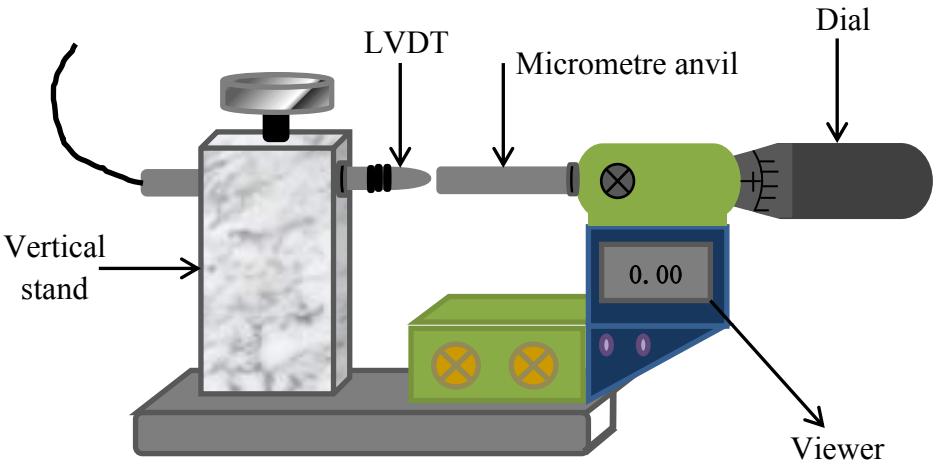

Figure 4.7 Schematic drawing of the digital micrometer used for LVDT calibration; LVDT clamped to a vertical stand opposite the micrometer anvil.

The displacements in µm were subsequently plotted against Pico units (in mV) in order to calculate the voltage/displacement calibration factor by linear regression analysis (r=0.9999) (Figure 4.8).

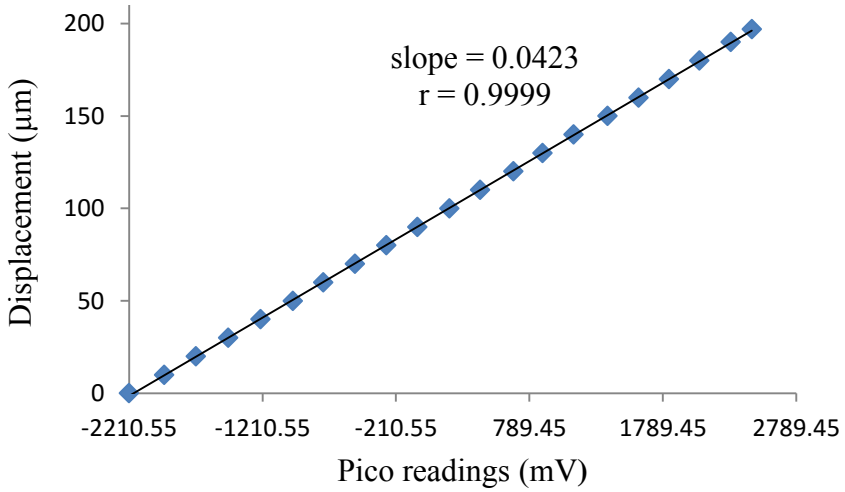

Figure 4.8 Calibration of the LVDT probe by linear regression from a plot of displacement (*µ*m) versus output (in mV).

4.3.5.3 Experimental procedure - shrinkage strain:

A total of 60 samples divided into 12 groups (n=5) for all compositions (Fuji Plus and RelyX Luting commercial, home and novel- F1, F2, F3, F4, R1, R2, R3 and R4) were investigated for polymerisation shrinkage strain and exotherm using the bonded-disk technique.

The experiments were conducted at both 23 ± 1°C (~room temperature) and at 37 ± 1°C (body temperature); the temperature was controlled through a metal plate on which the sample assembly was placed. The instrument was switched on and left to equilibrate to the desired temperature for 2 hours prior to starting the testing. Powder and liquid were mixed following the manufacturers recommendation (2:1 g:g for FP and 1.6:1 g:g for RX). The mix was then placed on the glass slab within the wax ring and covered with the glass cover-slip while inserting the thermocouple through the drilled groove and into the mixed material (Figure 4.11). The cover-slip was pressed

using a microscope glass slide in order to flatten the material and to achieve a standard thickness of the tested material each time; this was the thickness of the brass ring. Afterwards, the assembly (the glass slide and the cover-slip) was transferred to the aluminium stand and placed horizontally on the metal base. The probe of the LVDT was carefully placed to lightly touch the surface of the cover-slip. The test was started at this point and the output (in mV) and rise in temperature (^oC) were recorded simultaneously for a period of 60 minutes.

4.3.5.4 Treatment of polymerisation shrinkage strain data:

A baseline of 60 seconds was performed prior to starting each sample, which was then subtracted and the data was rescaled to time=0 and voltage=0.

The final specimen thickness (L) was measured using a digital micrometre accurate to 10µm. The calibration coefficient of displacement/voltage, calculated as described in 4.3.5.2, was used to calculate the displacement of the cover slip during the experiment (dL), which was then used to determine the original specimen thickness (L_0) in µm, following Equation 4.5.

$$L_0 = dL + L \qquad \text{(Equation 4.5)}$$

The percentage shrinkage strain was calculated using Equation 4.6.

$$Shrinkage\ strain\ \% = \left(\frac{dL}{L_0}\right) * 100 \qquad \text{(Equation 4.6)}$$

The shrinkage strain (%) values were calculated for each material using equation 4.6. These values were then plotted against time (seconds) to originate the shrinkage strain kinetic curve from the start to the end of experiment. Figure 4.9 is a

representative plot of shrinkage strain for FP group materials (commercial, home and novel) up to 3600 seconds (1 hour).

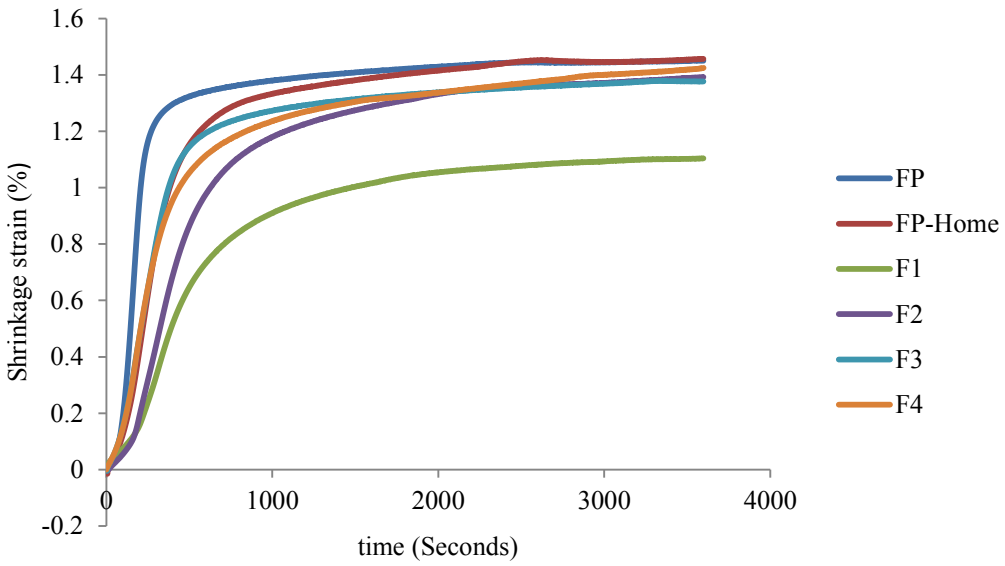

Figure 4.9 Representative plot of mean percentage shrinkage strain for FP group materials (commercial, home and novel) up to 3600 seconds.

The shrinkage strain values at 5, 15, 30 and 60 minutes, were used to determine any statistical significance differences between the materials under investigation and were analysed using one-way ANOVA followed by post- hoc Tukey test at a significance level of p=0.05.

The shrinkage strain rate (%.s^{-1}) was plotted against time (sec) in order to calculate the maximum shrinkage strain rate (shown as a peak) for each sample and the time to reach this peak temperature. Figure 4.10 is a representative plot of shrinkage strain rate curve versus time (seconds) for Fuji Plus.

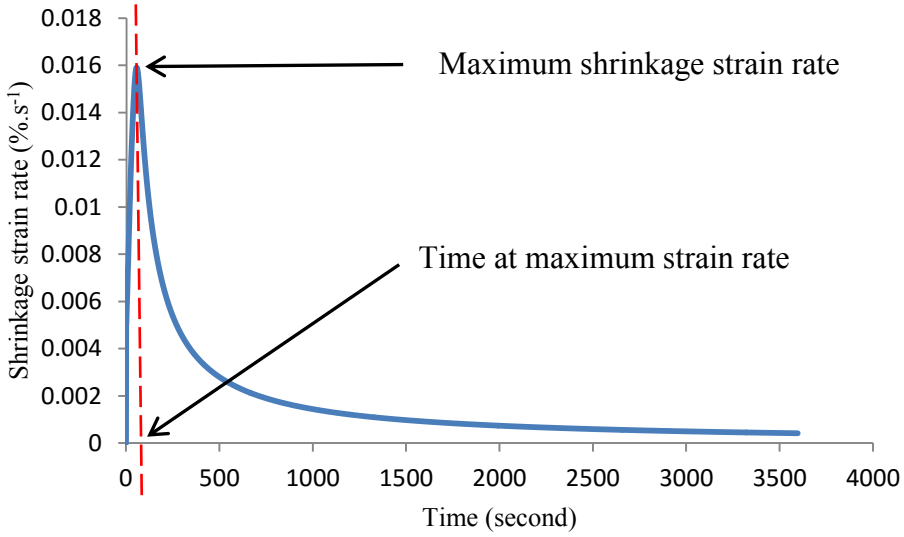

Figure 4.10 Representative plot of shrinkage strain rate (%.s^{-1}) versus time (in seconds) and the time to reach the maximum strain rate for Fuji Plus.

4.3.6 Polymerisation exotherm:

4.3.6.1 Polymerisation exotherm experiment procedure:

All materials (commercial, home, and novel) were tested using bonded-disk technique in order to determine their polymerisation exotherm following the procedure published by Alnazzawi and Watts (2012). The exotherm data were recorded simultaneously with the shrinkage strain measurements, for a period of 60 minutes at both 23 and 37°C.

A K-type thermocouple was used to measure the polymerisation exotherm; its free end was connected to a K-type thermocouple amplifier (TCK-4, Audon Electronics, Nottingham, UK) and the latter was attached to a ADC-20 unit. The free end of the thermocouple was inserted in the centre of the sample as it passed through a carefully drilled groove to the centre of the glass slide underneath the brass and the wax rings (Figure 4.11).

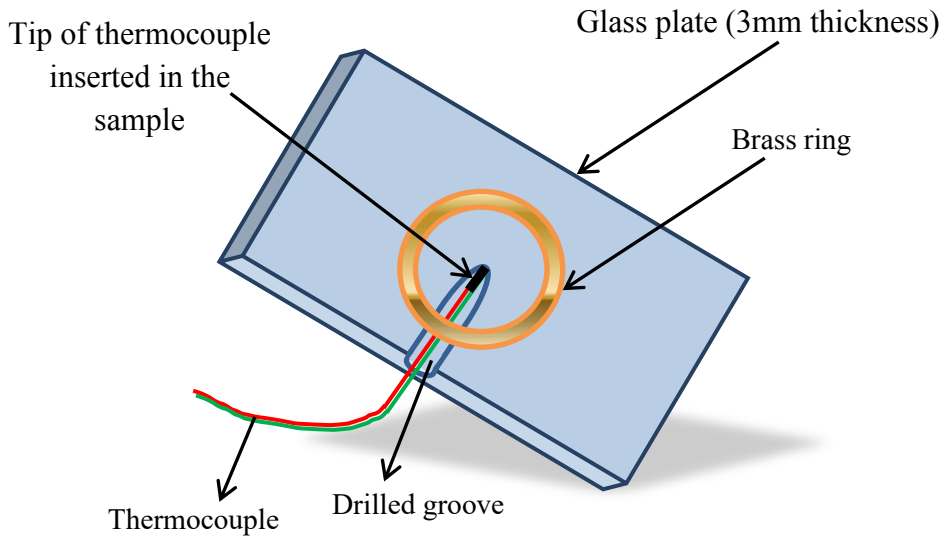

Figure 4.11 Schematic drawing showing the thermocouple passing through the groove to the centre of the glass plate underneath the brass ring.

4.3.6.2 Treatment of polymerisation exotherm data:

The temperature was recorded for 60 seconds before the start of the experiment to create the baseline, which was subsequently subtracted and, the polymerisation temperature of each specimen, was plotted against time. The maximum temperature reached was recorded and compared for significant differences between the materials using one-way ANOVA followed by post-hoc Tukey test at a significant level of $p=0.05$. Moreover, the time to reach the peak temperature was also recorded as the period from the start of mixing to the time required to reach the maximum temperature.

4.3.7 Monomer release study using high performance liquid chromatography (HPLC):

The release of four monomers (HEMA, THFM, HPM and UDMA; used in RMGICs) was analysed using HPLC in DW and 75:25% ethanol:DW. HPLC is a very sensitive technique that can detect, and subsequently quantify, the amount of each component released; this gives an indication of the extent of free monomer within each material.

Despite the availability of different methods published in the literature regarding the detection of released monomers, a novel method had to be developed for the HPLC analysis of HEMA, THFM, HPM and UDMA since there were variations in the materials reported and differences in column type/size used in the experiments. Furthermore, in this study two new monomers were used in the novel compositions that have not been previously reported in the literature with respect to HPLC (e.g. THFM and HPM), so detection was not optimum using published methods for both groups (FP and RX). Pilot studies were conducted in order to select the optimum test parameters for sufficient detection of the released monomers, as discussed below.

4.3.7.1 HPLC pilot studies:

Pilot studies involved selection of the most effective mobile phase ratio, sample size, solution amount, follow-up time, etc.

The first pilot study was conducted using acetonitrile (ACN)-52%, DW-47.9% and formic acid-0.1% as solvents under isocratic conditions (the mobile phase ratio was constant throughout the analysis time), for a period of 5 minutes. The test was performed using a reverse phase column Zorbax Eclipse® XDB-C18 (Agilent

Technologies, USA), 4.6×75 mm^2 i.d. and 5 µm particle size and wavelength detector of 210 nm. This method allowed detection of different concentrations of HEMA (1, 10 and 100 ppm) and gave a linear calibration curve using the peak area. However, the separation of the peak was not optimum, since the peak height of HEMA did not give a linear calibration, which made it necessary to use the peak area instead, but this proved to be difficult due to the subjectivity in determining the base of the peak (Figure 4.12). Moreover, the 100 ppm peak for HEMA was flat and broad, which indicated that the retention time of HEMA had increased and its concentration was too high. This indicated that the system was overloaded with HEMA.

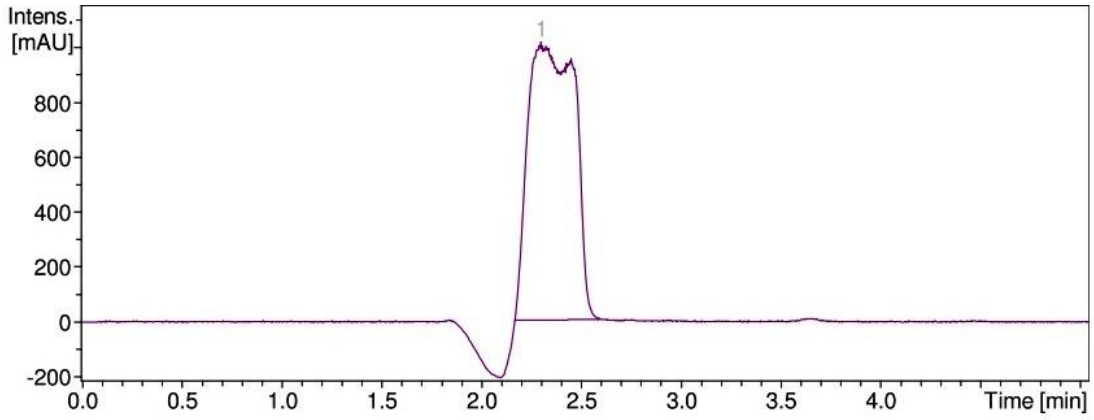

Figure 4.12 Chromatogram of 100 ppm HEMA based on the first HPLC pilot study.

In order to attain a sharper peak with a defined baseline a different method was tried, consisting of gradient conditions (the instrument altered the concentration of solvents during the analysis), with ACN and DW as solvents (this method will be described in 4.3.7.2), and was used for the identification of monomers released from FP samples. This modification proved more successful in separating all monomers (Figure 4.13). However, the disadvantage of this method was the long runtime needed (30

minutes). Therefore, to decrease the runtime and the overall cost of the experiment, a different method was tried using a shallow gradient condition of ACN in DW (increasing the ACN solvent concentration by only 5% between 5 and 6 minutes). This method allowed detection of three monomers (HEMA, THFM and HPM) while reducing the runtime to 8 minutes, but was unsuccessful in detecting UDMA. Therefore, this method was used only for the analysis of monomer release from the RX group, which did not contain UDMA in their compositions (Figure 4.14). In all pilot studies the molecular weights of all monomers were identified and confirmed using HPLC–mass spectrometry (HPLC-MS) to ensure correct assignment of each peak with the relevant monomer.

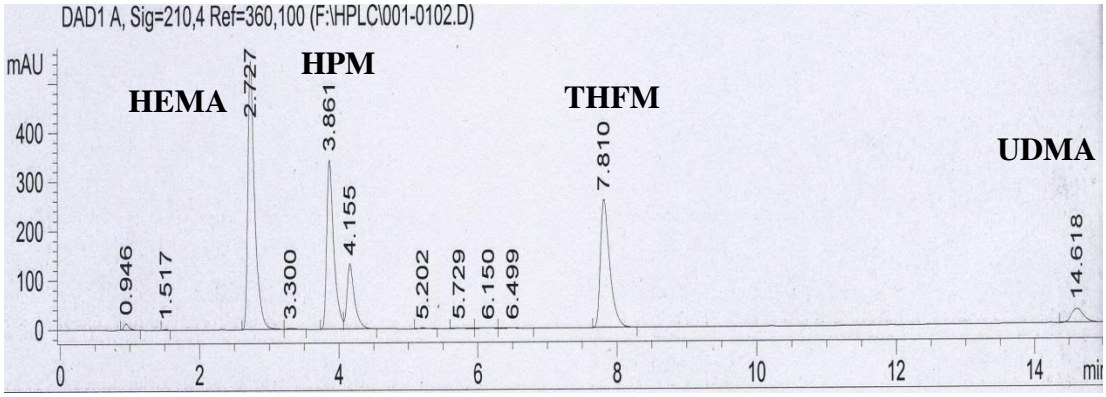

Figure 4.13 Chromatogram of all monomers following new method for FP group.

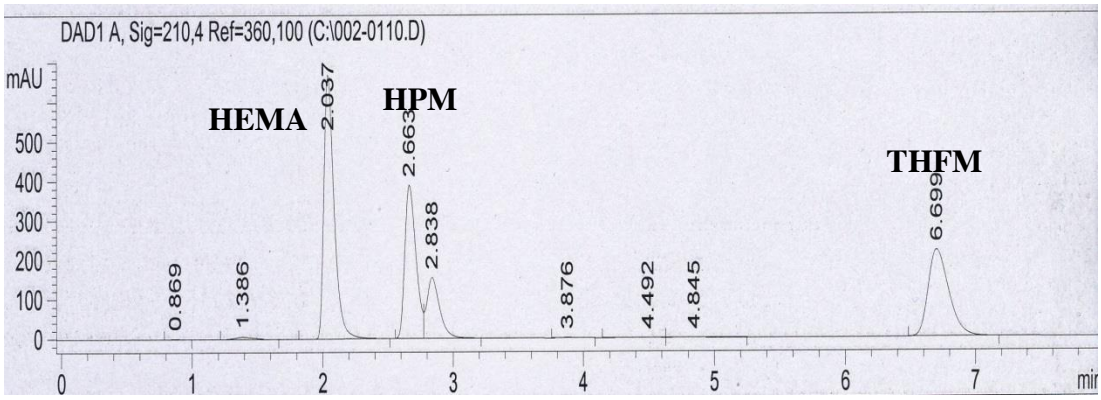

Figure 4.14 Chromatogram of HEMA, THFM and HPM following method used for RX group.

The HPLC system was run for 10 minutes at 2mL/min using each mobile phase ratio, every time the mobile phase was changed, in order to keep the system equilibrated. Moreover, the system was washed with 50:50% isopropyl alcohol (IPA) and DW between different sample injections, in order to eliminate contamination from the previous sample. Furthermore, blank samples consisting of DW were run before each batch of samples and were later compared with spectra of standards and samples to ensure that all separated compounds were from the sample and standard solutions only.

The release of monomers from samples immersed in 100 mL DW used in the water uptake experiment could not be detected (possibly due to a small amount released in a large volume of liquid), so another set of samples with different dimensions (10mm diameter and 1mm thickness) were tried by immersing in a lower amount of water (50 mL and 20 mL; (Palmer *et al*., 1999; Beriat and Nalbant, 2009); again leached monomers could not be detected after 1 week immersion. Therefore, a new set of samples with similar dimensions (10mm diameter and 1mm thickness) were immersed in 10mL DW or 10mL 75:25% ethanol:DW; this resulted in successful

identification and quantification of released monomers from commercial, home and novel (experimental) materials (sample preparation is fully described in section 4.3.7.7).

4.3.7.2 HPLC method for monomer release of FP group:

HPLC with UV-Vis spectrometric detector was used to analyse and quantify the release of monomers from commercial, home and novel RMGICs used in this study.

The exact parameters of this method were: reverse-phase column C18 Zorbax Eclipse® XDB-C18 (Agilent Technologies, USA), 4.6×75 mm^2 i.d. and 5 μm particle size. The mobile phase used consisted of ACN and DW at a flow rate of 1 mL/min, injection volume 10μL; the UV detector absorbance was at 210 nm; the column temperature was set at 30°C and the run time was 30 minutes.

The mobile phase ratio was performed under gradient conditions as follows: 0min, ACN 30%, 15min, ACN 70%; 17min, ACN 70%; 20min, ACN 100%; 21min, ACN 30%; 30min ACN 30%. Under all these conditions, ACN was combined with DW. The initial mobile phase (ACN 30%) was run at the end of each test sample for 9 minutes to eliminate any possibility of compounds carrying over following separation, as contamination of the column with hydrophobic elements was noticed during pilot studies, which made it necessary to wash the retained components following each sample analysis. Figure 4.13 presented earlier in 4.3.7.1 is a representative chromatogram of all compounds tested using HPLC method for FP group.

4.3.7.3 HPLC method for monomer release of RX group:

The same parameters detailed in section 4.3.7.1 were used for identification and quantification of monomer release from the RX group. The only difference between the two methods was the mobile phase gradient ratio and run time. The mobile phase conditions for the RX group was as follows: 0min, ACN 30%, 5min, ACN 35%; 6min, ACN 35%; 6:05 ACN 30%; 8min ACN 30%, runtime 8 minutes (shallow gradient). Figure 4.14 presented earlier in 4.3.7.1 is a representative chromatogram of all compounds tested using the HPLC method for RX group. All HPLC parameters for both methods are presented in Table 4.7.

Table 4.7 HPLC parameters for the two methods for FP and RX.

Instrument	**HPLC**
Detector and system controller	Agilent 1100 HPLC with UV detector.
Column	A reverse-phase column C18 Zorbax Eclipse® XDB-C18
Flow rate	1 mL/min
Volume injected	10 µL
Run time (FP group)	30 minutes
Run time (RX group)	8 minutes
Wavelength	210 nm
Mobile phase	ACN in water (gradient condition)

4.3.7.4 Calibration and preparation of standard solutions:

The HPLC system was calibrated prior to testing each batch of samples for every compound by running different concentrations of standard solutions 1, 5, 10, 25 and 100 ppm of HEMA, THFM, HPM or UDMA. These concentrations were selected since the maximum release of all monomers, in all samples, was lower than 100 ppm, with the exception of HPM release from F1 in 75:25% ethanol:DW, which was higher than 100 ppm. Therefore another 2 standard solutions of 200 and 300 ppm HPM in 75:25% ethanol:DW were prepared.

Preparation of 100 ppm standard solutions was performed by pipetting 9.3 μL of HEMA, or 9.6 μL of THFM, or 9.4 μL of HPM into a 100mL amber volumetric flask and mixing vigorously with 50 mL of DW for 10 minutes. Then the flask was filled with a further 50 mL DW and mixed again for an extra 10 minutes. Due to the higher viscosity of UDMA, it was not possible to pipette this compound; therefore it was dissolved in a similar weight of ACN solvent. Then a standard solution was prepared by pipetting 21.7 μL of 50/50% ACN/UDMA mixture in 100mL amber volumetric flask, filled with 50mL DW, mixed vigorously for 10 minutes, followed by the addition of 50 mL DW and mixed again for another 10 minutes. All 100 ppm solutions were used as stock solutions and different volumes (1, 5, 10 and 25 mL) of this solution were diluted in DW to the mark of 100 in a 100mL volumetric flask in order to prepare solutions for the calibration curve (Table 4.8).

Table 4.8 Preparation of standard solutions for all monomers tested.

Volume of DW or 75:25% ethanol:DW (mL)	Volume of stock solution (mL)	Concentration (ppm)
99	1	1
95	5	5
90	10	10
75	25	25

All analyses were performed from the lowest to highest concentrations (from 0 to 100-300 ppm) of standard solutions to eliminate the possibility of compounds carrying over. Moreover, blank samples of DW were also injected prior to each batch of standard and sample analyses. The data obtained from a standard HPLC solution was plotted as concentration (ppm) versus peak height to produce a calibration curve that was essential for the quantification of released monomers. Figure 4.15 is a representative calibration curve for HEMA standard solutions 1, 5, 10, 25 and 100 ppm concentrations, displaying the equation and regression correlation coefficients at 210nm.

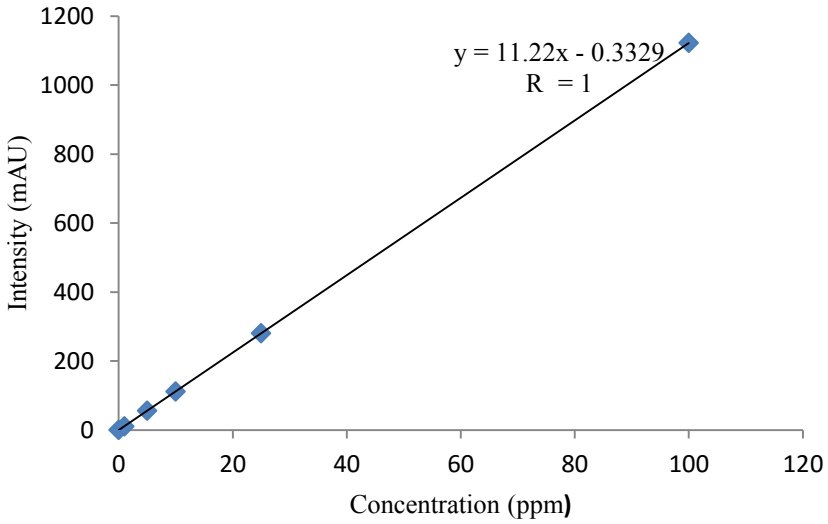

Figure 4.15 Representative calibration curve of 0, 1, 5, 10, 25 and 100 ppm HEMA at 210 nm.

4.3.7.5 Reproducibility of HPLC results:

HPLC results were tested for the ability to produce identical measurements of the same compound, of the same concentration, using the same method. The system was deemed suitable and the results were deemed reproducible, if the coefficient of variation (CoV) value, namely the standard deviation divided by the mean, was below 8% (Crawley, 2005), after injecting and testing the sample ten consecutive times (Table 4.9).

Table 4.9 CoV of four leached monomers analysed using HPLC following the RX and FP HPLC methods.

Monomer	CoV of peak heights (%)-RX method in DW	CoV of peak heights (%)-FP method in DW	CoV of peak heights (%)-RX method in ethanol:DW	CoV of peak heights (%)-FP method in ethanol:DW
HEMA	1.43	0.48	2.82	1.19
HPM	2.12	0.48	0.98	0.85
THFM	2.74	0.42	0.68	0.91
UDMA	No peak	3.46	No peak	0.64

4.3.7.6 Considerations during running the two HPLC methods:

The HPLC system was run for 10 minutes at 2mL/min using each mobile phase ratio, every time the mobile phase was changed, in order to keep the system equilibrated. Additionally, the system was washed through with 50:50% Isopropyl alcohol (IPA) and DW between different sample injections in order to eliminate contamination from the last sample, and this was done for all samples (FP and RX). This procedure was different from the washing procedure described in the FP group analysis, since FP contained UDMA (hydrophobic), which made it necessary to wash the system following each sample as described in 4.3.7.2. Blank samples consisting of DW, were run before each batch of test samples and were later compared with spectra of standards and samples to ensure that all separated compounds were from the sample and standard solutions only.

4.3.7.7 Sample and solution preparation:

Prior to starting the experiments, all glass tubes and flasks were washed with 10% HCl, then rinsed three times with DW and dried with acetone. Glass test tubes with curved internal bases were used to allow for maximum contact between the samples and the solution, and 'minimum contact' with the test tube (Figure 4.16). Glass test tubes were filled with 10mL DW and kept at 37°C for at least 24 hours before immersing samples. Six discs of each material were prepared by mixing the manufacturers recommended powder: liquid mixing ratio of commercial, home and novel materials as previously described in 4.3.1, and then packing the mix in a PTFE mould with different internal dimensions of 10mm diameter and 1mm thickness (Figure 4.16) compared to water uptake experiment. It was recommended to use smaller samples compared to the ones used in the water uptake experiment as a result of the pilot studies already mentioned in 4.3.7.1.

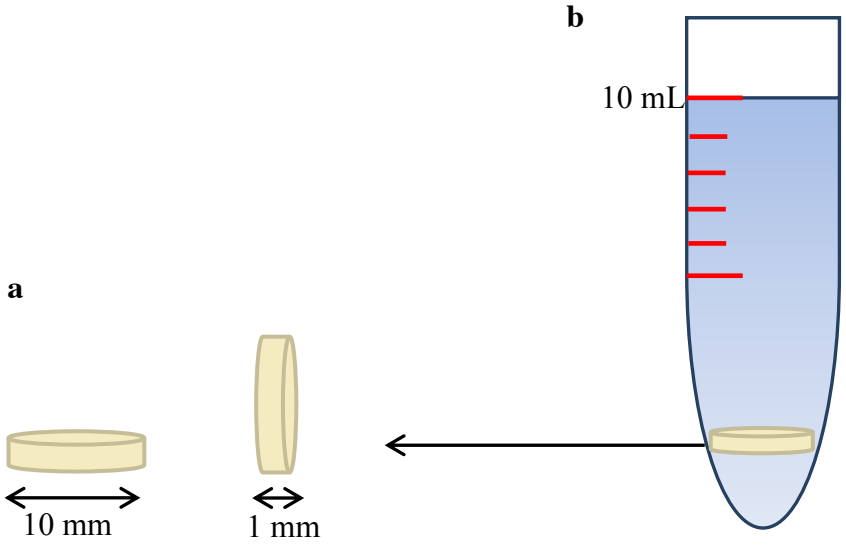

Figure 4.16 Schematic drawing of HPLC samples dimensions (a) and samples immersed in a curved bottom glass test tube containing 10 mL DW (b).

After setting, the samples were de-moulded, checked for any irregularities, weighed and then immersed in individual glass test tubes.

1mL of immersion solution was extracted at pre-determined time points, 1 hour, 4 hours, 24 hours and 168 hours after initial immersion. The solution was changed at the last time point (168 hours) plus an extra one after 672 hours (4 weeks). Glass amber vials were used to store the extracted solutions and were kept in the refrigerator at 2-4°C prior to analysis. 1mL of DW was added to the glass test tube each time an aliquot (1mL) was extracted, in order to maintain the volume of solution at 10mL.

4.3.7.8 Treatment of HPLC data:

Measurements were taken twice for each of the extracts and calibration solutions and then the mean of the peak heights was calculated. For every batch of samples at each time point (n=6), calibration curves were calculated by plotting the known concentration of each standard solution (ppm) versus the peak height obtained. The concentration of all monomers was then calculated using the correlation coefficient obtained from linear regression analyses of the calibration curves. A representative linear calibration equation, correlation coefficient and retention times of all monomers, following RX and FP HPLC methods, are presented in Table 4.10. Means of monomer release were then statistically compared using SPSS IBM statistics version 22 (Chicago, IL, USA) using One-way ANOVA followed by post-hoc Tukey test at significance level of p=0.05.

Table 4.10 A representative of linear calibration equation, correlation coefficient and retention times for HEMA, HPM, THFM and UDMA from the two methods used (FP and RX).

Monomer	Equation	R^2	Retention time (RX group), min	Retention time (FP group), min
HEMA	Y = 11.22x-0.3329	1	2.037	2.727
HPM	Y=7.2054x-1.401	0.9995	2.663	3.861
THFM	Y=4.3446x+0.2612	0.9998	6.699	7.810
UDMA	Y=0.6365x+1.869	0.9983	-	14.618

4.3.8 Compressive fracture strength test (CFS):

4.3.8.1 Sample preparation:

A total of 240 RMGICs cylindrical samples (n=20) of commercial, home and novel RMGICs (6.0 ± 0.1 mm height and 4.0 ± 0.1 mm diameter) were prepared for CFS tests following ISO 9917-1:2010 (Figure 4.17), using a stainless-steel split-mould. This was lightly covered with petroleum jelly (Vaseline, Sigma-Aldrich, St. Louis, Missouri, USA) before each use to prevent sample adhesion to the moulds. Powder and liquid were mixed as described previously in 4.3.1. One sample was prepared at a time and this required 0.4g powder: 0.2g liquid of FP and 0.4g powder: 0.25g liquid of RX. The mix was transferred to a metal mould (which was placed on a metal plate covered with an acetate sheet); then covered with another acetate sheet and metal plate before clamping together using bulldog clips, to give uniform surfaces. The assembly was transferred to an oven maintained at 37 ± 1°C and 100% humidity for 60 minutes to allow the setting of GIC.

After 60 minutes, the sample assembly was removed from the oven, samples were de-moulded and visually inspected for any defects or impurities (e.g. bubbles or chipped edges). The selected samples were then hand-lapped using P600 silicon carbide abrasive paper (Buehler, IL, USA) to remove any residual flash, stored in plastic test tubes filled with 50 mL of DW, and transferred to an incubator (LTE Qualicool, Scientific Laboratory Supplies, Yorkshire, UK), maintained at 37 ± 1°C, for a further 23 hours before testing.

4.3.8.2 Compressive fracture testing procedure:

24 hours from the start of mixing, the samples were removed from the test tubes and blotted on filter paper as fast as possible to remove surface water (Whatman No. 1, Whatman Inernational Ltd., Maidstone, England). A digital micrometre, accurate to 1μm (Mitutoyo, Kawasaki, Japan), was used to measure the thickness and diameter of the specimens. The diameter was measured (measurements made at three different points – top, middle and bottom) and the mean was calculated. Samples were processed as fast as possible to minimise desiccation. Two pieces of wet filter paper were placed on the two loading platens of the universal testing machine (Instron model 5567, High Wycombe, England) in order to test the specimens in a wet environment, in accordance with ISO 9917-1:2010. The specimen was then placed on the wet filter paper on the loading platen of the testing machine and a compressive load was applied vertically at a loading rate of 1 mm/min (Figure 4.17). The maximum load-to-failure was recorded and CFS was calculated for each specimen using Equation 4.7.

$$CFS = \frac{4P}{\pi d^2} \qquad \text{(Equation 4.7)}$$

where P was the load-to-failure in Newtons and d the mean specimen diameter in mm.

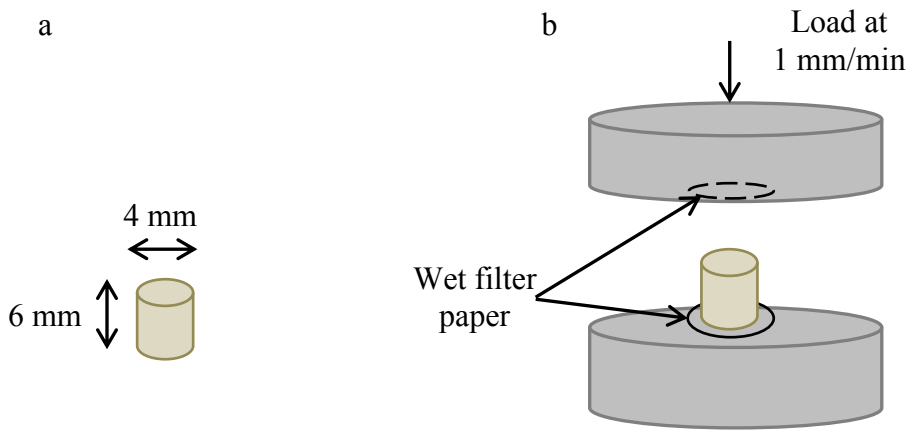

Figure 4.17 Schematic drawing of CFS sample dimensions (a) and test (b).

CFS value is dependent on the specimen dimensions because the height and diameter of each sample have an effect on the load-to-failure, and hence can influence the CFS value calculated. However, Ritter (1995) reported that the probability of samples containing defects and impurities was positively affected by increasing the specimen dimensions (height or diameter) and this will therefore negatively affect the CFS value recorded. Therefore, it was suggested that determining the compressive modulus (CM) value for each material is advantageous since CM is considered 'an intrinsic materials property' and it is not influenced by the sample's dimensions (Dowling and Fleming, 2008; Dowling and Fleming, 2009). CM was calculated by measuring the slope of the initial linear segment of the stress-strain plot (Fig 4.18) for each specimen tested for compressive strength using Equation 4.8.

$$CM\ (GPa) = \frac{stress\ (MPa)}{Strain\ (\%)} / 1000 \qquad \text{Equation (4.8)}$$

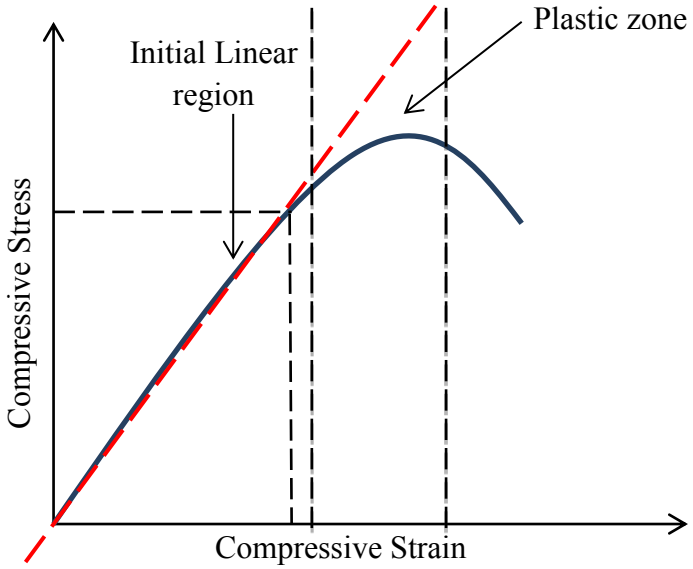

Figure 4.18 Schematic of stress-strain plot showing the initial linear region used to calculate the CM.

4.3.8.3 Treatment of CFS and CM data:

Means and standard deviations (SD) were calculated for samples of each material (n=20), and the results were statistically compared using IBM SPSS Version 22 (Chicago, IL, USA), One-way ANOVA test followed by the post-hoc Tukey test, at a significance level of p=0.05.

4.3.9 Three point flexure strength test (TFS):

4.3.9.1 Sample preparation:

This test and sample manufacture was performed in the Materials Science Unit, Dublin Dental University Hospital, Trinity College, Ireland under the supervision of Dr. Garry JP Fleming. The order in which samples of the RMGIC control materials (Fuji Plus and RelyX Luting) and the experimental variants of the control materials was chosen using a randomisation method whereby selection bias was avoided. Each

of the twelve groups, which consisted of twenty specimens (four batches of five) were prepared for each material (n=20). Every batch was assigned a number and prior to cement mixing the material under investigation was chosen at random. The powder and liquid were mixed as described previously in 4.3.1. (0.4g of powder and 0.2g of liquid was required to fabricate one sample of Fuji Plus group compared to 0.4g of powder and 0.25g of liquid for RelyX Luting group). Polytetrafluoroethylene (PTFE) bar-shaped moulds with internal dimensions of 25.0 ± 0.1 mm (length), 2.0 ± 0.1 mm (thickness), 2.0 ± 0.1 mm (width) were used to manufacture the samples (Figure 4.19). The mould was placed on a glass microscope slide, covered with acetate and filled with the mixed material from left to right. A second acetate strip was placed on the mould followed by a glass microscope slide and the mould assembly was clamped using two bulldog clips. The mould assembly was transferred to a water-bath maintained at 37 ± 1°C for 1 hour. Then the samples were removed from the water-bath, de-moulded and checked for any defects. Samples with defects or impurities (e.g. bubbles or chipped edges) were discarded. Flash was removed by hand-lapping the sample using P600 silicon carbide abrasive paper. Samples were then numbered and transferred into glass tubes filled with 50 mL deionised water for a further 23 hours (each batch of samples, which included five of the same material prepared at the same time, were immersed in individual glass tubes).

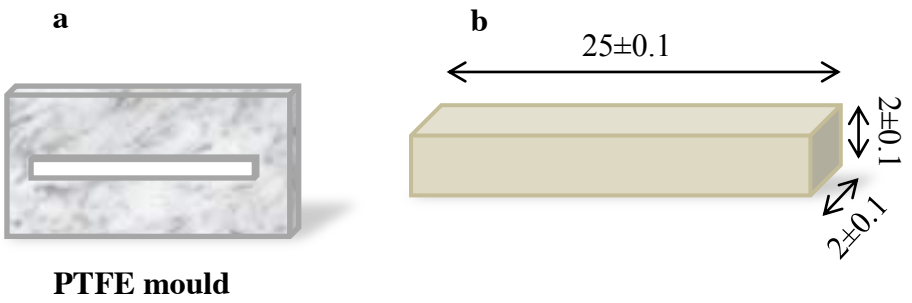

Figure 4.19 Schematic drawing of PTFE mould used to fabricate TFS specimens (a) and sample dimensions in mm.

4.3.9.2 Three point flexure strength testing (TFS) procedure:

24 hours from the start of mixing, samples were removed from the glass tubes, dried on filter paper as quickly as possible and loaded, in accordance with ISO 4049:2009, on a three-point flexure testing assembly, in a universal testing machine (Instron model 5565, High Wycombe, England). The three-point flexure apparatus included a central loading indenter and two point supports of 2mm diameter each, separated by a fixed loading span of 20mm. The bars were placed horizontally in the centre of the test apparatus supported by the two point support at each end (Figure 4.20).

A 100 N load cell was used at a cross-head speed of 1mm/min and the maximum load-to-failure (N) was recorded. The TFS was calculated using Equation (4.9).

$$TFS = 3PL/2bh^2 \qquad \text{(Equation 4.9)}$$

where P was the load to failure (N), L was the span which was constant (20 mm), b and h were the mean specimen thickness and mean specimen width (mm), which were measured using a digital micrometre accurate to 10 μm.

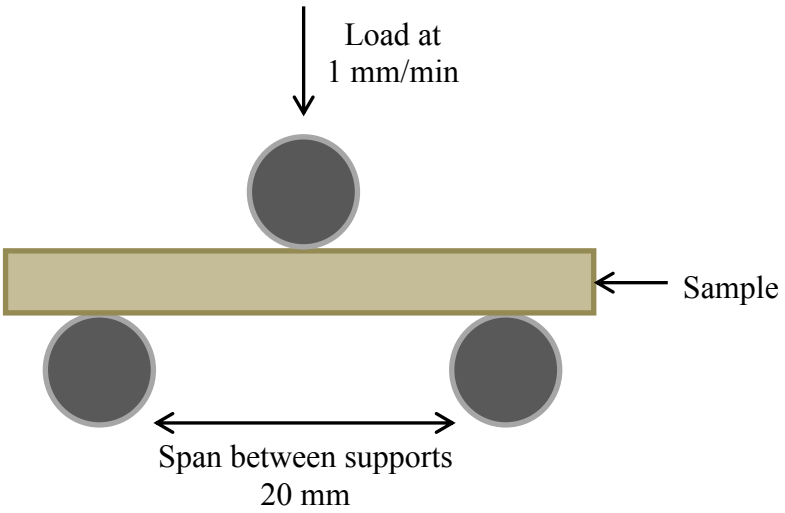

Figure 4.20 Schematic of TFS test apparatus.

Similar to CM, three-point flexure modulus (TFM) is an 'intrinsic material property' that can better highlight the overall structure of the material compared to the strength data (Braem, 1999). TFM takes into account both the specimen deflection following loading in the three-point flexure test and the load-to-failure. Therefore, TFM was calculated for each specimen using Equation 4.10.

$$TFM = \left(\frac{\Delta P}{\Delta D}\right) L^3/4bh^3 \qquad \text{(Equation 4.10)}$$

where $\frac{\Delta P}{\Delta D}$ was calculated as the slope of the steepest initial linear part of the load-deflection curve generated for each specimen, L, b and h have already been described above (Figure 4.21).

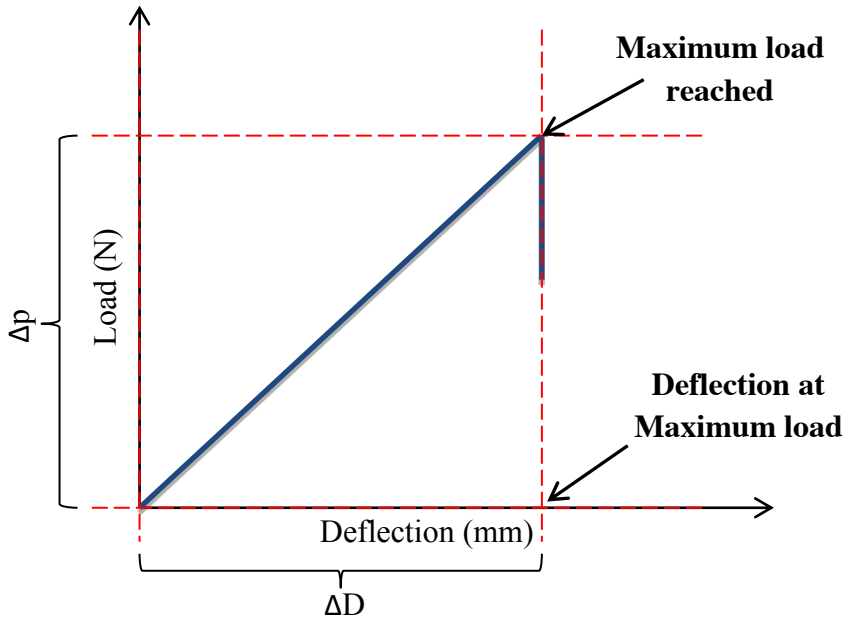

Figure 4.21 Schematic of load/deflection curve in TFS test used to calculate TFM.

4.3.9.3 Treatment of TFS and TFM data:

Means and standard deviations (SD) were calculated for samples of each material (n=20), and the results were subjected to statistically analyses using IBM SPSS Version 22 (Chicago, IL, USA) by comparing the means using One-way ANOVA test followed by the post-hoc Tukey test, at a significance level of p=0.05.

4.3.10 Cell culture:

The effect of the released components from RMGICs (commercial, home and novel) were tested on normal human dermal fibroblasts (NHDF) using a viability assay. The work was performed under the supervision of Professor Ken Parkinson in the Institute of Dentistry, Clinical for Diagnostic Oral Sciences, Queen Mary University of London.

4.3.10.1 Cells:

The normal human oral fibroblast line NHDF-1 fibroblast cells (Pitiyage *et al*., 2011) were obtained from a buccal mucosa biopsy, under ethical approval of the Dental Teaching Hospital, Peradeniya, Sri Lanka, following informed patient consent (Ethical Clearance Certificate No. FDS-ERC/2008/02/TIL). The cells were cultured and maintained at 37ºC in a humidified atmosphere of 10% CO_2/90% air in Dulbecco Modified Eagle's Medium (DMEM) supplemented with 10% vol/vol fetal bovine serum (FBS), penicillin, streptomycin and glutamine. Cells were seeded in a 96 well plate at a density of 9.32 x $10^3/cm^2$ in each well.

4.3.10.2 Sample preparation:

Samples were prepared according to the manufacturers recommendations (2:1 g:g of FP powder to liquid ratio for FP group materials and 1.6:1 g:g for the RelyX Luting group materials). The mixture was then packed in a teflon mould with internal dimensions of 5mm diameter and 2 mm thickness, placed on a glass slide/acetate sheet and then covered with another acetate sheet/glass slide. The assembly was then clamped together using bulldog clips and left to set in a temperature controlled room at 37ºC and ~30% humidity. Following setting, the samples were removed from the

moulds and each sample was then placed in a well containing 1-1.5 mL DMEM in a 24 well plate. Each sample had a surface area of 70.7 mm^2 and a surface to liquid ratio of 47.13 mm^2/mL. Afterwards, the 24 well plate containing one sample of each material (commercial FP and RX, Home, and novel RMGIC) and one well containing only medium, which served as negative control, were placed in an incubator maintained at 37°C and 10%CO_2/90% air for 24 hours. This experiment was repeated three times for the first set of samples and four times for the second set (see below).

4.3.10.3 Cytotoxicity testing procedure:

Following 24 hours, the medium containing the samples, and the negative control medium, were filter sterilised using Sterile Syringe Filter (VWR, Pennsylvania, USA). The medium in the wells containing the cells was gently aspirated and then 200 µL of the materials supernatants were placed in each well to a total of 4 wells per material; this was also performed for the negative control medium. The treated cells were then left in incubator for 72 hours at 37°C and 10%CO_2/90% air. This experiment was repeated 3 times to ensure reproducibility. Following incubation, the cell viability and number was tested using the MTT assay.

4.3.10.4 The MTT assay:

The MTT viability assay measures the mitochondrial dehydrogenase activity using MTT [3-(4, 5-dimethylthiazolyl-2)-2, 5-diphenyltetrazolium bromide], which is a yellow substrate that is then reduced by the active cells to generate a purple formazan. The latter can be subsequently measured using densitometry to give an indication of the amount of living cells.

Following 72 hours incubation of the cells, the medium in each well was gently aspirated and 200µL of MTT solution (0.5mg MTT to 1mL DMEM) was added to each well and incubated for 60 minutes at 37°C and 10%CO_2/90% air. Blank wells containing no cells were processed identically. At the end of one-hour incubation, medium containing MTT was carefully aspirated and then 200µL of dimethyl sulfoxide (DMSO) was suspended in each well. Then, the colour was quantified using a simple colorimetric assay at 570 nm absorbance to determine the optical density (OD) using an Optima Plate reader. The blank values were subtracted from the experimental values.

Cells viability was expressed as Equation 4.11:

$$Cell\ viability = {}^{OD\ (Test)}\Big/_{OD\ (Control)} \times 100 \qquad \text{(Equation 4.11)}$$

where OD (Test) was the optical density of the experimental medium and OD (Control) was that of the control medium.

As a result of the first triplicate experiment, no definite conclusion was drawn regarding the toxicity of the FP group materials, whilst RX group (commercial, home and novel) materials showed a definite cytotoxic reaction. Therefore, another set of experiments was performed which included only the FP group materials. The only difference between the first and the second set of experiments was that the samples had more surface area in the second experiment (282.8 mm^2) and the surface to liquid area was 141.4 mm^2/mL. The toxicity of the materials on cells was tested as neat aliquots with no dilution, and was also tested following dilution with a similar volume of DMEM.

4.3.10.5 Treatment of cell culture data:

Negative control data were used as 100% cell viability and compared with the viability of cells treated with materials substrate. Results were presented as mean ± standard deviation (SD) for all tested materials. Statistical significant differences were established using the unpaired Student's *t* test at a significance level of $p < 0.05$.

5 RESULTS

5.1 *Pilot studies:*

A significant amount of time was spent on conducting a number of pilot studies for:

1- Finding the optimum formulation for the novel liquid compositions (these results can be found in Appendix 1).

2- Water uptake - storage of samples prior to commencing both methods.

3- Developing and optimising HPLC techniques for each RMGIC (commercial, home and novel).

Pilot studies 2 and 3 were discussed in the materials and methods chapter.

5.2 *Water uptake, desorption, solubility, diffusion coefficient and dimensional changes of commercial and home materials following two methods: ISO 4049:2009 and without desiccation:*

The objective of this section was to compare water uptake/desorption and solubility of two commercial RMGICs and two home-made liquids with the corresponding commercial powder remaining the same (controls), in DW and AS following i) ISO-4049:2009, which involves desiccation of samples before immersion, and ii) immersion without desiccation. These experiments were carried out in order to choose an appropriate methodology to measure the water uptake of the novel cements since a suitable method for RMGICs has not been published in the literature. Manufacturers do not always give the exact composition of their products. Therefore two home liquids, corresponding to the respective commercial liquids, were also prepared so that any differences in results could be related back to the composition of the liquids.

In this project, labelling of materials will be as follows:

FP and RX = commercial materials, Fuji Plus and RelyX Luting, respectively.

FP home and RX home = home made liquids (were prepared according to the corresponding manufacturers MSDS) with commercial powders.

F1, F2, F3 and F4 = novel materials where liquids were prepared according to Fuji Plus formulation but with HEMA partially or fully replaced with THFM and/or HPM, and mixed with the corresponding commercial powder. Compositions are shown in Table 4.3.

R1, R2, R3 and R4 = novel materials where liquids were prepared according to RelyX Luting formulation but with HEMA partially or fully replaced with THFM and/or HPM, and mixed with the corresponding commercial powder. Compositions are shown in Table 4.4.

Water uptake and desorption data were obtained from commercial and home materials following the procedure described in 4.3.2. Percentage weight change was plotted against $t^{1/2}$ and the results were analysed for evidence of Fickian diffusion in the early stages of immersion during the two processes; a linear relationship indicated Fickian diffusion. Moreover, solubility and dimensional (volume) changes were also investigated for these materials.

5.2.1 Water uptake of commercial and home materials without desiccation in DW and AS:

Figures 5.1 and 5.3 plot percentage weight change (uptake) against square root of time (in seconds), for the commercial and home materials in this study (n=6),

immersed in DW and AS respectively without desiccation. Figures 5.2 and 5.4 show the initial water uptake up to 2 days (to demonstrate the relationship between uptake and square root of time during the initial stages), which were linear for both commercial and home materials. Figure 5.1 shows that in DW equilibrium appeared to be reached after $777s^{1/2}$ (~one week). At equilibrium, FP presented significantly higher weight change compared to all materials ($p<0.0001$). RX and RX home showed no significant differences in maximum weight change ($p=0.35$) but were higher than FP home ($p<0.0001$; FP 6.02 ± 0.33 %, RX 5.13 ± 0.25 %, RX home 4.80 ± 0.20 %, FP home 4.25 ± 0.20 %). The maximum percentage water uptake occurred in the first day for all materials (after $161.56s^{1/2}$ equivalent to ~7 hours) where FP (4.75 ± 0.37 %) and RX-Home (4.56 ± 0.18 %) had significantly higher uptakes compared to RX (4.17 ± 0.24 %) ($p\leq 0.013$) at this time point, and finally followed by FP home (3.10 ± 0.06 %; $p<0.0001$).

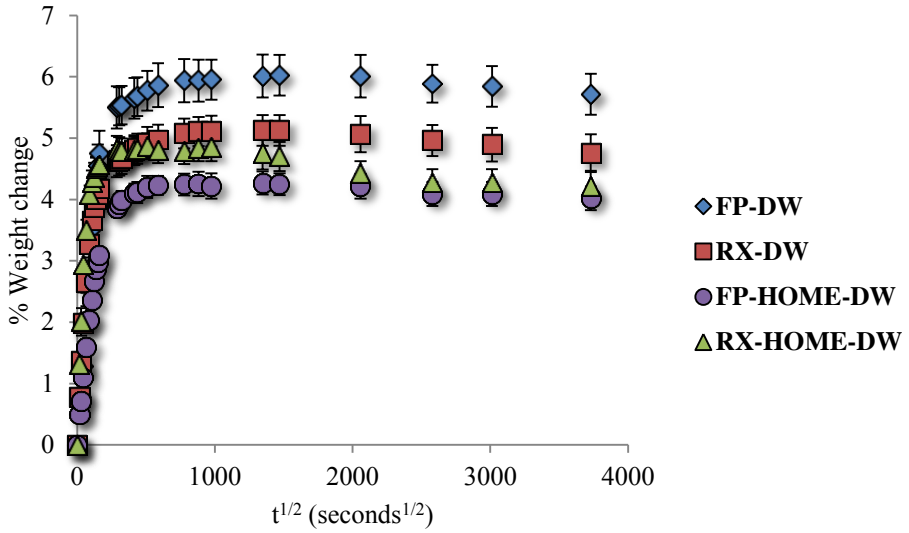

Figure 5.1 Percentage weight change of commercial (Fuji Plus, FP and RelyX Luting, RX) and home materials without desiccation (n=6) in DW up to 24 weeks.

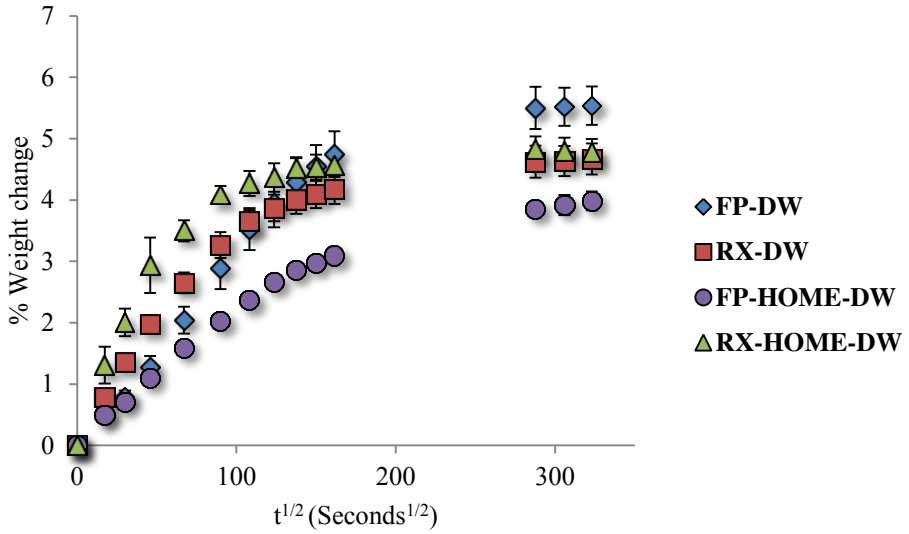

Figure 5.2 Early stages of water uptake for commercial and home materials (Fuji Plus, FP and RelyX Luting, RX up to two days; at ~323 $sec^{1/2}$) immersed in DW (without desiccation).

In AS (Figure 5.3) commercial materials FP and RX showed significantly higher maximum water uptake values (6.17 ± 0.08% and 5.95 ± 0.19% respectively) at ~1347$s^{1/2}$ (~4 weeks) compared to the home materials ($p<0.0001$). The maximum uptake appeared to occur in the first week. Both sets of materials began to lose weight after immersion in AS, after 3 weeks for the commercial materials, and 2 weeks for the home materials (Figure 5.3). All materials showed an initial linear region with $t^{1/2}$ (Figure 5.4).

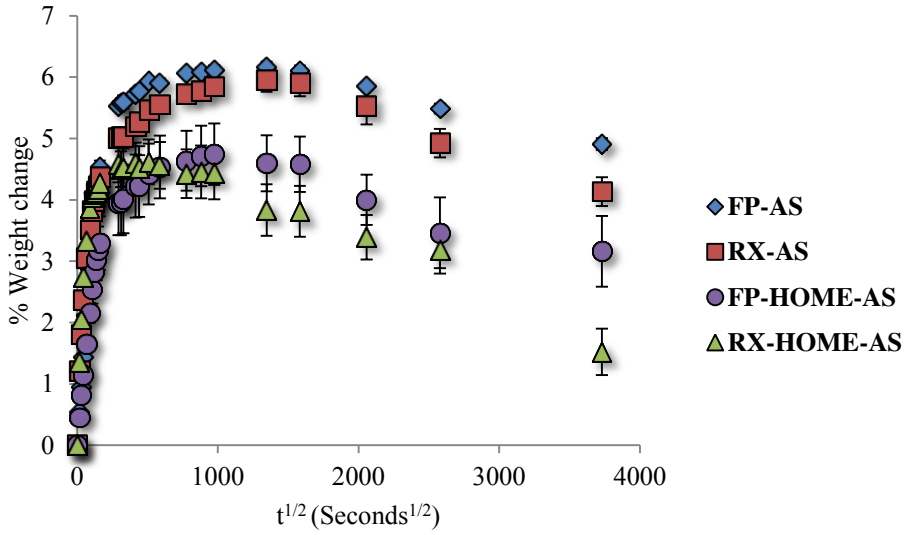

Figure 5.3 Percentage weight change of commercial and home materials (Fuji Plus and RelyX Luting) in AS up to 24 weeks (without desiccation).

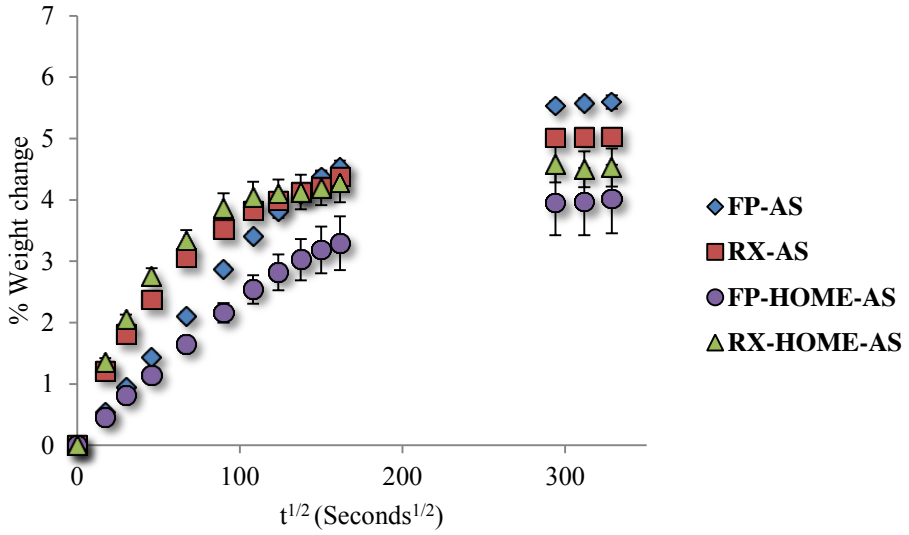

Figure 5.4 Early stages of water uptake for commercial and home materials (Fuji Plus and RelyX Luting up to two days; at ~323.11 $t^{1/2}$) immersed in AS (without desiccation).

5.2.2 Water desorption of commercial and home materials without desiccation:

After reaching equilibrium, samples were desorbed according to section 4.3.2. The desorption process was faster compared to water uptake, as it involved removing only water from the samples, whilst the water uptake consisted of, for example, water diffusing into the samples and components leaching out of the material. All the materials reached equilibrium weight loss in the first week. Figures 5.5 and 5.7 show plots of the percentage weight loss of commercial and home materials against time$^{1/2}$ in DW and AS, respectively and it can be seen that all materials appeared to have reached equilibrium, with significantly higher maximum loss values for RX home and RX compared to FP and FP home ($p<0.0001$) (12.50 ± 0.49 %, 11.74 ± 0.26 %, 8.95 ± 0.27 % and 8.33 ± 0.18 % respectively). Figures 5.6 and 5.8 show the early weight loss (up to 2 days) for all materials, which were linear to square root of time and thus followed Fick's law of diffusion (Figure 5.6 and 5.8).

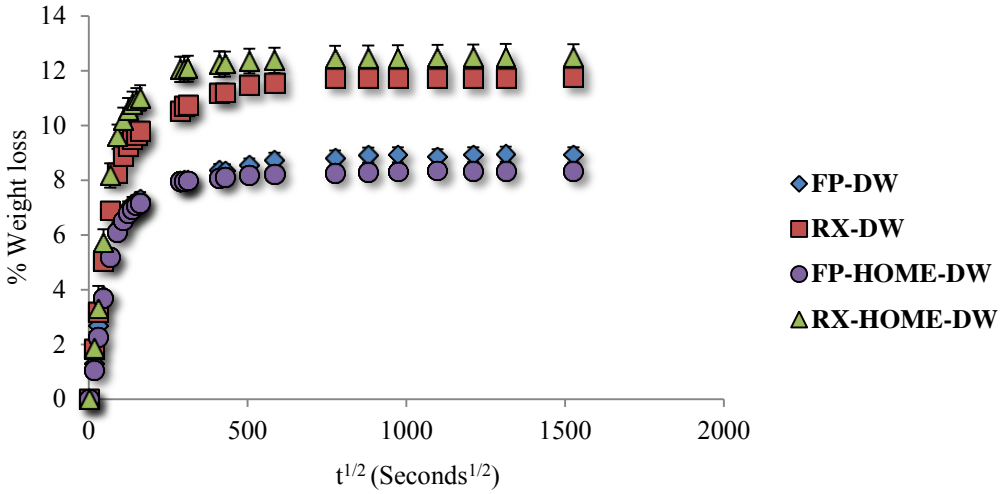

Figure 5.5 Percentage weight loss of commercial and home materials (Fuji Plus and RelyX Luting) (without desiccation-DW).

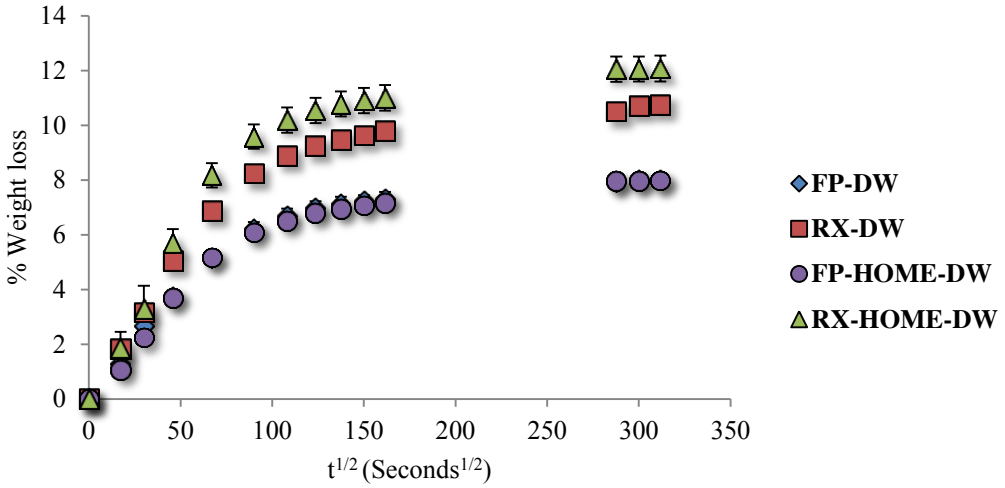

Figure 5.6 Early stages of desorption of commercial and home materials (Fuji Plus and RelyX Luting up to two days; at ~323.11 $t^{1/2}$) (without desiccation-DW).

The desorption plots of commercial and home materials immersed in AS showed similar trends to the materials immersed in DW with initial linear regions (Figure 5.8). Moreover, similarly to DW, weight loss from RX and RX home was significantly higher (12.43 ± 0.22% and 12.51 ± 0.19% respectively) compared to FP and FP home (9.22 ± 0.18% and 8.36 ± 0.19%; $p<0.0001$).

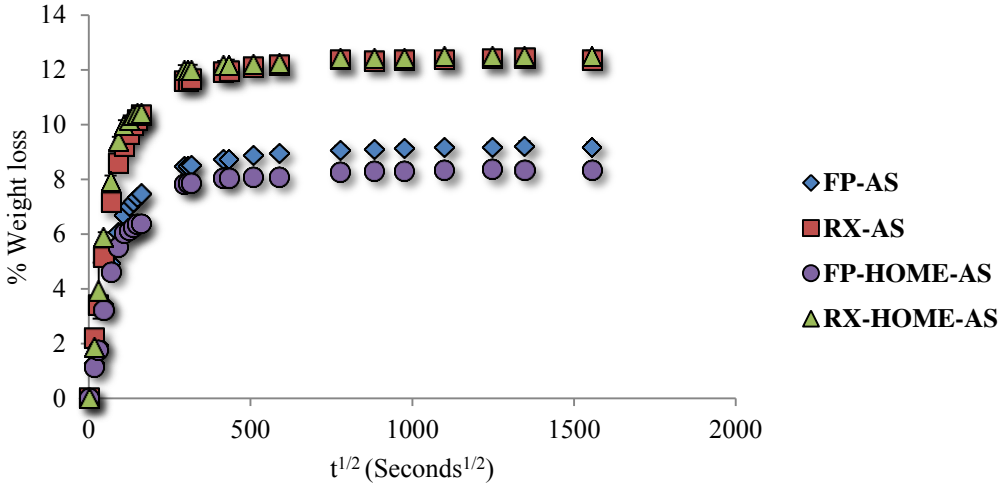

Figure 5.7 Percentage weight loss of commercial and home materials (Fuji Plus and RelyX Luting) (without desiccation-AS).

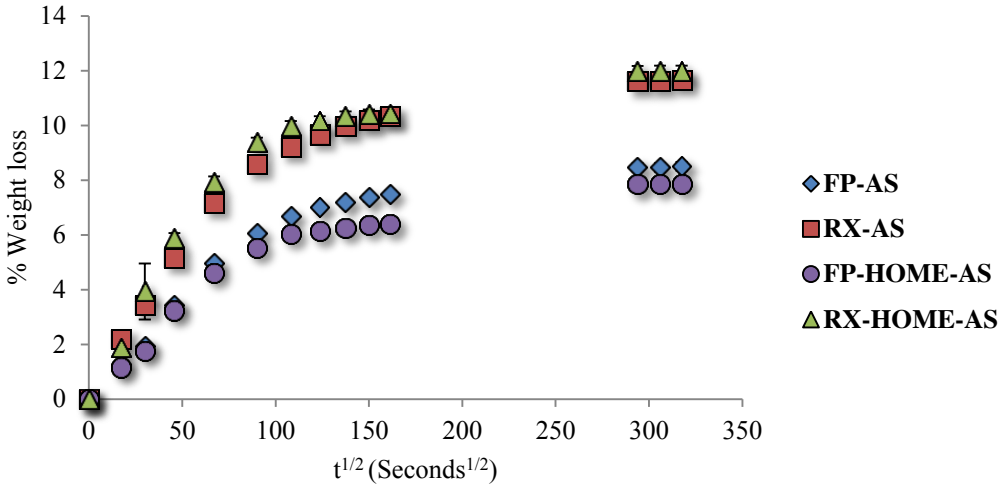

Figure 5.8 Initial desorption of commercial and home materials (Fuji Plus and RelyX Luting up to two days; at ~323.11 $t^{1/2}$) (without desiccation-AS).

5.2.3 Water uptake of commercial and home materials following ISO 4049:2009 in DW and AS:

The ISO 4049:2009 water uptake protocol involved desiccation of samples before immersion in solution. Samples were considered ready for the water uptake experiment when the change in sample weight was not more than 0.1 mg in any 24 hours' period; this process of sample desiccation took approximately 10 days. Following desiccation, the samples were immersed in the respective solutions (DW or AS) and the experiment was carried out as described in 4.3.2.1.

Figures 5.9 and 5.11 show the weight change of the commercial materials FP, RX and home controls in DW and AS respectively, with Figures 5.10 and 5.12 showing the initial 2-day period. All materials appeared to have reached equilibrium in DW. Noticeably, the uptake of all systems had increased from a maximum of 6% by the without desiccation method, to a maximum of ~14% by the ISO 4049:2009 method.

This will be discussed in the next chapter. In Figure 5.9 it can be seen that RX home had a higher maximum water uptake compared to RX in DW ($p<0.0001$; 14.27 ± 0.52 % and 13.30 ± 0.17 %) and the two values were higher than the ones noted for FP and FP home ($p<0.0001$; 10.07 ± 0.23 % and 9.56 ± 0.22 %). For all materials the majority of water uptake occurred in the first week of immersion followed by only a small increase until equilibrium was reached.

Initial water uptake region for all materials in DW (Figure 5.10) showed that uptake was not linear to $t^{1/2}$ and this is an indication that it was non-Fickian and thus Fick's second law of diffusion could not be applied and, consequently, diffusion coefficient values could not be calculated.

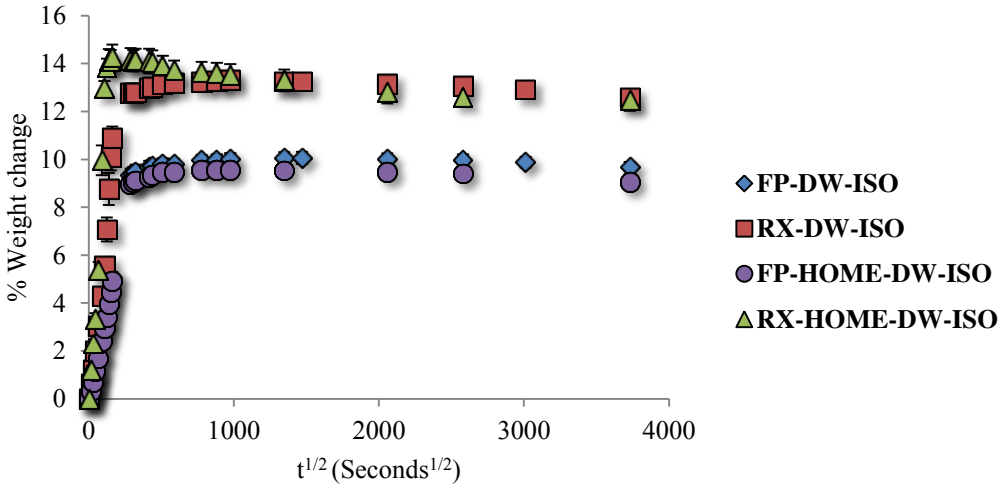

Figure 5.9 Mean water uptake of commercial and home materials (FP and RX) in DW following ISO 4049:2009 up to 24 weeks (~3729 $sec^{1/2}$).

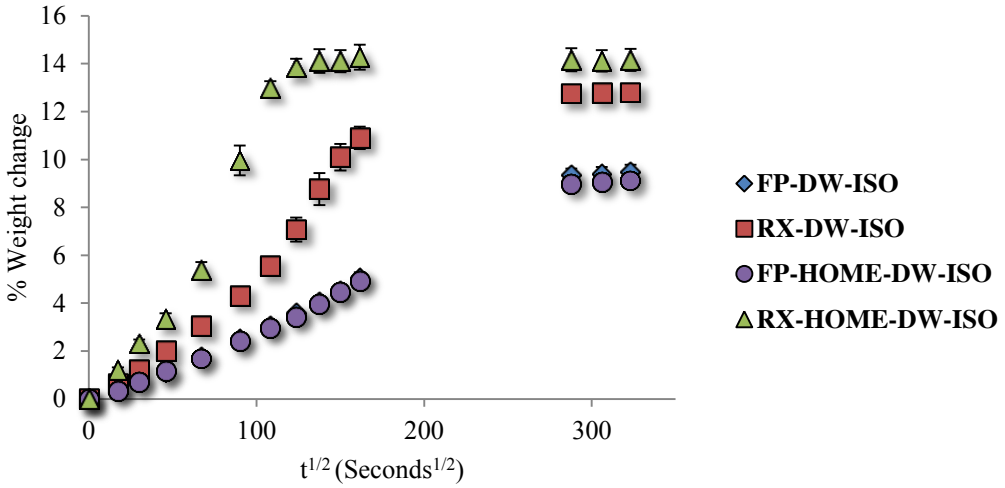

Figure 5.10 Early stages of water uptake of commercial and home (FP and RX) in DW following ISO 4049:2009 up to two days (at ~323.11 $t^{1/2}$).

In Figure 5.11 water uptake in AS following the ISO method for all materials showed comparable results to materials immersed in DW, with higher values for RX and RX home compared to FP and FP home ($p<0.0001$; 13.64 ± 0.20 %, 13.83 ± 0.15 %, 9.53 ± 0.14 %, 9.71 ± 0.15 respectively). Also, similar to the materials immersed in DW, the early uptake showed non-linear regions against $t^{1/2}$, which indicated non-Fickian diffusion (Figure 5.12). In order to identify the type of diffusion occurring in the ISO method, mean percentage water uptake for all materials (commercial and home) in DW and AS were plotted against linear time (seconds) in Figures 5.13 and 5.14. The plots were linear to time, which indicates Case II diffusion.

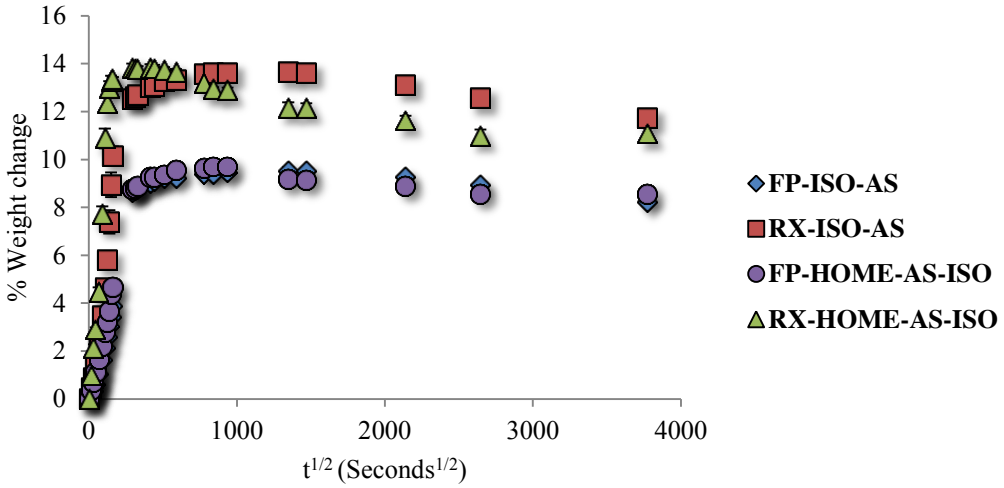

Figure 5.11 Mean water uptake of commercial and home materials (FP and RX) in AS following ISO 4049:2009 up to 24 weeks (~3729 $sec^{1/2}$).

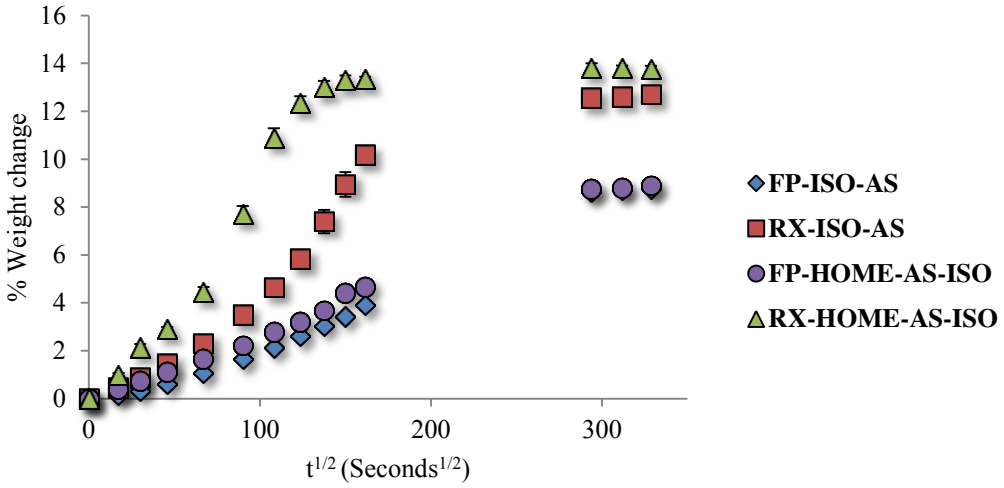

Figure 5.12 Early stages of water uptake of commercial and home (FP and RX) in AS following ISO 4049:2009 up to two days (~323.11 $t^{1/2}$).

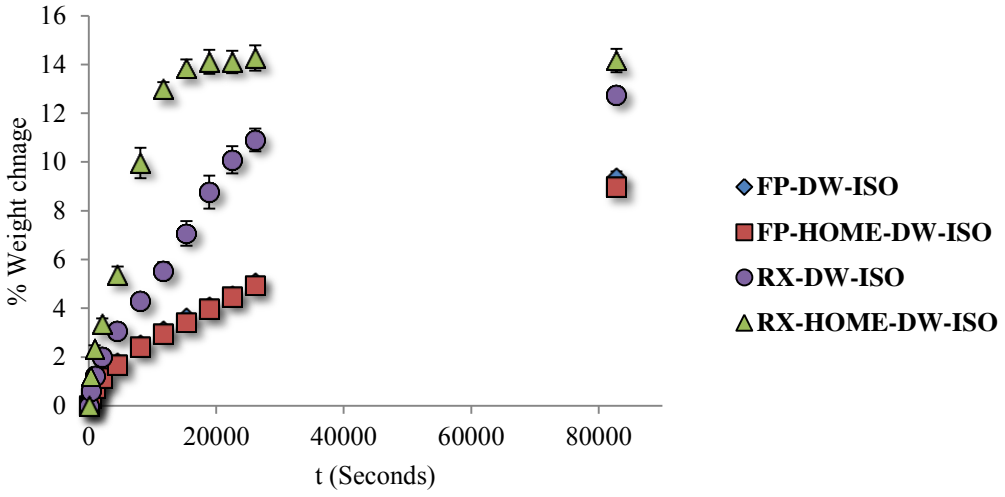

Figure 5.13 Early stages of water uptake of commercials and home (FP and RX) in DW following ISO 4049:2009 up to two days against time in seconds.

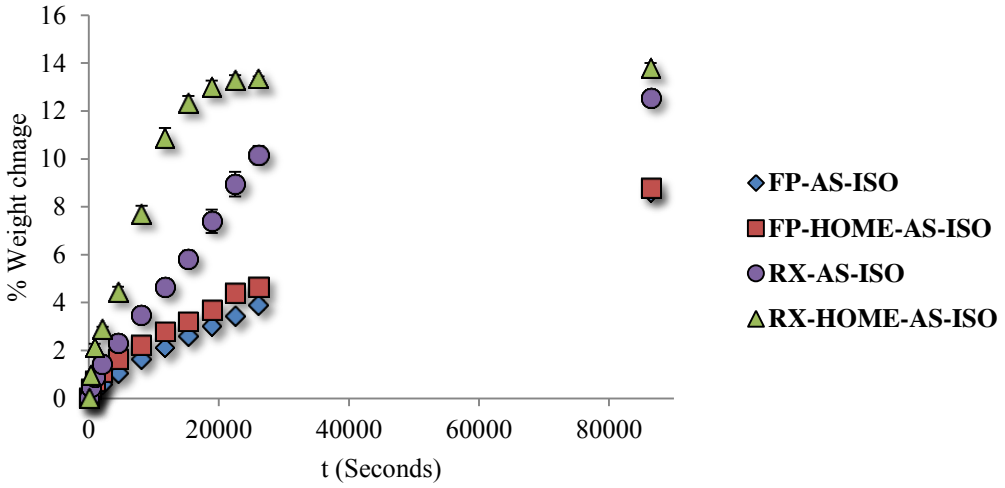

Figure 5.14 Early stages of water uptake of commercials and home (FP and RX) in AS following ISO 4049:2009 up to two days against time in seconds.

5.2.4 Desorption of commercial and home materials following ISO 4049:2009 in DW and AS:

Figures 5.15 and 5.16 give the desorption results for all materials in both DW and AS respectively and show comparable trends to those for water uptake (RX and its corresponding home exhibited higher values compared to FP and FP home;

p<0.0001). However, it was noticeable that the initial water loss behaviour plots were linear to $t^{1/2}$ indicating that desorption of all samples was by Fickian diffusion and not Case II as for the uptake process by this method.

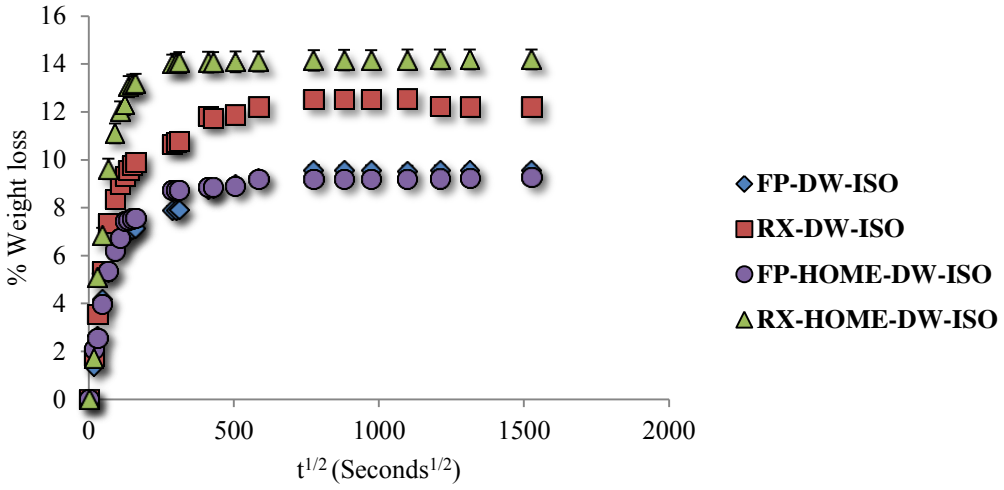

Figure 5.15 Mean percentage weight loss of commercial and home materials (FP and RX) following ISO 4049:2009 (DW) up to 5 weeks (~1528 $sec^{1/2}$).

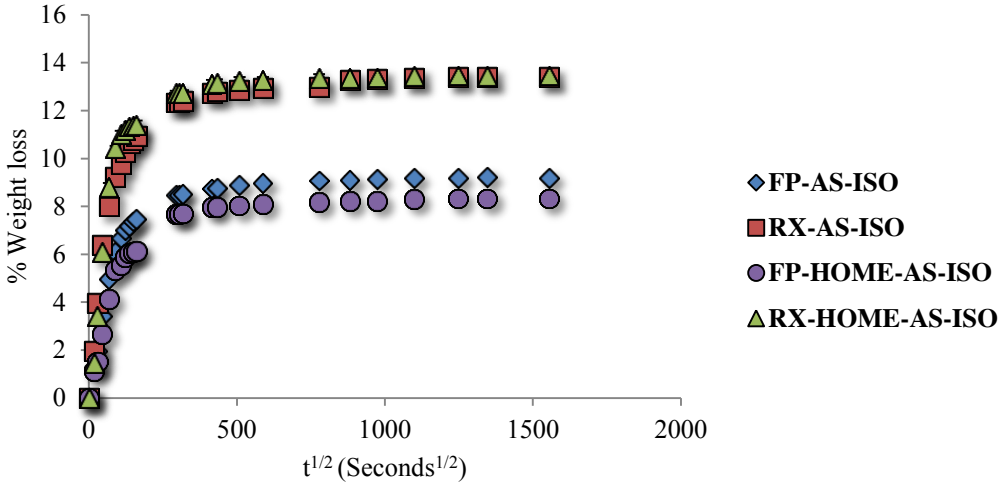

Figure 5.16 Mean percentage weight loss of commercial and home materials (FP and RX) following ISO 4049:2009 (AS) up to 5 weeks (~1528 $sec^{1/2}$).

5.2.5 Diffusion coefficient (Dabs) for water uptake:

Diffusion coefficients for the water uptake experiments were only calculated for samples under the without desiccation method, since plots from the ISO 4049:2009 method were non-linear to $t^{1/2}$; these did not follow Fick's laws of diffusion.

Figure 5.17 plots uptake for commercial and home materials as M_t/M_∞ against $t^{1/2}$ in DW (where M_t is uptake at a time and M_∞ is uptake at equilibrium). Plots for all materials were linear to $t^{1/2}$ in both solutions. The slope of the initial linear region up to $M_t/M_\infty = 0.05$ was determined and was used to calculate Dabs values according to Equation 2.4 in 2.3.1.2. The Dabs values are presented in Table 5.1 for samples immersed in DW. The diffusion coefficients for FP, both commercial and home were lower than the RX group, for water uptake. Dabs values for samples immersed in AS could not be calculated since they showed no signs of equilibrium after 24 weeks immersion.

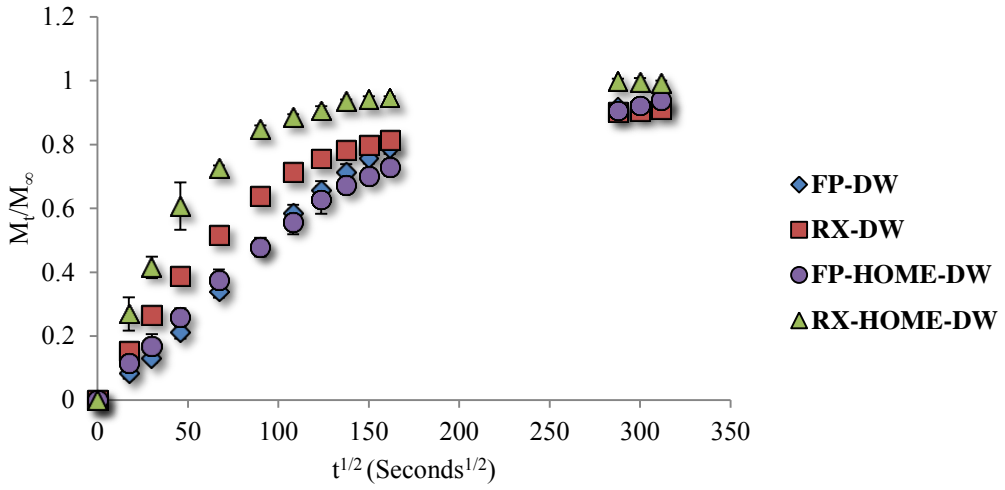

Figure 5.17 A representative figure of mean $M_t/M\infty$ uptake of commercial and home (FP and RX) in DW up to M_t/M_∞=1.

Table 5.1 Dabs values (m^2 sec^{-1}) of commercial and home materials immersed in DW for the without desiccation method.

Material	FP in DW (m^2 sec^{-1})	RX in DW (m^2 sec^{-1})
Commercial	$5.84X10^{-12}$	$1.92X10^{-11}$
Home	$7.72X10^{-12}$	$5.1X10^{-11}$

5.2.6 Diffusion coefficients for desorption (Ddes):

All materials from both experiments (without desiccation and ISO 4049:2009) showed a linear relationship when plotted as M_t/M_∞ against $t^{1/2}$ and, therefore, Ddes values were calculated as described in section 4.3.2.1. The results are presented in Table 5.2. Figure 5.18 is a representative example of M_t/M_∞ plots for desorption from which the slopes were obtained, and used to calculate Ddes values.

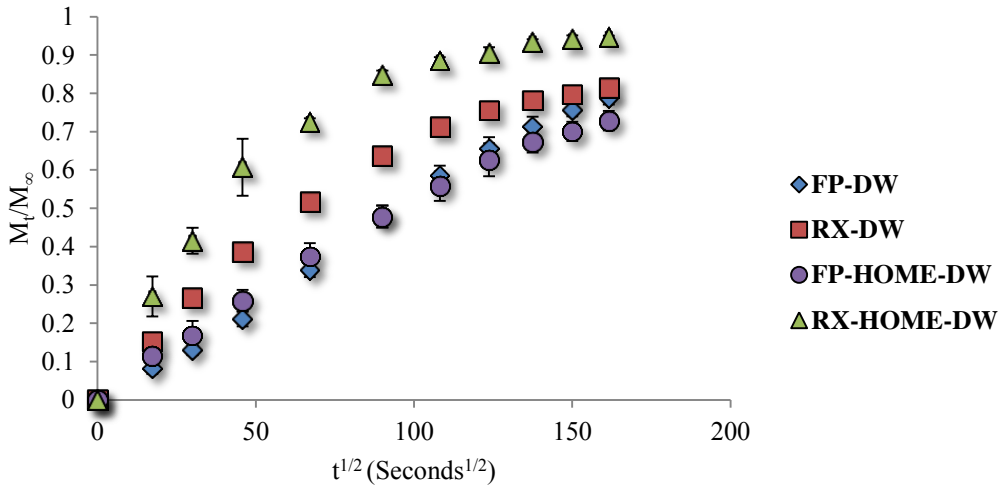

Figure 5.18 A representative figure of mean M_t/M_∞ desorption of commercial and home (FP and RX-DW) up to M_t/M_∞=1.

Table 5.2 Ddes values (m^2 sec^{-1}) of commercial and home in DW and AS following both methods-without desiccation (non-ISO) and ISO 4049:2009.

Material	FP in DW (m^2 sec^{-1})	RX in DW (m^2 sec^{-1})	FP in AS (m^2 sec^{-1})	RX in AS (m^2 sec^{-1})
Commercial (non –ISO)	$4.12X10^{-11}$	$3.86X10^{-11}$	$1.24X10^{-11}$	$2.22X10^{-11}$
Home (non-ISO)	$1.09X10^{-11}$	$2.67X10^{-11}$	$1.17X10^{-11}$	$1.62X10^{-11}$
Commercial ISO	$1.91X10^{-11}$	$1.87X10^{-11}$	$2.47X10^{-11}$	$1.04X10^{-11}$
Home ISO	$4.14X10^{-11}$	$1.69X10^{-11}$	$1.02X10^{-11}$	$1.55X10^{-11}$

Ddes values presented (Table 5.2) for the FP group showed faster diffusion compared to Dabs values (Table 5.1) for the same material. This is not the case for RX group with only small differences between Dabs and Ddes.

5.2.7 Solubility of commercial and home materials immersed in DW and AS in both methods:

Solubility was calculated as described in 4.3.2.1. and the results are presented in Table 5.3 below.

Table 5.3 Solubility % (SD) of commercial and home materials (FP and RX) in both DW and AS following both methods: without desiccation and the ISO 4049:2009.

Material	Method	Solution	Solubility % (SD)
FP	Without desiccation	DW	3.72 (0.14)
		AS	4.73 (0.15)
	ISO 4049	DW	0.77 (0.11)
		AS	1.78 (0.09)
FP Home	Without desiccation	DW	4.58 (0.15)
		AS	5.46 (0.43)
	ISO 4049	DW	0.73 (0.06)
		AS	0.45 (0.12)
RX	Without desiccation	DW	7.53 (0.31)
		AS	8.74 (0.06)
	ISO 4049	DW	1.17 (0.09)
		AS	3.23 (0.11)
RX Home	Without desiccation	DW	8.56 (0.2)
		AS	11.18 (0.36)
	ISO 4049	DW	3.38 (0.28)
		AS	3.89 (0.05)

Significantly lower solubility results were observed for the ISO 4049:2009 method compared to the method without desiccation for all materials tested ($p<0.0001$; Table 5.3). For the method without desiccation, higher solubility results were noticed for materials immersed in AS compared with DW ($p<0.0001$).

5.2.8 Dimensional (volume) changes of commercial and home materials prepared with and without desiccation:

Figures 5.19 and 5.20 show the mean dimensional (volume) changes (percentage) for samples without desiccation and following ISO 4049:2009 in DW and AS. Materials that underwent desiccation showed higher changes compared to the ones without desiccation ($P<0.0001$).

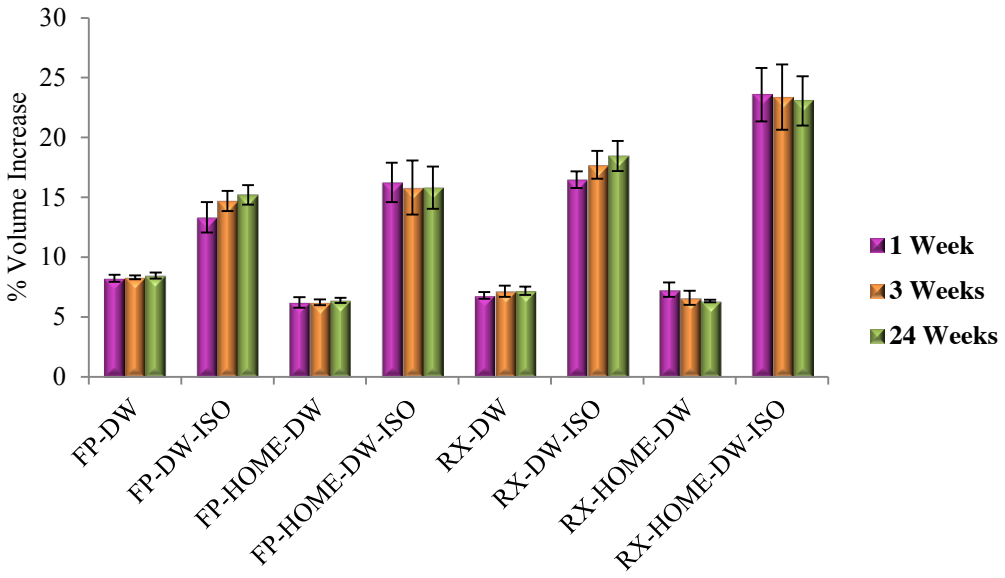

Figure 5.19 Percentage dimensional (volume) changes of commercial and home materials (FP and RX) prepared with (ISO) and without desiccation (non-ISO) immersed in DW at 1, 3 and 24 weeks immersion.

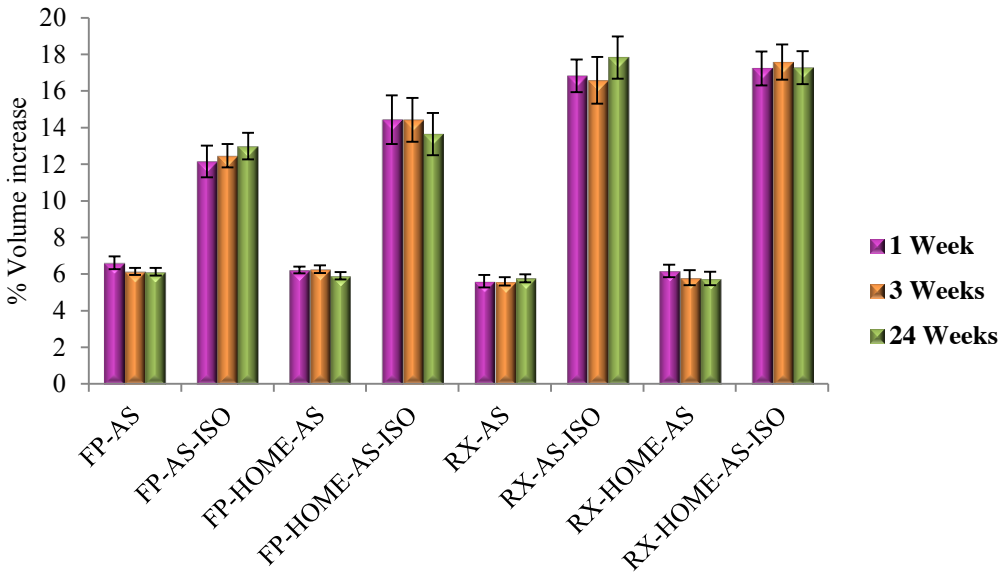

Figure 5.20 Percentage dimensional (volume) changes of commercial and home materials (FP and RX) prepared with (ISO) and without desiccation (non-ISO) and immersed in AS at 1, 3 and 24 weeks immersion.

5.3 *Water uptake, desorption, diffusion coefficient, solubility and dimensional (volume) changes of novel, commercial and home materials:*

At this stage it should be noted that the subsequent water uptake experiments on novel, commercial and home materials followed the method without desiccation (non-ISO). The latter showed water uptake and desorption results that were not exaggerated and, mimicked the clinical situation compared to the ISO 4049:2009 method, since these materials are placed directly in the mouth without initial desiccation.

5.3.1 Water uptake of novel materials in DW:

Percentage mean water uptake was plotted against $t^{1/2}$ and is presented in Figures 5.21 and 5.22 for FP and RX groups respectively. Commercial and home materials uptakes (previously presented in section 5.1) are also included in the plots in order to

show the differences between the novel compositions and the commercial/home materials.

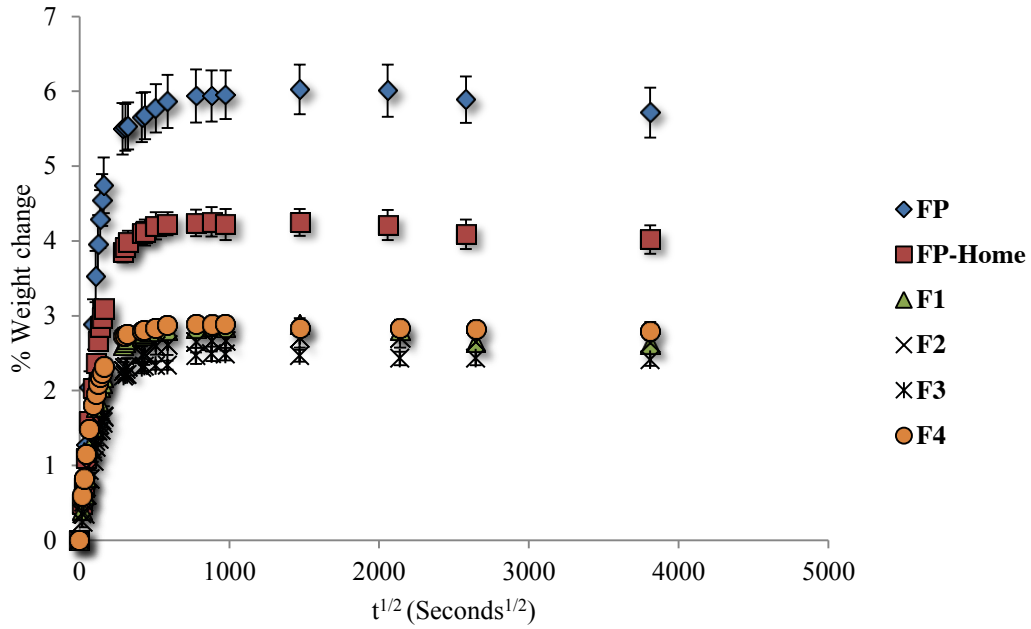

Figure 5.21 Mean water uptake of novel, commercial and home materials in the FP group immersed in DW for up to 24 weeks (~3729 $sec^{1/2}$).

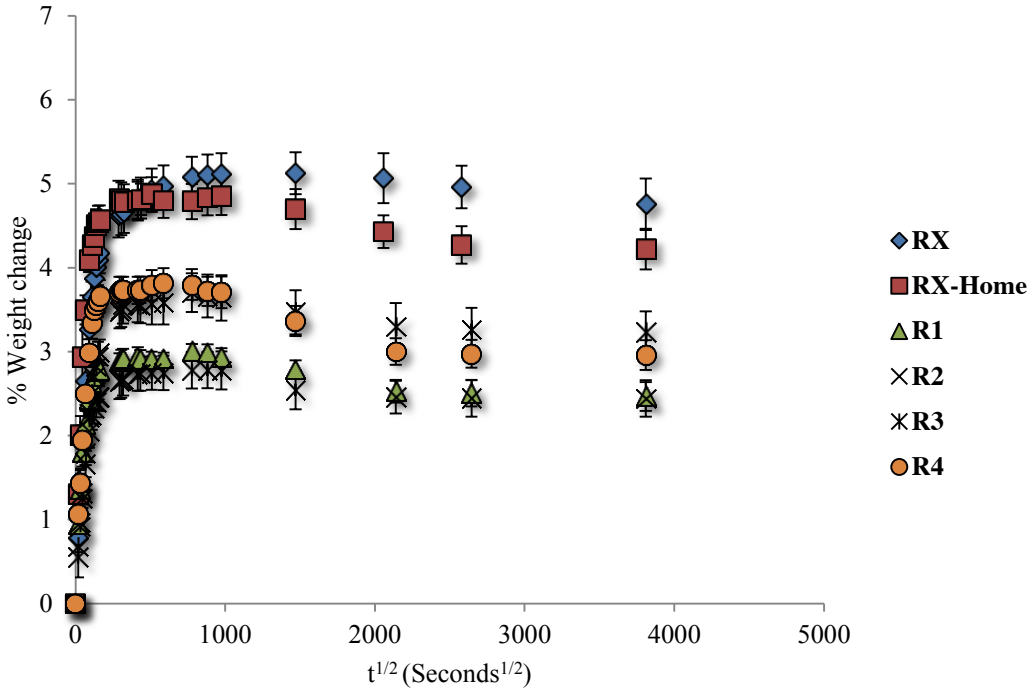

Figure 5.22 Mean water uptake of novel, commercial and home materials following RX composition immersed in DW for up to 24 weeks (~3729 $sec^{1/2}$).

All novel compositions showed lower maximum water uptake (weight changes) compared to their commercial and home counterparts ($p<0.0001$) up to 24 weeks. As shown in Figure 5.21, although FP home presented with lower water uptake (4.25 ± 0.19%) compared to the commercial FP (6.02 ± 0.33%: $p<0.0001$), it was higher than all novel materials ($p<0.0001$). Compositions F1, F2 and F4 showed similar water uptake ($p\leq1$), F3 exhibited the lowest maximum water uptake compared to all materials in the FP group except for F2 ($p=0.716$). The values for the novel compositions (F1, F2, F3 and F4) ranged from 2.89 ± 0.08 to 2.50 ± 0.10%.

As can be seen in Figure 5.22, a lower water uptake was shown for all RX novel compositions when compared with commercial and RX-Home ($P<0.0001$), especially for composition R1, which contained only HPM as a monomer, and R2 which contained THFM and HPM (3.00 ± 0.09% and 2.78 ± 0.22% respectively).

Higher water uptakes can be seen for compositions R3 and R4 (3.70 ± 0.23% and 3.81 ± 0.18% respectively), containing HEMA (50%)/THFM (50%) and HEMA (70%)/THFM (30%) respectively, which could be associated with HEMA. This water uptake behaviour was not seen in the novel FP group of materials containing THFM and HEMA (F3). The rationale behind proposing the compositions containing 70% HEMA and 30% THFM were to understand the higher values of R3. In theory, the increase in HEMA content in both liquids (FP and RX) should increase water uptake. This was not the case and so the proposed explanation is that there may be additional cross-linking occurring between HEMA and UDMA (a component of FP, not in RX), which could affect the uptake. The water uptake results for these two compositions are presented in Figure 5.23.

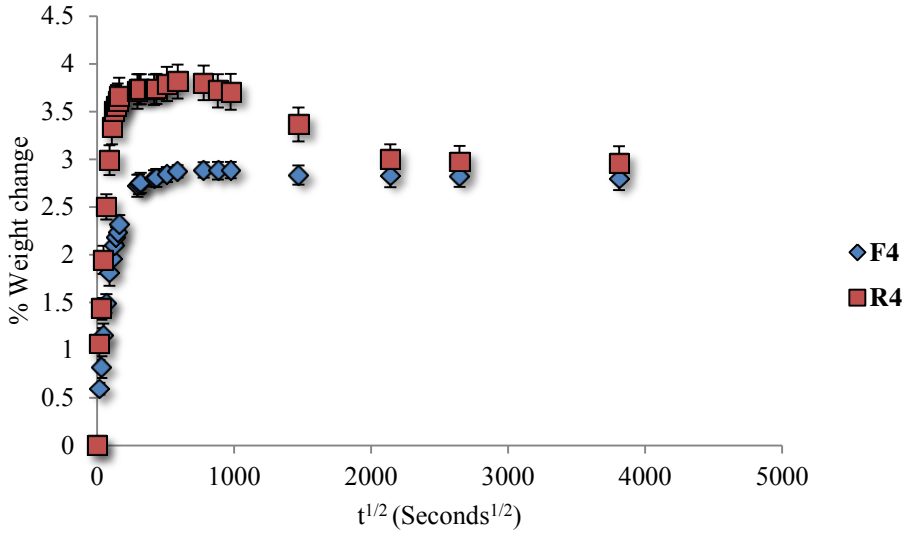

Figure 5.23 Percentage mean water uptake of compositions F4 and R4 replacing only 30% HEMA with THFM immersed in DW up to 24 weeks (~3729 $sec^{1/2}$).

In the FP group, even with a higher percentage of HEMA (70%) in F4, the water uptake was similar to F1 and F3 (%HEMA between 0 and 50; $p \leq 1$). This may indicate crosslinking between HEMA, THFM and UDMA that has led to a lower

water uptake, compared to the compositions in the RX group that do not contain UDMA. This will be discussed further in the discussion chapter.

5.3.2 Water uptake of novel materials in AS:

As with water uptake in DW, novel, commercial and home materials plots were presented against $t^{1/2}$ in Figures 5.24 and 5.25 for FP and RX groups respectively. Following an initial rapid weight increase, the materials lost weight and did not reach equilibrium during 24 weeks immersion.

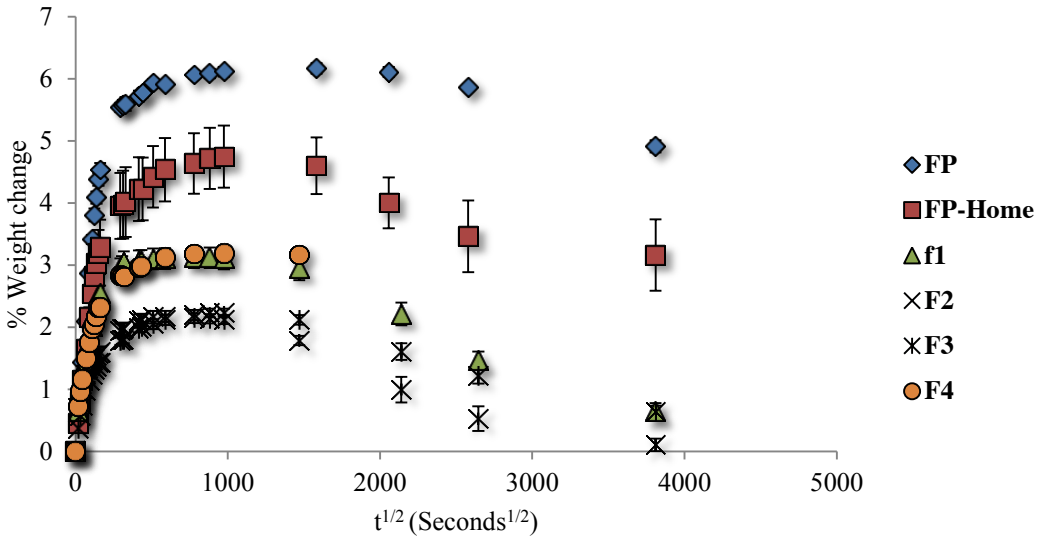

Figure 5.24 Mean water uptake of novel, commercial and home FP compositions in AS up to 24 weeks (~3729 $sec^{1/2}$).

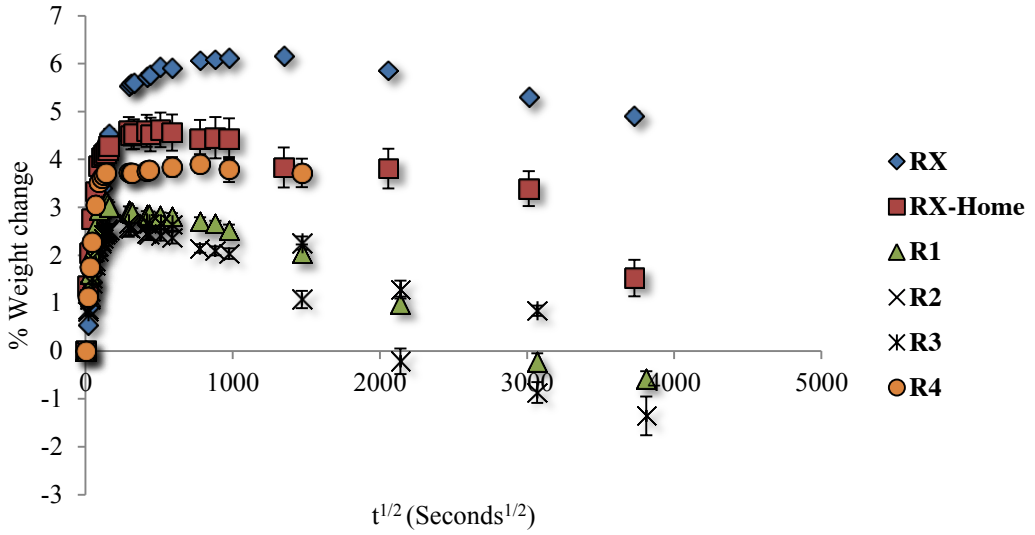

Figure 5.25 Mean water uptake of novel, commercial and home RX compositions in AS up to 24 weeks (~3729 $sec^{1/2}$).

All compositions immersed in AS showed similar trends, losing weight following the second week of immersion. Both commercial materials showed significantly higher maximum uptake in AS compared to all other compositions in their groups ($p<0.0001$). The two home materials had statistically similar maximum water uptake ($p=0.921$), which was lower than the two commercial materials but higher than all novel materials in both groups ($p<0.0001$). Figure 5.24 shows that compositions F2 (2.24 ± 0.06%) and F3 (2.14 ± 0.08%) had lower water uptake than all other FP materials in AS, compared to their commercial (6.11 ± 0.08%) and home (4.74 ± 0.50%) counterparts. Compositions F1 and F4 ($p=1$) presented significantly higher maximum water uptakes compared to the other novel compositions in their group ($p<0.0001$).

Comparing uptakes in DW and AS, maximum water uptake of FP commercial was statistically similar in DW and AS ($p=0.993$), while the home material had a higher uptake in AS compared to DW ($p<0.0001$). Similar water uptake values in DW and

AS were observed for composition F1 (that contained 100% HPM as a monomer; p=0.816), F3 (with similar amounts of HEMA and THFM; p=0.265) and F4 (containing 70% THFM and 30% HEMA; p=0.466). However, F2 (70% HPM and 30% THFM) had a higher maximum uptake in DW compared to when immersed in AS (p=0.026).

Figure 5.25 shows that all novel materials in the RX group had lower maximum water uptakes compared to their commercial and home counterparts in AS (p<0.0001). RX commercial (5.95 ± 0.19%) and RX home (4.62 ± 0.36%) had the highest maximum weight change values followed by R4 (3.92 ± 0.20%). Although compositions R2 and R3 presented with low water uptake in AS (2.56 ± 0.15% and 2.67 ± 0.14%), the uptakes of R3 and R1 were not statistically different (p=0.094).

Maximum water uptake of commercial RX was the highest compared to all materials in the RX group whether immersed in DW or AS (P<0.0001). R3 had a significantly higher water uptake (3.7 ± 0.23%) in DW compared with AS (2.66 ± 0.13%; P<0.0001). The other three compositions in the RX group (R1, R2 and R4) presented with comparable results, whether immersed in DW or AS (p≥0.809).

5.3.3 Desorption of novel materials in DW:

The procedure described in 4.3.2.1 was followed and results of mean weight loss against $t^{1/2}$ in seconds are presented in Figures 5.26 and 5.27 for FP and RX respectively. All formulations, except F4 in the FP group, showed lower weight losses compared to the commercial FP (P<0.0001). However, the compositions containing 50% and 70% HEMA with THFM (F3 and F4) showed comparable maximum weight losses (8.22 ± 0.13%) compared to the home material (8.33 ±

0.18%) ($p \leq 0.999$). Statistically similar weight losses were observed for F1 and F2 in DW (7.27 ± 0.18% and 6.85 ± 0.10%) ($p=0.092$), which were lower than all other materials in FP group ($p<0.0001$).

All materials appeared to have reached an apparent equilibrium and the weight was virtually stabilised after only one week ($t^{1/2}$ ~777).

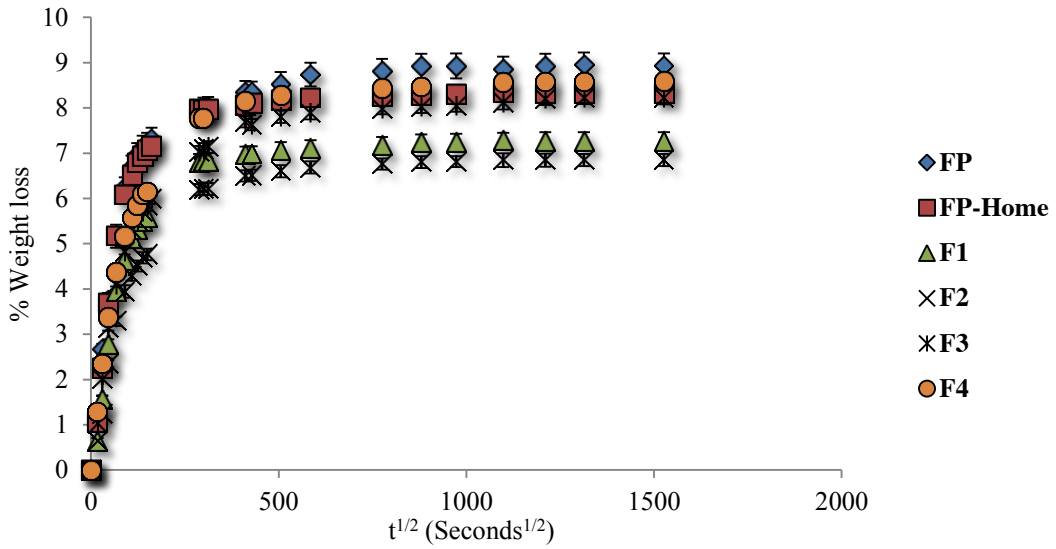

Figure 5.26 Mean percentage weight loss of commercial, home and novel FP materials in DW up to 5 weeks.

Weight losses for all novel compositions were lower than RX (11.74 ± 0.26%) and RX-home (12.49 ± 0.49%; $p<0.0001$; Figure 5.27). Compositions R1, R2 and R3 showed similar maximum weight losses following 5 weeks of desorption, ranging from 10.64 ± 0.25% for composition R1, 10.38 ± 0.15% for composition R2 and 10.46 ± 0.16% for composition R3 ($p \leq 1$). Although for R4 the weight loss was higher than R2 and R3 ($p \leq 0.013$) it was similar to R1 ($p=0.313$) and lower than both commercial and home RX ($p<0.0001$). Similar to the FP group, main weight loss appeared to be reached following one week of desorption ($t^{1/2}$ ~777)

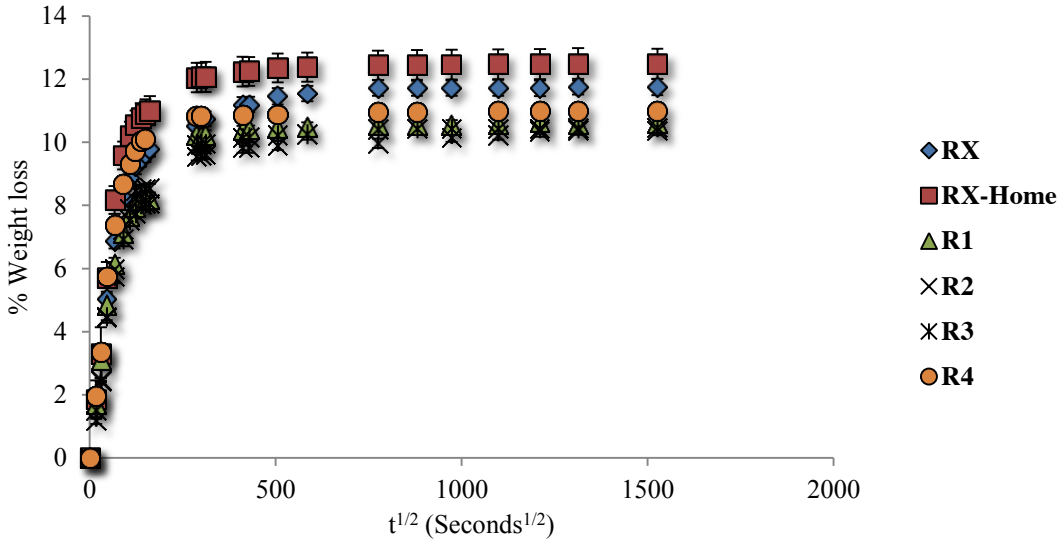

Figure 5.27 Mean percentage weight loss of commercial, home and novel RX materials in DW up to 5 weeks.

Initial desorption results for all materials (FP and RX groups) were linear to $t^{1/2}$, and thus, the diffusion of water out of the samples followed Fick's law of diffusion; hence Ddes values were calculated.

5.3.4 Desorption of novel materials in AS:

Figures 5.28 and 5.29 show the mean weight losses of commercial, home and novel materials in FP and RX groups respectively (following immersion in AS). FP commercial showed the highest weight loss (9.22 ± 0.18%) compared to all other materials in this group (home and novel; $p<0.0001$). This was followed by F1 and FP home, both with similar weight losses (8.55 ± 0.24% and 8.36 ± 0.19%; $p=0.887$) but higher than F2, F3 and F4. F4 showed the lowest value compared to all materials but the difference was not significant compared to F3 ($p=0.575$).

In the RX group, R1 and R2 showed statistically similar weight losses compared to commercial and home RX ($p \leq 1$). Weight loss of R3 was lower than the former compositions but still significantly higher than R4 ($p<0.0001$), which exhibited with the lowest water loss compared to all other compositions in the same group ($p<0.0001$).

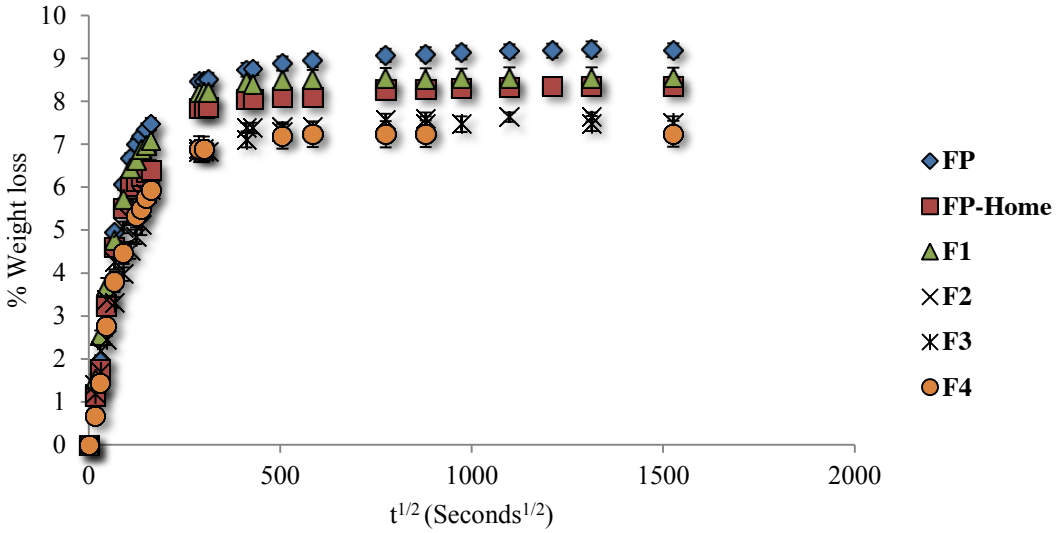

Figure 5.28 Mean weight loss of commercial, home and novel materials in the FP group-AS up to 5 weeks.

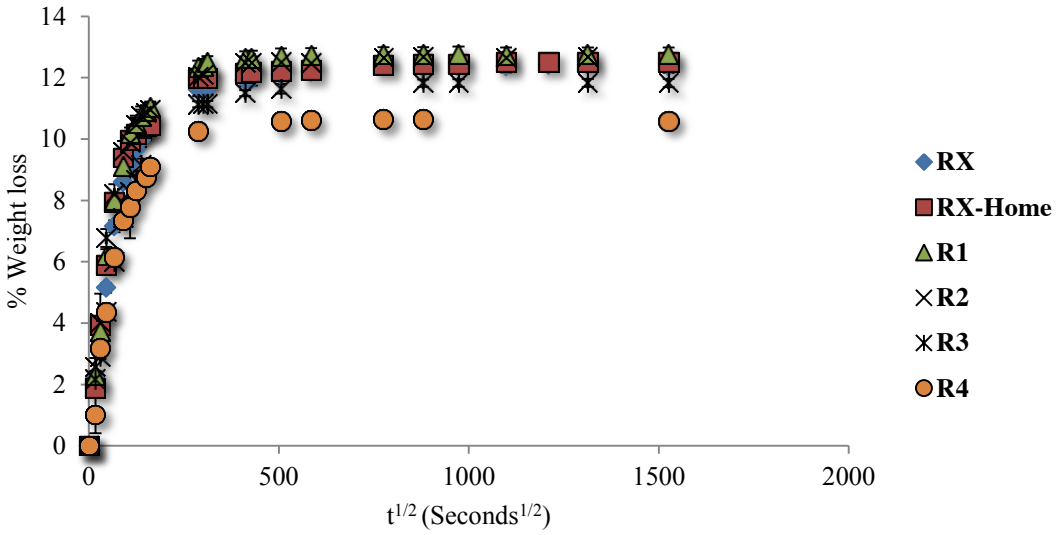

Figure 5.29 Mean weight loss of commercial, home and novel materials in the RX group-AS up to 5 weeks.

Figures 5.30 and 5.31 represent the early stages of desorption for commercial, home and novel materials in both groups (FP and RX) immersed in AS. The initial weight losses were linear to $t^{1/2}$, thus following Fick's law of diffusion and Ddes values were calculated for all materials.

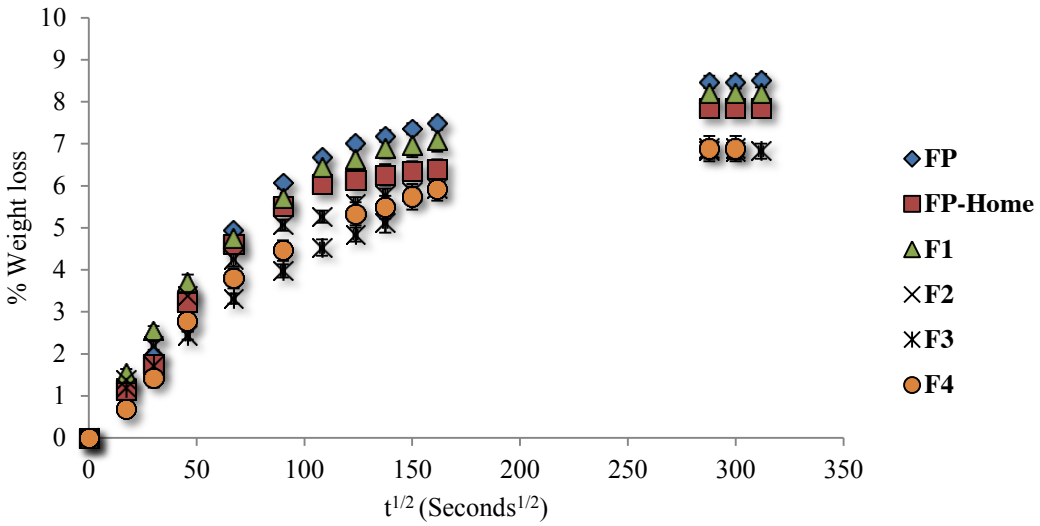

Figure 5.30 Initial mean percentage weight loss up to two days (at ~ 323 $t^{1/2}$) for FP commercial, home and novel materials -AS.

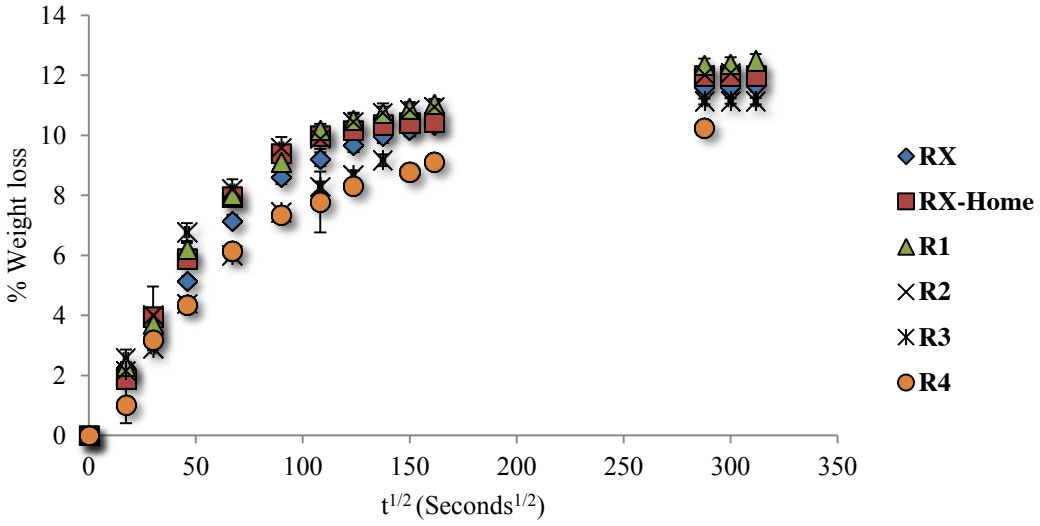

Figure 5.31 Initial mean percentage weight loss up to two days (at ~ 323 $t^{1/2}$) for RX commercial, home and novel materials -AS.

5.3.5 Solubility and diffusion coefficient (DC) results for novel materials:

The solubility and diffusion coefficient (DC) results of novel materials in FP and RX groups are presented in Tables 5.4 and 5.5 respectively, while those for the corresponding commercial/home FP and RX materials are presented in sections 5.2.5, 5.2.6 and 5.2.7. (Tables 5.1, 5.2 and 5.3).

FP commercial showed the lowest solubility in DW and AS compared to all other compositions in the same group ($p \leq 0.002$), except for F4 in AS, which was statistically similar ($p=0.304$). All FP compositions showed lower solubility results in DW compared to RX compositions ($p<0.0001$).

Similar to DW, the solubility of FP in AS was the lowest compared to all compositions in the same group ($p \leq 0.002$), with the exception of F4 ($p=0.304$). F1 showed the highest solubility while that for FP home was 5.46 ± 0.43%, which was lower than F3 and F2

FP novel compositions, similar to their commercial and home counterparts, showed slower diffusion in uptake compared to desorption, with the exception of F4 that showed comparable results in Dabs and Ddes values.

Table 5.4 Diffusion coefficients for absorption (Dabs), desorption (Ddes) and solubility %(SD) in DW and AS for commercial, home and novel FP materials.

	F1	F2	F3	F4
Dabs (DW) (m^2sec^{-1})	$9.83X10^{-12}$	$4.69X10^{-12}$	$8.73X10^{-12}$	$1.44X10^{-11}$
Ddes (DW) (m^2sec^{-1})	$1.41X10^{-11}$	$0.97X10^{-11}$	$1.19X10^{-11}$	$1.84X10^{-11}$
Ddes (AS) (m^2sec^{-1})	$2.25X10^{-11}$	$2.12X10^{-11}$	$1.12 X 10^{-11}$	$0.88 X 10^{-11}$
Solubility (DW) %(SD)	4.83(0.21)	4.37(0.14)	6.04 (0.15)	6.1 (0.14)
Solubility (AS) %(SD)	7.96(0.23)	7.54(0.15)	7.01(0.28)	4.31(0.09)

RX commercial and R3 in DW presented with the lowest solubility compared to all other compositions in their group ($p<0.0001$) (Table 5.5). All other compositions in the RX group did not show any significant difference in solubility in DW ($p\leq1$). R4 had the lowest solubility in AS ($p<0.0001$) followed by RX commercial, then RX home, R3, R1 and R2.

The diffusion coefficients for the absorption process for commercial, home and novel FP were lower than desorption diffusion coefficients. Conversely, for the entire RX group the diffusion coefficients for both processes were similar. Furthermore, the absorption diffusion coefficients for the RX group were higher than those for the FP group.

Table 5.5 Diffusion coefficients for absorption (Dabs), desorption (Ddes) and solubility %(SD) in DW and AS for commercial, home and novel RX materials.

	R1	R2	R3	R4
Dabs (DW) (m^2sec^{-1})	$1.85X10^{-11}$	$3.94X10^{-11}$	$1.32X10^{-11}$	$0.958X10^{-11}$
Ddes (DW) (m^2sec^{-1})	$2.56X10^{-11}$	$1.49X10^{-11}$	$1.62X10^{-11}$	$1.97X10^{-11}$
Ddes (AS) (m^2sec^{-1})	$2.27X10^{-11}$	$3.1X10^{-11}$	$1.48X10^{-11}$	$0.96 X 10^{-11}$
Solubility (DW) %(SD)	8.34(0.22)	8.18(0.31)	7.54 (0.22)	8.49 (0.24)
Solubility (AS) %(SD)	13.27(0.25)	13.9(0.56)	11.89 (0.16)	7.27(0.19)

5.3.6 Dimensional changes:

Dimensional changes for all materials were calculated as described in section 4.3.2.1. Figures 5.32 and 5.33 show mean percentage dimensional changes at 1, 3 and 24 weeks for all materials in DW and AS respectively.

FP commercial exhibited 8.24 ± 0.29% volume change after 1 week, which was higher than all other materials investigated ($p \leq 0.002$). RX and RX home did not show any significant differences in dimensional changes following 1 week immersion; however they were higher than all the corresponding novel materials ($p < 0.0001$). Although FP home had lower volume increase compared to commercial FP, after one week in DW, the value was higher than all novel materials in the same group ($p < 0.0001$). All novel compositions in both groups showed lower volume increase after one week immersion in DW compared to both commercial and home

materials ($p<0.0001$). Similar results to one week immersion were seen after 3 and 24 weeks immersion in DW, except after 24 weeks composition R1 showed a significantly lower volume change compared to all commercial, home and novel compositions in both groups ($p\leq0.001$).

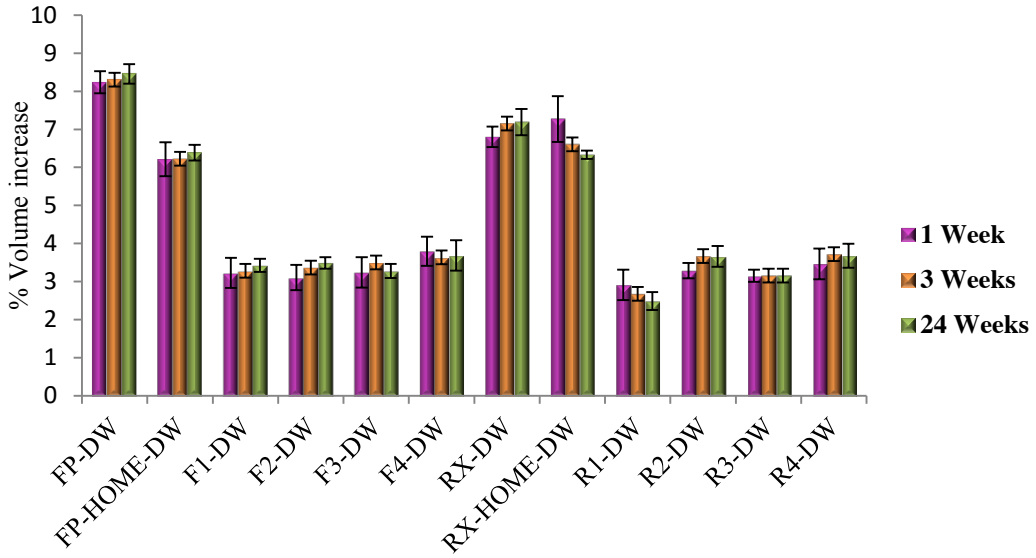

Figure 5.32 Mean percentage dimensional change of commercial, home and novel FP and RX in DW following 1, 3 and 24 weeks immersion in DW.

Similar to DW, novel materials showed significant lower volume increase following immersion in AS after 1, 3 and 24 weeks compared to commercial and home FP and RX. Compositions F4 and R4, containing 70% HEMA and 30% THFM, showed higher volume increase in AS compared to the other novel compositions ($p\leq0.03$); this was not evident in DW.

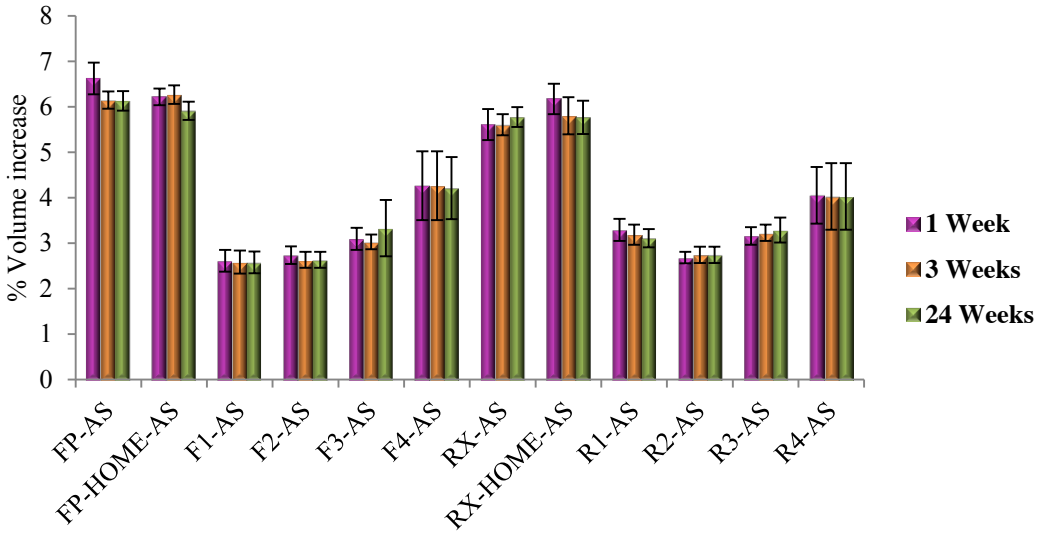

Figure 5.33 Mean percentage dimensional change of commercial, home and novel FP and RX in DW following 1, 3 and 24 weeks immersion in AS.

5.4 *Composition, analysis of reaction and degree of conversion for novel, commercial and home materials:*

5.4.1 Composition analysis:

5.4.1.1 Composition analysis of commercial and home liquids:

Spectra of both the commercial and the equivalent home-made liquids were obtained (Figure 5.34) and used to compare any differences between them. Spectra of commercial and home compositions for both FP and RX were comparable. Differences were observed between the spectra of the two liquids, FP and RX. FP contained UDMA, which gave additional weak peaks at ~1270 cm^{-1} and 1550 cm^{-1} for both commercial and home liquids. The peaks were weak since only a small percentage (~4%) was present. Peaks at 1631 cm^{-1} represented the C=C stretch in the monomers, whilst those at 1701 cm^{-1} represent the C=O group. Peaks at 1301 cm^{-1} and 1324 cm^{-1} represent C-O stretch and 1086 cm^{-1} represent tartaric acid (Young *et al*., 2004); the latter is present at 5-10% according to the manufacturer's MSDS in commercial materials and at 5% in the home and novel liquids.

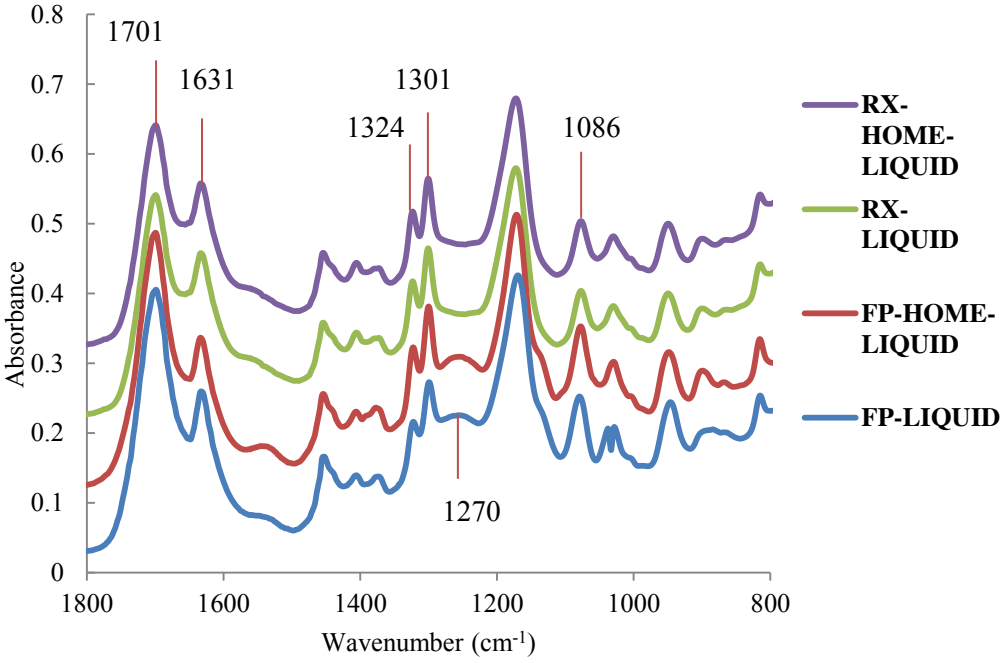

Figure 5.34 FTIR spectra of RMGIC liquids FP and RX (commercial and home).

Figure 5.35 shows FTIR spectra for the four monomers that were used in the commercial, home and novel materials; peaks for C=C, C=O and C-O were present in all four monomers. The peaks wavenumber (in cm^{-1}) and assignments are summarised in Table 5.6. HPM showed an additional peak at 1059 cm^{-1} corresponding to the –OH group in its structure, while HEMA and THFM showed additional peaks at ~1020 cm^{-1} and 1086, corresponding to the –OH group in HEMA's structure and the ring stretch in THFM (Stepanian *et al*., 1996; Rivera-Armenta *et al*., 2012). However, the UDMA spectrum was different compared to these three monomers with additional peaks at 1059 cm^{-1} (C-N stretch), 1250 and 1535 cm^{-1} (N-H bond).

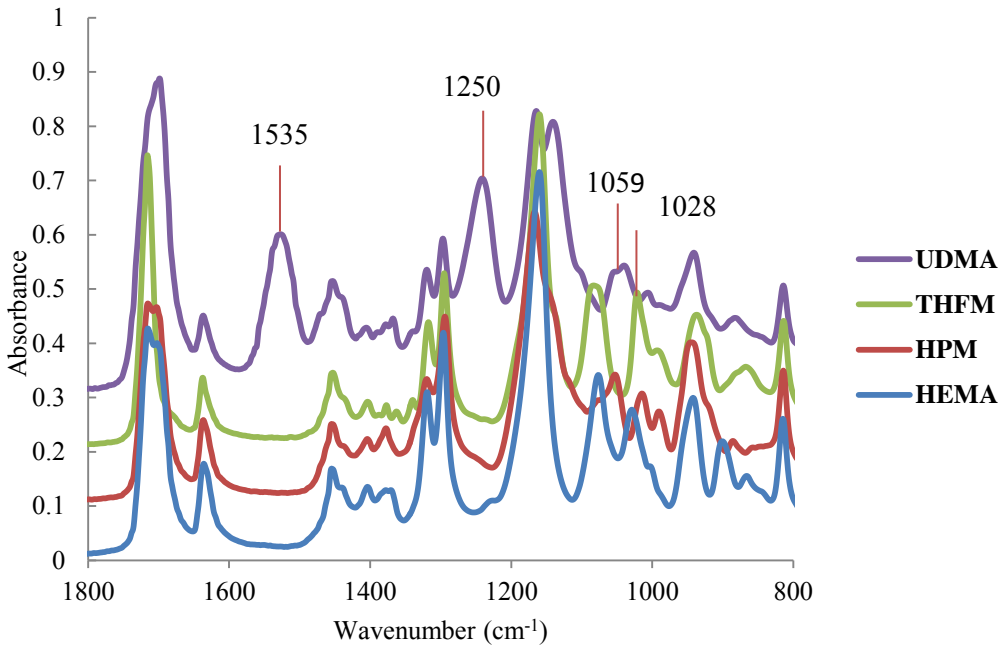

Figure 5.35 FTIR spectra of four monomers (HEMA, HPM, THFM and UDMA) used in RMGIC home and novel liquids.

Table 5.6 RMGIC liquid components FTIR analyses with the corresponding wavenumber (cm^{-1}) and assignment of each component (Stepanian *et al.*, 1996; Rivera-Armenta *et al.*, 2012, Young *et al.*, 2004).

FTIR Wavenumber (cm^{-1})	Assignment	Component
1020	-OH Ring stretch	HEMA THFM
1059	-OH C-N	HPM UDMA
1086	-OH Ring stretch	HEMA THFM
1250	N-H	UDMA
1300	C-O	Monomer (all three)
1320	C-O	Monomer (all three)
1379	C-H	PAA and monomer (all three)
1405	C-H	PAA and monomer (all three)
1450	C-H	PAA and monomer (all three)
1535	N-H	UDMA
1630	C=C	Monomer (all three)
1630	O-H	Water
1700	C=O	Monomer (all three)

5.4.1.2 Composition analysis of novel liquids:

Figures 5.36 and 5.37 show the FTIR spectra of novel liquid compositions in the FP and RX groups respectively (between wavenumbers of 800 cm^{-1} and 1800 cm^{-1}). Compositions of cements containing HPM, from both groups (F1, F2, R1 and R2), showed an additional peak at about 1059 cm^{-1} representing the OH stretch.

Moreover, peaks at ~1084 cm^{-1} were sharper in compositions containing THFM and HEMA (F3, F4, R3, R4). The peak at about 1539 cm^{-1} (seen in Figure 5.36), is assigned to the monomer UDMA, and was only present in the FP compositions; the RX group did not contain this monomer (Figure 5.37).

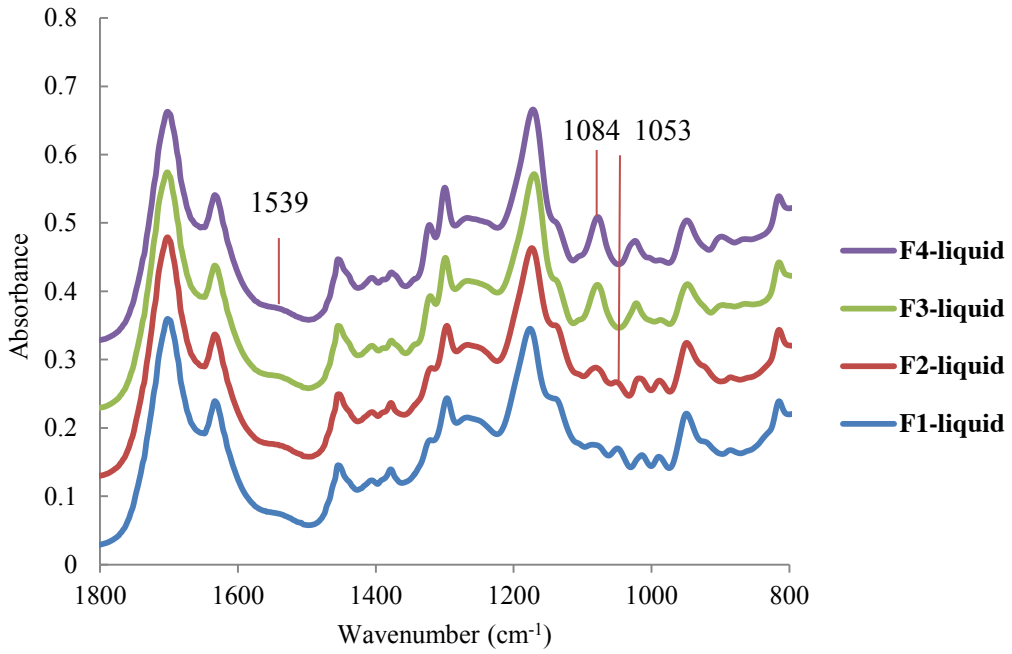

Figure 5.36 FTIR spectra of novel liquid compositions (F1, F2, F3 and F4).

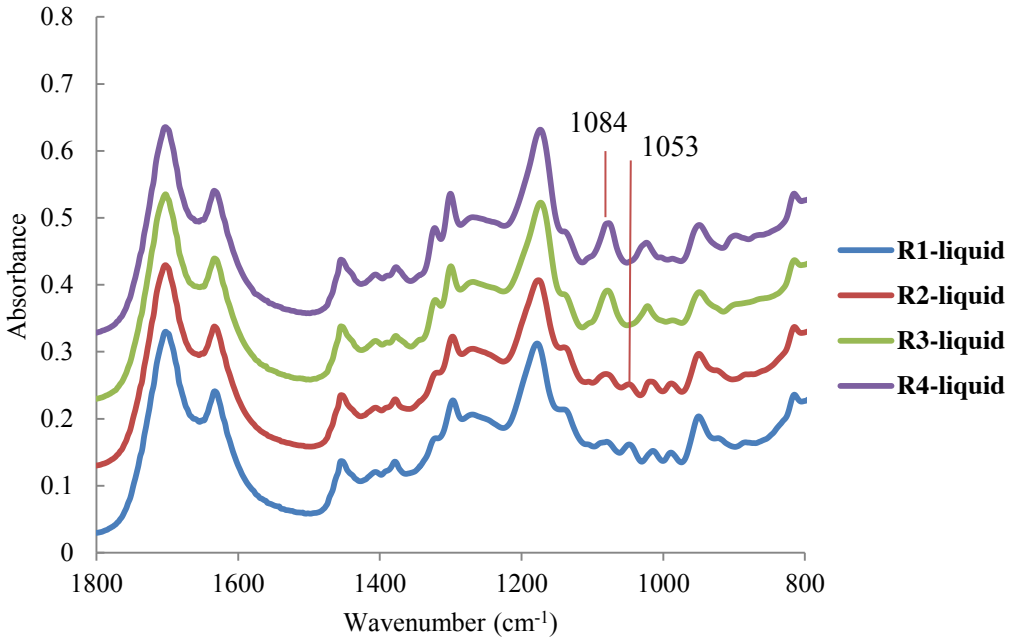

Figure 5.37 FTIR spectra of novel liquid compositions (R1, R2, R3 and R4).

5.4.2 Analysis of Reaction:

5.4.2.1 Analysis of reaction of commercial and home cements:

Figures 5.38 and 5.39 are representative FT-IR spectra taken during the setting of Fuji Plus commercial and home respectively, as soon as the cement was applied to the ATR crystal (0 minutes); this was done as fast as possible and took no longer than 50 seconds from the start of mixing. Spectra were obtained at 5, 10 and 30 minutes from the start of mixing. As can be seen in Figure 5.38, changes in absorbance occurred in FP (commercial) in the 5 minutes' spectrum when compared to that at 0 minutes. These changes included loss of C=C at 1630 cm^{-1}, 1320 and 1300 cm^{-1} and the shift of the latter two wavenumbers to 1275 and 1253 cm^{-1}. Small changes also occurred at 1700 and 975 cm^{-1} representing C=O and glass Si-O stretch respectively (Fareed and Stamboulis, 2014). These changes also occurred in FP Home (Figure 5.39) but at later time points, thus indicating a slower reaction.

Spectral changes due to the acid-base reaction were noticed due to the formation of 1400, 1492 and 1563 cm^{-1} peaks, which can be assigned to the polyacrylate salts formed (C=O stretching of Ca-polyacrylate, Al-polyacrylate, Ca-polyacrylate respectively) (Fareed and Stamboulis, 2014). Again, a faster reaction occurred in FP compared to FP home.

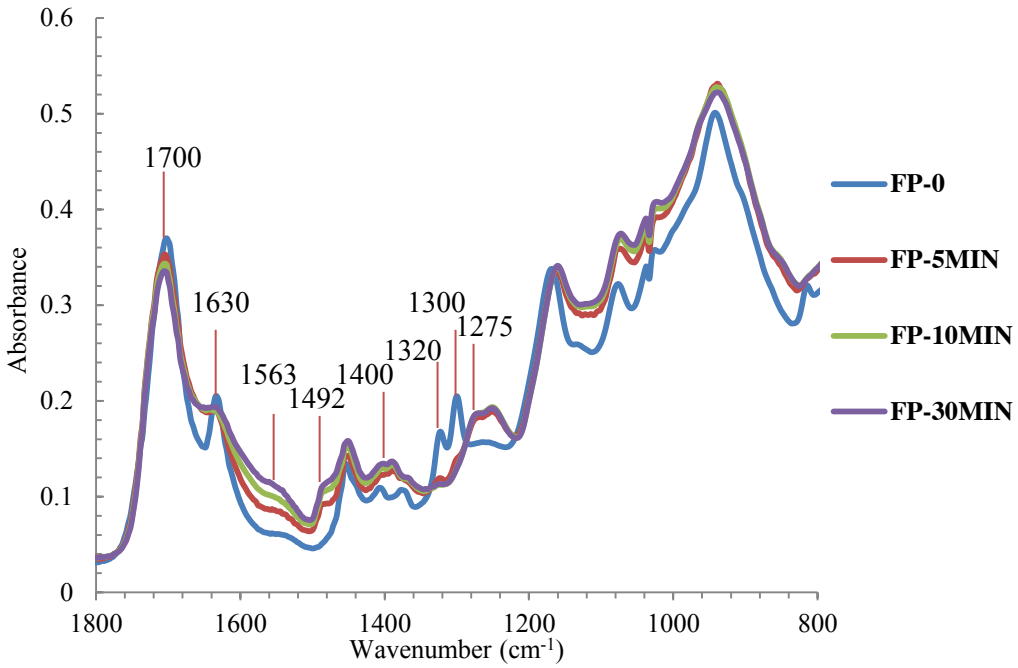

Figure 5.38 Representative FT-IR spectra of the setting reaction of commercial FP at 0, 5, 10 and 30 minutes from the start of mixing.

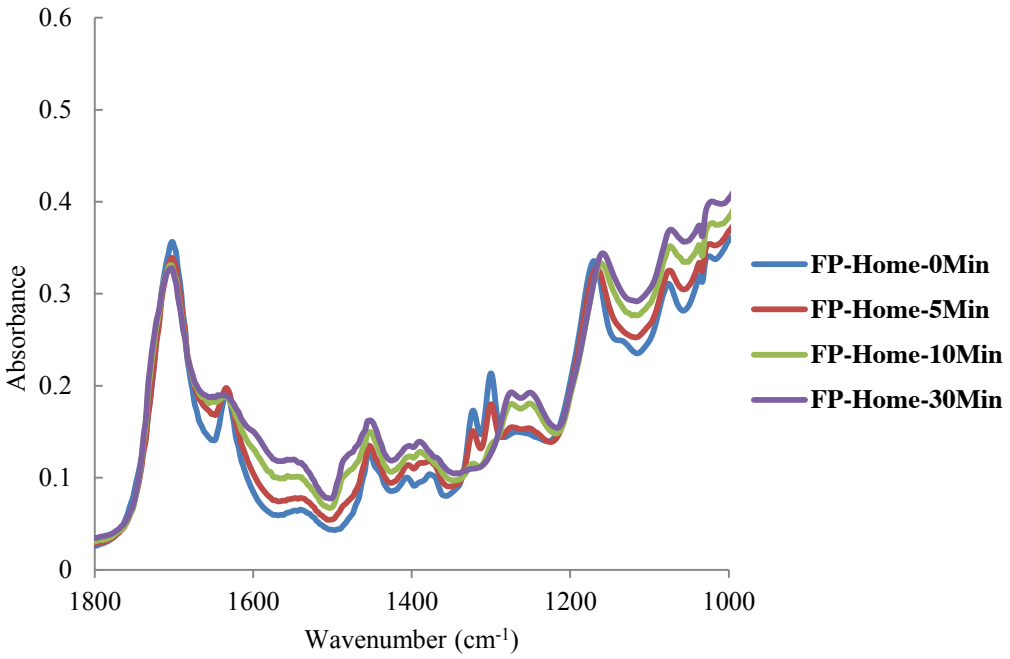

Figure 5.39 Representative FT-IR spectra of the setting reaction of FP-Home at 0, 5, 10 and 30 minutes from the start of mixing.

Figures 5.40 and 5.41 represent the FT-IR spectra taken at 0, 5, 10 and 30 minutes during the setting of RX and RX home respectively, from the start of mixing. Main changes in the spectra occurred following 5 minutes from the start of mixing, where the peaks at 1300 and 1320 cm^{-1} were still visible, but at lower absorbance values. These two peaks shifted to 1264 and 1285 cm^{-1} at 5 minutes but had higher absorbance values at 10 and 30 minutes. Similar to FP and FP home spectra, the peak at 1638 cm^{-1} disappeared as a result of the setting reaction and the conversion of the methacrylate C=C bond to C-C.

Glass and polyacrylate peaks at 970, 1405, 1480 and 1556 cm^{-1} can be observed from the 5 minutes time points, which increase in intensity from10 minutes.

RX home spectrum presented in Figure 5.41 showed a slower polymerisation reaction compared to RX commercial. In both spectra, peaks at 1300 and 1320 cm^{-1}

shifted to 1264 and 1285 cm^{-1}, and there was a difference in the time the shifts occurred (5 minutes in RX and 10 minutes in RX home). These two peaks were used to calculate the degree of conversion of monomer in the cements. There were signs of the acid-base reaction occurring in RX commercial and home following 10 minutes.

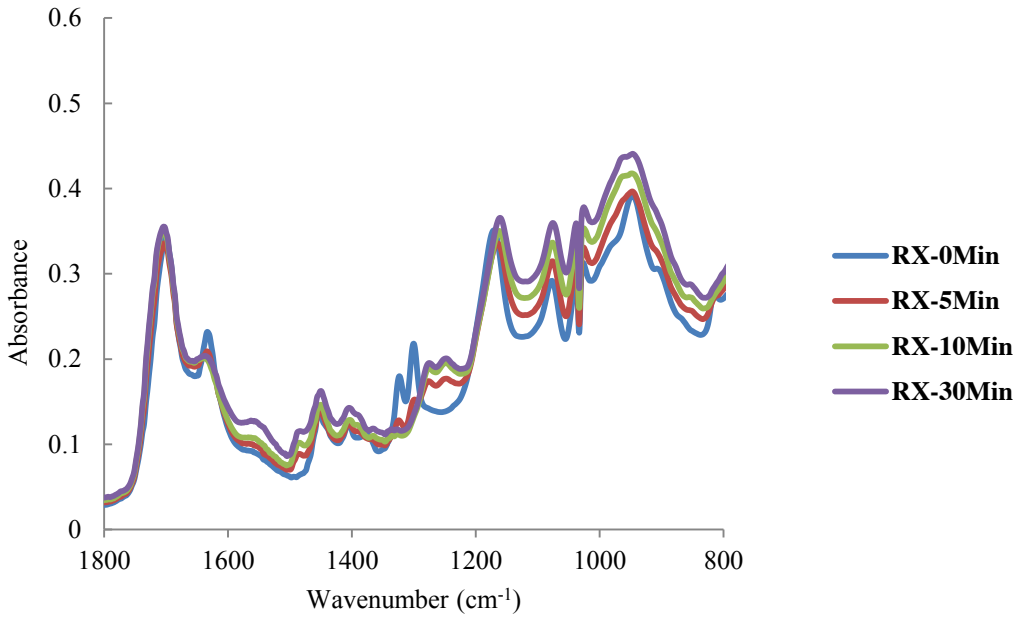

Figure 5.40 Representative FT-IR spectra of the setting reaction of RX at 0, 5, 10 and 30 minutes from the start of mixing.

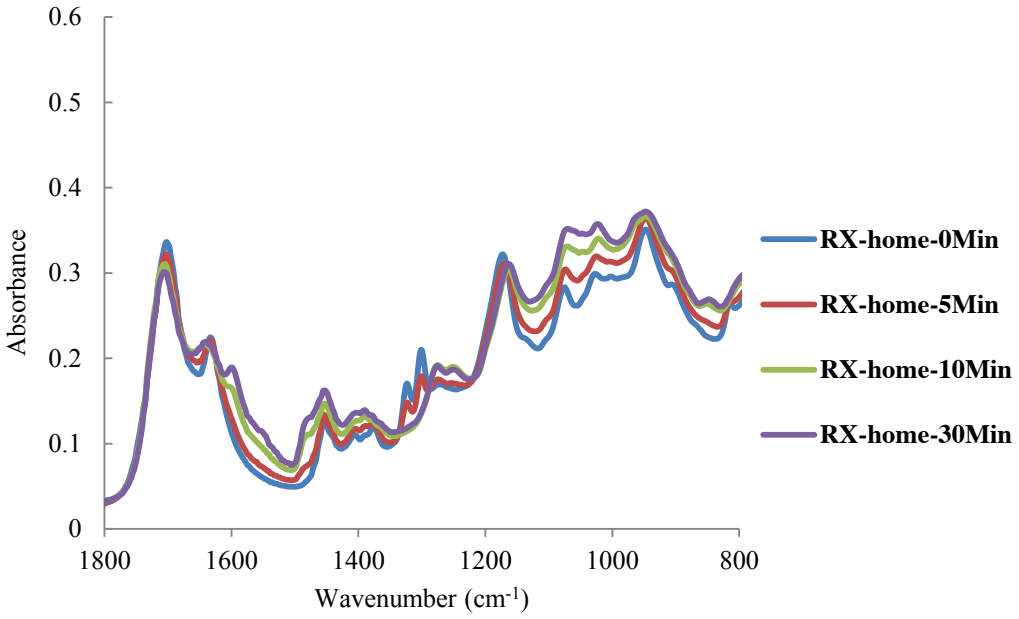

Figure 5.41 Representative FT-IR spectra of the setting reaction of RX-Home at 0, 5, 10 and 30 minutes from the start of mixing.

5.4.2.2 Analysis of reaction for novel cements:

Figures 5.42, 5.43, 5.44 and 5.45 are representatives of the spectra obtained during the setting reaction of F1, F2, F3 and F4 respectively. On comparing Figures 5.42 and 5.43, changes in the polymerisation of the methacylate group (at 1300 and 1320 cm^{-1}) in both spectra were obvious at 10 and 30 minutes following mixing; there was evidence of this in F1 at 5 minutes.

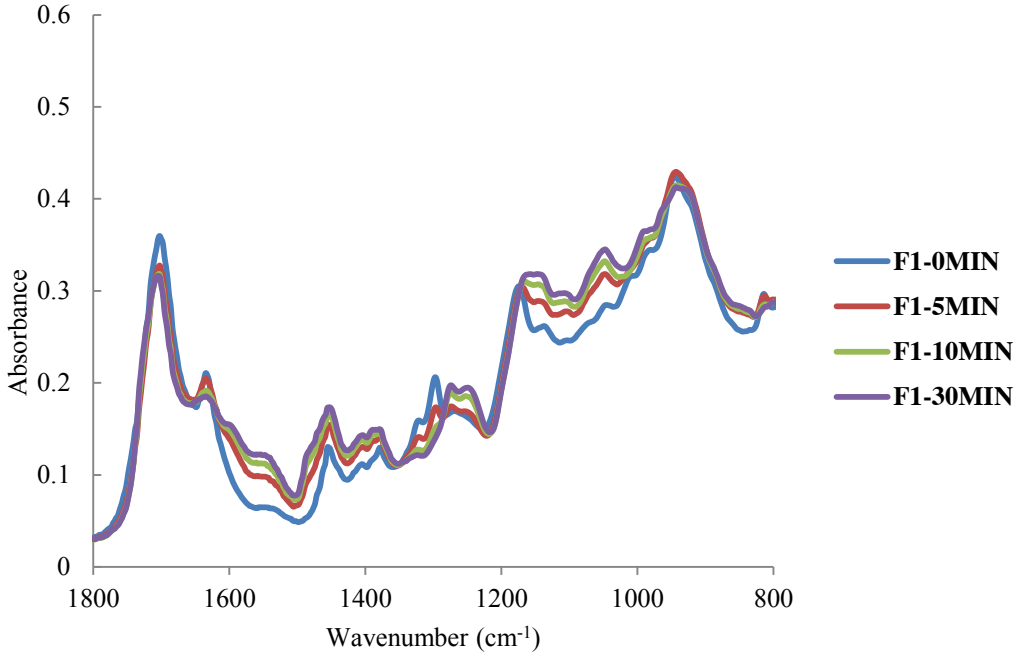

Figure 5.42 Representative FT-IR spectra of the setting reaction of F1 at 0, 5, 10 and 30 minutes from the start of mixing.

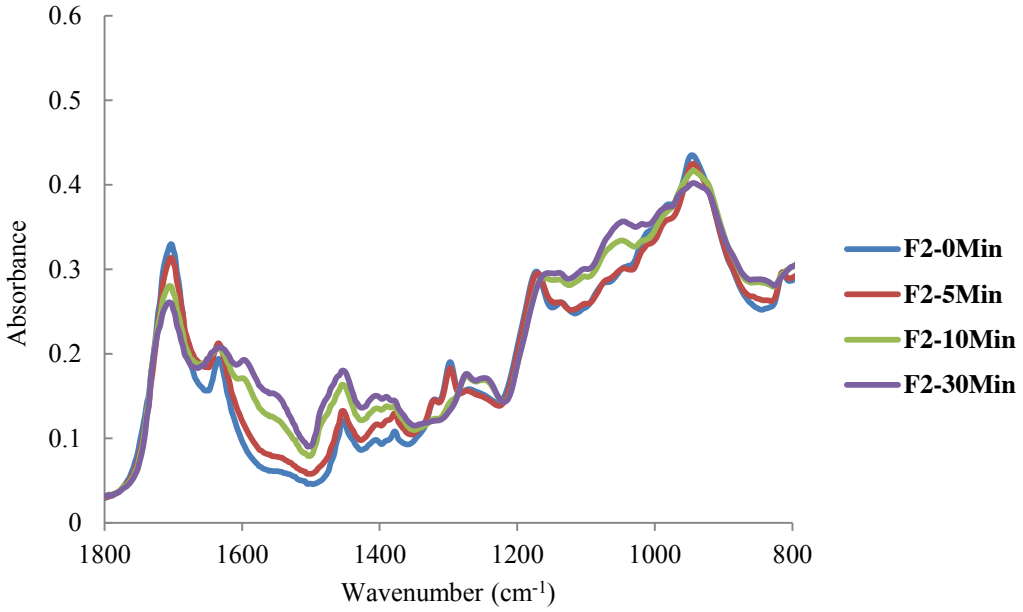

Figure 5.43 Representative FT-IR spectra of the setting reaction of F2 at 0, 5, 10 and 30 minutes from the start of mixing.

As can be seen in Figure 5.44 the F3 spectrum was different to all other materials in the FP group with respect to the loss of methacrylate group peaks (at 1300 and 1320 cm^{-1}), which shifted to 1264 and 1280 cm^{-1} at 5 minutes; in all other FP group materials they shifted after 10 and 30 minutes. Moreover, the spectrum also shows the formation of GIC salts and neutralisation of the acid (at 1550, 1484 and 1402 cm^{-1} COO^- stretch) at 5 minutes compared to later time points for the other materials in the same group. This possibly indicates that the reaction is occurring faster in F3 compared to the other materials.

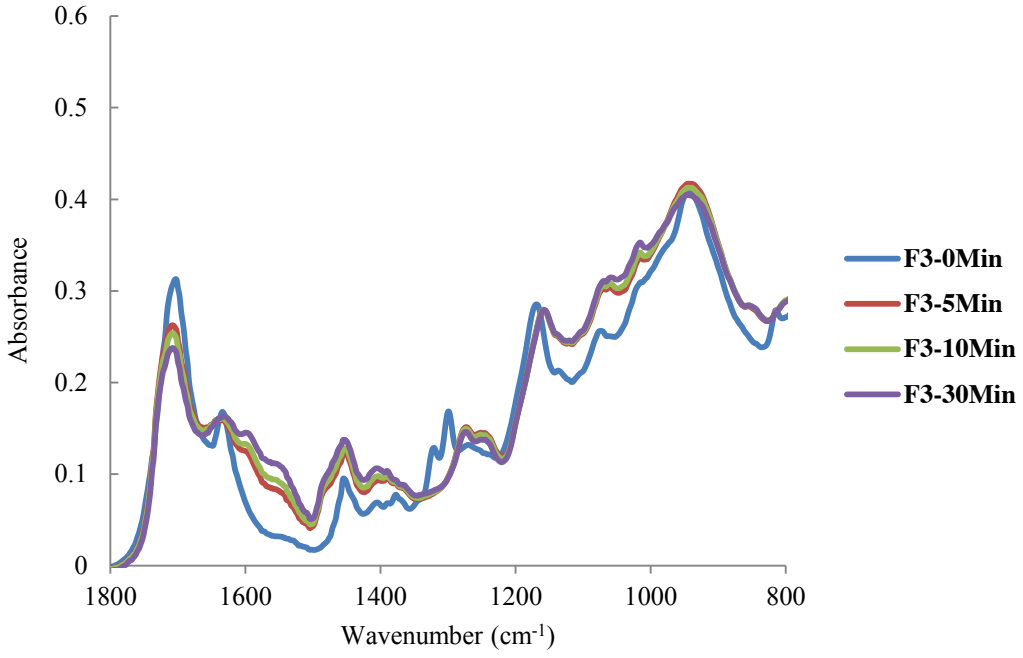

Figure 5.44 Representative FT-IR spectra of the setting reaction of F3 at 0, 5, 10 and 30 minutes from the start of mixing.

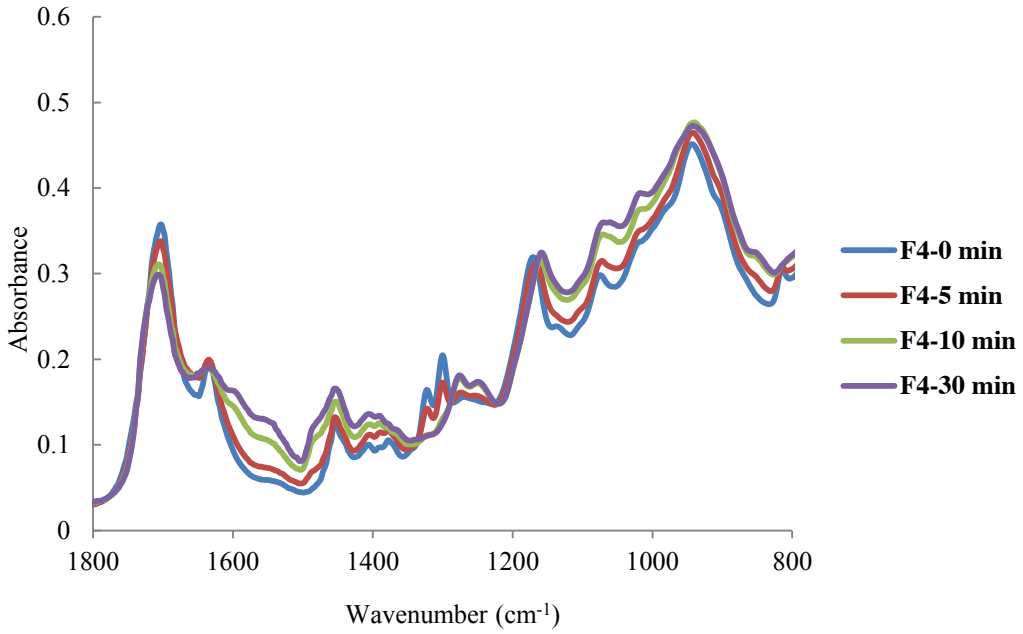

Figure 5.45 Representative FT-IR spectra of the setting reaction of F4 at 0, 5, 10 and 30 minutes from the start of mixing.

As can be seen in Figures 5.46, 5.47, 5.48 and 5.49, representing spectra of novel cements in the RX group, similar peaks are present in the spectra of the liquids and those of the cements, following mixing and placing the cement on the crystal (50 seconds) to the 0 time point spectrum, with the exception of the higher absorbance of the glass peak at 970 cm^{-1}. This indicates that the polymerisation reaction had not yet commenced.

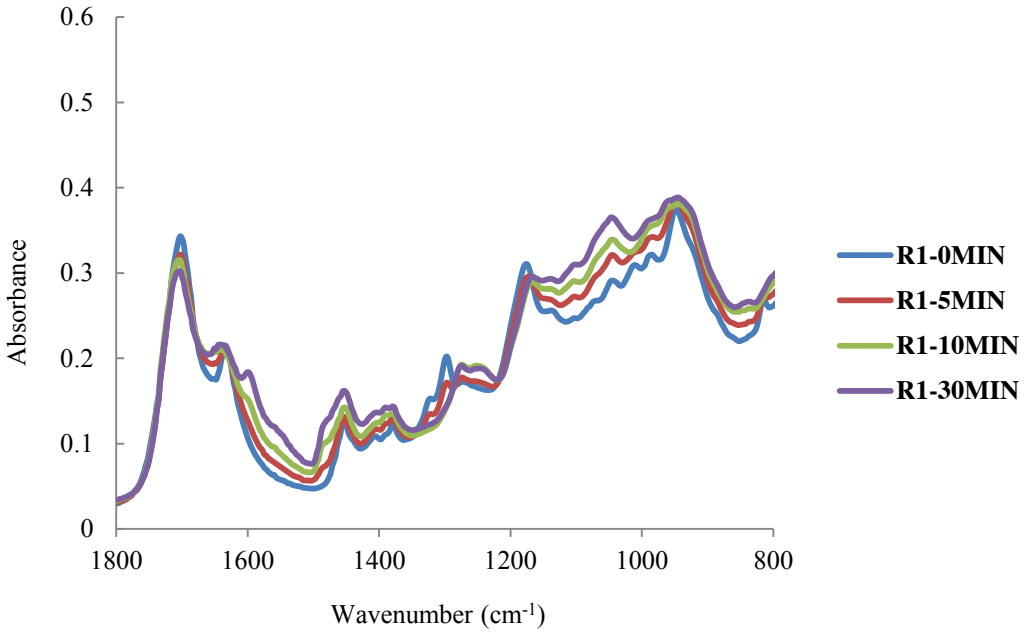

Figure 5.46 Representative FT-IR spectra of the setting reaction of R1 at 0, 5, 10 and 30 minutes from the start of mixing.

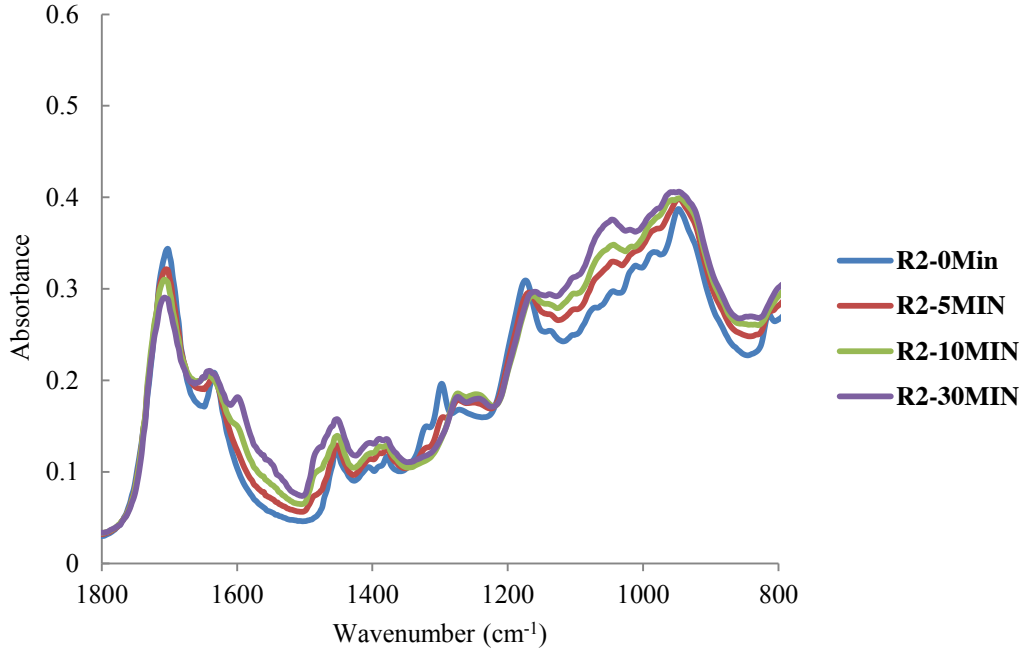

Figure 5.47 Representative FT-IR spectra of the setting reaction of R2 at 0, 5, 10 and 30 minutes from the start of mixing.

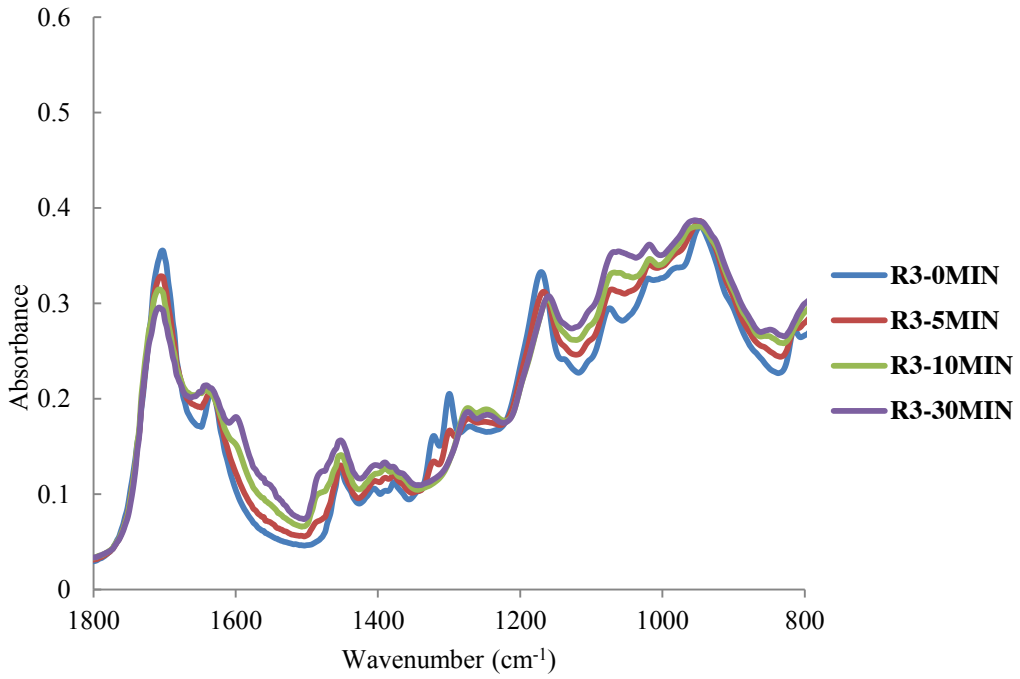

Figure 5.48 Representative FT-IR spectra of the setting reaction of R3 at 0, 5, 10 and 30 minutes from the start of mixing.

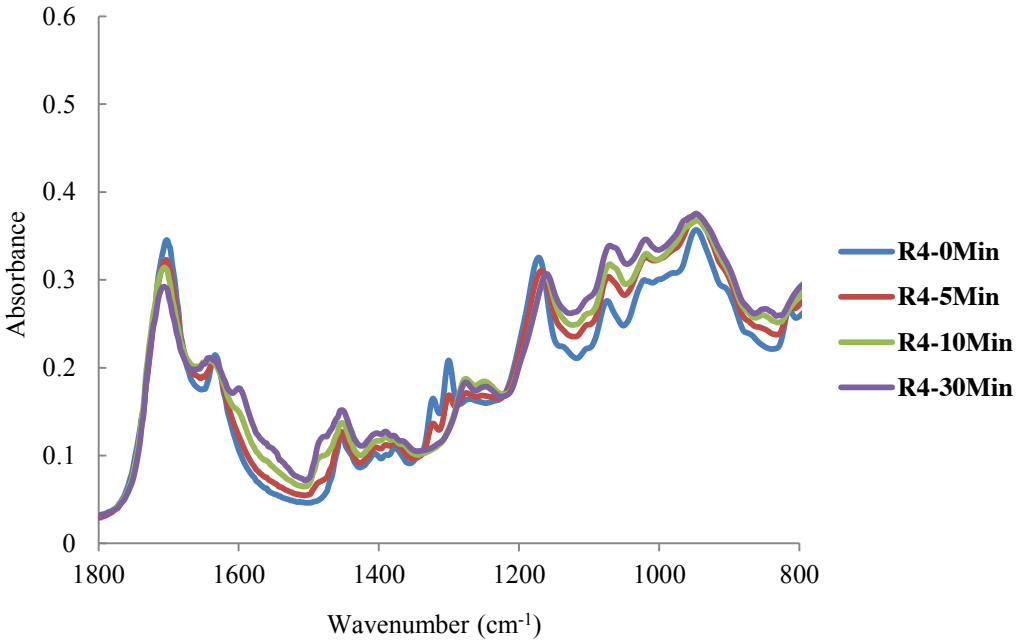

Figure 5.49 Representative FT-IR spectra of the setting reaction of R4 at 0, 5, 10 and 30 minutes from the start of mixing.

5.4.3 Percentage degree of conversion of commercial, home and novel materials:

Figure 5.50 shows the mean percentage degree of conversion of FP commercial, home and novel materials in the FP group, calculated as the change in peak height of the methacrylate group in each cement at 5, 10 and 30 minutes from the start of mixing. At 5 minutes interval, F3, FP and FP-Home showed statistically higher degree of conversion values (33.75 ± 4.25%, 28.12 ± 2.13% and 21.92 ± 9.46% respectively) compared to F4, F1 and F2 (14.91 ± 2.12%, 7.80 ± 3.01 and 6.58 ± 1.27% respectively; $p \leq 0.039$). F3, FP-Home, FP and F4 showed statistically comparable degree of conversion values at 10 minutes from the start of mixing (33.50 ± 3.83%, 33.12 ± 3.63%, 31.63 ± 1.32% and 25.94 ± 5.93%) ($p \leq 0.73$). The degree of conversion values at 10 minutes for F2 and F1 were the lowest in the FP group (18.79 ± 5.80% and 14.26 ± 4.93%; $p \leq 0.002$); there was no significant difference between degree of conversion values at 10 minutes and 30 minutes of each material.

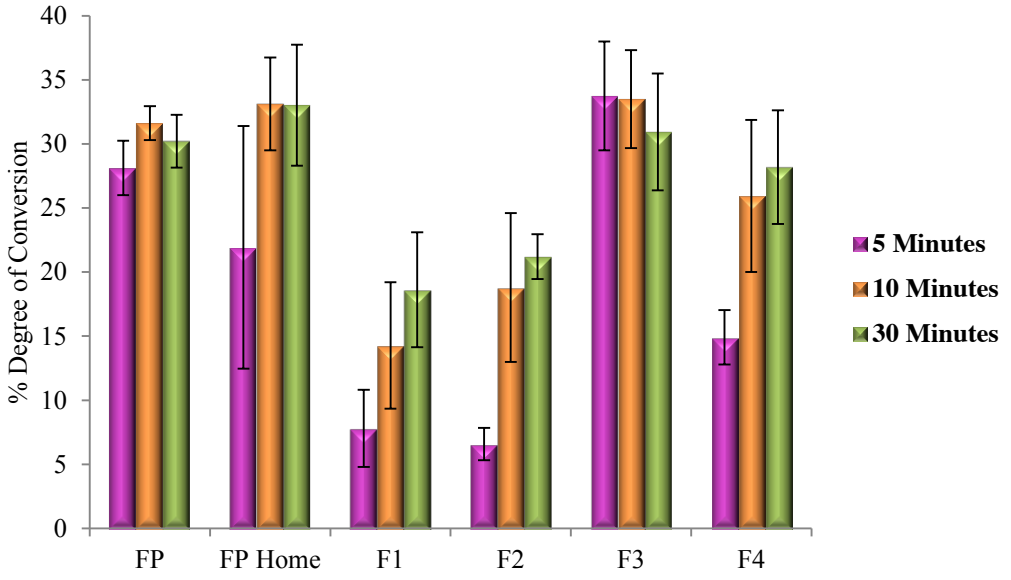

Figure 5.50 Mean percentage degree of conversion of FP commercial, home and novel materials measured at 5, 10 and 30 minutes, calculated from the start of mixing.

Figure 5.51 shows the mean percentage degree of conversion of RX commercial, home and novel materials in the RX group. Only R1 showed a significantly lower degree of conversion (9.47 ± 1.86%) compared to the commercial RX (23.15 ± 5.84%; p=0.029) at 5 minutes, but this was not significantly different compared to all other materials in the group (R3 - 17.10 ± 2.76%, RX-Home - 14.90 ± 5.81%, R2 - 14.63 ± 2.19% and R4 - 13.62 ± 4.09%; p≤0.987). Following 10 minutes from the start of mixing, RX and R4 showed significantly higher monomer conversion (37.02 ± 1.91% and 34.08 ± 3.22%) compared to R2 and R1 (24.74 ± 0.01% and 22.84 ± 1.68%; p≤0.004), but they were not significantly different compared to R3 and RX-Home (31.13 ± 0.48% and 30.95 ± 3.96%; p≤0.79). Similar trends were noticed in the degree of conversion values at 30 minutes intervals in the RX group.

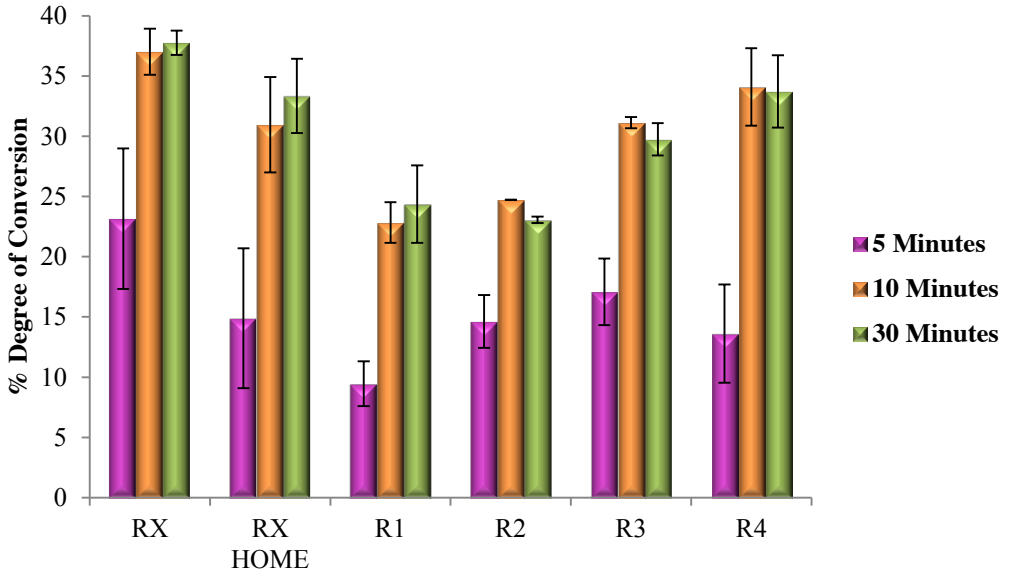

Figure 5.51 Mean percentage degree of conversion of RX commercial, home and novel materials measured at 5, 10 and 30 minutes, calculated from the start of mixing.

5.5 *Working and setting times of commercial, home and novel materials:*

A representative rheometer trace of FP-Home, as an example, is presented in Figure 5.52. Traces were obtained for all materials (commercial, home and novel materials in both groups).

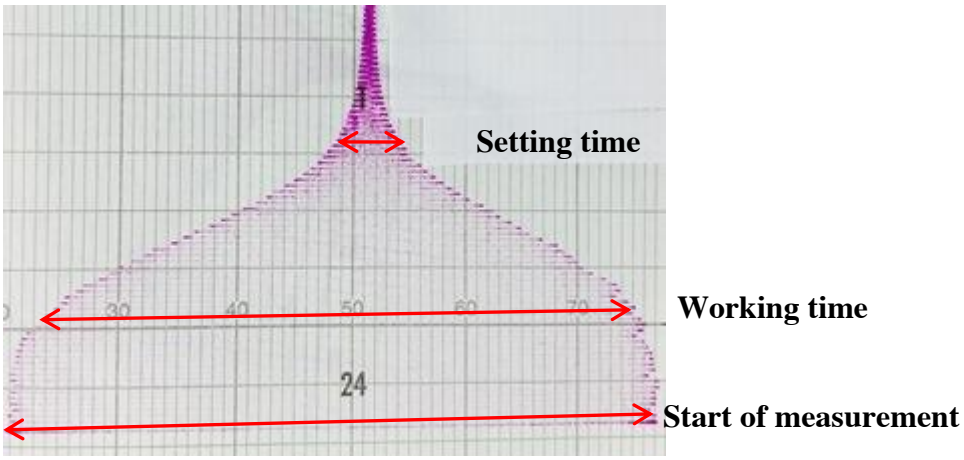

Figure 5.52 Representative oscillating rheometer trace of FP-Home cement.

5.5.1 Working times:

Figure 5.53 and Table 5.7 present the mean working times (± SD) for all materials tested.

Table 5.7 Mean ± SD of working times for all materials in both groups (FP and RX), measured in seconds. Similar superscript letters indicate no significant difference between materials (p>0.05).

Material	Working time (sec)(SD)
FP	137 (7.97)^{d,e,f}
FP-Home	135 (6.29)^{d,e,f}
FI	191 (11.64)^{a,b}
F2	162 (17.80)^{c}
F3	113 (4.52)^{f}
F4	125 (8.83)^{f}
RX	206 (19.22)^{a}
RX-Home	151 (11.01)^{c,d,e}
R1	157 (7.01)^{c,d}
R2	134 (6.20)^{d,e,f}
R3	129 (6.29)^{e,f}
R4	173 (23.21)^{b,c}

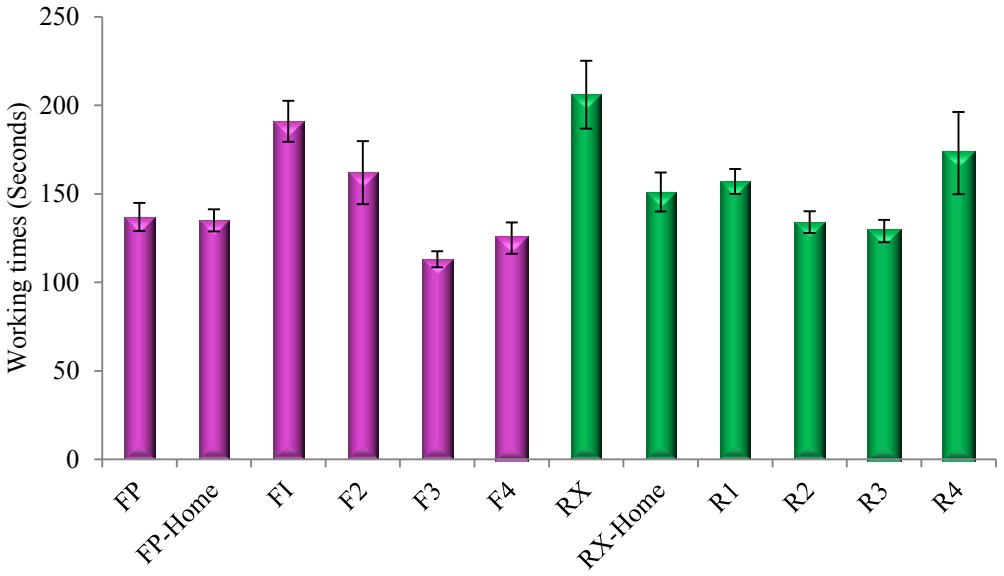

Figure 5.53 Working times of all materials (commercial, home and novel) with FP group presented as the purple bars and RX group as the green bars.

In the FP group, F1 showed a significantly longer working time compared to all other materials (191 ± 11.64 seconds; $p \leq 0.007$), followed by F2 (162 ± 17.80 seconds; $p \leq 0.036$). FP (commercial), FP-Home, F4 and F3 presented statistically comparable working times (137 ± 7.97 seconds, 135 ± 6.29 seconds, 125 ± 8.83 seconds and 113 ± 4.52 seconds, respectively; $p \geq 0.052$).

There was a significant difference in the RX group between the commercial, home and novel materials; commercial RX showed a significantly longer working time compared to all other cements (206 ± 19.22; $p \leq 0.001$). R3 (129 ± 6.29 seconds) presented the shortest working time compared to all materials in the group, although it was not statistically different ($p \geq 0.106$) from R2 (134 ± 6.20 seconds) and RX-Home (151 ± 11.01 seconds).

There was a significant difference in working times ($p < 0.0001$) between the two commercial materials (FP and RX), with RX showing a longer working time than FP by about 69 seconds (this is ~ 50% of the total working time of FP), which indicates a clinically significant difference in the working time between the two materials). There was no significant difference between the two home materials when comparing their working times ($p = 0.518$).

5.5.2 Setting times:

Figure 5.54 and Table 5.8 show the mean setting times (± SD) of all materials tested.

Table 5.8 Mean ± SD of setting times for all materials in both groups (FP and RX), measured in seconds. Similar superscript letters indicate no significant difference between materials (p>0.05).

Material	Setting times (sec)(SD)
FP	207 (9.86)
FP-Home	339 (21.38)^{d,e}
FI	363 (14.07)^{d}
F2	310 (14.03)^{e,f}
F3	273 (11.22)^{f}
F4	286 (12.96)^{f}
RX	465 (31.23)^{a,b,c}
RX-Home	476 (27.80)^{a,b}
R1	497 (34.24)^{a}
R2	422 (10.51)^{c}
R3	442 (32.57)^{b,c}
R4	472 (22.34)^{a,b}

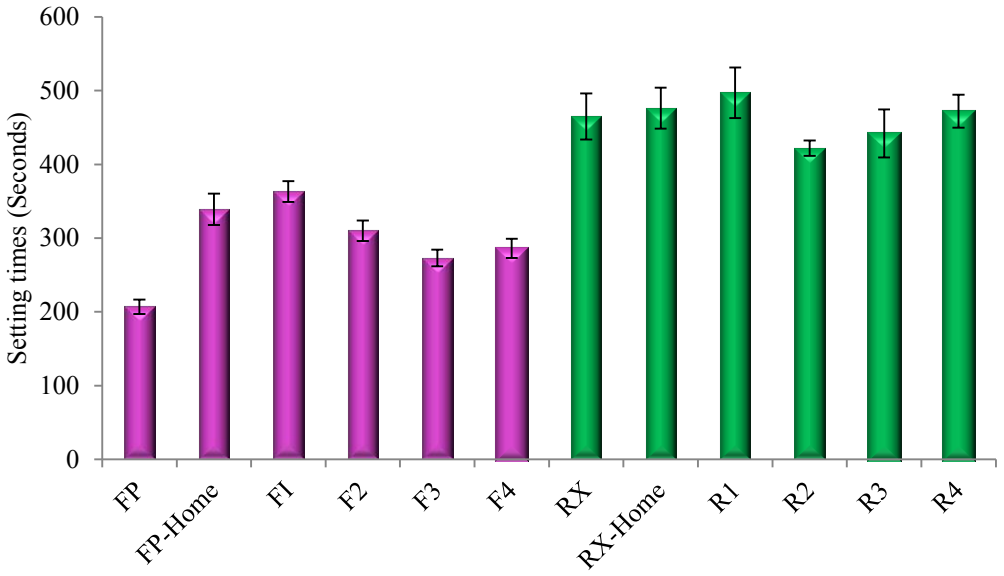

Figure 5.54 Setting times of all materials (commercial, home and novel) in the FP group presented as the purple bars and RX group as the green bars.

The setting time for commercial FP (207 ± 9.86 seconds) was significantly lower than all other materials in the FP group ($p<0.0001$). This was followed by F3 (273 ± 11.22 seconds), F4 (286 ± 12.96 seconds) and F2 (339 ± 21.38 seconds). Composition F1 had the longest setting time in the FP group (363 ± 14.07 seconds) although it was not statistically significant from FP-Home ($p=0.763$).

In the RX group, RX commercial showed comparable setting times (465 ± 31.23 seconds) compared to all materials in the same group ($p\geq0.053$). Although the setting time of R2 (422 ± 10.51 seconds) was not significantly different from RX and R3 (442 ± 32.57 seconds; $p\geq0.053$), it was shorter than R4, RX-Home and R1 (472 ± 22.34 seconds, 476 ± 27.80 seconds and 497 ± 34.24 seconds; $p\leq0.011$).

All FP compositions (commercial, home and novel materials) demonstrated significantly shorter setting times compared to all materials in the RX group (commercial, home and novel materials) as can be seen in Figure 5.54.

5.6 *Mechanical properties of commercial, home and novel materials:*

5.6.1 Compressive fracture strength (CFS) and compressive modulus (CM):

Mean compressive fracture strength for twenty samples of each material (n=20) (commercial, home and novel), in both groups (FP and RX), are presented in Table 5.9 and plotted in Figure 5.55.

Following statistical analyses using one-way ANOVA and post-hoc Tukey's test for comparison between groups, FP presented with the highest CFS value compared to all materials in both groups ($p<0.0001$), followed by F3, F4 and F2; there was no statistically significant difference ($p\geq0.097$) between the latter three materials. F1 containing 100% HPM showed the lowest CFS compared to all novel materials ($p<0.0001$). There was no statistically significant difference in CFS between RX home, R1, R2 and R3. The mean CFS for R4 was the highest compared to home and novel materials in the same group ($p\leq0.002$), but it was still lower than commercial RX ($p<0.0001$).

On comparing the CFS of the two groups, RX compositions showed lower values compared to their FP counterparts, in particular the home and novel materials. Commercial RX did not show any significant difference when compared to composition F1 ($p=1$) but it was still lower than all the other compositions in the FP group.

The CoV, which is the SD divided by the mean, for FP materials ranged from 0.7 to 0.11, whilst in the RX group it ranged from 0.3 to 0.8; this indicates good reproducibility of the CFS data.

Table 5.9 Mean compressive fracture strength (CFS), standard deviations (SD) and coefficient of variation (CoV) for all materials (commercial, home and novel). Groups sharing same superscript letter indicates no statistically significant difference (p>0.05).

Material	CFS (MPa)	SD (MPa)	CoV
FP	131.75	8.97	0.07
FP-Home	77.38	5.26	0.07
F1	87.09[b]	9.97	0.11
F2	96.81[a]	7.21	0.07
F3	103.25[a]	10.46	0.10
F4	101.83[a]	7.39	0.07
RX	88.27[b]	7.41	0.08
RX-Home	54.06[c]	2.80	0.05
R1	53.72[c]	1.94	0.03
R2	52.24[c]	2.93	0.06
R3	57.54[c]	3.87	0.07
R4	66.46	4.06	0.06

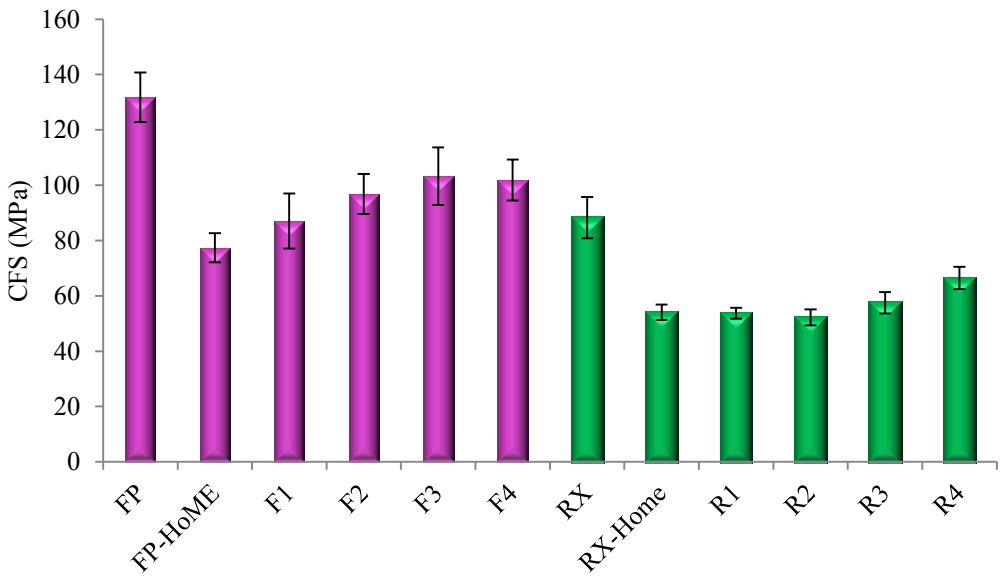

Figure 5.55 Mean compressive fracture strength (CFS) with error bars representing standard deviations (SD) for all materials (commercial, home and novel).

Table 5.10 highlights mean CM values for all materials. FP showed the highest compressive modulus compared to all other materials ($p<0.001$), similar to the CFS (Table 4.9). Also like the CFS data, CM of RX novel and home materials were lower than all FP compositions (commercial, home and novel) ($p\leq0.032$). Commercial RX had comparable CM to FP-Home, F1 and F4 (Figure 5.56).

Table 5.10 Mean compressive modulus (CM), standard deviations (SD) and coefficient of variation (CoV) for all materials (commercial, home and novel). Groups sharing same superscript letter indicate no statistically significant difference (p>0.05).

Material	CM (GPa)	SD (GPa)	CoV
FP	1.18	0.22	0.19
FP-Home	$0.59^{d,e}$	0.12	0.20
F1	$0.70^{c,d}$	0.21	0.30
F2	0.87^{a}	0.13	0.15
F3	$0.85^{a,b}$	0.15	0.18
F4	$0.84^{a,b,c}$	0.12	0.14
RX	$0.70^{b,c,d}$	0.21	0.30
RX-Home	0.43^{f}	0.07	0.16
R1	0.41^{f}	0.07	0.18
R2	0.43^{f}	0.10	0.22
R3	0.43^{f}	0.11	0.25
R4	$0.53^{e,f}$	0.09	0.16

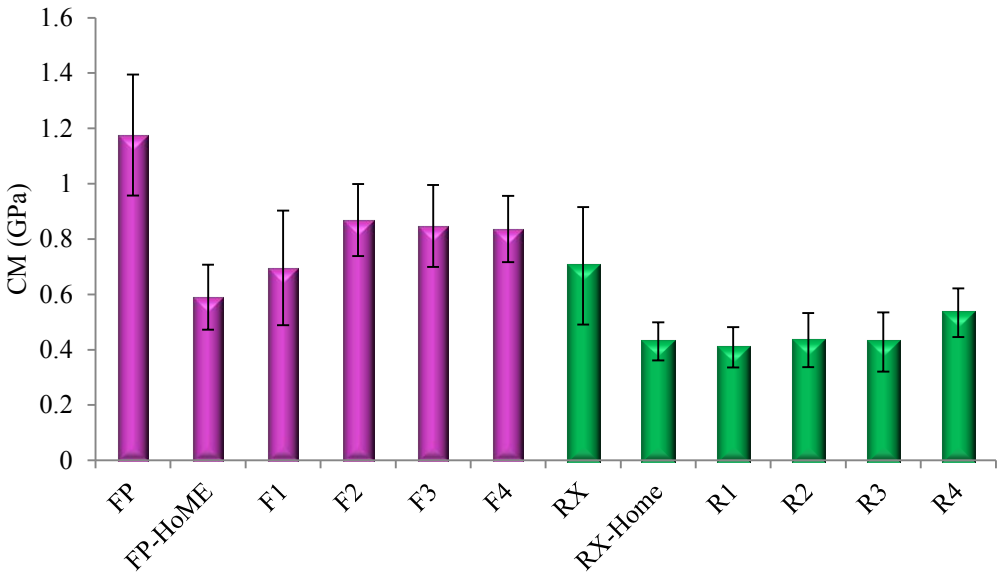

Figure 5.56 Mean compressive modulus (CM) with error bars representing standard deviations (SD) for all materials (commercial, home and novel).

5.6.2 Three-point Flexure strength (TFS) and three-point flexure modulus (TFM):

For all materials investigated in both groups (FP and RX) the TFS are presented in Table 5.11 and Figure 5.57.

The one-way ANOVA analyses showed a significant difference between groups ($p<0.0001$); the post-hoc Tukey's test confirmed that TFS for RX was the highest compared to all materials in both groups ($p<0.0001$), followed by FP commercial ($p<0.0001$). Conversely, the two home materials showed lower TFS results compared to their commercial counterparts and were also lower than some of the corresponding novel compositions. As an example, F3 and F4 showed higher TFS compared to the home material ($p\leq0.017$), whilst only R3 in the RX group presented with a higher value compared to the home material in the same group ($p=0.014$).

Table 5.11 Mean of three point flexural strength (TFS), standard deviations (SD) and coefficient of variation (CoV) for all materials (commercial, home and novel). Groups sharing same superscript letter indicate no statistically significant difference (p>0.05).

Material	TFS (MPa)	SD (MPa)	CoV
FP	17.20	3.85	0.22
FP-Home	$7.75^{d,e}$	1.59	0.21
F1	7.19	2.73	0.38
F2	$8.03^{c,d,e}$	1.99	0.25
F3	$10.37^{a,b}$	1.29	0.12
F4	$10.28^{a,b,c}$	0.92	0.09
RX	20.85	3.86	0.19
RX-Home	$8.40^{b,c,d,e}$	1.65	0.20
R1	$9.48^{a,b,c,d}$	1.19	0.13
R2	$9.91^{a,b,c,d}$	1.81	0.18
R3	10.96^{a}	1.35	0.12
R4	$8.87^{a,b,c,d,e}$	1.58	0.18

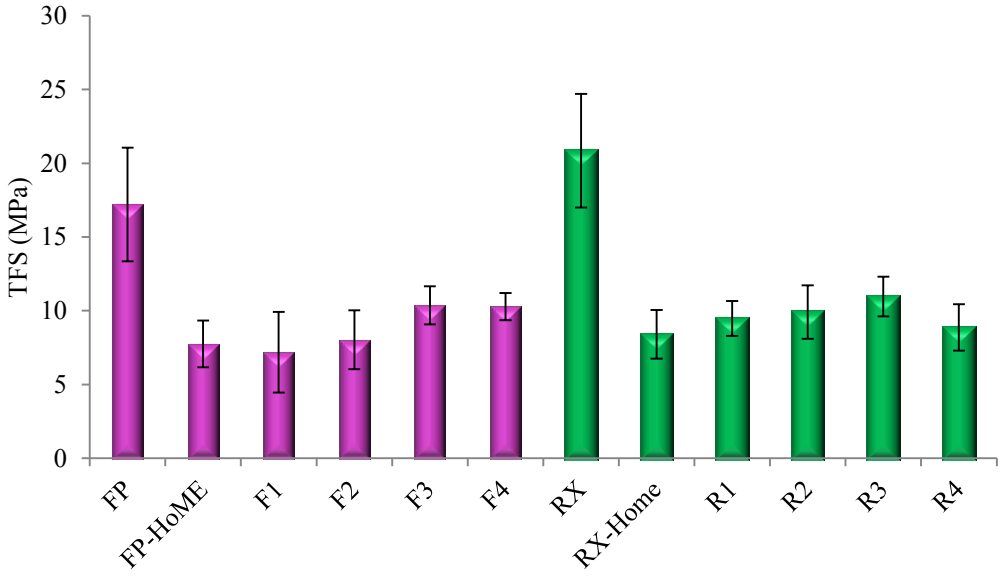

Figure 5.57 Mean of three point flexural strength (TFS) test with error bars representing standard deviations (SD) for all materials tested (commercial, home and novel).

During testing it was noted that some materials demonstrated different load/deflection curves. Commercial FP and RX, and home materials showed a linear load/deflection curve typically associated with brittle materials, whilst novel materials showed plastic deformation (plastic curving area) before fracture; this is indicative of the material being ductile rather than brittle. Differences between the brittle and ductile materials curves are presented in Figure 5.58. Therefore, the load at fracture value, needed for the measurement of TFM of ductile materials, was determined from the initial linear region of the curve (up to the elastic limit) rather than the load at fracture. Moreover the deflection of the sample was taken at the same point.

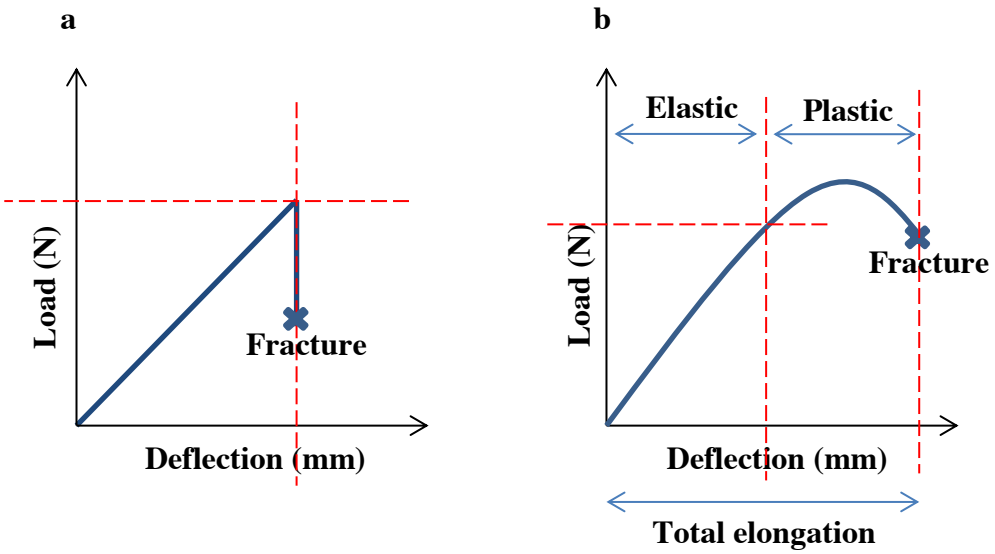

Figure 5.58 Schematic of load/deflection curve in TFS test used to calculate TFM where a: is a typical load/deflection curve for brittle materials and b: represents the curve associated with ductile materials.

Table 5.12 represents the TFM data for all materials. One-way ANOVA confirmed a significant difference of $p<0.0001$ between groups. According to Tukey's test, FP showed the highest TFM compared to all materials in both groups ($p<0.0001$). However, there were no significant differences in the TFM between FP-home and F1, F2 and F4 ($p\geq0.608$), but the values were lower than those for F3 ($p=0.018$). In the RX group, RX-Home was not significantly different compared to all the novel materials ($p\geq0.125$).

Table 5.12 Mean of three-point flexural modulus (TFM), standard deviations (SD) and coefficient of variation (CoV) for all materials (commercial, home and novel). Groups sharing same subscript letter indicate no statistically significant difference (p>0.05).

Material	TFM (GPa)	SD (GPa)	CoV
FP	4.77	0.53	0.11
FP-Home	2.39^{b}	0.34	0.14
F1	$2.28^{b,c}$	0.96	0.42
F2	$2.73^{a,b}$	0.92	0.34
F3	2.98^{a}	0.50	0.17
F4	$2.58^{a,b}$	0.66	0.25
RX	$2.32^{b,c}$	0.24	0.10
RX-Home	$1.67^{d,e}$	0.22	0.13
R1	$1.48^{d,e}$	0.36	0.24
R2	$1.79^{c,d}$	0.19	0.11
R3	$1.32^{d,e}$	0.16	0.12
R4	1.19^{e}	0.16	0.13

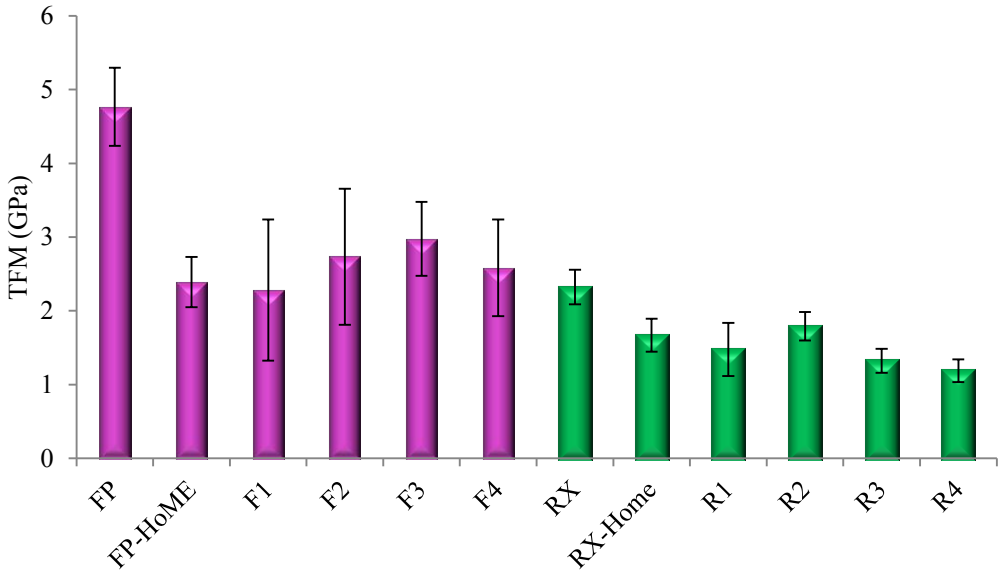

Figure 5.59 Mean of three point flexural modulus (TFM) with error bars representing standard deviations (SD) for all materials (commercial, home and novel).

5.7 *Polymerisation shrinkage strain for all materials (commercial, home and novel):*

5.7.1 Polymerisation shrinkage strain at 23°C:

Mean percentage shrinkage strain at 23°C for FP group were plotted against time, up to 3600 seconds (60 minutes). Figure 5.60 is an example of a percentage shrinkage strain plot for one sample of each material in this group. Mean percentage shrinkage strains (n=5) for the same group (FP) are summarised in Table 5.13 and Figure 5.61 for measurements taken at 5, 15, 30 and 60 minutes.

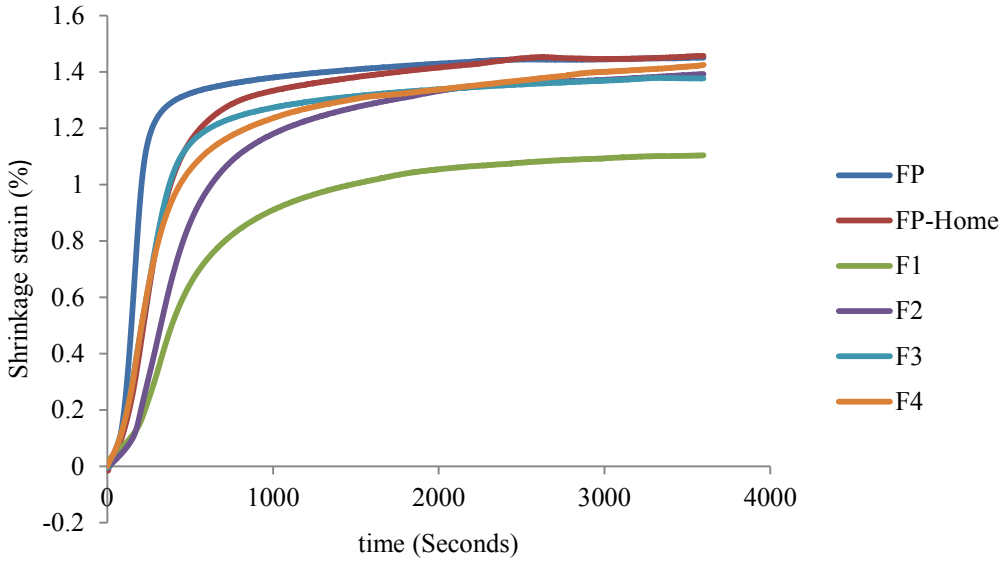

Figure 5.60 Representative plot of mean percentage shrinkage strain at 23°C for FP group materials (commercial, home and novel) up to 3600 seconds (1 hour).

Table 5.13 Mean percentage shrinkage strain values and standard deviation (SD) at 5, 15, 30 and 60 minutes, from the start of measurement, at 23°C for FP group (commercial, home and novel). Similar superscript letters indicates no statistically significant difference between materials at each time point (p>0.05).

Material	Shrinkage strain at 5 minutes % (SD)	Shrinkage strain at 15 minutes % (SD)	Shrinkage strain at 30 minutes % (SD)	Shrinkage strain at 60 minutes % (SD)
FP	1.19 (0.02)	1.34 (0.02)[a]	1.39 (0.02)[a,b]	1.41 (0.02)[a,b]
FP-Home	0.74 (0.06)[a]	1.31 (0.03)[a,b]	1.41 (0.03)[a]	1.46 (0.04)[a]
F1	0.35 (0.07)	0.95 (0.09)	1.12 (0.08)	1.21 (0.09)[c]
F2	0.47 (0.07)	1.19 (0.09)[b,c]	1.31 (0.05)[a,b,c]	1.39 (0.05)[a,b]
F3	0.77 (0.05)[a]	1.21 (0.04)[b,c]	1.28 (0.04)[b,c]	1.32 (0.05)[b,c]
F4	0.72 (0.07)[a]	1.14 (0.09)[c]	1.26 (0.09)[c]	1.35 (0.10)[a,b]

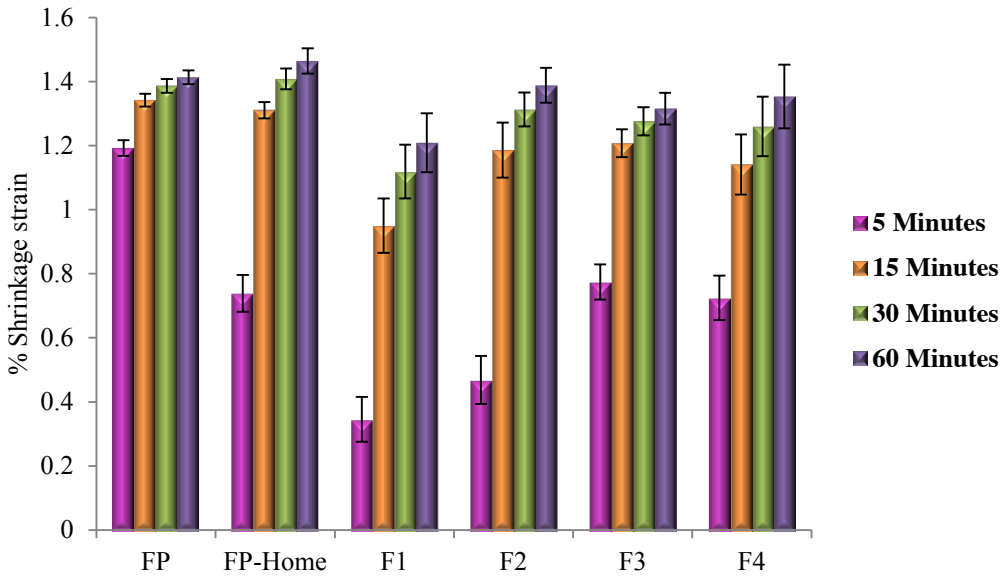

Figure 5.61 Mean shrinkage strain of FP group (commercial, home and novel) at 5, 15, 30 and 60 minutes measured at 23°C with error bars representing the standard deviation (n=5 per material).

At 23°C, five minutes from the start of the shrinkage measurement, commercial FP showed the highest shrinkage, which was significantly different compared to all materials in the group (home and novel; p<0.0001). Interestingly, shrinkage values for compositions containing HEMA (F3, FP-Home and F4) were significantly lower

than commercial FP (also containing HEMA) at this time point ($p<0.0001$); furthermore, they were significantly higher than the compositions containing HPM (F1; $p<0.0001$) and, composition F2, where the HEMA was replaced by 30% THFM and 70% HPM ($p<0.0001$). F1 presented with a significantly lower shrinkage at this time point compared to all materials in this group ($p\leq0.041$), and to all materials at all time points ($p\leq0.041$), except when compared to F3 at the 60 minutes ($p=0.146$). FP and FP-Home showed statistically similar results at 15, 30 and 60 minutes ($p\geq0.822$) (Table 5.13).

Similar to the FP group, the mean percentage shrinkage strains of the RX group, at 23°C, were also plotted against time up to 3600 seconds (1 hour), where Figure 5.62 is an example for one sample of each material in this group. Mean percentage shrinkage strain (n=5) for the RX group are also summarised in Table 5.14 and Figure 5.63 taken at 5, 15, 30 and 60 minutes.

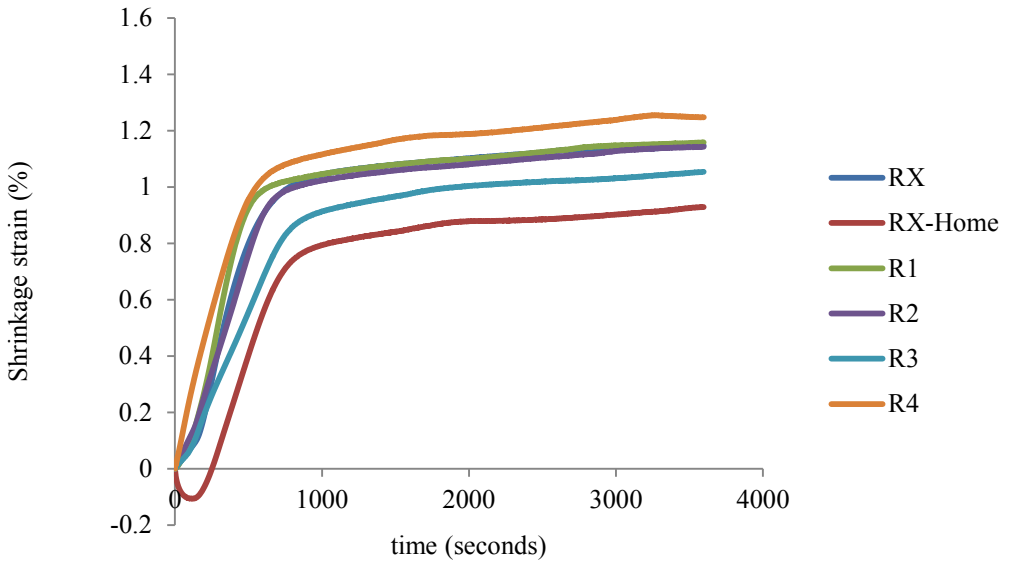

Figure 5.62 Shrinkage strain at 23°C for RX group materials (commercial, home and novel) plotted against time, up to 3600 seconds (1 hour).

Table 5.14 Mean percentage shrinkage strain values and standard deviation (SD) at 5, 15, 30 and 60 minutes from the start of measurement, at 23°C for RX group (commercial, home and novel). Similar superscript letters indicates no statistically significant difference between materials at each time point (p>0.05).

Material	Shrinkage strain at 5 minutes % (SD)	Shrinkage strain at 15 minutes % (SD)	Shrinkage strain at 30 minutes % (SD)	shrinkage strain at 60 minutes % (SD)
RX	0.59 (0.19)[a]	1.02 (0.05)[a]	1.07 (0.06)[a,b]	1.12 (0.06)[a,b]
RX-Home	0.23 (0.15)[b]	0.83 (0.11)[b]	0.90 (0.10)[b]	0.96 (0.10)[b]
R1	0.50 (0.07)[a,b]	1.01 (0.06)[a]	1.08 (0.06)[a,b]	1.14 (0.07)[a,b]
R2	0.56 (0.14)[a]	0.97 (0.03)[a,b]	1.03 (0.04)[a,b]	1.09 (0.03)[a,b]
R3	0.43 (0.12)[a,b]	0.94 (0.08)[a,b]	1.02 (0.07)[a,b]	1.08 (0.07)[a,b]
R4	0.51 (0.15)[a]	1.04 (0.16)[a]	1.13 (0.16)[a]	1.20 (0.17)[a]

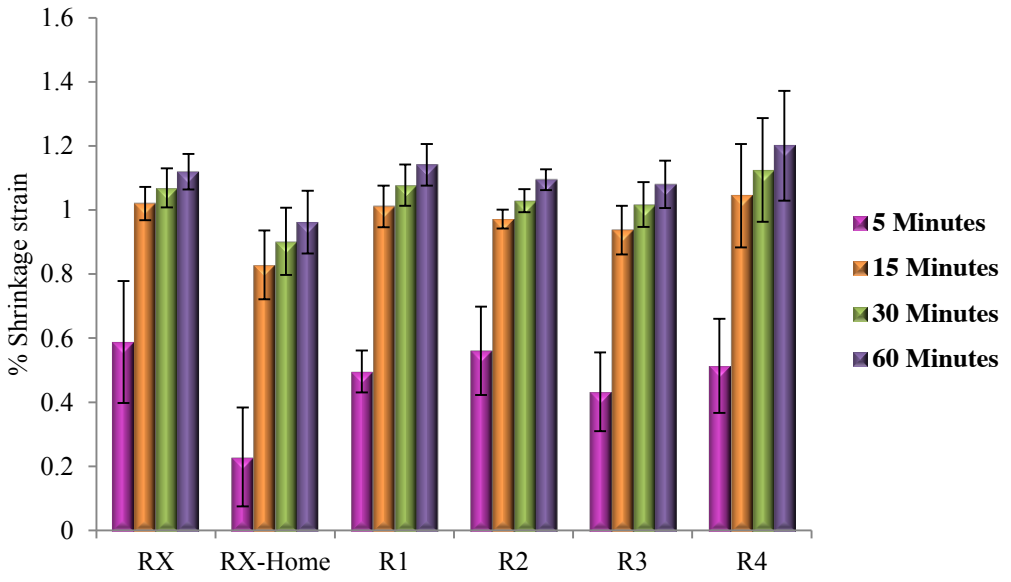

Figure 5.63 Mean shrinkage strain of RX group (commercial, home and novel) at 5, 15, 30 and 60 minutes measured at 23°C with error bars representing the standard deviation (n=5 per material).

RX-Home presented with the lowest shrinkage, which was statistically significant from most of other materials in the group especially at earlier time points (5 and 15 minutes) (Table 5.14). Moreover, as can be seen in Figure 5.62, the plot for RX-Home was different compared to other materials in the RX group; it showed a small expansion prior to the start of polymerisation shrinkage. All novel materials in the RX group (R1, R2, R3 and R4) had statistically comparable shrinkage values compared to commercial RX, at all time points, at 23°C ($p \geq 0.526$).

5.7.2 Polymerisation shrinkage strain at 37°C:

Figure 5.64 is a polymerisation shrinkage strain graph for one sample of each material in FP group, plotted against time in seconds, at 37°C up to 3600 seconds. Table 5.15 and Figure 5.65 highlight the mean percentage shrinkage values recorded at 5, 15, 30 and 60 minutes (37°C).

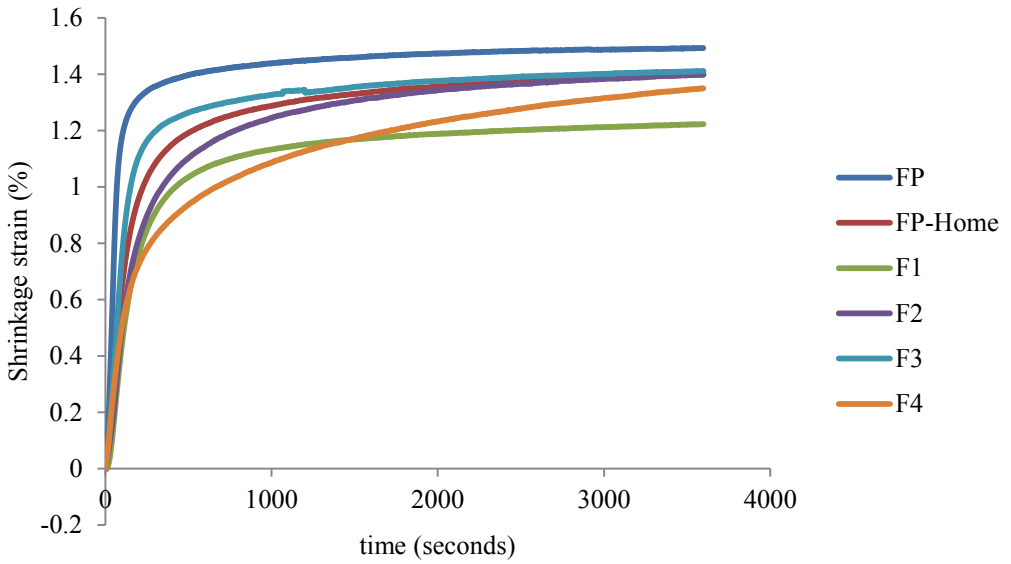

Figure 5.64 Shrinkage strain at 37°C for FP group materials (commercial, home and novel) up to 3600 seconds (60 minutes).

Table 5.15 Mean percentage shrinkage strain values and standard deviation (SD) at 5, 15, 30 and 60 minutes from the start of measurement, at 37°C, for FP group (commercial, home and novel). Similar superscript letters indicates no statistically significant difference between materials at each time point (p>0.05).

Material	Shrinkage strain at 5 minutes % (SD)	Shrinkage strain at 15 minutes % (SD)	Shrinkage strain at 30 minutes % (SD)	Shrinkage strain at 60 minutes % (SD)
FP	1.31 (0.05)	1.38 (0.06)^{a}	1.41 (0.06)^{a}	1.44 (0.07)^{a}
FP-Home	1.09 (0.04)^{a,b}	1.29 (0.04)^{a,b}	1.36 (0.04)^{a,b}	1.41 (0.03)^{a}
F1	0.94 (0.04)^{c,d}	1.18 (0.04)^{b,c}	1.25 (0.05)^{b}	1.29 (0.05)^{a}
F2	1.00 (0.08)^{b,d}	1.26 (0.09)^{a,b}	1.35 (0.08)^{a,b}	1.42 (0.08)^{a}
F3	1.19 (0.05)^{a}	1.30 (0.05)^{a,b}	1.34 (0.05)^{a,b}	1.38 (0.05)^{a}
F4	0.85 (0.06)^{c,d}	1.10 (0.09)^{c}	1.24 (0.11)^{b}	1.35 (0.14)^{a}

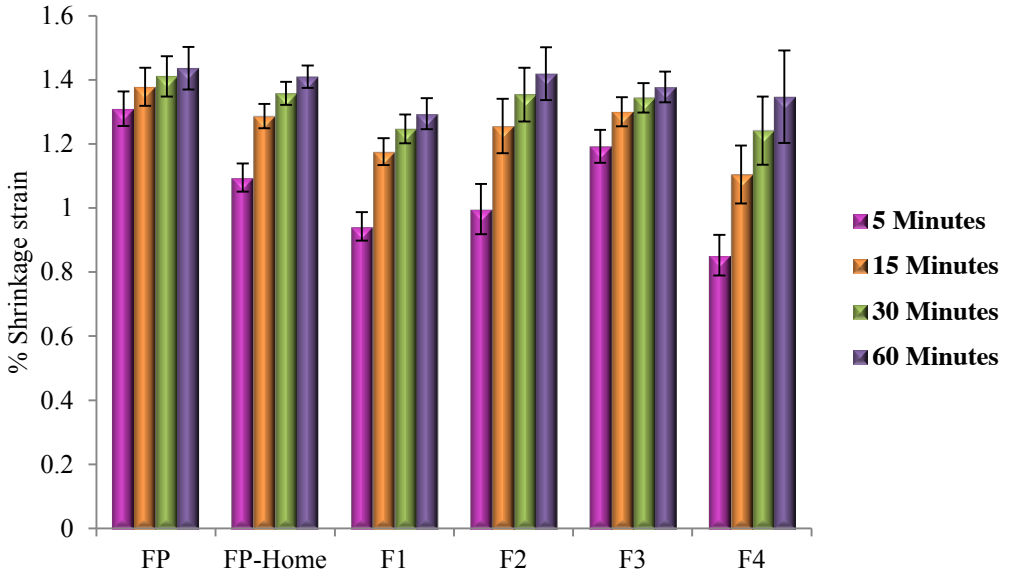

Figure 5.65 Mean shrinkage strain of FP group (commercial, home and novel) at 5, 15, 30 and 60 minutes, at 37°C, with error bars representing the standard deviation (n=5).

Similar to the polymerisation shrinkage behaviour at 23°C, FP showed the highest shrinkage at 5 minutes, which was significantly different from all materials in the FP group ($p \leq 0.037$). Following 60 minutes from the start of the shrinkage measurement, all materials in the FP group showed statistically comparable shrinkage values ($p=0.085$) (Table 5.15).

Figure 5.66 is a polymerisation shrinkage strain graph for one sample of all materials in the RX group at 37°C. Table 5.16 and Figure 5.67 illustrate the mean shrinkage strain values for all materials tested in the RX group (n=5) at 5, 15, 30 and 60 minutes.

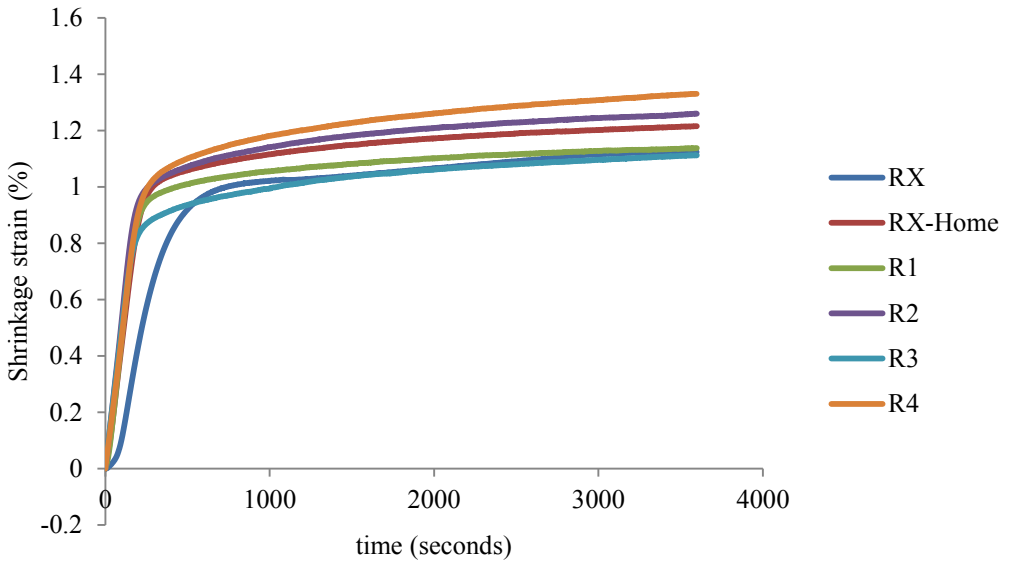

Figure 5.66 Shrinkage strain at 37°C for RX group materials (commercial, home and novel), up to 3600 seconds (1 hour).

Table 5.16 Mean percentage shrinkage strain values and standard deviation (SD) at 5, 15, 30 and 60 minutes from the start of measurement, at 37°C for RX group (commercial, home and novel). Similar superscript letters indicates no statistically significant difference between materials at each time point (p>0.05).

Material	Shrinkage strain at 5 minutes % (SD)	Shrinkage strain at 15 minutes % (SD)	Shrinkage strain at 30 minutes % (SD)	Shrinkage strain at 60 minutes % (SD)
RX	0.95 (0.05)^{a,b}	1.07 (0.05)^{a,b}	1.11 (0.05)^{a,b}	1.16 (0.05)^{a,b}
RX-Home	0.97 (0.05)^{a,b}	1.06 (0.05)^{a,b}	1.11 (0.06)^{a,b}	1.17 (0.05)^{a,b}
R1	0.98 (0.03)^{a,b}	1.07 (0.05)^{a,b}	1.13 (0.07)^{a,b}	1.19 (0.09)^{a,b}
R2	1.04 (0.04)^{a}	1.14 (0.04)^{a}	1.21 (0.05)^{a}	1.27 (0.05)^{a}
R3	0.92 (0.02)^{b}	1.01 (0.02)^{b}	1.07 (0.02)^{b}	1.13 (0.03)^{b}
R4	0.94 (0.07)^{b}	1.07 (0.08)^{a,b}	1.14 (0.08)^{a,b}	1.20 (0.10)^{a,b}

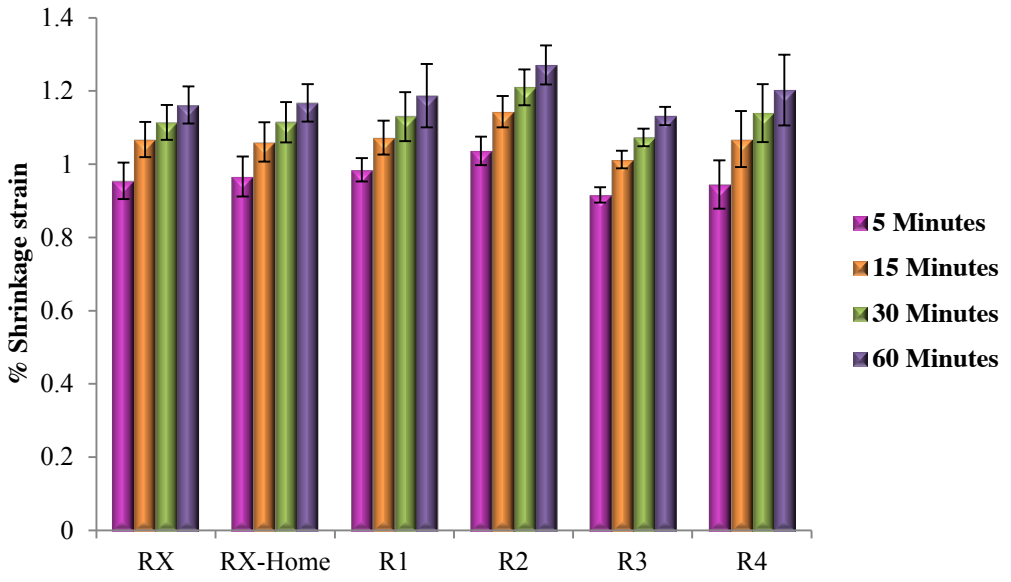

Figure 5.67 Mean shrinkage strain of RX group (commercial, home and novel) at 5, 15, 30 and 60 minutes, at 37°C, with error bars representing the standard deviation (n=5).

At 37°C, materials in the RX group showed a similar trend in the polymerisation shrinkage data to RX commercial, at different time points; there were no significant differences in shrinkage between all materials (commercial, home, and novel) ($p \leq 1$). This was also noted when the experiment was performed at 23°C (mentioned in 5.7.1). It should be noted that there was no initial expansion for RX Home at 37°C, as was evident at 23°C.

5.7.3 Polymerisation shrinkage rate ($\%.s^{-1}$):

Percentage shrinkage rate and, the time to reach the maximum rate in seconds (from the start of mixing), at 23°C and 37°C, were calculated for each material in both groups (n=5).

5.7.3.1 Polymerisation shrinkage rate (%.s^{-1}) of FP group:

Figures 5.68 and 5.70 are representative plots of shrinkage strain rate (%.s^{-1}) for the FP group materials (commercial, home and novel) measured at 23°C and 37°C respectively, up to 3600 seconds. Figures 5.69 and 5.71 represent mean of shrinkage strain rate (%.s^{-1}) for FP group materials (with error bars for the standard deviation of 5 samples per material) at 23°C and 37°C respectively. Moreover, Tables 5.17 and 5.18 highlight the mean of maximum shrinkage strain rate values recorded for each material in the FP group, at 23°C and 37°C respectively.

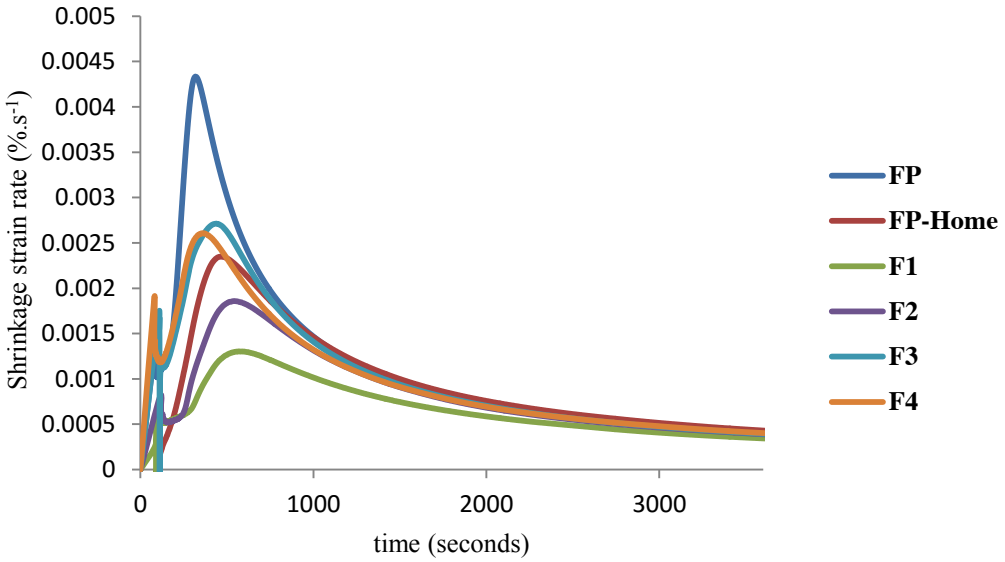

Figure 5.68 Representative shrinkage strain rate curve for FP group (commercial, home and novel) up to 3600 seconds, at 23°C.

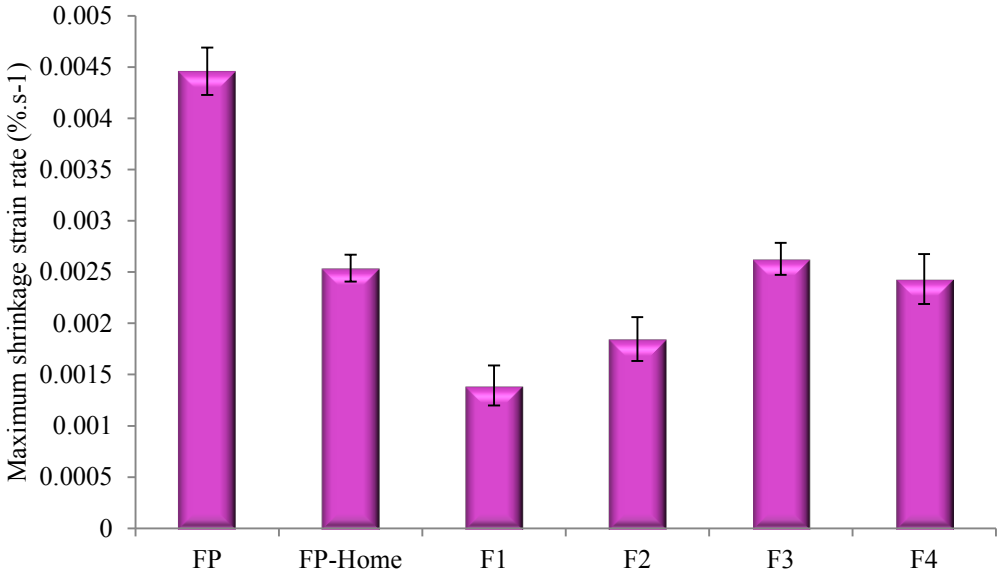

Figure 5.69 Mean percentage maximum shrinkage strain rate (%.s^{-1}) for FP group (commercial, home and novel) with error bars representing standard deviation (n=5 per material), at 23°C.

Table 5.17 Mean percentage maximum shrinkage strain rate (%.s^{-1}), time at the maximum shrinkage strain rate (seconds) and CoVs (23°C). Similar superscript letters indicates no statistically significant difference between materials (p>0.05).

Material	Shrinkage rate at 23°C (%.s^{-1}) (SD)	CoV	Time at maximum shrinkage rate (seconds) (SD)	CoV
FP	0.0045 0.0002)	0.05	327.80 (9.15)^{c}	0.03
FP-Home	0.0025 (0.0001)^{a}	0.05	440.80 (18.67)^{b}	0.04
F1	0.0014 (0.0002)	0.14	552.20 (33.11)^{a}	0.06
F2	0.0018 (0.0002)	0.12	545.40 (17.59)^{a}	0.03
F3	0.0026 (0.0002)^{a}	0.06	443.00 (12.55)^{b}	0.03
F4	0.0024 (0.0002)^{a}	0.10	339.80 (16.90)^{c}	0.05

One-way ANOVA analyses showed a highly significant difference between materials ($p<0.0001$), therefore the post-hoc Tukey test was applied to compare results between all materials at a significance level of $p<0.05$. It was noticed that shrinkage strain rate measured at 23°C was significantly lower for F1 and F2, which did not contain HEMA and, they required more time to reach this rate, compared to other materials in the group ($p\leq0.001$). Commercial FP had a significantly higher shrinkage rate value compared to all materials in the group ($p<0.0001$) and required less time to reach this rate ($p<0.0001$) (Table 5.17).

CoV values for shrinkage strain rate (0.05-0.14; 5-14%) and time to reach maximum strain rate (0.03-0.06; 3-6%) generally demonstrated acceptable reproducibility of the results, particularly with respect to the latter. However, F1 and F2 maximum strain rate CoV had a value greater than 10% but, they can be accepted as being reliable since they had lower values compared with other materials (Table 5.17).

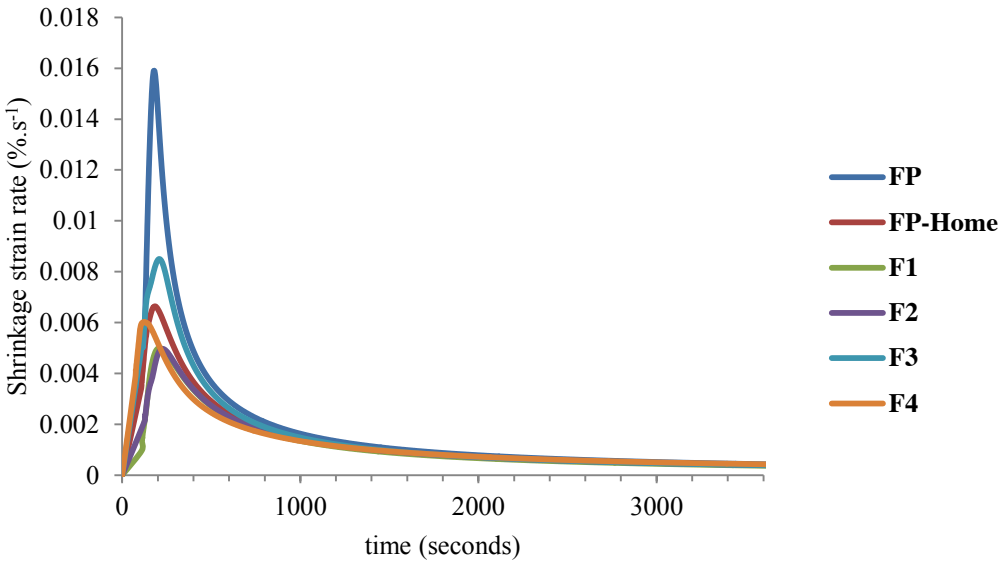

Figure 5.70 Representative shrinkage strain rate curve for FP group (commercial, home and novel) up to 3600 seconds at 37°C.

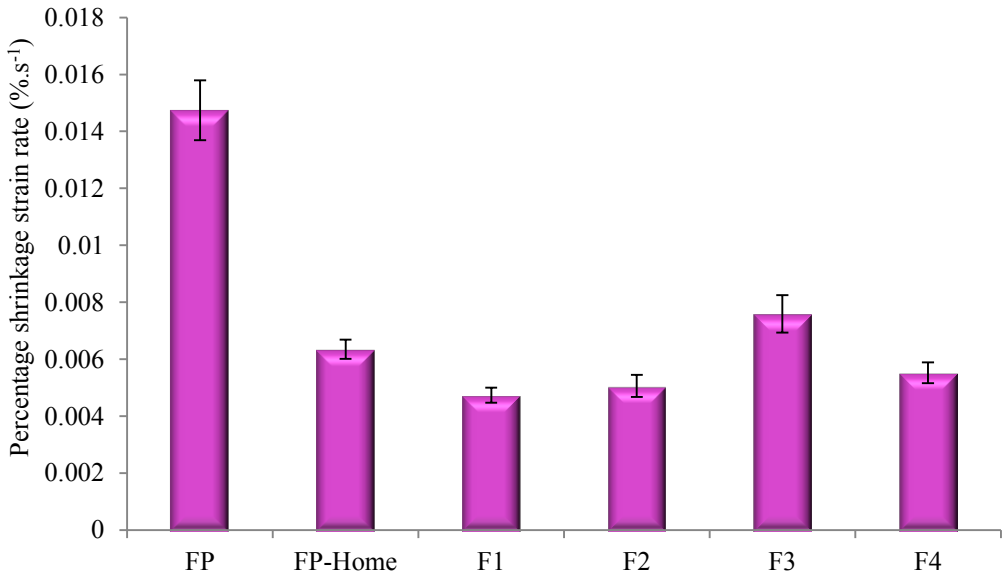

Figure 5.71 Mean percentage maximum shrinkage strain rate (%.s^{-1}) for FP group (commercial, home and novel) with error bars representing standard deviation (n=5 per material) at 37°C.

Table 5.18 Mean percentage maximum shrinkage strain rate (%.s^{-1}), time at the maximum shrinkage strain rate (seconds) and CoV for both means of FP group (commercial, home and novel) at 37°C. Similar superscript letters indicates no statistically significant difference between materials (p>0.05).

Material	shrinkage rate at 37°C (%.s^{-1}) (SD)	CoV	Time at maximum shrinkage rate (seconds) (SD)	CoV
FP	0.0147 (0.0011)	0.07	172.60 (5.98)	0.03
FP-Home	0.0063 (0.0003)^{a}	0.05	193.80 (3.49)	0.02
F1	0.0047 (0.0003)^{b}	0.06	208.00 (2.12)^{a}	0.01
F2	0.0051 (0.0004)^{b}	0.08	220.80 (5.31)	0.02
F3	0.0076 (0.0007)	0.09	206.60 (7.20)^{a}	0.03
F4	0.0055 (0.0004)^{a,b}	0.07	131.80 (6.10)	0.05

At 37°C, FP commercial has a significantly higher shrinkage strain rate compared to all materials in the same group ($p<0.0001$), similar to the trend obtained at 23°C. Once more, the shrinkage strain rate values recorded for F1 and F2 were significantly lower than other materials in the group ($p\leq0.019$), with the exception of F4 ($p\geq0.298$; Table 5.18).

Only F3 and F1 showed no significant difference in their time to reach the maximum shrinkage strain rate ($p=0.998$), while all other FP materials were statistically different (F4 took less time to reach the maximum rate followed by commercial FP). The calculated CoVs for the time to reach maximum shrinkage strain rate (mean) at 37°C, were very low, ranging from 1-5%, which demonstrates low variability between the measurements for each material (Table 5.18).

5.7.3.2 Polymerisation shrinkage rate ($\%.s^{-1}$) of RX group:

Shrinkage strain rate ($\%.s^{-1}$) were plotted against time up to 3600 seconds for all materials. Figures 5.72 and 5.74 are example plots for the RX group materials (commercial, home and novel) at 23°C and 37°C respectively. Mean shrinkage strain rates ($\%.s^{-1}$) (5 samples per material; n=5), at 23°C and 37°C, are presented in Figures 5.73 and 5.75, and summarised in Tables 5.19 and 5.20 respectively.

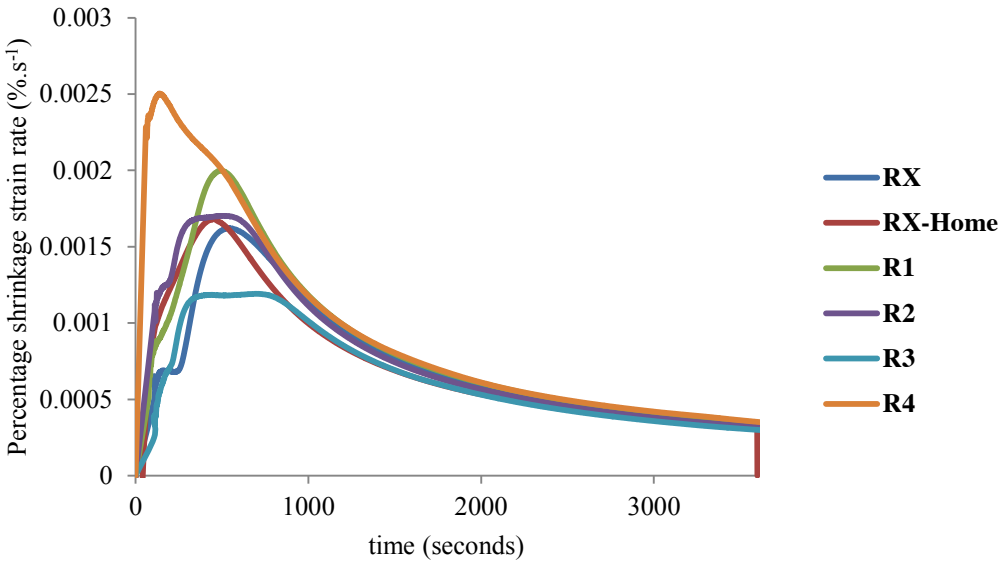

Figure 5.72 Representative shrinkage strain rate curve for RX group (commercial, home and novel) up to 3600 seconds, at 23°C.

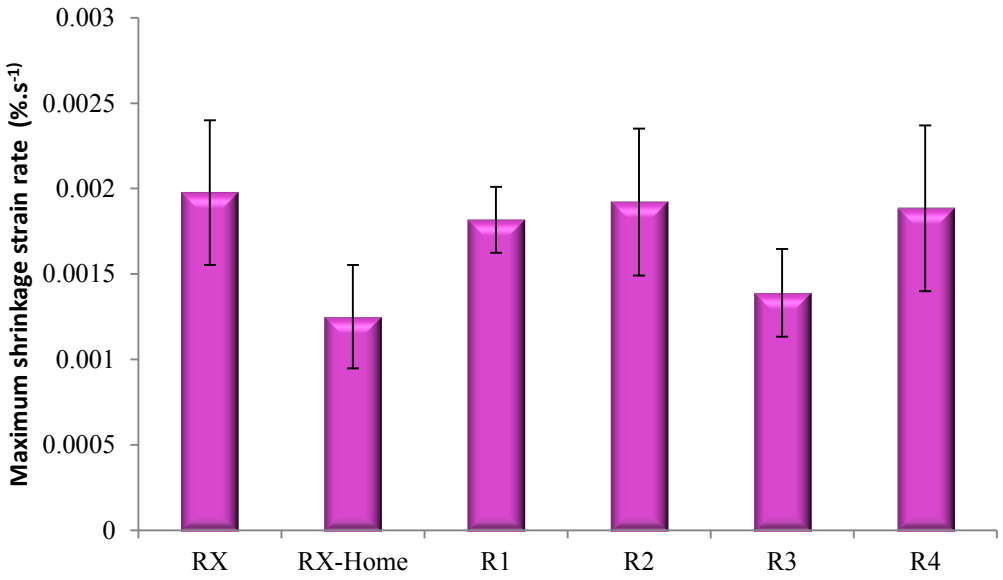

Figure 5.73 Mean percentage maximum shrinkage strain rate ($\%.s^{-1}$) for RX group (commercial, home and novel) with error bars representing standard deviation (n=5 per material), at 23°C.

Table 5.19 Mean percentage maximum shrinkage strain rate ($\%.s^{-1}$), time at the maximum shrinkage strain rate (seconds) and CoVs of RX group (commercial, home and novel), at 23°C. Similar superscript letters indicates no statistically significant difference between materials (p>0.05).

Material	Shrinkage strain rate at 23°C ($\%.s^{-1}$) (SD)	CoV	Time at maximum shrinkage strain rate (seconds) (SD)	CoV
RX	0.0020 (0.0004)[a]	0.21	471.00 (100.83)[a,b]	0.21
RX-Home	0.0013 (0.0003)[b]	0.24	640.00 (95.00)[a]	0.15
R1	0.0018 (0.0002)[a,b]	0.11	524.40 (79.99)[a,b]	0.15
R2	0.0019 (0.0004)[a,b]	0.22	450.20 (152.73)[a,b]	0.34
R3	0.0014 (0.0003)[a,b]	0.19	643.00 (86.39)[a]	0.13
R4	0.0019 (0.0005)[a,b]	0.26	399.80 (167.03)[b]	0.42

P value of 0.015 between materials in the RX group was noticed following one-way ANOVA analyses, which demonstrated statistically significant difference between some materials' shrinkage strain rate values. The post-hoc Tukey test confirmed that the only significant difference in the maximum shrinkage rate was between RX and RX-Home (p=0.043), whilst for all other materials there was no significant difference (p≥0.149). Moreover, it is worth noting the high CoV for strain rate values, which indicates variation in the values obtained and will be discussed in the discussion chapter.

Furthermore, time to reach the maximum strain rate showed high CoV values (42% for R4), which, similar to the shrinkage strain data, indicates a great variability in the results for RX, at 23°C; therefore the reliability of these results is debatable (Table 5.19).

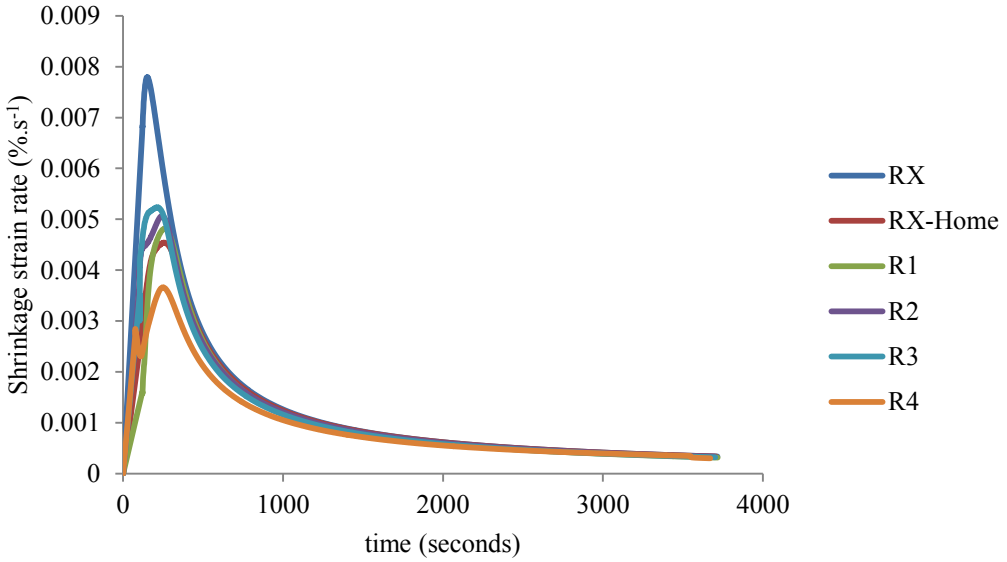

Figure 5.74 Representative shrinkage strain rate curve for RX group (commercial, home and novel) up to 3600 seconds at 37°C.

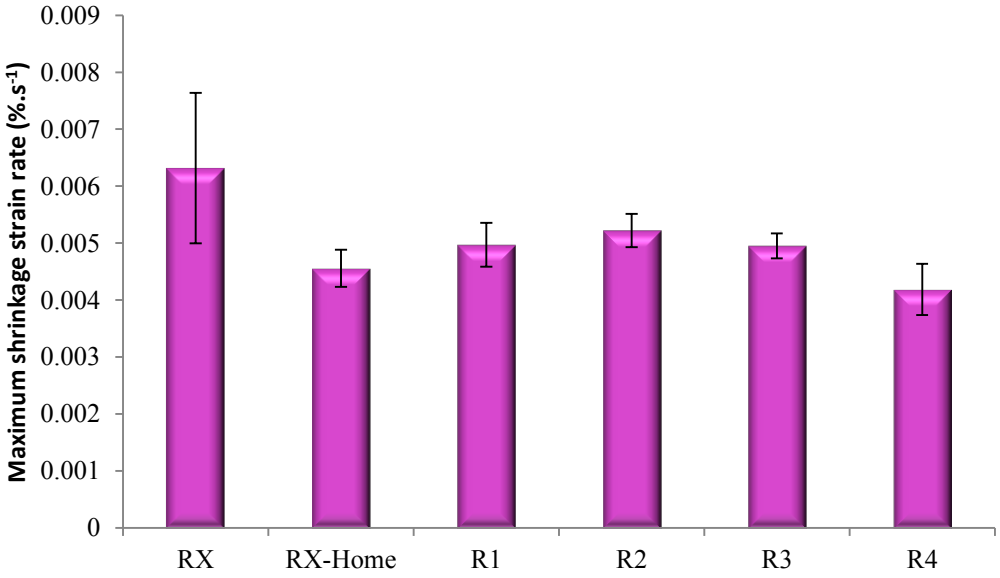

Figure 5.75 Mean percentage maximum shrinkage strain rate ($\%.s^{-1}$) for RX group (commercial, home and novel) with error bars representing standard deviation (n=5 per material) at 37°C.

Table 5.20 Mean percentage maximum shrinkage strain rate ($\%.s^{-1}$), time at the maximum shrinkage strain rate (seconds) and CoVs of RX group (commercial, home and novel) at 37°C. Similar superscript letters indicates no statistically significant difference between materials (p>0.05).

Material	Shrinkage strain rate at 37°C ($\%.s^{-1}$) (SD)	CoV	Time at maximum shrinkage rate (seconds) (SD)	CoV
RX	0.0063 (0.0013)[a]	0.21	168.80 (13.19)	0.08
RX-Home	0.0046 (0.0003)[b]	0.07	259.60 (7.13)[a]	0.03
R1	0.0050 (0.0004)[b]	0.08	263.00 (16.36)[a]	0.06
R2	0.0052 (0.0003)[a,b]	0.06	246.80 (11.73)[a,b]	0.05
R3	0.0049 (0.0002)[b]	0.04	220.00 (13.19)[c]	0.06
R4	0.0042 (0.0004)[b]	0.11	232.40 (13.41)[b,c]	0.06

RX commercial had a significantly higher shrinkage rate value, at 37°C, compared to all other materials in the group, except for R2 ($p=0.097$). Post-hoc Tukey test did not result in any significant differences, which indicates similar values were obtained for those materials ($p\geq0.130$). CoV values for home and novel materials were equal to, or less than, 11% indicating acceptable variability, with the exception of the RX CoV value, which reached 21% (Table 5.20).

As can be seen in Figure 5.74, sharper peaks were associated with strain rate measured at 37°C compared those obtained at 23°C, which were broad and not well defined (Figure 5.72).

RX commercial reached the maximum strain rate at 168.80 ± 13.19 seconds from the start of mixing and this was significantly faster than all other materials (home and novel cements) ($p<0.0001$). These results indicated a low variability between repeats ($n=5$), with CoV ranging from 3-8% (Table 5.20).

5.8 *Polymerisation exotherm of all materials (commercial, home and novel):*

5.8.1 Polymerisation exotherm of FP group materials:

Figures 5.76 and 5.77 are representative exotherm curves for materials, up to 3600 seconds, measured at both 23 and 37°C respectively. Tables 5.21 and 5.22 summarise polymerisation exotherm of FP group materials and the time taken to reach this temperature, from the start of the measurement, for 5 samples per material (n=5).

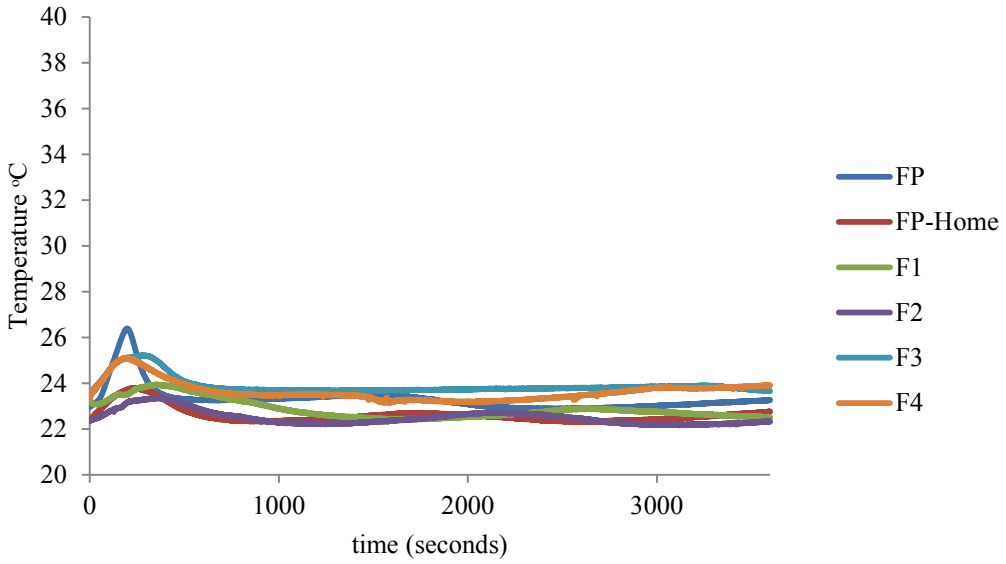

Figure 5.76 Representative temperature/time curve for FP group (commercial, home and novel) up to 3600 seconds, at 23°C.

Table 5.21 Polymerisation exotherm and time at exotherm for FP group (commercial, home and novel), with standard deviations and CoV (n=5 per material), at 23°C. Similar superscript letters indicates no statistically significant difference between materials (p>0.05).

Material	Peak exotherm temperature (SD)	CoV	Time at peak exotherm temperature at (SD)	CoV
FP	3.57 (0.13)	0.04	202.60 (9.71)[c]	0.05
FP-Home	1.46 (0.23)[a]	0.15	258.60 (23.38)[b]	0.09
F1	0.81 (0.12)	0.14	329.40 (14.40)[a]	0.04
F2	1.33 (0.29)[a]	0.22	348.20 (10.71)[a]	0.03
F3	1.85 (0.22)	0.12	285.00 (16.72)[b]	0.06
F4	1.45 (0.11)[a]	0.07	191.40 (15.11)[c]	0.08

FP commercial had a significantly higher exotherm at 23°C compared to all materials in the group ($p<0.0001$), and it also reached this exotherm faster than other materials, except for F4 ($p=0.864$). Although there was a statistically significant difference in reaching the peak temperature for FP-Home, F4 and F2 ($p<0.0001$), all three presented with comparable exotherm results ($p=0.896$). F1 increased in temperature by only 0.81 ± 0.12°C, which was significantly lower than all other materials in the group ($p\leq0.003$). Moreover, F1 took more time to reach this temperature, compared to the other materials ($p<0.0001$), with the exception of F2 ($p=0.427$) (Table 5.21).

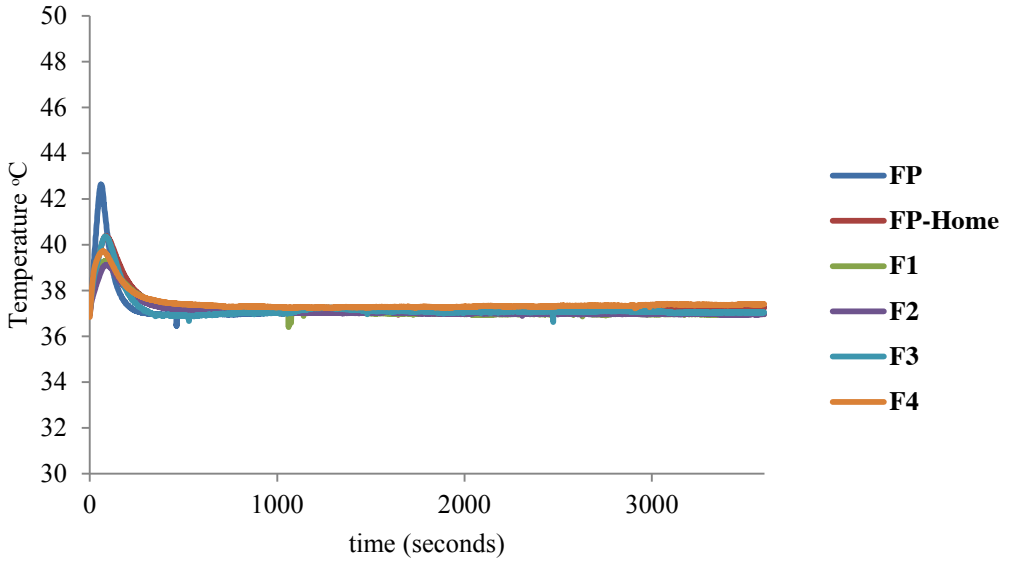

Figure 5.77 Representative temperature/time curve for FP group (commercial, home and novel) up to 3600 seconds at 37°C.

Table 5.22 Polymerisation exotherm and time at exotherm for FP group (commercial, home and novel) with standard deviations and CoV (n=5 per material), at 37°C. Similar superscript letters indicates no statistically significant difference between materials (p>0.05).

Material	Peak exotherm temperature at 37°C (°C) (SD)	CoV	Time at peak exotherm temperature at 37°C (seconds) (SD)	CoV
FP	6.12 (0.48)	0.08	56.20 (2.28)	0.04
FP-Home	3.01 (0.32)[a]	0.11	81.20 (1.10)[b]	0.01
F1	2.34 (0.16)[b]	0.07	89.80 (6.87)[a]	0.08
F2	2.32 (0.21)[b]	0.09	86.80 (3.19)[a,b]	0.04
F3	3.39 (0.36)[a]	0.11	87.20 (3.35)[a,b]	0.04
F4	2.77 (0.37)[a,b]	0.13	68.00 (3.46)	0.05

A similar trend in the exotherm was noticed at 37°C in that FP commercial had a significantly higher exotherm compared to all materials in the group ($p<0.0001$) and, moreover, less time was needed to reach this temperature ($p\leq0.001$). However, the

exotherm noted at 37°C was ~ 43% higher than that recorded at 23°C, reaching 6.12 ± 0.48°C, as a result of the polymerisation reaction. F1 exhibited a lower exotherm but the value recorded at 37°C was not significantly different to F4 and F2 values (p=0.301). There was no significant difference between the exotherms at 37°C (p=0.068) (Table 5.22) for compositions containing HEMA (FP-Home, F3 and F4).

5.8.2 Polymerisation exotherm of RX group materials:

Figures 5.78 and 5.79 are representatives of time dependent temperature curves at 23 and 37°C, up to 3600 seconds. Recorded exotherm values and time to reach this temperature, with standard deviations and CoV for all samples, are given in Tables 5.23 and 5.24.

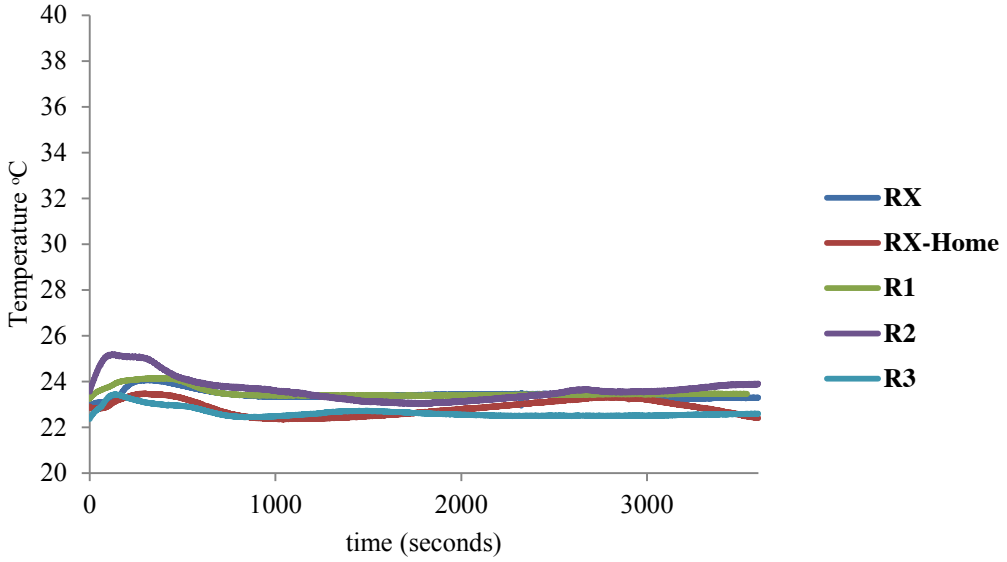

Figure 5.78 Representative temperature/time curve for RX group (commercial, home and novel) up to 3600 seconds at 23°C.

Table 5.23 Polymerisation exotherm and time at exotherm for RX group (commercial, home and novel) with standard deviations and CoV (n=5 per material) at 23°C. Similar superscript letters indicates no statistically significant difference between materials (p>0.05).

Material	Peak exotherm temperature at 23°C (°C) (SD)	CoV	Time at peak exotherm temperature at 23°C (seconds) (SD)	CoV
RX	1.42 (0.25)[a]	0.18	229.40 (70.37)[a,b]	0.31
RX-Home	0.96 (0.34)[a,b]	0.35	225.00 (65.15)[b,c]	0.29
R1	1.08 (0.21)[a,b]	0.20	309.60 (5.18)[a]	0.02
R2	0.95 (0.35)[a,b]	0.37	144.80 (26.17)[c]	0.18
R3	0.80 (0.22)[b]	0.28	183.20 (29.35)[b,c]	0.16
R4	1.09 (0.17)[a,b]	0.15	156.00 (10.63)[b,c]	0.07

The only significant difference between materials, with respect to exotherm data, measured at 23°C, was found between RX and R3 (p=0.013), despite these two materials showing similar results in their time taken to reach the maximum temperature recorded (p=0.563). R1 required a significantly longer time than all other materials in the same group to reach the maximum temperature recorded, except when compared to RX (p=0.064).

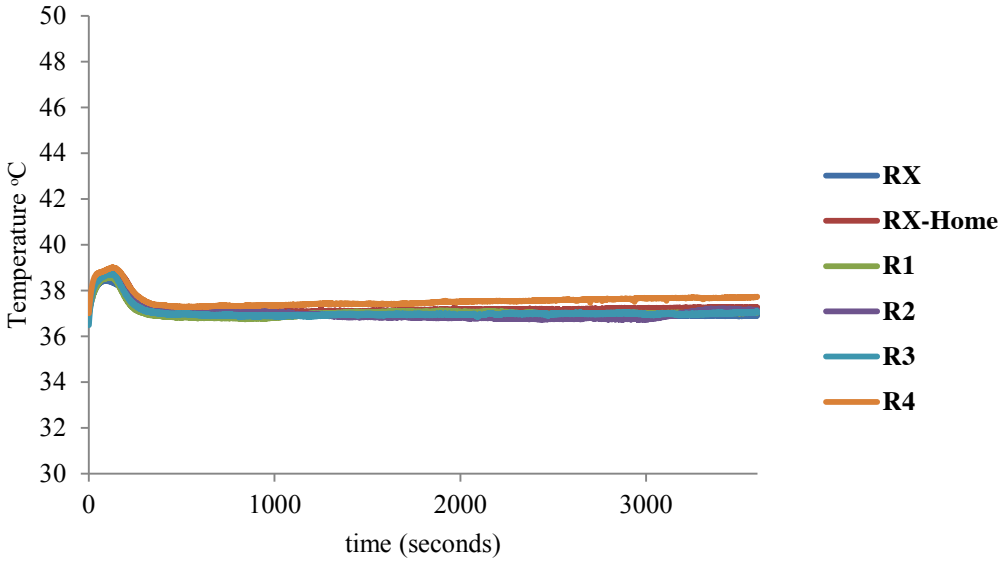

Figure 5.79 Representative temperature/time curve for RX group (commercial, home and novel) up to 3600 seconds at 37°C.

Table 5.24 Polymerisation exotherm and time at exotherm for RX group (commercial, home and novel) with standard deviations and CoV (n=5 per material) at 37°C. Similar superscript letters indicates no statistically significant difference between materials (p>0.05).

Material	Peak exotherm temperature at 37°C (°C) (SD)	CoV	Time at Peak exotherm temperature at 37°C (seconds) (SD)	CoV
RX	1.82 (0.28)[a]	0.15	75.40 (13.16)	0.17
RX-Home	1.91 (0.13)[a]	0.07	127.60 (9.48)[a,b]	0.07
R1	1.95 (0.23)[a]	0.12	122.40 (7.20)[b]	0.06
R2	1.93 (0.07)[a]	0.04	133.00 (8.25)[a,b]	0.06
R3	1.94 (0.21)[a]	0.11	115.40 (4.83)[b]	0.04
R4	2.07 (0.15)[a]	0.07	143.40 (12.93)[a]	0.09

Mean peak exotherm temperatures for RX materials at 37°C ranged from 1.82 to 2.07°C. Following one-way ANOVA testing, there was no significant difference between the peak exotherm of all materials in this group (p=0.491). Despite this, RX

required significantly less time to reach the peak temperature compared to all materials (home and novel) in the same group ($p<0.0001$).

5.9 *Identification and quantification of monomer release from all materials (commercial, home and novel):*

5.9.1 Identification of monomer release from FP group:

All monomer release analyses were performed following a novel HPLC method, which was developed in order to identify monomers included in the FP sample. This novel method was crucial since there was no available method published in the literature for detecting these monomers in RMGICs.

Monomers released from FP samples were detected using an HPLC technique and compared with their respective standard solutions (HEMA and UDMA). Peaks of HEMA (retention time ~3.351) and UDMA (retention time ~15.707), acquired from ChemStation software plotted as absorbance (mAU) against time (minutes), were identified in solutions taken at 1, 4 hours, 1day and 1 week following immersion of FP and FP-Home samples in DW, as can be seen in the typical chromatograms in Figures 5.80 and 5.81 respectively.

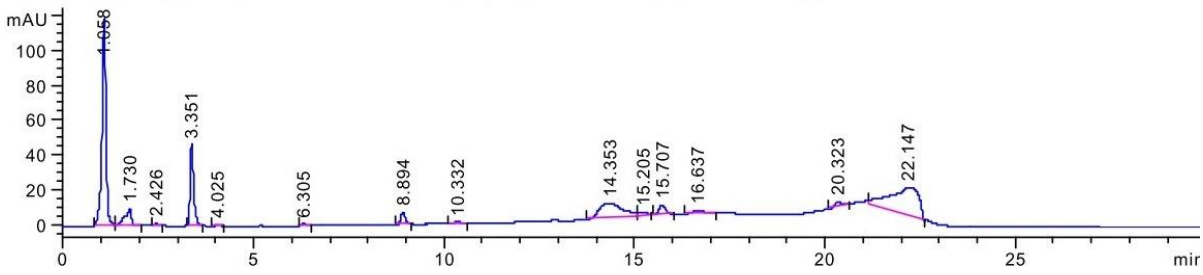

Figure 5.80 A typical HPLC chromatogram of commercial FP sample following 1 day immersion in DW.

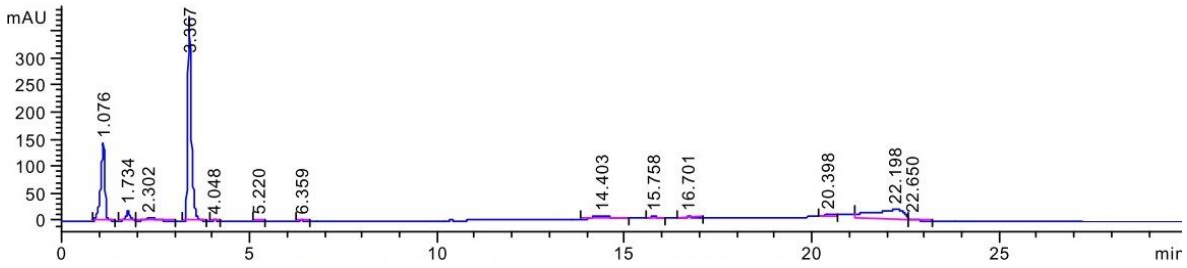

Figure 5.81 A typical HPLC chromatogram of FP-Home sample following 1 day immersion in DW.

A peak with a retention time of ~8.89 minutes was also detected in FP commercial sample (Figure 5.80). This peak's retention time did not match with any of the ingredients mentioned in the manufacturers MSDS of FP commercial liquid. Therefore, the commercial liquid of FP was further analysed using HPLC-mass spectrometer (HPLC-MS) in order to confirm the identification of this composition and, to make sure that this peak was associated with it, rather than it being a result of contamination. Hence, two batches of the liquid were analysed to rule out the possibility of batch contamination. Three peaks were identified following analyses, one associated with HEMA (at ~3.38 minutes), one with UDMA (at a retention time of ~15.74 minutes) and the additional peak (retention time of ~8.941 minutes), the latter being similar to the peak noticed in the sample solution extracts. The HPLC-MS showed that the component's molecular weight/charge was 211.5 but it could not be identified at this stage (Figure 5.82).

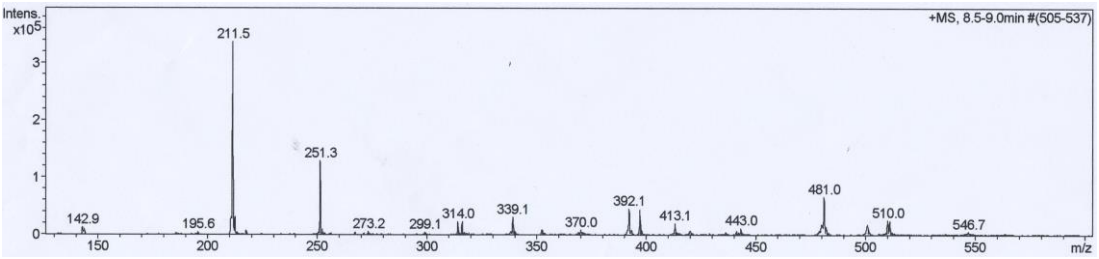

Figure 5.82 Mass spectrum of monomer eluted from commercial FP sample to confirm an additional component at a retention time of ~8.9 minutes.

Representative HPLC chromatogram of novel F1, F2, F3 and F4 are presented in Figures 5.83, 5.84, 5.85 and 5.86 respectively. It can be seen that monomers (HEMA, THFM, HPM and UDMA) were released from cement samples, which were detected following immersion either in DW or 75:25% ethanol:DW.

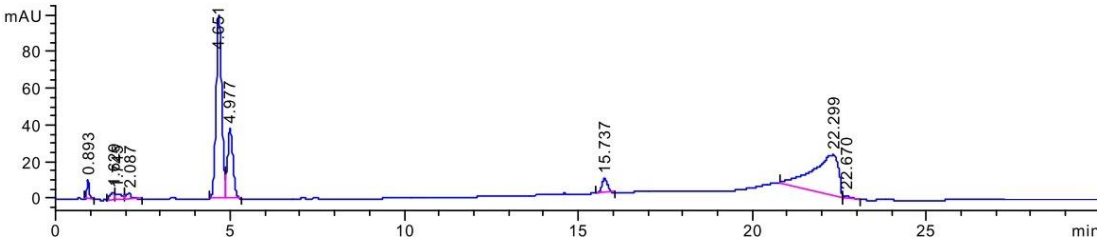

Figure 5.83 A typical HPLC chromatogram of F1 sample following 1 day immersion in 75:25 ethanol:DW.

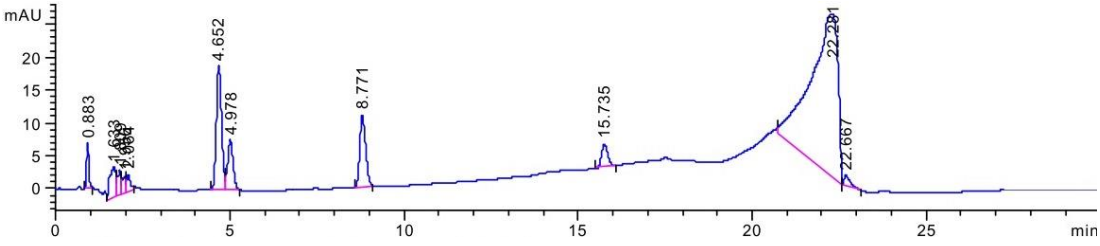

Figure 5.84 A typical HPLC chromatogram of F2 sample following 1 day immersion in DW.

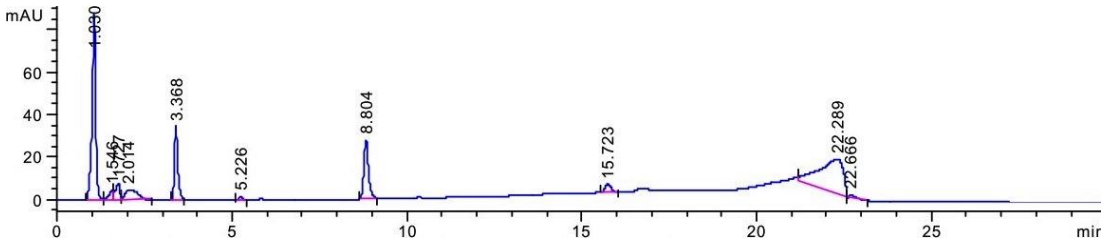

Figure 5.85 A typical HPLC chromatogram of F3 sample following 1 day immersion in DW.

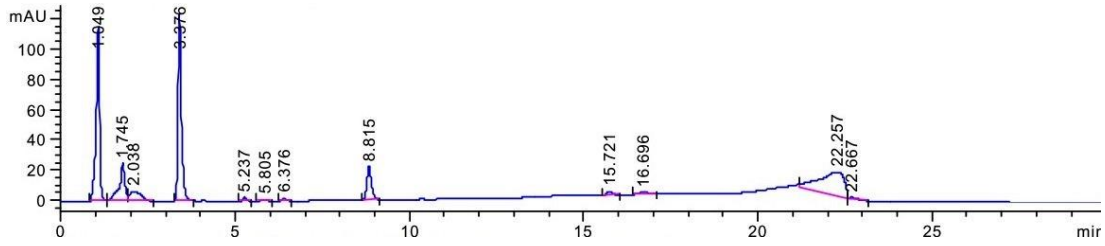

Figure 5.86 A typical HPLC chromatogram of F4 sample following 1 day immersion in 75:25 ethanol:DW.

5.9.2 Identification of monomer release from RX group:

Representative HPLC chromatograms of RX, RX-Home, R1, R2, R3 and R4 are presented in Figures 5.87, 5.88, 5.89, 5.90, 5.91 and 5.92 respectively.

Similar to the FP group, a novel method had to be developed for the identification of monomers released from the RX group. Although the novel method used for FP could have been used, a further novel method had to be developed for RX to allow identification of extracts in less time (8 minutes in the RX group compared to 30 minutes in the FP group), and thus reducing the costs of the experiments.

Extracted solutions from RX samples showed peaks that were attributed to the monomers included in each corresponding liquid. RX and RX-Home showed peaks for HEMA only, whereas HPM was present in HPLC spectra of F1 and F2, along

with THFM in the latter material; HEMA and THFM were found in F3 and F4 spectra.

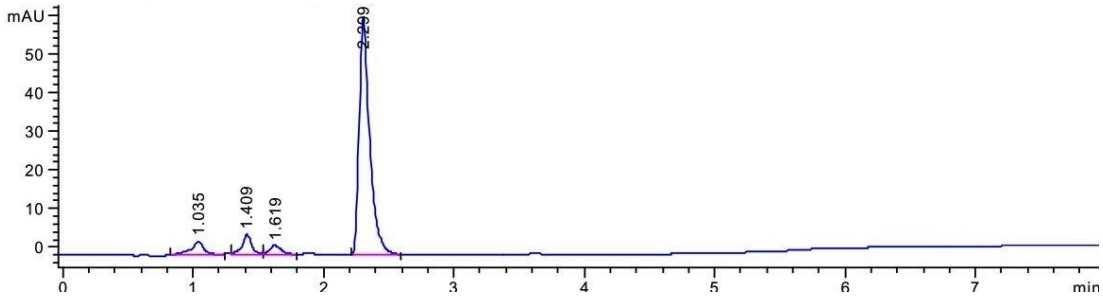

Figure 5.87 A typical HPLC chromatogram of commercial RX sample following 1 day immersion in DW.

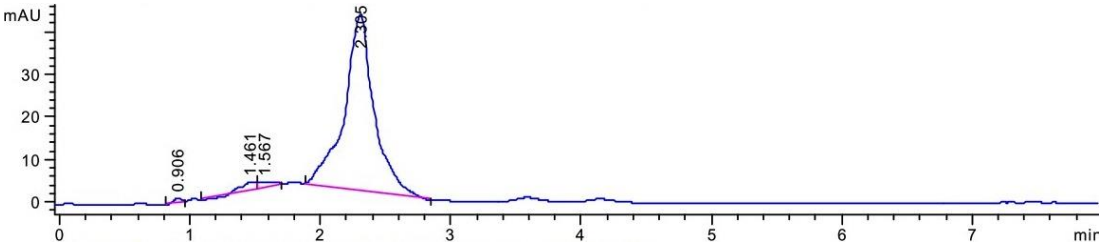

Figure 5.88 A typical HPLC chromatogram of RX-Home sample following 1 day immersion in 75:25 ethanol:DW.

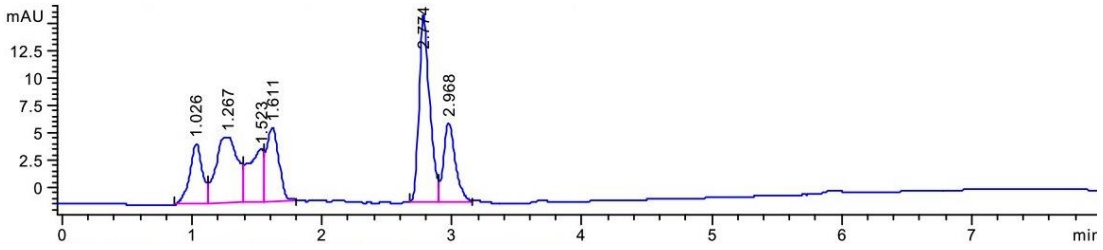

Figure 5.89 A typical HPLC chromatogram of R1 sample following 1 hour immersion in 75:25 ethanol:DW.

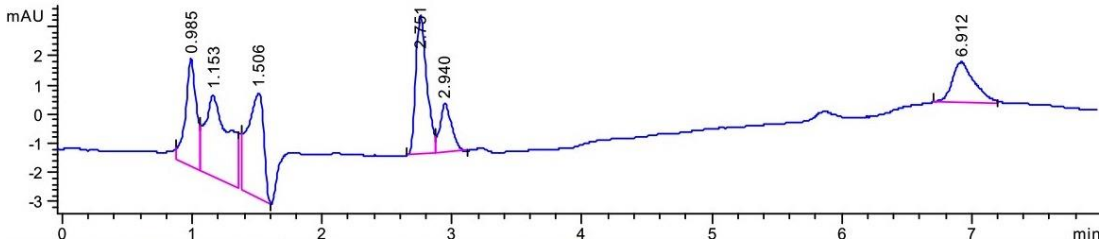

Figure 5.90 A typical HPLC chromatogram of R2 sample following 1 hour immersion in 75:25 ethanol:DW.

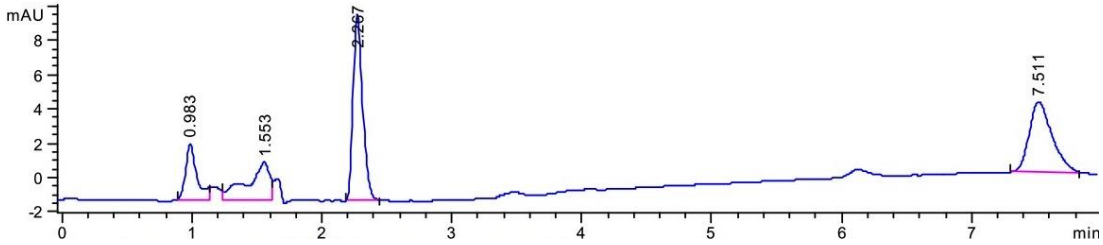

Figure 5.91 A typical HPLC chromatogram of R3 sample following 1 hour immersion in DW.

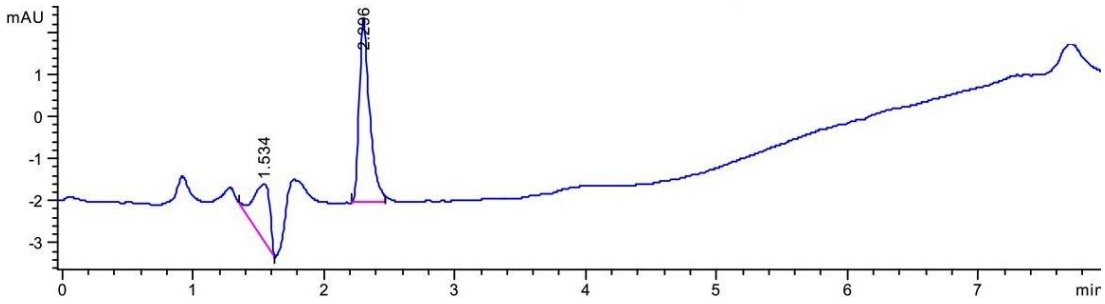

Figure 5.92 A typical HPLC chromatogram of R4 sample following 1 hour immersion in DW.

5.9.3 Quantification of monomer release (ppm) in DW:

Mean cumulative monomer release from FP group samples, following immersion in DW after 1, 4 hours, 1 day and 1 week are presented in Figure 5.93 and moreover Table 5.25 summarises the release data from all materials at the same time points.

Following one-hour immersion in DW at 37°C, FP and FP-Home showed significantly higher release of HEMA compared to F3 and F4 ($p \leq 0.001$), although there was no significant difference between the cumulative release of monomers from these four materials ($p \geq 0.810$). F3 and F4 additional released the monomer THFM, which was not present in FP and FP-Home. A maximum release was noticed in solutions from F1 samples, at 1 hour, which continued to show significantly higher release than all other materials in the same group, at all time points ($p \leq 0.001$). Furthermore, at all-time points, F1 showed a significantly higher release of HPM and a cumulative monomer release (HPM and UDMA) than F2 ($p < 0.0001$) (Figure 5.97). Lower amounts of residual monomers were released from F3 and commercial FP at 1 day and 1 week compared to all other materials ($p \leq 0.023$).

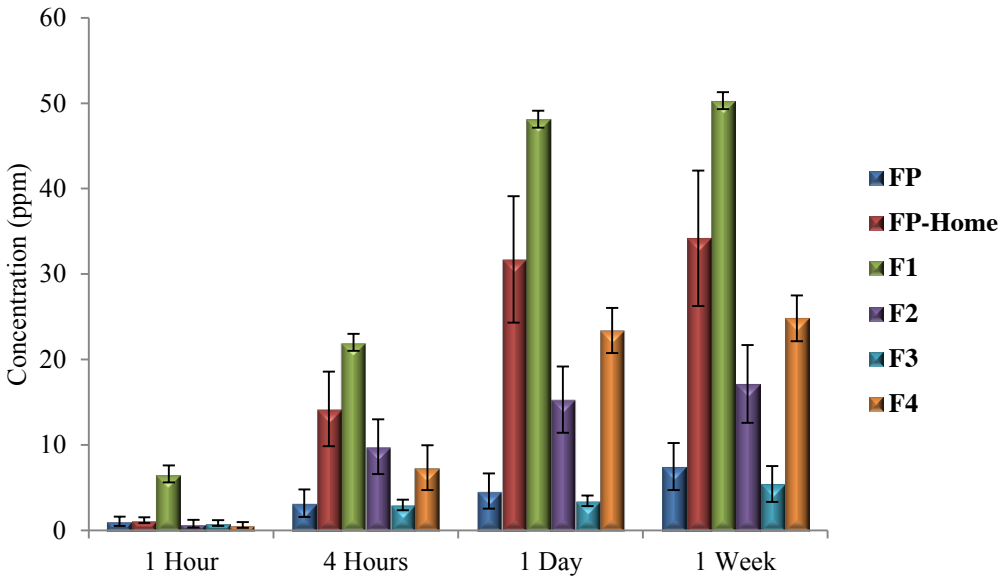

Figure 5.93 Mean concentration (ppm) of all monomers (HEMA, HPM, THFM, UDMA) released from FP group materials in DW at 1 hour, 4 hours, 1 day and 1 week. Error bars represent standard deviations of the mean of 6 samples per materials (n=6).

Table 5.25 Mean release and cumulative release of all monomers (ppm) (SD) from each material in the FP group in DW at different time points (1 hour, 4 hours, 1 day and 1 week). Similar superscript letters indicate no significant difference (p>0.05).

Time	Monomer	FP	FP-Home	F1	F2	F3	F4
1 Hour	HEMA	1.07 (0.55)[a]	1.19 (0.35)[a]	-	-	0.32 (0.10)[b]	0.41 (0.19)[b]
	HPM	-	-	6.60 (1.61)	0.78 (0.45)	-	-
	THFM	-	-	-	0	0.53 (0.24)	0.28 (0.12)
	UDMA	0	0	0	0	0	0
	All monomers	1.07 (0.55)[a]	1.19 (0.35)[a]	6.60 (1.61)	0.78 (0.45)[a]	0.86 (0.34)[a]	0.64 (0.33)[a]
4 Hours	HEMA	3.18 (1.61)[a]	14.21 (4.37)	-	-	1.01 (0.26)[a]	3.11 (0.96)[a]
	HPM	-	-	17.70 (2.60)	3.96 (1.97)	-	-
	THFM	-	-	-	2.07 (0.95)[a]	1.96 (0.35)[a,b]	1.27 (0.43)[b]
	UDMA	0	0	4.31 (0.64)[a]	3.76 (0.30)[a]	0	4.43 (0.43)[a]
	All monomers	3.18 (1.61)[c]	14.21 (4.37)[a]	22.01 (2.86)	9.79 (3.20)[a,b]	2.97 (0.61)[c]	7.34 (2.62)[b,c]
1 Day	HEMA	3.23 (1.59)[a]	30.00 (7.20)	-	-	1.21 (0.24)[a]	12.91 (2.25)
	HPM	-	-	36.24 (7.88)	5.47 (1.99)	-	-
	THFM	-	-	-	2.85 (0.99)[a]	2.25 (0.38)[a]	4.16 (0.91)
	UDMA	1.37 (0.75)[b]	1.70 (0.92)[b]	11.89 (1.04)	6.98 (1.12)[a]	0	6.30 (0.81)[a]
	All monomers	4.60 (2.07)[c]	31.70 (7.41)[a]	48.13 (7.32)	15.31 (3.88)[b]	3.45 (0.62)[c]	23.38 (2.65)[a,b]
1 Week	HEMA	3.88 (1.58)[a]	31.86 (7.46)	-	-	1.60 (0.46)[a]	12.35 (1.83)
	HPM	-	-	37.86 (7.37)	6.06 (1.74)	-	-
	THFM	-	-	-	3.02 (0.82)[a]	2.36 (0.55)[a]	5.48 (1.28)
	UDMA	3.58 (1.22)[b]	2.33 (0.61)[b]	12.43 (1.07)	8.06 (2.27)[a]	2.40 (0.72)[b]	6.98 (0.42)[a]
	All monomers	7.46 (2.76)[b]	34.20 (7.93)	50.29 (6.70)	17.14 (4.55)[a]	5.42 (2.11)[b]	24.81 (2.68)[a]

Mean cumulative monomers (HEMA, HPM and THFM) concentrations (ppm), which were released from RX materials in DW at all time points were plotted and presented in Figure 5.94. Table 5.26 summarises the monomers released from RX group materials at 1, 4 hours, 1 day and 1 week time intervals following immersion in DW (6 samples for each material; n=6).

Commercial RX released significantly more HEMA than home and novel RX materials at all time points ($p \leq 0.015$). However, similar amounts of HEMA were released from R3 and R4 at all time points ($p \geq 0.403$), which was significantly lower than commercial and home materials following the one hour interval ($p \leq 0.013$). R1 and R2 presented similar HPM release values at 1, 4 hours and 1 day ($p \geq 0.153$). Materials containing THFM in their composition showed variation in its amounts released. As an example, R3 (which contains a higher percentage of THFM monomer in its liquid composition) showed a greater release compared to the other two materials that contained less THFM (R2 and R4) ($p \leq 0.007$). On comparing all monomers released from RX and RX-Home, the post-hoc Tukey test showed no significant differences between RX and RX-Home, at 1 hour and 1 day immersion. However, at 1 week, the concentration of released monomers was lower in the RX-Home solution, which indicates a decrease in the amount of monomer released following 1 day, compared to the corresponding commercial material (Figure 5.94).

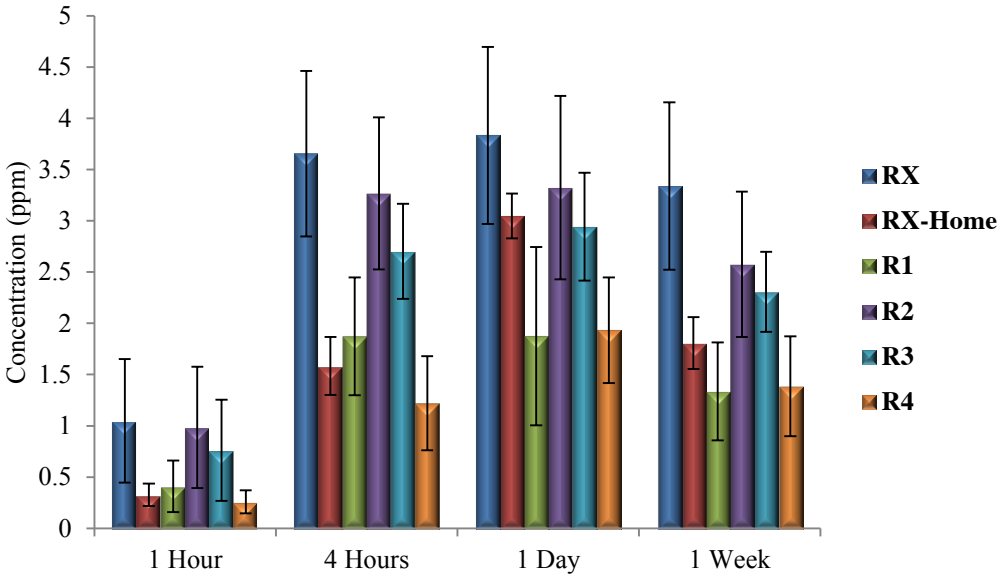

Figure 5.94 Mean concentration (ppm) of all monomers (HEMA, HPM and THFM) released from RX group materials in DW at 1 hour, 4 hours, 1 day and 1 week. Error bars represent standard deviations of the mean of 6 samples per materials (n=6).

Table 5.26 Mean release of each monomer and cumulative release of all monomers (ppm) (SD) of each material in the RX group in DW at different time points (1 hour, 4 hours, 1 day and 1 week). Similar superscript letters indicate no significant difference (p>0.05).

Time	Monomer	RX	RX-Home	R1	R2	R3	R4
1 Hour	HEMA	1.05 (0.60)	0.33 (0.11)^{a}			0.29 (0.18)^{a}	0.26 (0.11)^{a}
	HPM			0.49 (0.17)^{b}	0.69 (0.39)^{b}		
	THFM					0.56 (0.26)	
	All monomers	1.05 (0.60)^{a}	0.33 (0.11)^{a,b}	0.41 (0.25)^{a,b}	0.69 (0.39)^{a,b}	0.76 (0.49)^{a,b}	0.26 (0.11)^{b}
4 Hours	HEMA	3.65 (0.81)	1.58 (0.28)			0.82 (0.16)^{a}	0.66 (0.23)^{a}
	HPM			1.87 (0.57)^{a}	2.21 (0.56)^{a}		
	THFM				1.06 (0.26)	1.88 (0.35)	0.56 (0.23)
	All monomers	3.65 (0.81)^{a}	1.58 (0.28)^{c}	1.87 (0.57)^{b,c}	3.27 (0.74)^{a}	2.70 (0.46)^{a,b}	1.22 (0.46)^{c}
1 Day	HEMA	3.83 (0.86)	3.05 (0.22)			0.85 (0.16)^{a}	1.28 (0.26)^{a}
	HPM			1.88 (0.87)^{a}	2.13 (0.58)^{a}		
	THFM				1.19 (0.32)	2.09 (0.41)	0.66 (0.27)
	All monomers	3.83 (0.86)^{a}	3.05 (0.22)^{a,b}	1.88 (0.87)^{b}	3.32 (0.90)^{a}	2.94 (0.53)^{a,b}	1.93 (0.52)^{b}
1 Week	HEMA	3.34 (0.82)	1.81 (0.25)			0.87 (0.18)^{a}	0.74 (0.23)^{a}
	HPM			1.34 (0.48)	1.92 (0.53)		
	THFM				0.66 (0.19)^{a}	1.44 (0.41)	0.64 (0.27)^{a}
	All monomers	3.34 (0.82)^{a}	1.81 (0.25)^{b,c}	1.34 (0.48)^{c}	2.58 (0.71)^{a,b}	2.31 (0.39)^{b,c}	1.39 (0.49)^{c}

5.9.4 Quantification of monomer release (ppm) in 75:25 ethanol:DW:

75:25 ethanol:DW was chosen as an immersion solution following the recommendations of the United States food and drug administration (US FDA), which consider this solvent to be clinically relevant to testing in artificial saliva. It is reported to mimic the effect of human saliva tested on dental materials, food or drugs (Altintas and Usumez, 2012).

Figures 5.95 and 5.96 represent concentration of monomers (ppm) released from FP and RX materials following immersion in 75:25 ethanol:DW, up to 1 week, at 37°C. The release data are summarised in in Tables 5.27 and 5.28 respectively.

HEMA release from FP-Home solutions was significantly greater than commercial FP, F3 and F4 at all time points ($p<0.0001$). FP and F3 did not show any significant difference in HEMA release at 4 hours, 1 day and 1 week time points ($p\geq0.124$). Similar to the results obtained from samples immersed in DW, F1 samples released greater amounts of HPM than F2 ($p<0.0001$) and moreover showed higher release compared to all other materials in the FP group ($p<0.0001$) (Figure 5.95; Table 5.27).

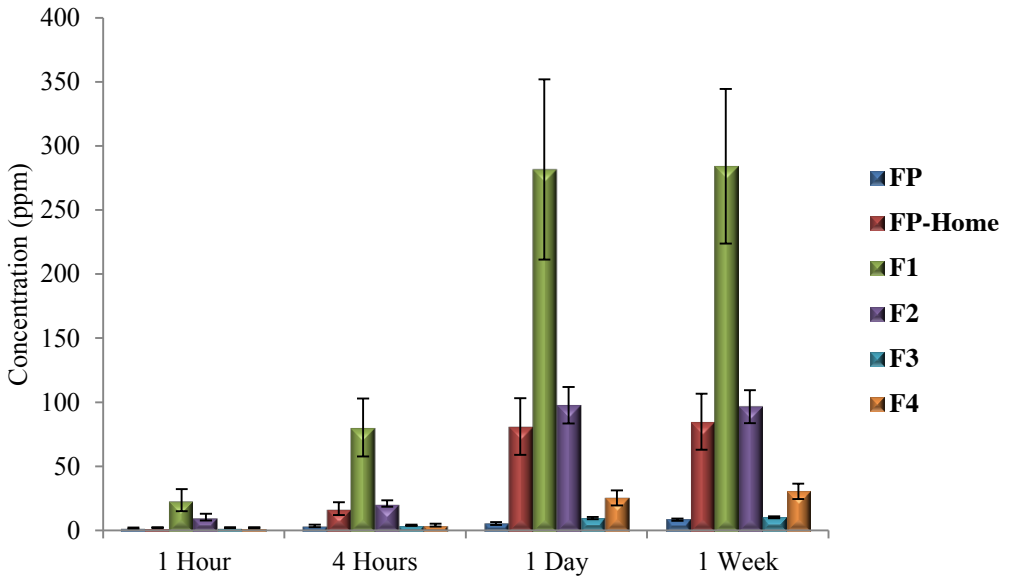

Figure 5.95 Mean concentration (ppm) of all monomers (HEMA, HPM, THFM, UDMA) released from FP group materials in 75:25 ethanol:DW at 1 hour, 4 hours, 1 day and 1 week. Error bars represent standard deviations of the mean of 6 samples per materials (n=6).

Table 5.27 Mean cumulative release of each monomer (ppm) (SD) from material the FP group materials in 75:25 ethanol:DW. Similar superscript letters indicate no significant difference (p>0.05).

Time	Monomer	FP	FP-Home	F1	F2	F3	F4
1 Hour	HEMA	1.06 (0.42)[a]	1.91 (0.29)			0.55 (0.11)[b]	0.84 (0.24)[a,b]
	HPM			22.10 (8.38)	6.01 (1.76)		
	THFM				2.66 (0.66)	1.19 (0.20)[a]	0.69 (0.14)[a]
	UDMA	0.67 (0.19)[b]	0.14 (0.23)[b]	1.44 (0.61)[a,b]	1.57 (0.34)[a,b]	0.40 (0.06)[b]	0.41 (0.07)[b]
	All monomers	1.73 (0.56)[a]	2.06 (0.46)[a]	23.55 (8.55)	10.24 (2.61)	2.15 (0.35)[a]	1.93 (0.39)[a]
4 Hours	HEMA	2.00 (0.71)[a]	15.04 (5.09)			1.15 (0.20)[a]	2.06 (0.76)[a]
	HPM			77.66 (22.50)	11.78 (1.84)		
	THFM				6.32 (1.82)	2.10 (0.27)[a]	1.43 (0.34)[a]
	UDMA	1.41 (0.33)[c,d]	1.83 (0.38)[b,c]	2.63 (0.68)[a,b]	2.88 (0.89)[a]	0.66 (0.07)[d]	0.62 (0.11)[d]
	All monomers	3.41 (1.00)[b]	16.86 (4.98)[a,b]	80.29 (22.65)	20.98 (2.43)[a]	3.91 (0.53)[b]	25.34 (5.91)[a]
1 Day	HEMA	2.56 (0.84)[a]	75.54 (21.64)			3.21 (0.33)[a]	14.25 (3.65)
	HPM			266.20 (65.76)	64.83 (9.50)		
	THFM				27.35 (3.66)	5.43 (0.58)	10.13 (2.82)
	UDMA	2.79 (0.48)[a,b]	5.46 (0.62)[a]	15.36 (4.56)	5.47 (1.23)[a]	0.91 (0.06)[b]	0.97 (0.12)[b]
	All monomers	5.35 (1.19)[b]	81.00 (22.11)[a]	281.55 (70.30)	97.66 (14.24)[a]	9.54 (0.83)[b]	25.34 (5.91)
1 Week	HEMA	3.47 (0.75)[a]	76.41 (20.85)			3.35 (0.28)[a]	16.39 (3.22)
	HPM			267.05 (56.18)	63.84 (8.54)		
	THFM				26.75 (3.44)	5.04 (0.56)	11.54 (3.19)
	UDMA	4.85 (0.32)[b,c]	8.29 (1.14)[a]	17.04 (4.21)	5.96 (1.08)[a,b]	1.77 (0.06)[c]	2.46 (0.29)[c]
	All monomers	8.32 (0.95)[b]	84.69 (21.90)[a]	284.10 (60.37)	96.55 (12.92)[a]	10.16 (0.78)[b]	30.40 (6.04)

Similar residual HEMA concentrations were noted from commercial RX, RX-Home ($p \geq 0.174$) and from R3 and R4 samples, following 1 day and 1 week immersion ($p \geq 0.944$) (Table 5.28). Novel compositions R3 and R4 released less HEMA than commercial and home RX materials following 1 day and 1 week immersion, similar to the release in DW ($p \leq 0.005$). In 75:25% ethanol:DW, R1 presented a greater release of HPM compared to R2 ($p < 0.0001$) and the cumulative release of monomers from it was higher than all other materials, at 1 hour ($p \leq 0.001$) (Figure 5.96).

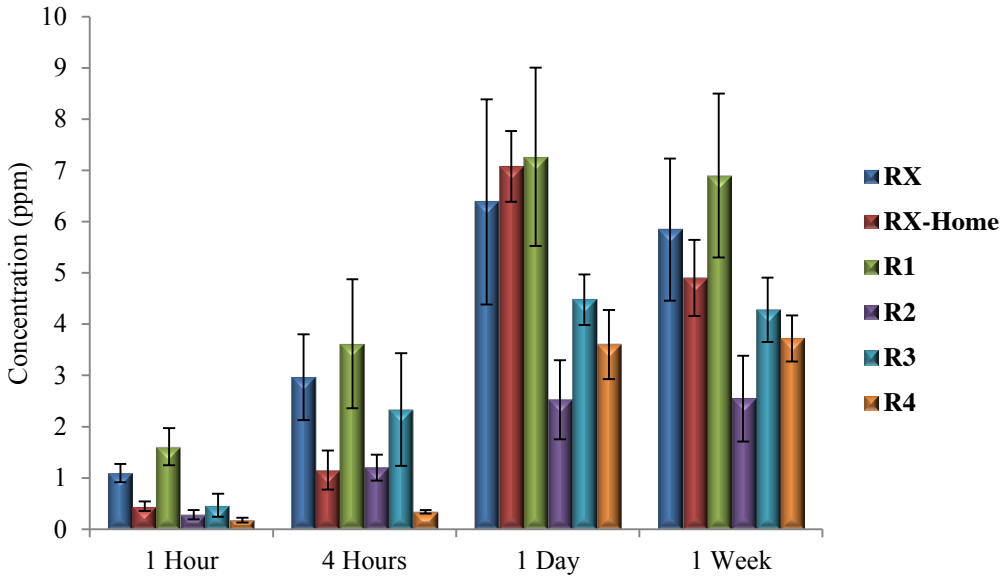

Figure 5.96 Mean concentration (ppm) of all monomers (HEMA, HPM and THFM) released from RX group materials in 75:25 ethanol:DW at 1 hour, 4 hours, 1 day and 1 week. Error bars represent standard deviations of the mean of 6 samples per materials (n=6).

Table 5.28 Mean and cumulative monomer release (ppm) (SD) of each material in the RX group in 75:25 ethanol:DW at different time points (1 hour, 4 hours, 1 day and 1 week). Similar superscript letters indicate no significant difference (p>0.05).

Time	Monomer	RX	RX-Home	R1	R2	R3	R4
1 Hour	HEMA	1.10 (0.18)	0.45 (0.09)			0.27 (0.08)[a]	0.18 (0.05)[a]
	HPM			1.61 (0.36)	0.28 (0.09)		
	THFM					0.19 (0.16)	
	All monomers	1.10 (0.18)	0.45 (0.09)[a]	1.61 (0.36)	0.28 (0.09)[a]	0.47 (0.23)[a]	0.18 (0.05)[a]
4 Hours	HEMA	2.96 (0.84)	1.15 (0.38)[a,b]			1.80 (0.88)[a]	0.34 (0.04)[b]
	HPM			3.62 (1.26)	0.99 (0.18)		
	THFM				0.22 (0.18)	0.54 (0.32)	
	All monomers	2.96 (0.84)[a]	1.15 (0.38)[b,c]	3.62 (1.26)[a]	1.20 (0.25)[b,c]	2.33 (1.10)[a,b]	0.34 (0.04)[c]
1 Day	HEMA	6.39 (2.00)[a]	7.08 (0.69)[a]			3.73 (0.39)[b]	3.26 (0.56)[b]
	HPM			7.27 (1.74)	1.91 (0.52)		
	THFM				0.61 (0.27)[a,b]	0.75 (0.23)[a]	0.34 (0.13)[b]
	All monomers	6.39 (2.00)[a,b]	7.08 (0.69)[a]	7.27 (1.74)[a]	2.52 (0.77)[c]	4.47 (0.49)[b,c]	3.60 (0.67)[c]
1 Week	HEMA	5.84 (1.39)[a]	4.90 (0.74)[a]			3.29 (0.29)[b]	3.36 (0.35)[b]
	HPM			6.90 (1.60)	1.97 (0.55)		
	THFM				0.57 (0.30)[a]	0.99 (0.39)	0.36 (0.11)[a]
	All monomers	5.84 (1.39)[a,b]	4.90 (0.74)[b,c]	6.90 (1.60)[a]	2.54 (0.84)[d]	4.28 (0.63)[b,c,d]	3.72 (0.45)[c,d]

5.10 *Cytotoxicity of materials (commercial, home and novel):*

5.10.1 First set of experiments on FP and RX group materials:

Mean percentage of active cells following exposure to aliquots (control medium in which the samples were immersed) of all RMGICs (commercial, home and novel) and, standard deviations of triplicate experiments, are presented in Table 5.29 and Figure 5.97. Table 5.29 includes the statistical analysis and comparison between i) materials (commercial, home and novel) versus medium; ii) materials (home and novel) versus commercial; and iii) novel materials versus home. P values less than 0.05 were used to confirm statistically significant differences between materials.

In the RX group, all materials (commercial, home and novel) showed significantly lower cell viability than the negative control. Only F2 in the FP group presented with a lower p value than 0.05 ($p=0.028$) and less viable cells, following 72 hours of exposure to the material's supernatant compared with the negative control medium. No significant differences were noted between both groups on comparing with the commercial and home counterparts (Table 5.29).

Table 5.29 The percentage of viable cells following treatment with materials' aliquots (commercial, home and novel) for both FP and RX groups and, p values comparing materials with medium (negative control), home and novel materials with commercials and novel materials with home.

Material	Mean cells viability (%) (SD)	p values of materials v medium	p values of materials v commercial	p values of materials v home
Medium	100.00 (0.00)	-	-	-
FP	85.95 (29.77)	0.4596	-	-
FP-Home	90.90 (9.29)	0.1651	0.7969	-
F1	75.95 (17.88)	0.0803	0.6440	0.2680
F2	82.96 (8.77)	0.0282	0.8755	0.3422
F3	107.29 (24.26)	0.6302	0.3903	0.3360
F4	94.06 (19.48)	0.6254	0.7131	0.8125
RX	-0.57 (4.67)	0.0000	-	-
RX-Home	0.44 (3.90)	0.0000	0.7878	-
R1	3.82 (1.87)	0.0000	0.2059	0.2478
R2	5.85 (3.80)	0.0000	0.1388	0.1606
R3	1.51 (3.87)	0.0000	0.5849	0.7533
R4	0.96 (4.65)	0.0000	0.7083	0.8894

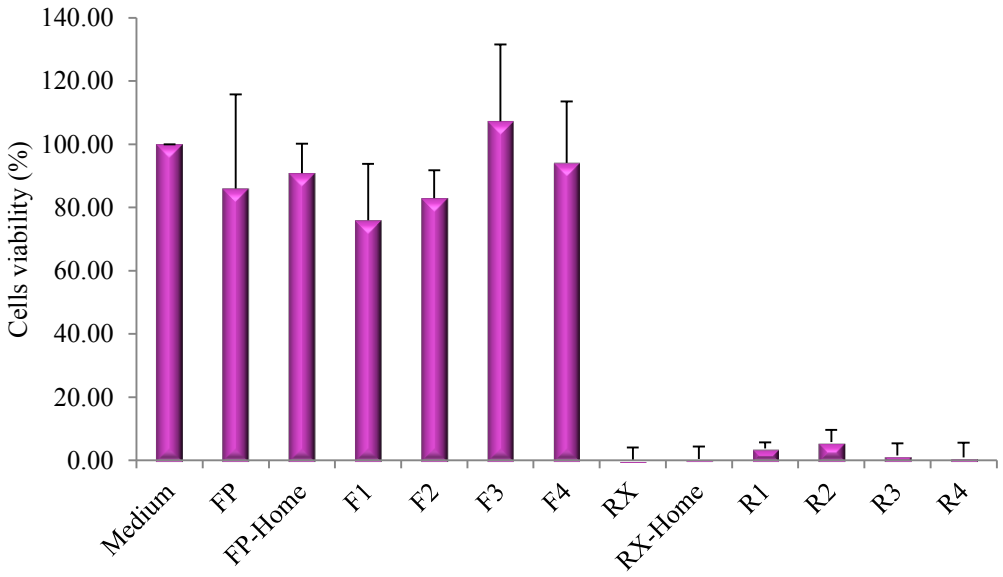

Figure 5.97 Cytotoxicity of FP and RX materials (commercial, home and novel). Error bars represent standard deviation of the mean of three experiments; each experiment included 4 readings of each materials' aliquot.

It is worth noting that the colour of the medium containing RX samples changed from pink to yellow, which indicates that this medium was more acidic compared to the medium containing FP samples; the latter did not show a change in colour and stayed pink throughout the experiment time (Figure 5.98). This will be discussed in discussion chapter.

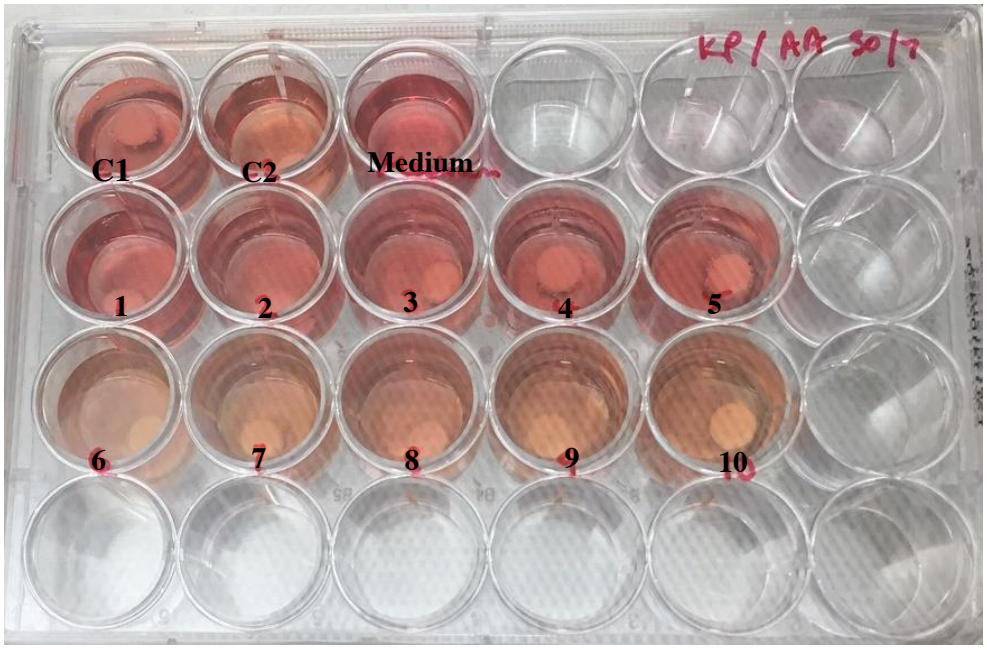

Figure 5.98 24 well plates containing samples immersed in 1.5 mL DMEM in each well. C1:FP, C2:RX, 1-5: FP-Home, F1, F2, F3, F4, 6-10:RX-Home, R1, R2, R3, R4.

Figure 4.99 (a-d) is example showing the effects of materials extracts (supernatant) and negative control in contact with cultured fibroblast cells. Figure 5.99 (a) shows healthy fibroblast cells that had a 'spindle like' shape, which were also present in Figure 5.99 (b), representing the fibroblast cells following exposure to FP aliquots. Cells exposed to RX samples exhibited a change in morphology from a spindle like shape to a round shape (Figure 5.99 (c)). F3 showed similar cell morphology to that of the cells in the control medium and FP cells, that were spindle like with long processes as can be seen in Figure 5.99 (d).

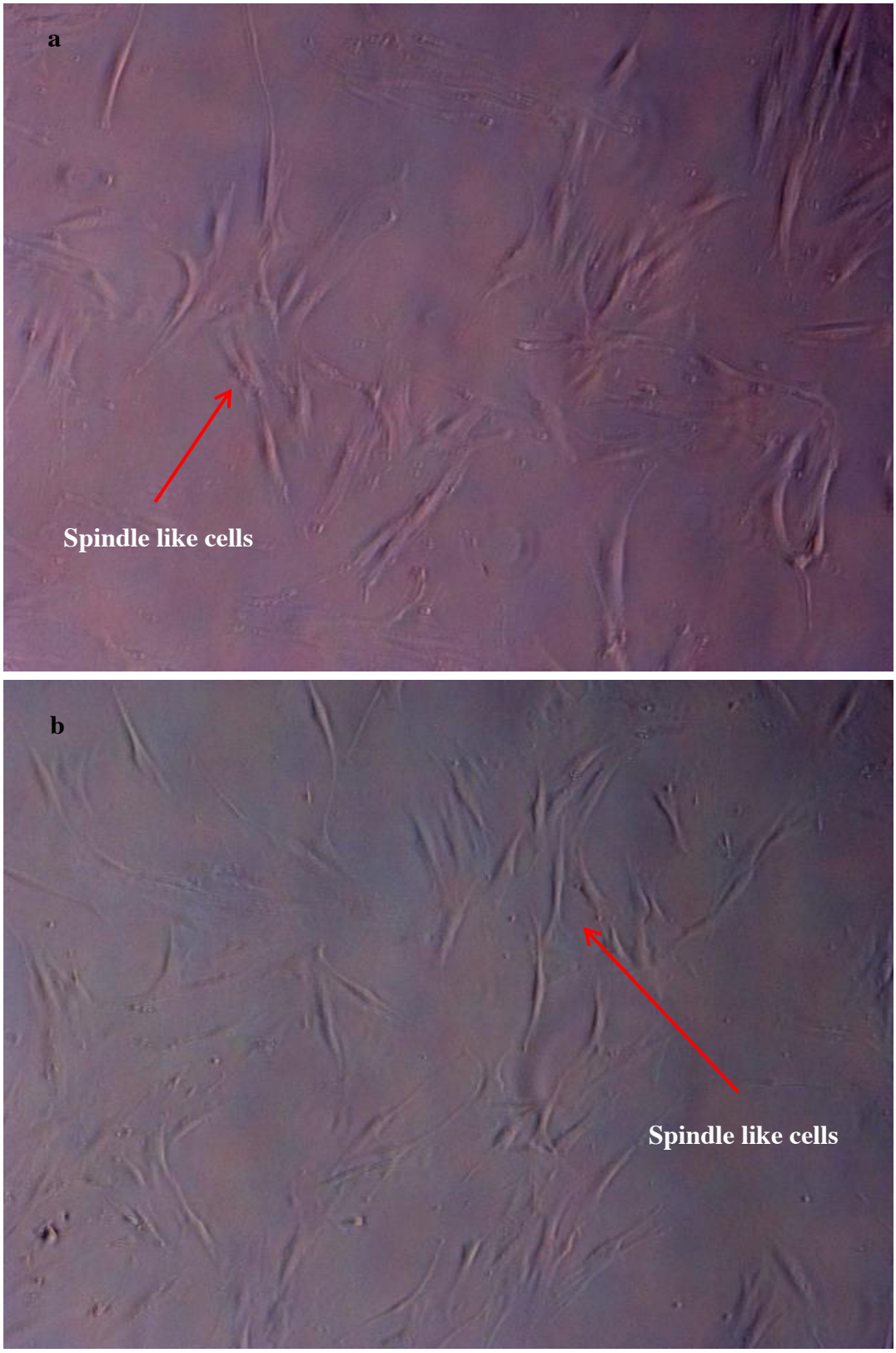
a
Spindle like cells
b
Spindle like cells

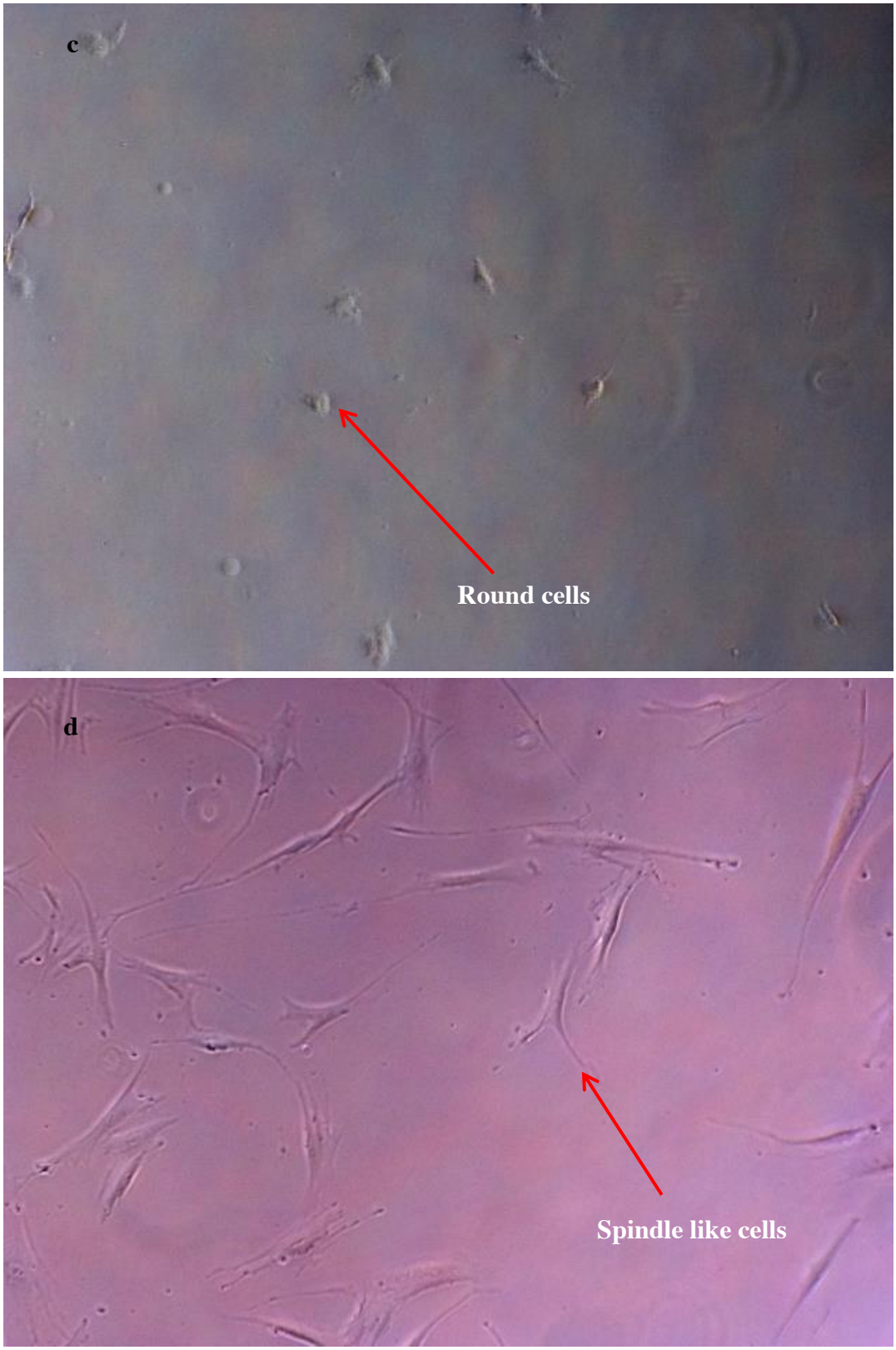

Figure 5.99 Effects of materials on NHDF cells in culture: (a) medium (negative control), (b) FP, (c) RX, (d) F3.

5.10.2 Second set of experiments on FP group materials:

The second set of experiments were only performed on the FP group, since the RX group showed high cytotoxicity in the first set of experiments and would be expected to behave in the same manner, in the second set, which included testing the materials with increased specimen surface area.

Table 5.30 and Figure 5.100 represent mean and standard deviations of viable cells following exposure to neat and diluted FP group solutions. Table 5.30 gives the p values for commercial, home and novel materials versus medium, home and novel materials versus medium and novel materials versus their home counterparts.

F3 and F4 neat aliquots showed similar effects on NHDF cells when compared with control medium ($p \geq 0.185$). Other compositions including commercial and home neat solutions were shown to be cytotoxic as results were statistically significant from the control medium ($p \leq 0.027$). All diluted solutions demonstrated similar effects on cells compared to the control medium, with the exception of F4 that presented with higher viability of cells, after 72 hours exposure to solution ($p=0.023$) (Table 5.30).

Table 5.30 The percentage of viable cells following treatment with materials' aliquots (commercial, home and novel) from the FP group both neat and diluted with similar volume of control medium, and p values comparing materials v medium (negative control), home and novel materials v commercials and novel materials v home.

Material	Mean cells viability (%) (SD)	p values of materials v medium	p values of materials v commercial	p values of materials v home
Medium	100 (0.00)	-	-	-
FP	25.18 (16.19)	0.0001	-	-
FH	36.88 (43.19)	0.0265	0.6299	-
F1	20.88 (25.11)	0.0007	0.7831	0.5453
F2	13.87 (8.90)	0.0000	0.2667	0.3367
F3	55.04 (60.12)	0.1854	0.3744	0.6411
F4	69.62 (55.77)	0.3177	0.1768	0.3892
Medium 1:1	100 (0.00)	-	-	-
FP 1:1	114.12 (22.35)	0.2534	-	-
FH 1:1	123.33 (45.67)	0.3464	0.7296	-
F1 1:1	47.55 (70.67)	0.1883	0.1226	0.1218
F2 1:1	141.56 (41.97)	0.0949	0.2922	0.5779
F3 1:1	129.23 (37.92)	0.1741	0.5179	0.8489
F4 1:1	154.75 (36.01)	0.0228	0.1036	0.3214

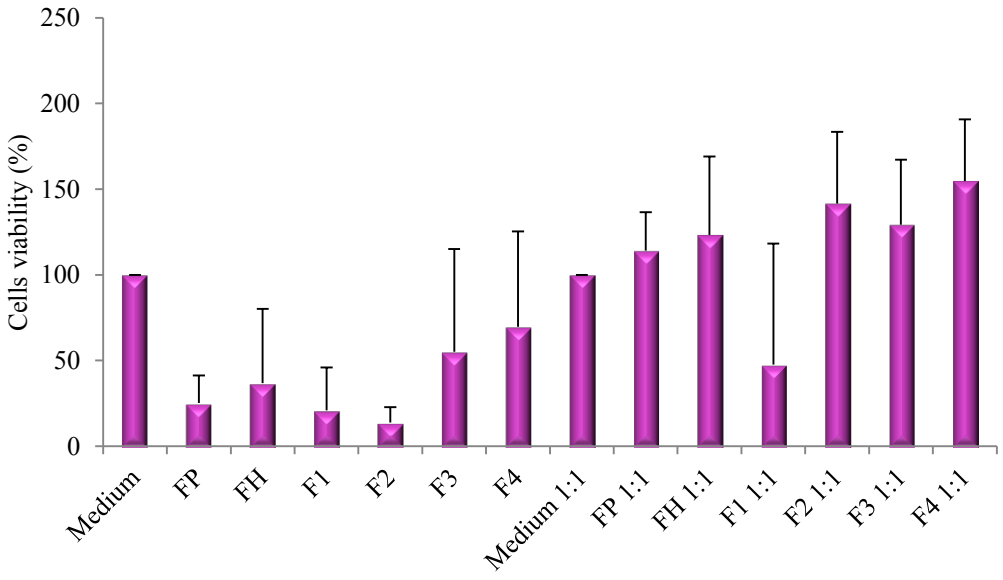

Figure 5.100 Cytotoxicity of FP group materials (commercial, home and novel), both neat and diluted solution, calculated as percentage of the negative control (medium). Error bars represent the standard deviation of the mean of three experiments; each experiment included 4 readings of each material aliquot.

6 DISCUSSION

6.1 *Introduction:*

Before discussing the results of this research, it should be mentioned that in order to achieve the aims, it was essential to initially carry out a set of pilot studies, on which a vast amount of time was spent. These are briefly summarised here.

In order to develop novel RMGICs, it was necessary to know the exact compositions of the two commercial materials (FP and RX), which were used as comparisons. The improved physico-mechanical and biological properties could then be correlated with the various components incorporated. However, this proved difficult, since manufacturers do not supply such information. Therefore, much time was spent on formulating the home-made liquids (to similarly match the commercial liquids), and novel liquid compositions. Problems were encountered in formulating both sets of liquids; with the home liquids, FT-IR was used to match commercial liquid compositions, but, towards the end of the project it was evident that this technique was not as effective in highlighting all the ingredients. With the novel liquids, phase separation was a problem where the monomers, THFM and HPM, phase separated due to their more hydrophobic nature, compared with HEMA. Further difficulties occurred in finding an optimum method for measuring the water uptake of RMGICs since they already contain water. Also, effective techniques for analysing residuals from the cements were not in published literature, and hence novel methods had to be developed. Eventually, a set of eight novel liquid formulations and two home liquids were successfully prepared, some of which presented with improved properties compared to the two commercial materials. These are discussed subsequently.

6.2 *Water uptake, desorption, diffusion coefficient and solubility of commercial and control materials following two methods: ISO 4049 and without desiccation:*

Although several articles on RMGICs have documented water uptake of these materials, a standard method has not been used. Researchers have used the ISO standard 4049 method, but this is essentially for resin based cements, and not for RMGICs, which contain water. Therefore, the initial part of this study addressed finding an appropriate method for measuring the water uptake of these materials, where the ISO standard method that requires desiccation of samples prior to water uptake was compared with a well documented method (Stafford and Braden, 1968) that does not require prior desiccation of samples. Two commercial materials Fuji Plus (FP) and RelyX Luting (RX) and, two home-made liquids, keeping the powder the same, were used for this experiment.

6.2.1 Differences between commercial and home materials following ISO 4049:2009 standard and the method without desiccation:

Commercial FP exhibited significantly higher water uptake compared to commercial RX in DW; this difference might be a result of the two acids used in RX (copolymer of acrylic and itaconic acids) compared to only one, poly(acrylic acid), in commercial FP. Itaconic acid contains two carboxyl groups and acrylic acid contains one. These groups potentially crosslink the matrix (via carboxyl groups in the acids and OH groups in HEMA), thus increasing the crosslinking potential of the set cement (Crisp *et al*., 1980). According to Cefaly *et al*. (2006), the uptake is negatively correlated with the crosslinking density, hence the lower uptake for RX (Cefaly *et al*., 2006).

Commercial FP had a significantly higher water uptake than its home counterpart in both DW and AS, which was not the case for commercial RX and RX-Home; this indicates that there was a difference between the liquid compositions of FP and FP-Home. The formation of home and novel liquid compositions followed data provided by the manufacturer in MSDS. Although theoretically the information provided (in MSDS) should be accurate, manufacturers are not required to mention the exact composition details, since some elements do not pose any hazard. Therefore, FT-IR was used as an initial guide for formulating and matching the home liquids composition with commercial liquids, to ensure similarity. However, as will be discussed later in the HPLC section, one monomer that was identified much later by HPLC, was not identified by FT-IR, and therefore it was not included in the home liquid compositions. Hence, this difference in liquid compositions may have caused the variation in the amount of water absorbed between commercial and home materials.

Both FP and RX as RMGICs undergo two setting reactions, the acid-base reaction and that of the polymerisation of the resin (Anstice and Nicholson, 1992). The resin matrix in RMGIC is responsible for the material's water uptake, and thus it was expected that different percentages of the monomer (e.g. HEMA) would lead to different values of water uptake (Li *et al*., 1985). Poly(HEMA) is known to absorb a vast amount of water (42-80%) since it is a hydrogel (Pinchuk *et al*., 1984; Patel and Braden, 1991a). Therefore it was hypothesised that RX would have a higher water uptake compared to FP because the latter was prepared in a higher powder: liquid ratio (2:1 g:g- FP vs 1.6:1 g:g-RX), and so there was more HEMA resin in RX (even

though similar amounts of HEMA were included in both liquids). However, this was not the case as discussed subsequently.

In this study, both FP and RX Home cements showed comparable results (with no statistically significant differences between the two materials), in both DW and AS, for the method without desiccation. This was not expected and contradicts Li et al (1985) findings. An explanation for these results could be argued as follows. Despite the higher powder: liquid ratio in FP, its composition included an additional monomer (UDMA, not in RX). This monomer (UDMA) is more hydrophobic than HEMA, but its hydroxyl (OH^-) and urethane ($NHCOO^-$) groups play a role in the water uptake through acquired hydrogen bonding with water (Sideridou *et al*., 2008). Hence, this theory agrees with the results obtained for the home materials.

The ISO 4049:2009 method for commercial and home materials, involved dehydration of the samples prior to the water uptake study. Obvious differences were observed between FP and RX group materials, with water uptake values being significantly higher for RX cements than FP, in both DW and AS. This difference may be attributed to RX's lower powder: liquid ratio and increased original water content in the liquid (35% compared to 30% in FP). Also, set RMGICs contain water in their structure, which is divided between 'loosely bound' and 'tightly bound' water associated with metal cations and poly(acrylic acid) chains (Lohbauer, 2009). With time, more loosely bound water converts to tightly bound water. When this cement is exposed to a dry environment, the loosely bound water evaporates and this procedure jeopardises the setting of the GIC component of RMGICs, since water is one of the essential components of the setting reaction (Wilson and Nicholson, 2005). Hence, to compensate for the water lost during desiccation (which could be

related to the cement's original water content), the samples essentially absorbed the amount of water that was lost, as well as absorbed further water to saturate the resin matrix, thus accounting for the higher uptake for the RX group.

A similar trend was observed in the desorption experiments for both methods (without desiccation and the one following ISO 4049:2009) in DW and AS. Although there was no significant difference between the commercial FP and home materials, and between commercial RX and its home counterpart, the latter exhibited higher weight losses compared to the FP group, thus reflecting the water uptake results. Upon desiccation, the samples lost both the water gained from the uptake process and the remaining unbound water within the samples, which in turn could be related to the differences in the powder: liquid ratios used for preparing the two materials.

Diffusion coefficients for the absorption process (Dabs) could not be calculated for samples following the ISO 4049:2009 method, since their uptake did not follow Fickian diffusion. For the method without desiccation, FP (commercial and home) diffusion coefficients, for both the water uptake and desorption processes in DW and AS, varied in accordance to the literature (Patel and Braden, 1991a). The diffusion coefficients for the absorption process (Dabs) were lower than those obtained for the desorption process (Ddes), thus implying that water was diffusing slowly ($x10^{-12}$ m^2sec^{-1}) into the materials during absorption compared to diffusing faster out of the materials ($x10^{-11}m^2sec^{-1}$) during desorption (Nazhat *et al*., 2001). This was expected, as the water uptake process is more complex compared to desorption, and involves water absorbing into the material and other components (e.g. unconverted monomers etc) leaching out of it. Alternatively, the desorption process involves only water

evaporating from samples. There was only a small difference between Dabs and Ddes values for RX. Home materials followed the same trend as their corresponding commercial materials. Based on the diffusion coefficients data, this indicates that water was diffusing faster into RX compared to FP.

FP and RX home materials showed higher solubility results compared to commercial FP and RX, in both DW and AS, for the method without desiccation and, for RX, following the ISO 4049:2009 method. This points to slight variations in the compositions of commercial versus home materials, which will be discussed further in the HPLC section.

6.2.2 Differences between the two water absorption methods (without desiccation and ISO 4049:2009:

Higher water uptake values were obtained for samples following the ISO 4049:2009 standard compared to the method without desiccation. This was a result of the different techniques involved, where ISO 4049:2009 included desiccation of samples before immersion. Thus the samples took up more water to compensate for the water lost during desiccation. This was not the case in the method without desiccation, as the original water content in the samples was not modified.

For the desorption process it was assumed that samples following ISO 4049:2009 would lose more water (due to their higher uptake associated with desiccation of samples immediately after setting), whereas in the method without desiccation, some of the unbound water in the structure would have had time to convert to tightly bound water, which would not evaporate during this process. However, desorption results for commercial and home materials from both groups (FP and RX) were generally comparable between the two methods, in both DW and AS. This may be

due to the level of tightly bound water being insignificant compared to the water that evaporated during the desiccation process. Therefore, it can be assumed for both methods that the evaporated water was a result of the original water content plus the water that was absorbed during the water uptake experiment.

Interestingly, two modes of diffusion were observed for the two water uptake methods. Whilst samples prepared without desiccation showed Fickian diffusion, those following the ISO 4049:2009 standard exhibited Case II diffusion. This can be explained by the fact that for the latter case, water absorbed by the material following desiccation resulted in filling the gaps in the matrix from where water was lost, and rehydration of HEMA (hydrogel); this will therefore not follow a Fickian process. In the former process (without desiccation), water was absorbed to saturate the material.

The solubility results varied between the two methods and these were significantly lower for the 'ISO' compared with the 'without desiccation' method, in both DW and AS. The ISO 4049:2009 solubilties were a result of the monomer leaching from the RMGICs, while with the alternative method they were due to the leaching of the monomer and unbound water from the samples. Hence, with the ISO 4049:2009 method, a possible explanation could be due to the initial dehydration of the samples, therefore water diffused into the sample to compensate for the lost water, during the 24 weeks experimental period, and so it was assumed that only residual monomer had time to leach out.

The dimensional changes in samples also showed differences between the two methods in both DW and AS. As expected, the ISO 4049:2009 (desiccated prior to

water uptake) samples had a greater change in dimensions compared to the ones that were directly immersed in water (without desiccation). This could be explained by the fact that during immersion, the water absorbed by the desiccated samples compensated for both the evaporated water and the water saturating the resin matrix, thus resulting in swelling of the samples.

It can be clearly seen that the method without desiccation appeared to be the method of choice for measuring the water uptake of novel materials. This decision was based on the results obtained that showed exaggerated absorption values following ISO 4049:2009, and moreover, since this method included desiccation of samples prior to the water uptake experiment, it does not mimic the clinical situation where the material is mixed and placed directly into the moist oral environment, without desiccation. Hence, for all commercial, home and novel materials, discussed in section 6.3, the method without desiccation was used for further water uptake measurements.

6.3 *Water uptake, desorption, diffusion coefficient, solubility and dimensional changes of commercial, home (control) and novel materials:*

One of the main aims of this study was to develop novel RMGICs with lower water uptake than the current commercial materials. Moreover, the selection of monomers to replace HEMA in the commercial products was based on monomers known for their low water uptake (Patel *et al*., 2001) and good biocompatibility in the oral environment (Pearson *et al*., 1986). Two commercial RMGICs (Fuji Plus, FP and RelyX Luting, RX) and two home liquid products were compared with eight novel

experimental compositions, four were based on FP and the other four on RX formulations.

Significantly lower water uptakes were attained for all novel compositions compared with their commercial counterparts in both DW and AS. The reduction in water uptake can be attributed to the replacement of HEMA in the novel compositions with the less hydrophilic monomers, THFM and HPM. These findings agree with published literature concerning these two monomers and their lower water uptake compared to HEMA (Sawtell *et al*., 1997; Patel *et al*., 2001).

Theoretically, the polymer's water uptake in AS has been reported to be lower than in water, due to the absence of clustering around water soluble entities within the materials, and to an osmotic potential gradient between the immersion solution and the absorbed solution (Sawtell *et al*., 1997). However, in this study, maximum water uptakes for all materials immersed in AS were comparable to those immersed in DW. These results indicate that clustering in the two media may not have occurred in all cements.

Interestingly, the noted difference, between samples immersed in DW compared with AS, was that the samples in the latter medium started to lose weight from ~975 second$^{1/2}$ (~two weeks) for the FP group, and from ~294 second $^{1/2}$ (~two days) for the RX group. This may be explained by the fact that AS contains components that are not present in DW, and some of its (AS) components diffused into the samples, and did not bind to any chemical groups. But due to a chemical potential gradient, after reaching a maximum weight change, these components diffused out of the material, thus accounting for the weight loss (Riggs *et al*., 2001). Another

explanation is that weight loss due to leaching of residuals was more than weight gain due to water uptake (AS), which also explains the higher solubility results for materials in AS compared to DW.

The solubility reflected the amount of residuals leaching out from the system. Solubility levels were generally comparable between materials within each group (FP and RX), in DW and AS, but were higher for the RX group compared to the FP group. This variation between the two groups is likely to be due to the differences in composition between them (FP and RX), with FP containing UDMA and HEMA in its formulation, whilst RX contained only HEMA as a monomer. Since UDMA is a dimethacrylate, additional cross-linking may have occurred between HEMA and UDMA, UDMA and THFM, or UDMA and HPM, and thus the amount of residual (unconverted) monomers was lower in the FP formulations compared to RX; this will consequently decrease the solubility of the material.

In a study by Mese *et al*. (2008), commercial Fuji Plus (FP) showed lower solubility results compared to commercial Rely X Luting2, which agrees with the solubility results obtained in this project. Mese *et al*. (2008) reported that the reason for this difference was due to the presence of a filler in Rely X luting2 (zirconia silica filler) that is not present in FP, rather than the differences in the monomers within the two materials. This reason cannot be used in our study to describe the differences in solubility results, as commercial RX, according to the manufacturer's MSDS, does not contain this filler, and the only difference between RX and FP liquids was due to the addition of UDMA in the latter (manufacture's MSDS). A further explanation for the increased solubility in the RX group could be due some of the water diffusing out of these samples when immersed in solutions (DW or AS), as a result of the powder:

liquid ratio used, and the water content in the liquid (35% in RX liquids and 30% in FP). Moreover, in the HPLC experiment, only RX compositions also released poly(acrylic acid), but not FP compositions. Hence, all these factors may have accounted for the higher solubility results of RX compared to FP.

The FP group (commercial, home and novel) exhibited lower diffusion coefficients for the absorption process (Dabs) compared to the desorption ones (Ddes) for the reasons discussed earlier. The water uptake process was Fickian for all materials and this was in agreement with Kanchanavasita *et al*. (1997), Yap *et al*. (1997) and Nicholson (1997). Despite this agreement, different Dvalues were reported and could not be correlated with this study, due to the differences in the methods and the materials that were tested.

Following application in the oral environment, RMGICs undergo dimensional changes (expansion) as a result of the water uptake and polymerisation shrinkage. Whilst the expansion of RMGIC can be beneficial to compensate for the composite's polymerisation shrinkage (Kanchanavasita *et al*., 1995), this dimensional change may cause problems for the restored teeth, causing stress on the tissues and post-operative sensitivity. It may also cause fracture of the weak ceramic crown or tooth structure where RMGIC is used as luting cement. Therefore, decreasing the dimensional changes of commercial RMGIC is highly desirable. In this study, all sample dimensions (diameter and thickness) were measured prior to water uptake in both AS and DW, and at 1 week, 3 weeks and 24 weeks. All novel materials showed significantly lower dimensional changes compared to the commercial and control products, after immersion in both DW and AS. This finding is highly important for

the commercialisation of the novel RMGICs, as they will have wider applications compared to current commercially available products.

6.4 *Degree of conversion (DC):*

RMGICs contain materials required for both the acid-base and polymerisation reactions to occur. In this study, all materials were chemically activated and thus the two reactions occurred simultaneously following mixing. Spectra of commercial, home and novel materials showed acid neutralisation peaks (indicating that the acid-base reaction had taken place) at 1550, 1484 and 1402 cm^{-1}. The difference in the compositions of FP and RX (commercial, home and novel materials) was the inclusion of UDMA in FP. Spectra for all FP liquids showed small peaks for UDMA.

As discussed earlier in the literature survey, commonly the peaks used to identify the degree of conversion were at 1638 cm^{-1} and 1712 cm^{-1} (reference peak) (Kakaboura *et al*., 1996; dos Santos *et al*., 2012). These peaks could not be used in this study, as the peak at 1638 cm^{-1} was masked by the presence of water (in the material) that also absorbs at the same wavelength. Therefore, the DC was calculated using the peak at 1320 cm^{-1}, as reported by Young *et al*. (2004).

The analyses of reactions (both acid-base and polymerisation of the monomer) showed that the setting reaction occurred faster (by five minutes) in both commercial cements (FP and RX) compared to the home materials, as mentioned in 5.4.2.1. Despite this time difference and, using different peaks to identify the polymerisation reaction, there was no statistically significant difference between commercial and home materials with respect to the calculated degree of conversion of the

methacrylate monomers, at all time intervals; they also showed agreement with other studies on RMGIC in that the percentage maximum conversion occurred mainly in the first 10 minutes, following mixing or light activation (Rueggeberg and Caughman, 1993; Yan *et al*., 2010; Kim *et al*., 2015). According to Young (2002), differences in water content and the acids used in the products could affect the acid-base reaction times. Therefore, the differences between commercial RX and RX Home could be a result of the different acids used [(copolymer of acrylic and itaconic acid compared with poly(acrylic acid), respectively)] .

In this project, one of the main focusses was on the quantification of the degree of conversion of the monomers (discussed below) rather than the extent of the acid-base reaction. The former occurs in the first hour, from mixing the powder and liquid. The latter takes at least 24 hours, and sometimes months to complete (Kim *et al*., 2015). In this project this reaction was followed by the appearance of the salt peaks, where all materials (commercial, home and novel) showed the initiation of the acid-base reaction through formation of salt polyacrylate peaks at ~1550, 1484 and 1402 cm^{-1}.

In both groups (FP and RX), compositions, which contained HPM instead of HEMA, showed a lower degree of conversion. Atai *et al*. (2005) and Abed *et al*. (2015) reported that higher molecular weight monomers (like HPM) may contribute to an increase in viscosity and their movement within the matrix. HPM contains an additional CH_2 compared to HEMA and therefore it has a higher molecular weight. Hence this may have caused the lower degree of conversion values in this project. Another article (Patel *et al*., 2001) reported that THFM, partially replaced with either HEMA or HPM, showed reduced reactivity of a system containing HPM, compared

to a similar system containing HEMA. In order to make a full conclusion, this data will be correlated with HPLC data, which is discussed later.

6.5 *Working and setting times:*

The oscillating rheometer method, for measuring working and setting times, is useful for determining the clinical handling of materials. As the material begins to set there is a change in viscosity, which is directly related to the handling properties, and ease of use of each material. According to ISO standards 4049:2009, the polymerisation exotherm of the material is used to determine the working and setting times, while the rheometer method records the 'dynamic' setting of the material (rather than measuring of the temperature rise during setting) (Ogawa *et al*., 2001). All materials should be manipulated within the working time and adjusted and finished inside the mouth within the initial setting time. Any modifications beyond the setting time could compromise the material's physical properties, and those with a longer setting time require longer chairside time. Therefore, the preferred material property is longer working time and 'rapid' setting times (Ogawa *et al*., 2001).

Working times for the FP group showed similar trends to the degree of conversion, with F1 and F2 having longer working times compared to all other compositions; this indicates a slower setting reaction, which was also confirmed by the FT-IR experiment. The explanation for this is mentioned above in 6.4, where the higher molecular weight of HPM monomer, compared to HEMA, resulted in a slower reaction. It was difficult to correlate the results of the novel compositions with existing literature, since there were neither similar products, nor similar experimental compositions reported. The results obtained here were in agreement with the

'instruction for use leaflet' for commercial FP, which states that the working time of this cement is 2.30 minutes.

Setting times of all materials did not follow the same trend as the working times, therefore these two parameters could not be correlated with each other and, should be studied separately for each product, as stated in the literature (Ogawa *et al*., 2001).

RX group showed longer working and setting times (between 8.29 for R1 and 7.03 minutes for R2; with all other compositions falling between these two). The working and setting times could be associated with the powder: liquid ratio of each material. Following the manufacturers guidelines, the FP group materials were prepared with a higher powder: liquid ratio, compared to the RX group materials. This may have resulted in a higher viscosity for the FP materials that subsequently shortened their working and setting times, compared to those for the RX group. Although the shorter working times of all FP group materials (commercial, home and novel) may not be the choice for inexperienced clinicians, who may need more time to manipulate the restoration, the shorter setting times are an advantage since they reduce the chairside time.

A conclusion from this section is that although working and setting times varied between materials in each group, all novel compositions demonstrated working and setting times that are clinically acceptable and, more importantly, the satisfactory working times (not lower than the commercial materials) will allow clinicians to manipulate the cement and seat the crowns or bridges (Lad *et al*., 2014).

6.6 *Polymerisation shrinkage strain:*

The bonded disk method was used to measure the polymerisation shrinkage strain of all materials. It recorded the axial movement and shrinkage of the material in one direction, since the bottom surface of the specimen was directly attached to the 3mm thickness glass plate. This validated method was used to calculate the percentage shrinkage strain of each specimen, since it has been used previously for a variety dental materials, including resin composites, impression materials, GICs and RMGICs (Watts and Cash, 1991; Tolidis *et al*., 1998; Watts and Hindi, 1999; Watts and Marouf, 2000; Bryant and Mahler, 2007).

Shrinkage strain (shrinkage) data for F1 and F2 (compositions containing HPM), at 23°C, showed lower percentage shrinkage and shrinkage rate, and more time was taken to reach the maximum shrinkage rate, compared to all other FP materials. This data agrees with the degree of conversion results, measured by FT-IR, which showed a lower degree of conversion for F1 and F2, compared to the other materials in the same group. Hence, the degree of shrinkage could also give an indication of the degree of polymerisation in the material (Atai *et al*., 2005), since shrinkage is a result of the change of van-der-Waals forces to covalent single bonds in the methacrylate system. Differences in polymerisation shrinkage were observed between 23°C or 37°C, in the FP group materials in the first 5 minutes of the experiment. This could be a result of the increased mobility of the monomers at 37°C compared to 23°C, which allowed for the reaction to occur faster. Therefore more double bonds were converted to single bonds, subsequently resulting in higher shrinkage values at 37°C, which agree with published literature (Watts and Hindi, 1999).

All materials in the RX group (commercial, home and novel) did not show any significant differences between each other at 37°C and 23°C, with the exception of RX Home at 23°C, which demonstrated significantly lower shrinkage values at this temperature. This could be a result of the material exhibiting an expansion prior to shrinking, which may have affected the results obtained.

The data for the shrinkage strain rate (how fast the shrinkage is occurring) and the time to reach the maximum strain rate, for all materials in the RX group, were generally comparable, but did not agree with the degree of conversion values (using FT-IR); R1 and R2 had lower conversion compared to other materials in the same group. Shrinkage rate results reported in this project are lower than these reported for HEMA and HPM by Atai *et al*. (2005) for composite resins; note in this study RMGICs are the subject. The calculated percentage shrinkage could not be correlated with values reported in literature due to the different materials used, and various techniques employed to measure the shrinkage. One study (Bryant and Mahler, 2007) reported the relationship between the polymerisation shrinkage and powder: liquid ratios. The reported values in this project were in agreement with the data for lining materials tested by Bryant and Mahler (2007), when they increased the powder: liquid ratio from that recommended by the manufacturer.

The main purpose behind testing the shrinkage of the materials was to ensure that the novel materials did not shrink more than the commercial materials, so that they cannot be compensated by the water uptake, and this was confirmed for all novel materials.

6.7 *Polymerisation exotherm:*

The polymerisation reaction of monomers in dental materials generates heat (exotherm) following the conversion of the carbon-carbon double bonds to single bonds. This reaction occurs as a result of the initiation procedure that can be generated through heat, light or at room temperature (Ferracane, 2001). In this study, the reaction was initiated chemically (at room temperature), where in the presence of water, ascorbic acid reacted with potassium persulfate, generating free radicals that then reacted with the monomer, to convert the double bonds into single bonds (Antonucci *et al*., 1979). The latter resulted in heat generation, which further enhanced the polymerisation reaction and moreover increased the heat generated.

The polymerisation of monomers (in dental materials) in situ results in the generation of heat, which can cause 100% irreversible pulpal damage when the exotherm reaches 16.6°C (Zach and Cohen, 1965). Therefore, reducing the polymerisation exotherm of dental materials is highly desirable.

In this study, the exotherm of all materials was studied at both 37 ± 1°C (body temperature) and at ambient temperature of 23 ± 1°C, which was of clinical importance, due to the fact that although the body temperature is 37°C, the oral cavity baseline temperature has been recorded as 25.1°C with rubber dam application (Plasmans *et al*., 1994).

According to Hanning and Bott (1999), a temperature rise in light-cured dental cements is a result of the exotherm occurring from the light source and the polymerisation reaction itself (Hannig and Bott, 1999). However, in this study, the exotherm was solely a result of the polymerisation reaction since all materials were

chemically activated. At both temperatures, commercial FP showed a higher exotherm than home and novel materials, which although theoretically should agree with the degree of conversion values, as the heat produced is a result of the change in the C=C double bond to single bonds, it did not. One explanation for this is that commercial FP contained an additional monomer (glycerol dimethacrylate), which was not present in the home and novel FP materials. Therefore, the higher temperature of commercial FP could be due to the conversion of this additional monomer. This will be discussed further in the HPLC section. Novel F1 and F2 had lower exotherms at both temperatures (compared to other materials in the FP group); this data agrees with the corresponding degree of conversion and shrinkage results for F1 and F2, since they had lower shrinkage strain and degree of conversion, particularly F1.

The FP group had higher exotherms compared to the RX group. This could be due to the composition of FP containing UDMA in addition to the other monomers in the cement (HEMA, THFM and HPM), whereas RX did not. As mentioned earlier, UDMA monomer is a dimethacrylate containing C=C (vinyl group) at each end of the molecule, which took part in the polymerisation reaction. Since the exotherm is dependent on the conversion of the double bond, also as mentioned earlier, this can justify the higher exotherm temperature of the FP group.

Similar to the shrinkage strain results, all RX materials did not show any significant differences between each other with respect to exotherm. However, this does not agree with the degree of conversion results. It was expected that the RX compositions containing HPM would have a significantly lower exotherm compared to all other materials in that group since they showed a lower degree of conversion.

This may be due to the very low temperature increases recorded for this group, and therefore, the significancy between materials could not be calculated.

6.8 *Monomer release from materials:*

RMGICs were introduced to overcome weaknesses present in the conventional GICs while maintaining the benefits of this conventional cement (e.g. fluoride release and bonding to tooth tissue). This was achieved by incorporating a resin, commonly used is HEMA, in these cements in order to improve their strength and early sensitivity to moisture (Attin *et al*., 1996; Khoroushi and Keshani, 2013). Theoretically the setting reaction should continue until all the monomers are converted to polymers, but this is rarely the case (Ferracane, 2001); not all of the monomers in the cement are completely polymerised during this setting reaction. Therefore residual unreacted monomers can leach out into the oral environment, and can pass through the dentine to the pulp, causing cytotoxic effects (Aranha *et al*., 2006). Hence, it is crucial to measure the amount of monomers released from materials, which can give an indication on the biocompatibility and cytotoxicity of the cement and, moreover, the degree of polymerisation.

Initially, gas chromatography was tried to separate all monomers released from samples, but it was not successful. Identification and quantification of monomers is reported in the literature by mainly using HPLC, which is considered as a powerful and good analytical method that can give improved levels of control for the separation process of compounds (Moharamzadeh *et al*., 2007; Altintas and Usumez, 2008). Therefore, HPLC was tried and proved successful for the identification and quantification of all monomers released from all FP and RX materials. However, a considerable amount of time was taken to develop two novel methods for analysing

leachants from FP and RX, since these were not documented in the literature, due to variations in the materials and differences in the column type/size used

In this study, two immersion media were used, DW and 75%/25% ethanol/DW. Although AS components could be separated by HPLC, their peaks masked some of the monomer components peaks, since these were eluted at similar retention times. Also components from AS were difficult to wash away from the column following analysis of each sample, and this biased the results of the subsequent sample. Therefore, identification of monomer release was deemed unsuitable for release of cement components in AS, and an alternative solution was sought, this being 75%/25% ethanol/DW. Following the recommendation of the US FDA, which reveals that 75%/25% ethanol/DW mimics the oral environment more than pure water (Altintas and Usumez, 2012), an ethanol solution was selected as an organic solvent (in which samples were immersed). The organic solvent penetrates the cement matrix causing swelling of the polymer, hence facilitating the leaching of the unreacted monomers (Ferracane, 1994). Using this solvent as an immersion solution may exaggerate what really happens in the oral environment, but it is beneficial as it represents the worst-case scenario of the whole process. Also the results can be compared to immersion in DW. DW was chosen as it was one of the immersion solutions used in the water uptake experiments, and therefore, it would be beneficial to correlate the results obtained from the two experiments.

The peak at 8.89 minutes in the HPLC spectrum of the commercial FP sample could not be correlated with any of the components given in the manufacturer's MSDS; as mentioned earlier the latter was used as a guide to fabricate the home and novel liquids. FT-IR analyses of commercial FP liquid did not show any additional peaks

for this component. HPLC and HPLC-MS were also not successful for identification of this component. In August 2015, a newer version of the FP MSDS was published, which included an additional monomer (glycerol dimethacrylate, 1-5%). This monomers molecular weight is 228.24, which is between the two values that were observed by the HPLC-MS (211.5 and 251.3). Hence, even though this component was present in a very small quantity in the FP composition, and only a small amount was released, HPLC was able to identify it. This finding confirms the suitability of the HPLC technique, and the novel method developed, to identify released components from the cements.

It was unfortunate that the presence of glycerol dimethacrylate was detected towards the end of this project; this monomer was not included in the FP formulations or in the release analysis of the monomers eluted from the material, since it was only identified after the completion of the HPLC experiments. This finding can be related to, and explained by the higher water uptake value for FP, since it has been reported that glycerol dimethacrylate, like HEMA, increases water uptake (McCabe and Rusby, 2004). Furthermore, the addition of this monomer meant that additional crosslinking of the matrix and conversion of the double bonds would have occurred, during the polymerisation reaction, and this contributed to the increased exotherm and lower solubility noted with commercial FP, compared to all other FP compositions in the same group.

Commercial FP also showed less monomer release compared to home and novel materials, with the exception of F3. The latter demonstrated a higher degree of the polymerisation reaction occurring in both FP and F3. This agrees with published literature utilising the two monomers THFM and HEMA, in a 50/50% ratio, mixed

with PEM, which showed lower water uptake behaviour and higher exotherm (Patel *et al*., 2001), thus indicating a higher degree of polymerisation reaction occurring in the system.

Novel F1 showed the highest monomer release compared to all materials, which suggests a lower degree of conversion for this monomer (HPM) and this was generally confirmed in all of the experiments. This was also true for samples whether immersed in DW or ethanol/DW, the only difference was that samples immersed in ethanol/DW showed higher monomers release, as expected.

All RX samples also showed release of an additional compound, which was detected at a retention time of ~1 minute, using HPLC. Therefore, HPLC-MS was conducted on all samples in this group to identify this compound, where it emerged to have a molecular weight of ~1800. It was then confirmed that this compound was poly(acrylic acid), which according to the manufacturers MSDS for the acid used, had a molecular weight of ~2000. It should be noted that the release of this poly(acrylic acid) was not evident from the FP compositions. This finding may be explained by the silane treatment of glass (fluoroalumino-silicate) used in commercial RX powder, which rendered it more hydrophobic than the non-treated glass in the FP powder. This silane treated (hydrophobic) glass will not react with all of the hydrophilic poly(acrylic acid), and this will result in some of it being released. To confirm this, the commercial powders of both cements were dissolved in a similar amount of water. FP powder sank to the bottom of the plastic tube whilst some of the RX powder stuck to the sides of the tube (hydrophobic behaviour), and this confirms the hydrophobic nature of the RX powder.

In the RX group, R3 and R4 showed lower release of monomers compared to commercial and home materials, in both solutions, similar to the FP group. This agrees with what was discussed earlier. R1 in ethanol/DW solution showed higher HPM monomer release and this correlated with the degree of conversion experiment. Similar to F1, R1 showed a lower degree of polymerisation of the HPM monomer, when compared to HEMA monomer. This again may be due to the higher molecular weight of HPM compared to HEMA, hence less mobility of the monomer and thus a slower reaction.

6.9 *Mechanical properties of commercial, home and novel materials:*

One of the main benefits of incorporating a monomer (commonly used HEMA) into GICs in order to formulate a RMGIC is to improve their strength (McCabe, 1998). Therefore, it was crucial to test the mechanical properties of commercial, home materials and novel cements (the latter incorporating THFM and HPM), in order to make sure that the addition of new monomers did not adversely affect their strength.

Since there was no testing methodology recommended for RMGICs in the published literature, testing was performed using ISO 9917-1, which is recommended for GICs (for compressive fracture strength; CFS), ISO 4049 for resin cements and ISO 9917-2 for RMGICs (three-point flexural strength; TFS). According to Baig *et al*. (2015), CFS was the most reliable mechanical testing methodology for hand-mixed GICs, when compared to TFS, biaxial flexural strength (BFS) and Hertzian indentation (HI) (Baig *et al*., 2015). For resin cements, TFS is usually the test of choice since it is recommended by ISO 4049 (Chung *et al*., 2004). The latter author reported that

TFS results were more reliable than those obtained from BFS, which showed a higher CoV.

As speculated, novel F1, which showed a lower degree of conversion (compared to other novel FP materials), also had a significantly lower compressive strength compared to commercial and home FP materials. This can be explained by the fact that a higher degree of conversion leads to a more cross-linked structure, hence the material would have improved mechanical properties (Lovell *et al*., 2001). On comparing the home and novel materials, all novel materials showed higher CFS compared to the home material, especially F3, F4 and F2; these results did not reflect the trend observed in the degree of conversion experiment where the home material showed a similar degree of conversion to F3 and F4, while F2 presented with a significantly lower value. However, it should be noted that the degree of conversion of monomers was measured only up to 30 minutes, whilst CFS testing was performed after 24 hours from the start of mixing. This difference in time for CFS testing could potentially account for more monomer conversion occurring thus the improved strength. Also, the setting of RMGICs includes both an acid-base reaction of the GIC and polymerisation of the resin where both contribute to the ultimate strength of the material, whilst the degree of conversion only estimates the conversion of the monomers in the material. Hence, there may have been a difference in the extent of the acid-base reaction between the materials, which may have affected the CFS results.

Commercial FP had a higher CFS than all other compositions (home and novel) in the group. This could possibly be due to the molecular weight of poly(acrylic acid) being higher compared with a lower molecular weight grade used to formulate the

home and novel cement liquids (~2000). It should be noted that although the commercial materials did not specify the molecular weight range of poly(acrylic acid|) used, it is assumed that some of it was ~2000 (the lower end of the range), since it was detected by HPLS-MS. This was also speculated since this material is used as a luting cement. Although a high molecular weight poly(acrylic acid) would enhance the physical properties, it could also cause an increase in viscosity of the mixed cement (Dowling and Fleming, 2011), thus making it difficult to manipulate, especially when used as a luting cement.

Cements with higher molecular weight poly(acrylic acid) are expected to have more cross-linked polyacrlate chains and therefore higher strength (Wilson *et al*., 1977; Griffin and Hill, 1998). Wilson *et al*. (1989) reported an improvement in the GICs performance when increasing the poly(acrylic acid) molecular weight, due to longer polymer chains (Wilson *et al*., 1989). Other published literature reported on the relationship between molecular weight of poly(acrylic acid) and CFS, where higher molecular weight poly(acrylic acid) accounted for improved CFS of GICs (Griffin and Hill, 1998; Fennell and Hill, 2001).

All materials in the RX group showed lower CFS than the FP group. This could be due to the RX materials containing a higher water content in the liquid (35%) and a result of the lower powder: liquid ratio, and so it can be assumed that the liquid contained a higher percentage of water compared to FP. It was speculated that some of this water was lost in the immersion solution following setting of the cement; this was confirmed from the solubility results where a higher solubility was obtained for RX compared to FP. Bertenshaw and Piddock (1993) reported that water-based luting cements (zinc polycarboxylate, zinc phosphate and GICs) with a higher

solubility increased the percentage of pores/porosity within the materials (Bertenshaw and Piddock, 1993). Nomoto et al. (2004) confirmed that pores/porosity within the material contributed to the reduced strength in GICs (Nomoto *et al*., 2004), and hence this argument could apply to RMGICs.

Compressive modulus (CM) was also calculated for all samples in this study, which is considered as an intrinsic material property, compared to CFS, that can be influenced by different sample dimensions (Dowling and Fleming, 2008). Here, CM values were generally in agreement with CFS. As examples, commercial FP showed significantly higher CM and CFS values compared to all materials in both groups. CM and CFS of novel RX and home materials were lower than all corresponding FP compositions, which again could be attributed to the lower powder: liquid ratio and increased water content in the liquid (35% in RX compared with 30% in FP), thus reflecting the materials intrinsic properties.

Similar to CFS, TFS of the two commercial materials were higher than those obtained for home and novel cements, which again could be related to the higher molecular weight poly(acrylic acid) used in the commercial products. On comparing novel and home cements, promising CFS, CM and TFS results were obtained for F2, F3 and F4 (novel), which presented with higher values than the home material.

The load/deflection curve for novel materials showed ductile behaviour while home and commercial cements presented brittle behaviour. These materials did not fracture immediately after reaching the maximum stress point, but rather underwent some plastic deformation prior to fracture. This could be due to the lower degree of conversion of monomers in compositions containing HPM (F1, F2, R1 and R2), and

a result of the increased molecular weight of THFM monomer in F3, F4, R3 and R4 compositions. The ductility of THFM has also been confirmed by Patel and Braden when room temperature polymerising this monomer with PEM (Patel and Braden, 1991b; Moore and Turner, 2001).

As mentioned earlier, according to ISO 4049:2009, TFS is the test of choice for measuring the strength of polymer based materials. However, this test was questioned for its reliability due to the stresses developing in the specimen during testing (Kumar, 2013), with a compressive stress occurring in the top surface, a tensile stress at the bottom surface and no stress in the middle neutral region. Therefore, the different stresses occurring at top and bottom surfaces emphasise the effect of surface finishing; this could affect the values obtained from TFS test (Berenbaum and Brodie, 1959). Thus, all samples in this study were treated in the same way and, the two surfaces that were exposed to stresses (top and bottom), were the ones that were in contact with the acetate sheet during the setting of the sample. However, although all samples were treated similarly, the possibility of different surface textures on samples cannot be ruled out, which could have played a role in the high variation of the values obtained within each material. Therefore, TFM was calculated to give a better idea of the strength of the materials, as similar to CM, it is considered an intrinsic materials property. It should be noted that compositions F3, F4 and R3 passed the ISO 9917-2:2010 requirement of a minimum 10 MPa for TFS.

TFM data showed generally similar trends to CM, where commercial FP had higher values compared to all materials in both groups. Moreover, FP compositions presented with higher TFM compared to their RX counterparts. However, the CoV was relatively high (reaching 42%) in F1, which might have been a result of the

subjectivity in selecting the end-point value of the initial linear region of the load/deflection plot, which was used to calculate the TFM; for the brittle materials (home and commercial), the end of the initial linear region (where the sample fractured) represented the maximum load. CoV of CFS data were considerably low, ranging between 3-11%, compared to the higher CoV calculated for TFS (reaching 38% in F1). This implies that the CFS test is more reliable in determining the strength of the cements. The outcome of these results is in agreement with Baig *et al*. (2015), who concluded that the CFS is 'the only discriminatory performance indicator of hand-mixed GICs'.

6.10 *Cytotoxicity of materials (commercial, home and novel):*

Dental materials should undergo and pass several biocompatibility studies, whether *in vivo* or *in vitro*, before they can be recommended for patients. *In vitro* studies offer the advantage of control over the experiment variables that sometimes cannot be managed *in vivo*; they are less expensive and do not possess ethical difficulties compared to animal testing (Schmalz, 1994). Different cells and tests have been used to evaluate biocompatibility and cytotoxicity of dental materials. In this study, human fibroblasts were used since the materials under investigation are potential luting cements, and therefore, they would be in close contact with the gingival tissue following the application of a crown or bridge. In these situations, fibroblasts are considered the cells of choice for testing these materials (Willershausen *et al*., 1999; Wan *et al*., 2001; Engelmann *et al*., 2002; Szep *et al*., 2002; Janke *et al*., 2003; Issa *et al*., 2004). They are considered as 'highly sensitive' cells and demonstrate even minimal cytotoxic effects. They are moreover relatively easy to grow in the culture medium and easily obtained from patients (Moharamzadeh *et al*., 2009).

The biological endpoint used in the present study was the measurement of cells viability through the MTT [(3-(4,5-dmethylthiazol-2-yl)-2,5-diphenyltetrazolium bromide] assay. It has been used in studies to assess the cytotoxicity of dental materials (Geurtsen *et al*., 1998; Stanislawski *et al*., 1999; Schuster *et al*., 2001; Bouillaguet *et al*., 2002; Huang and Chang, 2002; Schmalz *et al*., 2002; Chen *et al*., 2003; Issa *et al*., 2004).

RX samples showed significantly lower cell viability compared to the control and FP group. The HPLC experiment results showed lower monomer release but higher poly(acrylic acid) release from the RX group, compared to FP. It can be assumed that the cytotoxicity was rather a result of the acid released (and not monomer leached). This was confirmed by the change in colour of the culture medium in which the samples were placed, which indicated acidity of the medium. Therefore, the cytotoxicity was linked to the high acidity rather than cytotoxicity of the monomers.

It can be confirmed that all RX group materials showed highly cytotoxic behaviour. This was in agreement with Pontes *et al*. (2014), as the authors concluded that RX produced a very 'intense' cytotoxic effect and moreover confirmed the acidity of RX supernatants (Pontes *et al*., 2014). However, our results did not agree with da Fonseca Roberti Garcia *et al*. (2015), who demonstrated that RX is not considered as a cytotoxic material. This could be explained by the different cells used in their study (odontoblast), which may have had a different reaction to the material compared to the NHDF cells used in the present study (da Fonseca Roberti Garcia *et al*., 2015).

In the first experiment (sample surface to liquid area = 47.13 mm^2/mL), the FP group did not show differences between materials and control medium, with the exception of F2 that showed lower cell viability. This could be a result of the higher standard deviations obtained for F2 (CoV =24%) rather than the actual cytotoxicity of this material. The second set of experiments included higher surface to liquid area (141.4 mm^2/mL; compared to 47.13 mm^2/mL in the first experiment), in an attempt to show if there were any differences between the FP materials in relation to the monomer used in each varying formulation. The diluted supernatants generally showed significantly similar cell viability compared to the control medium. The results from the second experiment demonstrated promising results for F3 and F4, despite the fact that they were not significantly different when compared to home and commercial materials. They were the only two materials that showed comparable results to the control medium (the negative control). The higher cell viability could be a result of the monomer used in this material (THFM), that partially replaced HEMA, which is known to be a biocompatible material when it was tested in the dental pulp of monkeys (Pearson *et al*., 1986).

General summary:

The physico-mechanical properties of two commercial RMGICs (Fuji Plus and RelyX Luting) were successfully compared with two-home (in-house) and eight novel RMGICs. The strength of the newly developed cements could be improved further with the inclusion of, for example, a higher molecular weight poly(acrylic acid) and glycerol dimethacrylate. The latter two materials presence in commercial materials was not evident until the end of the experimental period of the project. All eight novel compositions presented with lower water uptakes and dimensional

changes compared to commercial materials; they also demonstrated acceptable handling properties and comparable polymerisation shrinkage, and in some cases lower exotherms. It should be noted that the water uptake, although lower, would still be sufficient to allow the acid-base reaction to proceed, due to the water present in the cement (from the liquid; as characterised by FTIR); hence these novel formulations will therefore undergo less swelling, (compared to commercial materials), which is a potential advantage for luting all-ceramic crowns. Furthermore, promising biocompatibility results were obtained for two novel RMGICs (F3 and F4), which showed similar cell viability compared to the control medium. Hence, the overall encouraging results show that some of the novel formulations (e.g. F3 and F4) merit further research prior to taking them forward for potential commercialisation.

7 CONCLUSIONS AND FUTURE WORK

7.1 Conclusions:

The conclusions from this study can be summarised as follows:

- A suitable method (without desiccation of samples prior to water uptake) was found for measuring the water uptake of all materials (commercial, home and novel). It was more clinically relevant, because when the materials are used at the chairside, they are used as prepared (without desiccation). Since RMGICs contain water in their composition, the results of the ISO 4049:2009 method (which includes desiccation of samples prior to water uptake) were more exaggerated, compared to the method without desiccation, and so it was deemed unsuitable.

- Two modes of diffusion kinetics were associated for the two water uptake methods, Fickian (without desiccation method), and Case II (ISO 4049:2009 method). The latter is a result of molecular relaxation since water is acting as a plasticiser, while the former is the percentage of water required to saturate the resin matrix alone.

- Eight novel liquid compositions were successfully prepared based on pre-determined formulations of the commercial materials (FP and RX; using FT-IR and materials MSDS), where HEMA was partially or fully replaced with various percentages of THFM, HPM or both.

- As expected, with the incorporation of THFM and HPM, all novel compositions in both groups (FP and RX) showed lower water uptakes and

lower dimensional changes, compared to their commercial and home counterparts, both in both DW and AS.

- The water uptake of the novel materials, although reduced, would be sufficient to allow the acid base reaction to proceed, due to the water present in the cement (from the liquid; as characterised by FTIR). Additionally, these novel formulations will therefore undergo less swelling, (compared to commercial materials), which is a potential advantage for luting all-ceramic crowns.

- Both the acid-base and polymerisation reactions were successfully followed and analysed using FT-IR, where all novel compositions (with the exception of those containing HPM, F1, F2, R1 and R2), showed a comparable 'degree of conversion' compared with commercial and home materials.

- Handling properties (working and setting times) of all novel compositions were deemed to be clinically acceptable and were generally comparable to their commercial counterparts.

- All novel compositions showed comparable shrinkage values to the commercial and home materials. Therefore, it can be assumed that the shrinkage will be compensated by the water uptake of the material, and the marginal integrity of the cement will not be compromised.

- Novel FP RMGICs demonstrated a lower temperature rise on setting compared to commercial FP, at both temperatures 23°C and 37°C. Moreover, the FP group (containing UDMA in addition to the other monomers all with

C=C) showed higher exotherms, compared to the RX group, as a result of the conversion of C=C double bonds.

- Novel methods were developed for identifying residuals from RX and FP; these methods were deemed to be successful in identifying even small quantities of components released from materials (eg glycerol dimethacrylate).

- Compositions containing THFM (F3, R3 and R4) showed similar or lower release of all monomers, compared to commercial and home materials in both solutions (DW and 75%/25% ethanol/DW), thus indicating a higher, or similar, degree of polymerisation.

- Promising CFS, CM and TFS results were obtained for F2, F3 and F4 (novel), which presented with higher values than the home material.

- All novel materials passed the ISO 9917-1:2010 requirement for a minimum of 50 MPa for CFS, and moreover, F3, F4 and R3 passed the ISO 9917-2 requirement for a minimum of 10 MPa for TFS.

- Coefficient of variations (CoV) for CFS were considerably lower than those for TFS, which implies that the CFS test is more reliable in determining the strength of the cements (thus agreeing with published literature Baig et al. 2015).

- Promising results were obtained for F3 and F4 with respect to the cell culture study (second experiment on FP), which showed insignificant difference

compared to the control medium, despite not being significantly different to the home and commercial materials.

7.2 Future work:

- Further improvement on the degree of conversion with compositions containing HPM need to be considered, by for example, including a higher percentage of the dimethacrylate monomer (e.g. UDMA), to enhance cross-linking of the matrix. However, exotherm and shrinkage should also be taken into consideration.

- Compositions that showed promising cell viability results (especially F3 and F4) should be modified with the incorporation of glycerol dimethacrylate, to mimic the composition of commercial FP, and to improve the strength of the novel materials.

- Higher molecular weight poly(acrylic acids) should be incorporated in the liquid compositions from both groups to further improve their mechanical properties. Care should be taken not to increase the materials viscosity since the intended use of the material is as a luting cement.

- Development of a new glass powder with improved properties (e.g. remineralisation ability) to use with the novel liquids, especially those that showed promising results in the cell culture study (F3 and F4) to further improve properties of the resulting cements.

8 REFERENCES

Abed Y A, Sabry H A and Alrobeigy N A (2015). Degree of conversion and surface hardness of bulk-fill composite versus incremental-fill composite. Tanta Dental Journal 12(2): 71-80.

Adamson M, Lloyd C H and Watts D C (1988). The temperature rise beneath a light-cured cement lining during light curing. J Dent 16(4): 182-187.

Al-Qudah A A, Mitchell C A, Biagioni P A and Hussey D L (2005). Thermographic investigation of contemporary resin-containing dental materials. J Dent 33(7): 593-602.

Alnazzawi A and Watts D C (2012). Simultaneous determination of polymerization shrinkage, exotherm and thermal expansion coefficient for dental resin-composites. Dent Mater 28(12): 1240-1249.

Altintas S H and Usumez A (2008). Evaluation of monomer leaching from a dual cured resin cement. J Biomed Mater Res B Appl Biomater 86(2): 523-529.

Altintas S H and Usumez A (2012). Evaluation of TEGDMA leaching from four resin cements by HPLC. European Journal of Dentistry 6(3): 255-262.

Andrzejewska E, Andrzejewski M, Socha E and Zych-Tomkowiak D (2003). Effect of polyacid aqueous solutions on photocuring of polymerizable components of resin-modified glass ionomer cements. Dent Mater 19(6): 501-509.

Anstice H M, Kanchanavasita W, Pearson G J, Schottlander B D and Sherpa A L (2001). Polymerizable cement compositions.

Anstice H M and Nicholson J W (1992). Studies on the structure of light-cured Glass-ionomer cements. J Mater Sci Mater Med 3(6): 447-451.

Anstice H M, Nicholson J W and McCabe J F (1992). The effect of using layered specimens for determination of the compressive strength of glass-ionomer cements. J Dent Res 71(12): 1871-1874.

Antonucci J M, Grams C L and Termini D J (1979). New initiator systems for dental resins based on ascorbic acid. J Dent Res 58(9): 1887-1899.

Antonucci J M, McKinney J E and Stansbury R W (1988). Resin Modified glass ionomer Cement.

Antonucci J M and Toth E E (1983). Extent of polymerization of dental resins by differential scanning calorimetry. J Dent Res 62(2): 121-125.

Anusavice K J (1993). Recent developments in restorative dental ceramics. J Am Dent Assoc 124(2): 72-74, 76-78, 80-74.

Anusavice K J, Phillips R W, Shen C and Rawls H R (2012). Phillips' Science of Dental Materials, USA: Elsevier/Saunders.

Aquilino S A, Diaz-Arnold A M and Krueger G E (1990). Tensile bond strengths of an electrolytically and chemically etched base metal. Int J Prosthodont 3(1): 93-97.

Aranha A M, Giro E M, Souza P P, Hebling J and de Souza Costa C A (2006). Effect of curing regime on the cytotoxicity of resin-modified glass-ionomer lining cements applied to an odontoblast-cell line. Dent Mater 22(9): 864-869.

Aratani M, Pereira A C, Correr-Sobrinho L, Sinhoreti M A and Consani S (2005). Compressive strength of resin-modified glass ionomer restorative material: effect of P/L ratio and storage time. J Appl Oral Sci 13(4): 356-359.

Atai M, Watts D C and Atai Z (2005). Shrinkage strain-rates of dental resin-monomer and composite systems. Biomaterials 26(24): 5015-5020.

Attar N, Tam L E and McComb D (2003). Mechanical and physical properties of contemporary dental luting agents. J Prosthet Dent 89(2): 127-134.

Attin T, Vataschki M and Hellwig E (1996). Properties of resin-modified glass-ionomer restorative materials and two polyacid-modified resin composite materials. Quintessence Int 27(3): 203-209.

Babannavar R and Shenoy A (2013). Evaluation of shear bond strength of silorane resin to conventional, resin-modified glass ionomers and nano-ionomer cements. J Investig Clin Dent.

Baig M S, Dowling A H, Cao X and Fleming G J (2015). A discriminatory mechanical testing performance indicator protocol for hand-mixed glass-ionomer restoratives. Dent Mater 31(3): 273-283.

Bakopoulou A, Mourelatos D, Tsiftsoglou A S, Giassin N P, Mioglou E and Garefis P (2009). Genotoxic and cytotoxic effects of different types of dental cement on normal cultured human lymphocytes. Mutation Research/Genetic Toxicology and Environmental Mutagenesis 672(2): 103-112.

Bakopoulou A, Papadopoulos T and Garefis P (2009). Molecular Toxicology of Substances Released from Resin–Based Dental Restorative Materials. International Journal of Molecular Sciences 10(9): 3861-3899.

Baldissara P, Catapano S and Scotti R (1997). Clinical and histological evaluation of thermal injury thresholds in human teeth: a preliminary study. J Oral Rehabil 24(11): 791-801.

Barrie J A and Machin D (1969). The sorption and diffusion of water in silicone rubbers: Part I. Unfilled rubbers. J Macromol Sci Ph 3(4): 645-672.

Bausch J R, de Lange K, Davidson C L, Peters A and de Gee A J (1982). Clinical significance of polymerization shrinkage of composite resins. Journal of Prosthetic Dentistry 48(1): 59-67.

Becher R, Kopperud H M, Al R H, Samuelsen J T, Morisbak E, Dahlman H J, Lilleaas E M and Dahl J E (2006). Pattern of cell death after in vitro exposure to GDMA, TEGDMA, HEMA and two compomer extracts. Dent Mater 22(7): 630-640.

Behr M, Rosentritt M, Loher H, Kolbeck C, Trempler C, Stemplinger B, Kopzon V and Handel G (2008). Changes of cement properties caused by mixing errors: the therapeutic range of different cement types. Dent Mater 24(9): 1187-1193.

Behr M, Rosentritt M, Mangelkramer M and Handel G (2003). The influence of different cements on the fracture resistance and marginal adaptation of all-ceramic and fiber-reinforced crowns. Int J Prosthodont 16(5): 538-542.

Berenbaum R and Brodie I (1959). Measurement of tensile strength of brittle materials. British Journal of Applied Physics 10: 281-287.

Beriat N C and Nalbant D (2009). Water Absorption and HEMA Release of Resin-Modified Glass-Ionomers. Eur J Dent 3(4): 267-272.

Bertenshaw B W and Piddock V (1993). Porosity in water-based dental luting cements. Journal of Materials Science: Materials in Medicine 4(4): 415-417.

Bhusate M and Braden M (1983). Low shrinkage polymer/monomer mixtures for biomedical use.

Billington R W, Williams J A and Pearson G J (1990). Variation in powder/liquid ratio of a restorative glass-ionomer cement used in dental practice. Br Dent J 169(6): 164-167.

Botsali M S, Kusgoz A, Altintas S H, Ulker H E, Tanriver M, Kilic S, Basak F and Ulker M (2014). Residual HEMA and TEGDMA release and cytotoxicity evaluation of resin-modified glass ionomer cement and compomers cured with different light sources. ScientificWorldJournal 2014: 218295.

Bouillaguet S, Shaw L, Gonzalez L, Wataha J C and Krejci I (2002). Long-term cytotoxicity of resin-based dental restorative materials. J Oral Rehabil 29(1): 7-13.

Bouillaguet S, Wataha J C, Hanks C T, Ciucchi B and Holz J (1996). In vitro cytotoxicity and dentin permeability of HEMA. J Endod 22(5): 244-248.

Bouillaguet S, Wataha J C, Virgillito M, Gonzalez L, Rakich D R and Meyer J M (2000). Effect of sub-lethal concentrations of HEMA (2-hydroxyethyl

methacrylate) on THP-1 human monocyte-macrophages, in vitro. Dent Mater 16(3): 213-217.

Bovis S C, Harrington E and Wilson H J (1971). Setting characteristics of composite filling materials. Br Dent J 131(8): 352-356.

Brackett W W, Dib A, Brackett M G, Reyes A A and Estrada B E (2003). Two-year clinical performance of Class V resin-modified glass-lonomer and resin composite restorations. Oper Dent 28(5): 477-481.

Braden M, Causton E E and Clarke R L (1976). Diffusion of water in composite filling materials. J Dent Res 55(5): 730-732.

Braden M, Davy K W M, Downes S and Patel M P (1993). The use of biomaterials for tissue repair.

Braden M, Patel M P and Pearson G J F (2001). Fluoride releasing biomaterials.

Braem M (1999). Physical properites of glass ionomer cements: fatigue and elasticity. Advances in Glass Ionomer Cements. Berlin/Chicago: Quintessence Publishing Co: 67-84.

Braem M J, Lambrechts P, Gladys S and Vanherle G (1995). In vitro fatigue behavior of restorative composites and glass ionomers. Dent Mater 11(2): 137-141.

Brook I M and Hatton P V (1998). Glass-ionomers: bioactive implant materials. Biomaterials 19(6): 565-571.

Brunthaler A, Konig F, Lucas T, Sperr W and Schedle A (2003). Longevity of direct resin composite restorations in posterior teeth. Clin Oral Investig 7(2): 63-70.

Bryant R W and Mahler D B (2007). Volumetric contraction in some tooth-coloured restorative materials. Aust Dent J 52(2): 112-117.

Buonocore M G (1955). A simple method of increasing the adhesion of acrylic filling materials to enamel surfaces. J Dent Res 34(6): 849-853.

Cattani-Lorente M A, Dupuis V, Payan J, Moya F and Meyer J M (1999). Effect of water on the physical properties of resin-modified glass ionomer cements. Dent Mater 15(1): 71-78.

Cefaly D F, Wang L, de Mello L L, dos Santos J L, dos Santos J R and Lauris J R (2006). Water sorption of resin-modified glass-ionomer cements photoactivated with LED. Braz Oral Res 20(4): 342-346.

Chadwick R G and Woolford M J (1993). A comparison of the shear bond strengths to a resin composite of two conventional and two resin-modified glass polyalkenoate (ionomer) cements. J Dent 21(2): 111-116.

Charlton D G, Moore B K and Swartz M L (1991). Direct surface pH determinations of setting cements. Oper Dent 16(6): 231-238.

Chen C C, Chen R C and Huang S T (2002). Enzymatic responses of human deciduous pulpal fibroblasts to dental restorative materials. J Biomed Mater Res 60(3): 452-457.

Chen R S, Liu C C, Tseng W Y, Jeng J H and Lin C P (2003). Cytotoxicity of three dentin bonding agents on human dental pulp cells. J Dent 31(3): 223-229.

Cho S Y and Cheng A C (1999). A review of glass ionomer restorations in the primary dentition. J Can Dent Assoc 65(9): 491-495.

Chung S M, Yap A U, Chandra S P and Lim C T (2004). Flexural strength of dental composite restoratives: comparison of biaxial and three-point bending test. J Biomed Mater Res B Appl Biomater 71(2): 278-283.

Circu M L and Aw T Y (2012). Glutathione and modulation of cell apoptosis. Biochimica et Biophysica Acta (BBA) - Molecular Cell Research 1823(10): 1767-1777.

Cook W D, Forrest M and Goodwin A A (1999). A simple method for the measurement of polymerization shrinkage in dental composites. Dental Materials 15(6): 447-449.

Costa C A, Giro E M, do Nascimento A B, Teixeira H M and Hebling J (2003). Short-term evaluation of the pulpo-dentin complex response to a resin-modified glass-ionomer cement and a bonding agent applied in deep cavities. Dent Mater 19(8): 739-746.

Crank J (1979). The Mathematics of Diffusion, Oxford: Clarendon Press.

Crawley M J (2005). Fundamentals. Statistics, USA: John Wiley & Sons, Inc.**:** 1-14.

Crisp S, Jennings M A and Wilson A D (1978). A study of temperature changes occurring in setting dental cements. J Oral Rehabil 5(2): 139-144.

Crisp S, Kent B E, Lewis B G, Ferner A J and Wilson A D (1980). Glass-ionomer cement formulations. II. The synthesis of novel polycarobxylic acids. J Dent Res 59(6): 1055-1063.

Crisp S and Wilson A D (1976). Reactions in glass ionomer cements: V. Effect of incorporating tartaric acid in the cement liquid. J Dent Res 55(6): 1023-1031.

Croll T (1998). Alternatives to silver amalgam and resin composite in pediatric dentistry. Quintessence Int 29(11): 697-703.

Croll T P and Nicholson J W (2002). Glass ionomer cements in pediatric dentistry: review of the literature. Pediatr Dent 24(5): 423-429.

Czarnecka B, Limanowska-Shaw H and Nicholson J W (2002). Buffering and ion-release by a glass-ionomer cement under near-neutral and acidic conditions. Biomaterials 23(13): 2783-2788.

da Fonseca Roberti Garcia L, Pontes E C, Basso F G, Hebling J, de Souza Costa C A and Soares D G (2015). Transdentinal cytotoxicity of resin-based luting cements to pulp cells. Clin Oral Investig.

de Castilho A R, Duque C, Negrini Tde C, Sacono N T, de Paula A B, de Souza Costa C A, Spolidorio D M and Puppin-Rontani R M (2013). In vitro and in vivo investigation of the biological and mechanical behaviour of resin-modified glass-ionomer cement containing chlorhexidine. J Dent 41(2): 155-163.

de Castilho A R F, Duque C, Negrini T d C, Sacono N T, de Paula A B, Sacramento P A, de Souza Costa C A, Spolidorio D M P and Puppin-Rontani R M (2012). Mechanical and biological characterization of resin-modified glass-ionomer cement containing doxycycline hyclate. Archives of Oral Biology 57(2): 131-138.

de la Macorra J C and Pradies G (2002). Conventional and adhesive luting cements. Clin Oral Investig 6(4): 198-204.

Diaz-Arnold A M, Vargas M A and Haselton D R (1999). Current status of luting agents for fixed prosthodontics. J Prosthet Dent 81(2): 135-141.

do Nascimento A B, Fontana U F, Teixeira H M and Costa C A (2000). Biocompatibility of a resin-modified glass-ionomer cement applied as pulp capping in human teeth. Am J Dent 13(1): 28-34.

dos Santos R L, Pithon M M, Martins F O, Romanos M T V and Ruellas A C O (2012). Evaluation of cytotoxicity and degree of conversion of glass ionomer cements reinforced with resin. The European Journal of Orthodontics 34(3): 362-366.

Dowling A H and Fleming G J (2008). Is encapsulation of posterior glass-ionomer restoratives the solution to clinically induced variability introduced on mixing? Dent Mater 24(7): 957-966.

Dowling A H and Fleming G J P (2009). Are encapsulated anterior glass-ionomer restoratives better than their hand-mixed equivalents? Journal of Dentistry 37(2): 133-140.

Dowling A H and Fleming G J P (2011). The influence of poly(acrylic) acid number average molecular weight and concentration in solution on the compressive fracture strength and modulus of a glass-ionomer restorative. Dent Mater 27(6): 535-543.

Du M and Zheng Y (2008). Degree of conversion and mechanical properties studies of UDMA based materials for producing dental posts. Polymer Composites 29(6): 623-630.

Duarte S, Jr., Phark J H, Tada T and Sadan A (2009). Resin-bonded fixed partial dentures with a new modified zirconia surface: a clinical report. Journal of Prosthetic Dentistry 102(2): 68-73.

E L, Irie M, Nagaoka N, Yamashiro T and Suzuki K (2010). Mechanical properties of a resin-modified glass ionomer cement for luting: effect of adding spherical silica filler. Dent Mater J 29(3): 253-261.

Engelmann J, Leyhausen G, Leibfritz D and Geurtsen W (2002). Effect of TEGDMA on the intracellular glutathione concentration of human gingival fibroblasts. J Biomed Mater Res 63(6): 746-751.

Ergin S and Gemalmaz D (2002). Retentive properties of five different luting cements on base and noble metal copings. J Prosthet Dent 88(5): 491-497.

Ermis R B (2002). Two-year clinical evaluation of four polyacid-modified resin composites and a resin-modified glass-ionomer cement in Class V lesions. Quintessence Int 33(7): 542-548.

Ernst C P, Cohnen U, Stender E and Willershausen B (2005). In vitro retentive strength of zirconium oxide ceramic crowns using different luting agents. J Prosthet Dent 93(6): 551-558.

Fareed M A and Stamboulis A (2014). Effect of Nanoclay Dispersion on the Properties of a Commercial Glass Ionomer Cement. International Journal of Biomaterials 2014: 10.

Federlin M, Schmidt S, Hiller K A, Thonemann B and Schmalz G (2004). Partial ceramic crowns: influence of preparation design and luting material on internal adaptation. Oper Dent 29(5): 560-570.

Federlin M, Sipos C, Hiller K A, Thonemann B and Schmalz G (2005). Partial ceramic crowns. Influence of preparation design and luting material on margin integrity--a scanning electron microscopic study. Clin Oral Investig 9(1): 8-17.

Feilzer A J, De Gee A J and Davidson C L (1988). Curing contraction of composites and glass-ionomer cements. J Prosthet Dent 59(3): 297-300.

Felton D A, Kanoy B E and White J T (1987). Effect of cavity varnish on retention of cemented cast crowns. J Prosthet Dent 57(4): 411-416.

Fennell B and Hill R G (2001). The influence of poly(acrylic acid) molar mass and concentration on the properties of polyalkenoate cements Part III Fracture toughness and toughness. Journal of Materials Science 36(21): 5185-5192.

Ferracane J L (1994). Elution of leachable components from composites. J Oral Rehabil 21(4): 441-452.

Ferracane J L (2001). Polymeric materials: the basics. Materials in Dentistry: Principles and Applications. Lippincott Williams & Wilkins**:** 255-280.

Fleming G J, Dowling A H and Addison O (2012). The crushing truth about glass ionomer restoratives: exposing the standard of the standard. J Dent 40(3): 181-188.

Fleming G J P, Marquis P M and Shortall A C C (1999). The influence of clinically induced variability on the distribution of compressive fracture strengths of a hand-mixed zinc phosphate dental cement. Dent Mater 15(2): 87-97.

Forsten L (1995). Resin-modified glass ionomer cements: fluoride release and uptake. Acta Odontol Scand 53(4): 222-225.

Fouad A, Torabinejad M and Walton R E (2008). Endodontics: Principles and Practice, UK: Elsevier Health Sciences.

Franco E B, Benetti A R, Ishikiriama S K, Santiago S L, Lauris J R, Jorge M F and Navarro M F (2006). 5-year clinical performance of resin composite versus resin modified glass ionomer restorative system in non-carious cervical lesions. Oper Dent 31(4): 403-408.

Gaintantzopoulou M D, Willis G P and Kafrawy A H (1994). Pulp reactions to light-cured glass ionomer cements. Am J Dent 7(1): 39-42.

Galler K, Hiller K A, Ettl T and Schmalz G (2005). Selective influence of dentin thickness upon cytotoxicity of dentin contacting materials. J Endod 31(5): 396-399.

Gallorini M, Cataldi A and di Giacomo V (2013). HEMA-induced cytotoxicity: oxidative stress, genotoxicity and apoptosis. Int Endod J 47(9):813-8.

Galvão M R, Caldas S G F R, Bagnato V S, de Souza Rastelli A N and de Andrade M F (2013). Evaluation of degree of conversion and hardness of dental composites photo-activated with different light guide tips. European Journal of Dentistry 7(1): 86-93.

Gerdolle D A, Mortier E, Jacquot B and Panighi M M (2008). Water sorption and water solubility of current luting cements: an in vitro study. Quintessence Int 39(3): 107-114.

Gerzina T M and Hume W R (1996). Diffusion of monomers from bonding resin-resin composite combinations through dentine in vitro. J Dent 24(1-2): 125-128.

Geurtsen W (2000). Biocompatibility of resin-modified filling materials. Crit Rev Oral Biol Med 11(3): 333-355.

Geurtsen W, Lehmann F, Spahl W and Leyhausen G (1998). Cytotoxicity of 35 dental resin composite monomers/additives in permanent 3T3 and three human primary fibroblast cultures. J Biomed Mater Res 41(3): 474-480.

Geurtsen W, Spahl W and Leyhausen G (1998). Residual monomer/additive release and variability in cytotoxicity of light-curing glass-ionomer cements and compomers. J Dent Res 77(12): 2012-2019.

Glace W R and Ibsen R L (1981). Provisional crown-and-bridge resin containing tetrahydrofuryl methacrylate.

Gordan V V, Boyer D and Soderholm K J (1998). Enamel and dentine shear bond strength of two resin modified glass ionomers and two resin based adhesives. J Dent 26(5-6): 497-503.

Griffin S and Hill R (1998). Influence of poly(acrylic acid) molar mass on the fracture properties of glass polyalkenoate cements. Journal of Materials Science 33(22): 5383-5396.

Griffiths P R and De Haseth J A (2007). Fourier Transform Infrared Spectrometry, Interscience, USA: John Wiley & Sons.

Hamid A and Hume W R (1997). Diffusion of resin monomers through human carious dentin in vitro. Endod Dent Traumatol 13(1): 1-5.

Hamid A and Hume W R (1997). The effect of dentine thickness on diffusion of resin monomers in vitro. J Oral Rehabil 24(1): 20-25.

Hamid A, Okamoto A, Iwaku M and Hume W R (1998). Component release from light-activated glass ionomer and compomer cements. J Oral Rehabil 25(2): 94-99.

Hannig M and Bott B (1999). In-vitro pulp chamber temperature rise during composite resin polymerization with various light-curing sources. Dental Materials 15(4): 275-281.

Hasegawa T, Manabe A, Itoh K and Wakumoto S (1989). Investigation of self-etching dentin primers. Dent Mater 5(6): 408-410.

Hashiguchi Y, Morino Y, Segawa T and Suzuki N (1976). Dental cement composition.

Hashimoto M, Ito S, Tay F R, Svizero N R, Sano H, Kaga M and Pashley D H (2004). Fluid movement across the resin-dentin interface during and after bonding. J Dent Res 83(11): 843-848.

Hebling J, Lessa F C, Nogueira I, Carvalho R M and Costa C A (2009). Cytotoxicity of resin-based light-cured liners. Am J Dent 22(3): 137-142.

Heintze S D, Thunpithayakul C, Armstrong S R and Rousson V (2011). Correlation between microtensile bond strength data and clinical outcome of Class V restorations. Dental materials: official publication of the Academy of Dental Materials 27(2): 114-125.

Hoffman A S (2001). Hydrogels for biomedical applications. Ann N Y Acad Sci 944: 62-73.

Hofmann N, Hugo B and Klaiber B (2002). Effect of irradiation type (LED or QTH) on photo-activated composite shrinkage strain kinetics, temperature rise, and hardness. Eur J Oral Sci 110(6): 471-479.

Huang F-M and Chang Y-C (2002). Cytotoxicity of resin-based restorative materials on human pulp cell cultures. Oral Surgery, Oral Medicine, Oral Pathology, Oral Radiology, and Endodontology 94(3): 361-365.

Huang F-M, Tai K-W, Chou M-Y and Chang Y-C (2002). Resinous Perforation-Repair Materials Inhibit the Growth, Attachment, and Proliferation of Human Gingival Fibroblasts. Journal of Endodontics 28(4): 291-294.

Huang F M and Chang Y C (2002). Cytotoxicity of resin-based restorative materials on human pulp cell cultures. Oral Surg Oral Med Oral Pathol Oral Radiol Endod 94(3): 361-365.

Huget E F (1998). Compressive properties of chemically cured, resin modified glass ionomer luting cements. J Tenn Dent Assoc 78(2): 20-23.

Hussey D L, Biagioni P A and Lamey P J (1995). Thermographic measurement of temperature change during resin composite polymerization in vivo. Journal of Dentistry 23(5): 267-271.

Ilie N and Hickel R (2007). Mechanical behavior of glass ionomer cements as a function of loading condition and mixing procedure. Dent Mater J 26(4): 526-533.

Ilie N, Hickel R, Valceanu A S and Huth K C (2012). Fracture toughness of dental restorative materials. Clin Oral Investig 16(2): 489-498.

Imazato S, Horikawa D, Takeda K, Kiba W, Izutani N, Yoshikawa R, Hayashi M, Ebisu S and Nakano T (2010). Proliferation and differentiation potential of pluripotent mesenchymal precursor C2C12 cells on resin-based restorative materials. Dent Mater Journal 29(3): 341-346.

Imbery T A, Namboodiri A, Duncan A, Amos R, Best A M and Moon P C (2013). Evaluating dentin surface treatments for resin-modified glass ionomer restorative materials. Oper Dent 38(4): 429-438.

Irie M, Maruo Y, Nishigawa G, Suzuki K and Watts D C (2010). Physical properties of dual-cured luting-agents correlated to early no interfacial-gap incidence with composite inlay restorations. Dent Mater 26(6): 608-615.

Irie M and Nakai H (1998). Flexural properties and swelling after storage in water of polyacid-modified composite resin (compomer). Dent Mater J 17(1): 77-82.

Irie M and Suzuki K (2000). Marginal seal of resin-modified glass ionomers and compomers: effect of delaying polishing procedure after one-day storage. Oper Dent 25(6): 488-496.

International Standardization Organization. ISO 4049:2009. Dentistry-polymer-based restorative materials. Geneva: ISO;2009.

International Standardization Organization.ISO (9917-1:2010). Dentistry -- Water-based Cements: Geneva: ISO;2010.

International Standardization Organization.ISO (9917-2:2010). Dentistry -- Water-based Cements-Resin modified materials: Geneva: ISO;2010.

Issa Y, Watts D C, Brunton P A, Waters C M and Duxbury A J (2004). Resin composite monomers alter MTT and LDH activity of human gingival fibroblasts in vitro. Dent Mater 20(1): 12-20.

Janke V, von Neuhoff N, Schlegelberger B, Leyhausen G and Geurtsen W (2003). TEGDMA causes apoptosis in primary human gingival fibroblasts. J Dent Res 82(10): 814-818.

Jefferies S, Loof J, Pameijer C H, Boston D, Galbraith C and Hermansson L (2013). Physical properties and comparative strength of a bioactive luting cement. Compend Contin Educ Dent 34 Spec No 8: 8-14.

Jonke E, Franz A, Freudenthaler J, Konig F, Bantleon H P and Schedle A (2008). Cytotoxicity and shear bond strength of four orthodontic adhesive systems. Eur J Orthod 30(5): 495-502.

Jyothi K, Annapurna S, Kumar A S, Venugopal P and Jayashankara C (2011). Clinical evaluation of giomer- and resin-modified glass ionomer cement in class V noncarious cervical lesions: An in vivo study. J Conserv Dent 14(4): 409-413.

Kakaboura A, Eliades G and Palaghias G (1996). An FTIR study on the setting mechanism of resin-modified glass ionomer restoratives. Dent Mater 12(3): 173-178.

Kalachandra S and Kusy R P (1991). Comparison of water sorption by methacrylate and dimethacrylate monomers and their corresponding polymers. Polymer 32(13): 2428-2434.

Kan K C, Messer L B and Messer H H (1997). Variability in cytotoxicity and fluoride release of resin-modified glass-ionomer cements. J Dent Res 76(8): 1502-1507.

Kanca J, 3rd (1992). Improving bond strength through acid etching of dentin and bonding to wet dentin surfaces. J Am Dent Assoc 123(9): 35-43.

Kanchanavasita W, Pearson G J and Anstice H M (1995). Influence of humidity on dimensional stability of a range of ion-leachable cements. Biomaterials 16(12): 921-929.

Kanchanavasita W, Pearson G J and Anstice H M (1996). Factors contributing to the temperature rise during polymerization of resin-modified glass-ionomer cements. Biomaterials 17(24): 2305-2312.

Kanie T, Kadokawa A, Nagata M and Arikawa H (2013). A comparison of stress relaxation in temporary and permanent luting cements. J Prosthodont Res 57(1): 46-50.

Karaoglanoglu S, Akg, Uuml, L N, Ouml, Zdabak H N and L H M (2009). Effectiveness of surface protection for glass-ionomer, resin-modified glass-ionomer and polyacid-modified composite resins. Dent Mater 28(1): 96-101.

Kerby R E and Knobloch L (1992). The relative shear bond strength of visible light-curing and chemically curing glass-ionomer cement to composite resin. Quintessence Int 23(9): 641-644.

Khoroushi M and Keshani F (2013). A review of glass-ionomers: From conventional glass-ionomer to bioactive glass-ionomer. Dental Research Journal 10(4): 411-420.

Kim S H and Watts D C (2004). Polymerization shrinkage-strain kinetics of temporary crown and bridge materials. Dent Mater 20(1): 88-95.

Kim Y K, Kim K-H and Kwon T-Y (2015). Setting Reaction of Dental Resin-Modified Glass Ionomer Restoratives as a Function of Curing Depth and Postirradiation Time. Journal of Spectroscopy 2015: 8.

Knobloch L A, Kerby R E, McMillen K and Clelland N (2000). Solubility and sorption of resin-based luting cements. Oper Dent 25(5): 434-440.

Koenig J (1984). Fourier transform infrared spectroscopy of polymers. Spectroscopy: NMR, Fluorescence, FT-IR, Springer Berlin Heidelberg. 54**:** 87-154.

Krifka S, Hiller K A, Spagnuolo G, Jewett A, Schmalz G and Schweikl H (2012). The influence of glutathione on redox regulation by antioxidant proteins and apoptosis in macrophages exposed to 2-hydroxyethyl methacrylate (HEMA). Biomaterials 33(21): 5177-5186.

Kumar N (2013). Inconsistency in the strength testing of dental resin-based composites among researchers. Pakistan Journal of Medical Sciences 29(1): 205-210.

Lad P P, Kamath M, Tarale K and Kusugal P B (2014). Practical clinical considerations of luting cements: A review. Journal of International Oral Health : JIOH 6(1): 116-120.

Lad P P, Kamath M, Tarale K and Kusugal P B (2014). Practical clinical considerations of luting cements: A review. J Int Oral Health 6(1): 116-120.

Ladha K and Verma M (2010). Conventional and contemporary luting cements: an overview. J Indian Prosthodont Soc 10(2): 79-88.

Lai J H and Johnson A E (1993). Measuring polymerization shrinkage of photo-activated restorative materials by a water-filled dilatometer. Dent Mater 9(2): 139-143.

Lan W H, Lan W C, Wang T M, Lee Y L, Tseng W Y, Lin C P, Jeng J H and Chang M C (2003). Cytotoxicity of conventional and modified glass ionomer cements. Oper Dent 28(3): 251-259.

Lee I-B, Cho B-H, Son H-H, Um C-M and Lim B-S (2006). The effect of consistency, specimen geometry and adhesion on the axial polymerization shrinkage measurement of light cured composites. Dent Mater 22(11): 1071-1079.

Leevailoj C, Platt J A, Cochran M A and Moore B K (1998). In vitro study of fracture incidence and compressive fracture load of all-ceramic crowns cemented with resin-modified glass ionomer and other luting agents. J Prosthet Dent 80(6): 699-707.

Leirskar J, Nordbø H, Mount G J and Ngo H (2003). The influence of resin coating on the shear punch strength of a high strength auto-cure glass ionomer. Dent Mater 19(2): 87-91.

Li J, Liu Y, Liu Y, Soremark R and Sundstrom F (1996). Flexure strength of resin-modified glass ionomer cements and their bond strength to dental composites. Acta Odontol Scand 54(1): 55-58.

Li Y, Lin H, Zheng G, Zhang X and Xu Y (2015). A comparison study on the flexural strength and compressive strength of four resin-modified luting glass ionomer cements. Biomed Mater Eng 26 Suppl 1: S9-17.

Li Y, Swartz M L, Phillips R W, Moore B K and Roberts T A (1985). Effect of filler content and size on properties of composites. J Dent Res 64(12): 1396-1401.

Li Z C and White S N (1999). Mechanical properties of dental luting cements. The Journal of Prosthetic Dentistry 81(5): 597-609.

Lim H N, Kim S H, Yu B and Lee Y K (2009). Influence of HEMA content on the mechanical and bonding properties of experimental HEMA-added glass ionomer cements. J Appl Oral Sci 17(4): 340-349.

Lloyd C H (1984). A differential thermal analysis (DTA) for the heats of reaction and temperature rises produced during the setting of tooth coloured restorative materials. J Oral Rehabil 11(2): 111-121.

Lloyd C H, Joshi A and McGlynn E (1986). Temperature rises produced by light sources and composites during curing. Dent Mater 2(4): 170-174.

Lohbauer U (2009). Dental Glass Ionomer Cements as Permanent Filling Materials? – Properties, Limitations and Future Trends. Materials 3(1): 76-96.

Lonnroth E C and Dahl J E (2003). Cytotoxicity of liquids and powders of chemically different dental materials evaluated using dimethylthiazol diphenyltetrazolium and neutral red tests. Acta Odontol Scand 61(1): 52-56.

Lovell L G, Lu H, Elliott J E, Stansbury J W and Bowman C N (2001). The effect of cure rate on the mechanical properties of dental resins. Dent Mater 17(6): 504-511.

Malacarne J, Carvalho R M, de Goes M F, Svizero N, Pashley D H, Tay F R, Yiu C K and Carrilho M R (2006). Water sorption/solubility of dental adhesive resins. Dent Mater 22(10): 973-980.

Malkoc S, Corekci B, Botsali H E, Yalçın M and Sengun A (2010). Cytotoxic effects of resin-modified orthodontic band adhesives. The Angle Orthodontist 80(5): 890-895.

Mallmann A, Ataide J C, Amoedo R, Rocha P V and Jacques L B (2007). Compressive strength of glass ionomer cements using different specimen dimensions. Braz Oral Res 21(3): 204-208.

Marchi J J, de Araujo F B, Froner A M, Straffon L H and Nor J E (2006). Indirect pulp capping in the primary dentition: a 4 year follow-up study. J Clin Pediatr Dent 31(2): 68-71.

Mathis R S and Ferracane J L (1989). Properties of a glass-ionomer/resin-composite hybrid material. Dent Mater 5(5): 355-358.

McCabe J F (1985). Cure performance of light-activated composites by differential thermal analysis (DTA). Dent Mater 1(6): 231-234.

McCabe J F (1998). Resin-modified glass-ionomers. Biomaterials 19(6): 521-527.

McCabe J F and Carrick T E (1986). A statistical approach to the mechanical testing of dental materials. Dent Mater 2(4): 139-142.

McCabe J F and Rusby S (2004). Water absorption, dimensional change and radial pressure in resin matrix dental restorative materials. Biomaterials 25(18): 4001-4007.

McCabe J F and Walls A (2009). Applied Dental Materials, USA: John Wiley and Sons.

McCabe J F and Walls A (2013). Applied Dental Materials, USA: John Wiley and Sons.

McCabe J F and Wilson H J (1980). The use of differential scanning calorimetry for the evaluation of dental materials. I. Cements, cavity lining materials and anterior restorative materials. J Oral Rehabil 7(2): 103-110.

McLean J W (1988). Glass-ionomer cements. Br Dent J 164(9): 293-300.

McLean J W (1992). Clinical applications of glass-ionomer cements. Oper Dent Suppl 5: 184-190.

McLean J W (1994). Evolution of glass-ionomer cements: a personal view. J Esthet Dent 6(5): 195-206.

McLean J W, Wilson A D and Prosser H J (1984). Development and use of water-hardening glass-ionomer luting cements. J Prosthet Dent 52(2): 175-181.

Melo de Mendonça A A, Chaves Souza P P, Hebling J and de Souza Costa C A (2007). Cytotoxic effects of hard-setting cements applied on the odontoblast cell line MDPC-23. Oral Surgery, Oral Medicine, Oral Pathology, Oral Radiology, and Endodontology 104(4): 102-e108.

Mendonça A A M d, Oliveira C F d, Hebling J and Costa C A d S (2012). Influence of thicknesses of smear layer on the transdentinal cytotoxicity and bond strength of a resin-modified glass-ionomer cement. Brazilian Dental Journal 23: 379-386.

Mese A, Burrow M F and Tyas M J (2008). Sorption and solubility of luting cements in different solutions. Dent Mater J 27(5): 702-709.

Meyer J M, Cattani-Lorente M A and Dupuis V (1998). Compomers: between glass-ionomer cements and composites. Biomaterials 19(6): 529-539.

Michelsen V B, Moe G, Strom M B, Jensen E and Lygre H (2008). Quantitative analysis of TEGDMA and HEMA eluted into saliva from two dental composites by use of GC/MS and tailor-made internal standards. Dent Mater 24(6): 724-731.

Mickenautsch S, Yengopal V and Banerjee A (2010). Pulp response to resin-modified glass ionomer and calcium hydroxide cements in deep cavities: A quantitative systematic review. Dent Mater 26(8): 761-770.

Milhem M M, Al-Hiyasat A S and Darmani H (2008). TOXICITY TESTING OF RESTORATIVE DENTAL MATERIALS USING BRINE SHRIMP LARVAE (ARTEMIA SALINA). Journal of Applied Oral Science 16(4): 297-301.

Milia E, Cumbo E, Cardoso R J and Gallina G (2012). Current dental adhesives systems. A narrative review. Curr Pharm Des 18(34): 5542-5552.

Mitra S and Mitra S B (1992). Universal water-based medical and dental cement.

Mitra S B (1991). Adhesion to dentin and physical properties of a light-cured glass-ionomer liner/base. J Dent Res 70(1): 72-74.

Mitra S B (1992). Photocurable ionomer cement systems.

Moharamzadeh K, Brook I and Van Noort R (2009). Biocompatibility of Resin-based Dental Materials. Materials 2(2): 514.

Moharamzadeh K, Van Noort R, Brook I M and Scutt A M (2007). HPLC analysis of components released from dental composites with different resin compositions using different extraction media. J Mater Sci Mater Med 18(1): 133-137.

Mohd Zainal Abidin R, Luddin N, Shamsuria Omar N and Mohamed Aly Ahmed H (2015). Cytotoxicity of Fast-set Conventional and Resin-modified Glass Ionomer Cement Polymerized at Different Times on SHED. J Clin Pediatr Dent 39(3): 235-240.

Momoi Y, Hirosaki K, Kohno A and McCabe J F (1995). Flexural properties of resin-modified "hybrid" glass-ionomers in comparison with conventional acid-base glass-ionomers. Dent Mater J 14(2): 109-119.

Moore D R and Turner S (2001). Mechanical Evaluation Strategies for Plastics, UK: Elsevier Science.

Moraes L G P, Rocha R S F, Menegazzo L M, de AraÚjo E B, Yukimitu K and Moraes J C S (2008). INFRARED SPECTROSCOPY: A TOOL FOR DETERMINATION OF THE DEGREE OF CONVERSION IN DENTAL COMPOSITES. Journal of Applied Oral Science 16(2): 145-149.

Mortier E, Gerdolle D A, Jacquot B and Panighi M M (2004). Importance of water sorption and solubility studies for couple bonding agent--resin-based filling material. Oper Dent 29(6): 669-676.

Moshaverinia A, Roohpour N, Chee W W L and Schricker S R (2011). A review of powder modifications in conventional glass-ionomer dental cements. Journal of Materials Chemistry 21(5): 1319-1328.

Mosmann T (1983). Rapid colorimetric assay for cellular growth and survival: application to proliferation and cytotoxicity assays. J Immunol Methods 65(1-2): 55-63.

Mount G J (1994). Glass ionomer cements and future research. Am J Dent 7(5): 286-292.

Mount G J, Patel C and Makinson O F (2002). Resin modified glass-ionomers: Strength, cure depth and translucency. Australian Dental Journal 47(4): 339-343.

Mulder R, Grobler S R and Osman Y I (2013). Volumetric change of flowable composite resins due to polymerization as measured with an electronic mercury dilatometer. Oral Biology and Dentistry 1(1).

Munksgaard E C, Hansen E K and Kato H (1987). Wall-to-wall polymerization contraction of composite resins versus filler content. Scand J Dent Res 95(6): 526-531.

Nakamura T, Wakabayashi K, Kinuta S, Nishida H, Miyamae M and Yatani H (2010). Mechanical properties of new self-adhesive resin-based cement. J Prosthodont Res 54(2): 59-64.

Nazhat S N, Parker S, Patel M P and Braden M (2001). Isoprene-styrene copolymer elastomer and tetrahydrofurfuryl methacrylate mixtures for soft prosthetic applications. Biomaterials 22(17): 2411-2416.

Neve A D, Piddock V and Combe E C (1992). Development of novel dental cements. I. Formulation of aluminoborate glasses. Clinical Materials 9(1): 7-12.

Neve A D, Piddock V and Combe E C (1993). The effect of glass heat treatment on the properties of a novel polyalkenoate cement. Clin Mater 12(2): 113-115.

Nicholson J W (1998). Chemistry of glass-ionomer cements: a review. Biomaterials 19(6): 485-494.

Nicholson J W and Anstice H M (1994). The Physical-Chemistry of Light-Curable Glass-Ionomers. J Mater Sci Mater Med 5(3): 119-122.

Nicholson J W, Anstice H M and McLean J W (1992). A preliminary report on the effect of storage in water on the properties of commercial light-cured glass-ionomer cements. Br Dent J 173(3): 98-101.

Nicholson J W, Brookman P J, Lacy O M and Wilson A D (1988). Fourier transform infrared spectroscopic study of the role of tartaric acid in glass-ionomer dental cements. J Dent Res 67(12): 1451-1454.

Nicholson J W and Croll T P (1997). Glass-ionomer cements in restorative dentistry. Quintessence Int 28(11): 705-714.

Nicholson J W and Czarnecka B (2007). Kinetic studies of the effect of varnish on water loss by glass-ionomer cements. Dent Mater 23(12): 1549-1552.

Nicholson J W and Czarnecka B (2008). The biocompatibility of resin-modified glass-ionomer cements for dentistry. Dent Mater 24(12): 1702-1708.

Nicholson J W and Czarnecka B (2008). Kinetic studies of water uptake and loss in glass-ionomer cements. J Mater Sci Mater Med 19(4): 1723-1727.

Nicholson J W, McKenzie M A, Goodridge R and Wilson A D (2001). Variations in the compressive strength of dental cements stored in ionic or acidic solutions. J Mater Sci Mater Med 12(7): 647-652.

Nicholson J W and Wilson A D (2000). The effect of storage in aqueous solutions on glass-ionomer and zinc polycarboxylate dental cements. J Mater Sci Mater Med 11(6): 357-360.

Nomoto R, Komoriyama M, McCabe J F and Hirano S (2004). Effect of mixing method on the porosity of encapsulated glass ionomer cement. Dent Mater 20(10): 972-978.

Ogawa T, Tanaka M, Matsuya S, Aizawa S and Koyano K (2001). Setting characteristics of five autopolymerizing resins measured by an oscillating rheometer. J Prosthet Dent 85(2): 170-176.

Oilo G (1991). Luting cements: a review and comparison. Int Dent J 41(2): 81-88.

Oliva A, Della Ragione F, Salerno A, Riccio V, Tartaro G, Cozzolino A, D'Amato S, Pontoni G and Zappia V (1996). Biocompatibility studies on glass ionomer cements by primary cultures of human osteoblasts. Biomaterials 17(13): 1351-1356.

Orimoto A, Suzuki T, Ueno A, Kawai T, Nakamura H and Kanamori T (2013). Effect of 2-hydroxyethyl methacrylate on antioxidant responsive element-mediated transcription: a possible indication of its cytotoxicity. PLoS One 8(3): e58907.

Oysaed H and Ruyter I E (1986). Composites for use in posterior teeth: mechanical properties tested under dry and wet conditions. J Biomed Mater Res 20(2): 261-271.

Palacios R P, Johnson G H, Phillips K M and Raigrodski A J (2006). Retention of zirconium oxide ceramic crowns with three types of cement. J Prosthet Dent 96(2): 104-114.

Palmer G, Anstice H M and Pearson G J (1999). The effect of curing regime on the release of hydroxyethyl methacrylate (HEMA) from resin-modified glass-ionomer cements. Journal of Dentistry 27(4): 303-311.

Palmer G, Anstice H M and Pearson G J (1999). The effect of curing regime on the release of hydroxyethyl methacrylate (HEMA) from resin-modified glass-ionomer cements. J Dent 27(4): 303-311.

Pameijer C H (2012). A review of luting agents. Int J Dent 2012: 752861.

Pameijer C H, Garcia-Godoy F, Morrow B R and Jefferies S R (2015). Flexural strength and flexural fatigue properties of resin-modified glass ionomers. J Clin Dent 26(1): 23-27.

Pamir T, Sen B H and Evcin O (2012). Effects of etching and adhesive applications on the bond strength between composite resin and glass-ionomer cements. J Appl Oral Sci 20(6): 636-642.

Pastila P, Lassila L V, Jokinen M, Vuorinen J, Vallittu P K and Mantyla T (2007). Effect of short-term water storage on the elastic properties of some dental restorative materials--A resonant ultrasound spectroscopy study. Dent Mater 23(7): 878-884.

Patel M P and Braden M (1991a). Heterocyclic methacrylates for clinical applications. III. Water absorption characteristics. Biomaterials 12(7): 653-657.

Patel M P and Braden M (1991b). Heterocyclic methacrylates for clinical applications. I. Mechanical properties. Biomaterials 12(7): 645-648.

Patel M P and Braden M (1991c). Heterocyclic methacrylates for clinical applications. II. Room temperature polymerizing systems for potential clinical use. Biomaterials 12(7): 649-652.

Patel M P, Braden M and Davy K W (1987). Polymerization shrinkage of methacrylate esters. Biomaterials 8(1): 53-56.

Patel M P, Johnstone M B, Hughes F J and Braden M (2001). The effect of two hydrophilic monomers on the water uptake of a heterocyclic methacrylate system. Biomaterials 22(1): 81-86.

Patil S G, Sajjan M S and Patil R (2015). The effect of temperature on compressive and tensile strengths of commonly used luting cements: an in vitro study. J Int Oral Health 7(2): 13-19.

Pearson G J and Atkinson A S (1987). Effects of temperature change on the working and setting characteristics of water-based dental cements. Dental Materials 3(5): 275-279.

Pearson G J, Picton D C, Braden M and Longman C (1986). The effects of two temporary crown materials on the dental pulp of monkeys (Macaca fascicularis). Int Endod J 19(3): 121-124.

Pedley D G, Skelly P J and Tighe B J (1980). Hydrogels in Biomedical Applications. Brit Polymer J 12(3): 99-110.

Percq A, Dubois D and Nicholson J W (2008). Water transport in resin-modified glass-ionomer dental cement. J Biomater Appl 23(3): 263-273.

Pinchuk L, Eckstein E C and Van De Mark M R (1984). Effects of low levels of methacrylic acid on the swelling behavior of poly(2-hydroxyethyl methacrylate). Journal of Applied Polymer Science 29(5): 1749-1760.

Pinchuk L, Eckstein E C and Van De Mark M R (1984). The interaction of urea with the generic class of poly(2-hydroxyethyl methacrylate) hydrogels. J Biomed Mater Res 18(6): 671-684.

Pitiyage G N, Slijepcevic P, Gabrani A, Chianea Y G, Lim K P, Prime S S, Tilakaratne W M, Fortune F and Parkinson E K (2011). Senescent mesenchymal cells accumulate in human fibrosis by a telomere-independent mechanism and ameliorate fibrosis through matrix metalloproteinases. J Pathol 223(5): 604-617.

Piwowarczyk A and Lauer H C (2003). Mechanical properties of luting cements after water storage. Oper Dent 28(5): 535-542.

Plasmans P J M M, Creugers N H J, Hermsen R J and Vrijhoef M M A (1994). Intraoral humidity during operative procedures. Journal of Dentistry 22(2): 89-91.

Pontes E C, Soares D G, Hebling J and Costa C A (2014). Cytotoxicity of resin-based luting cements to pulp cells. Am J Dent 27(5): 237-244.

Powers J M and Sakaguchi R L (2006). Craig's Restorative Dental Materials. Michigan: Mosby Elsevier.

Prosser H J, Powis D R and Wilson A D (1986). Glass-ionomer cements of improved flexural strength. J Dent Res 65(2): 146-148.

Qvist V (1993). Resin restorations: leakage, bacteria, pulp. Endod Dent Traumatol 9(4): 127-152.

Rao A (2008). Principles and Practice of Pedodontics. London: Jaypee Brothers Medical Publishers (P) Ltd.

Reis J M, Jorge E G, Ribeiro J G, Pinelli L A, Abi-Rached Fde O and Tanomaru-Filho M (2012). Radiopacity evaluation of contemporary luting cements by digitization of images. ISRN Dent 2012: 704246.

Rezk-Lega F, Ogaard B and Rolla G (1991). Availability of fluoride from glass-ionomer luting cements in human saliva. Scand J Dent Res 99(1): 60-63.

Ribeiro B C I, Boaventura J M C, de Brito-GonÇAlves J, Rastelli A N d S, Bagnato V S and Saad J R C (2012). Degree of conversion of nanofilled and microhybrid composite resins photo-activated by different generations of LEDs. Journal of Applied Oral Science 20(2): 212-217.

Riggs P D, Kinchesh P, Braden M and Patel M P (2001). Nuclear magnetic imaging of an osmotic water uptake and delivery process. Biomaterials 22(5): 419-427.

Riggs P D, Parker S, Braden M and Kalachandra S (2001). Development of novel elastomer/methacrylate monomer soft lining materials. J Mater Sci Mater Med 12(4): 359-364.

Ritter J E (1995). Predicting lifetimes of materials and material structures. Dental Materials 11(2): 142-146.

Rivera-Armenta J L, Martínez-Hernández A L, Mendoza-Martínez A M, Velasco-Santos C, Flores-Hernández C G and Angel-Aldana R Z D (2012). Evaluation of Graft Copolymerization of Acrylic Monomers Onto Natural Polymers by Means Infrared Spectroscopy, INTECH Open Access Publisher, from https://books.google.co.uk/books?id=wafSoAEACAAJ.

Robbins J W and Cooley R L (1988). Microleakage of Ketac-Silver in the tunnel preparation. Oper Dent 13(1): 8-11.

Rodriguez I A, Ferrara C A, Campos-Sanchez F, Alaminos M, Echevarria J U and Campos A (2013). An in vitro biocompatibility study of conventional and resin-modified glass ionomer cements. J Adhes Dent 15(6): 541-546.

Rodríguez O, Fornasiero F, Arce A, Radke C J and Prausnitz J M (2003). Solubilities and diffusivities of water vapor in poly(methylmethacrylate), poly(2-hydroxyethylmethacrylate), poly(N-vinyl-2-pyrrolidone) and poly(acrylonitrile). Polymer 44(20): 6323-6333.

Rogalewicz R, Batko K and Voelkel A (2006). Identification of organic extractables from commercial resin-modified glass-ionomers using HPLC-MS. J Environ Monit 8(7): 750-758.

Rosenstiel S F, Land M F and Crispin B J (1998). Dental luting agents: A review of the current literature. J Prosthet Dent 80(3): 280-301.

Rueggeberg F A and Caughman W F (1993). The influence of light exposure on polymerization of dual-cure resin cements. Oper Dent 18(2): 48-55.

Ryan A K, Mitchell C A and Orr J F (2002). Fracture mechanics analysis of the dentine-luting cement interface. Proc Inst Mech Eng H 216(4): 271-276.

Ryan A K, Orr J F and Mitchell C A (2001). A comparative evaluation of dental luting cements by fracture toughness tests and fractography. Proc Inst Mech Eng H 215(1): 65-73.

Saskalauskaite E, Tam L E and McComb D (2008). Flexural strength, elastic modulus, and pH profile of self-etch resin luting cements. J Prosthodont 17(4): 262-268.

Sawtell R M, Downes S, Patel M P, Clarke R L and Braden M (1997). Heterocyclic methacrylates for clinical applications-further studies of water sorption. J Mater Sci Mater Med 8(11): 667-674.

Sced I and Wilson A (1980). Hardenable compositions.

Scheerer E W, Swartz M L, Norman R D and Phillips R W (1964). RESIDUAL MONOMER OF RESTORATIVE RESINS. J Dent Res 43: 672-677.

Schmalz G (1994). Use of cell cultures for toxicity testing of dental materials--advantages and limitations. J Dent 22 Suppl 2: S6-11.

Schmalz G, Schuster U, Koch A and Schweikl H (2002). Cytotoxicity of low pH dentin-bonding agents in a dentin barrier test in vitro. J Endod 28(3): 188-192.

Schmid-Schwap M, Franz A, Konig F, Bristela M, Lucas T, Piehslinger E, Watts D C and Schedle A (2009). Cytotoxicity of four categories of dental cements. Dent Mater 25(3): 360-368.

Schuster U, Schmalz G, Thonemann B, Mendel N and Metzl C (2001). Cytotoxicity testing with three-dimensional cultures of transfected pulp-derived cells. J Endod 27(4): 259-265.

Schweikl H, Spagnuolo G and Schmalz G (2006). Genetic and cellular toxicology of dental resin monomers. J Dent Res 85(10): 870-877.

Scott A, Egner W, Gawkrodger D J, Hatton P V, Sherriff M, van Noort R, Yeoman C and Grummitt J (2004). The national survey of adverse reactions to dental materials in the UK: a preliminary study by the UK Adverse Reactions Reporting Project. Br Dent J 196(8): 471-477; discussion 465.

Scoville R K, Foreman F and Burgess J O (1990). In vitro fluoride uptake by enamel adjacent to a glass ionomer luting cement. ASDC J Dent Child 57(5): 352-355.

Selby A, Maldonado-Codina C and Derby B (2013). Influence of specimen thickness on the nanoindentation of hydrogels: Measuring the mechanical properties of soft contact lenses. J Mech Behav Biomed Mater.

Selimovic-Dragas M, Hasic-Brankovic L, Korac F, Dapo N, Huseinbegovic A, Kobaslija S, Lekic M and Hatibovic-Kofman S (2013). In vitro fluoride release from a different kind of conventional and resin modified glass-ionomer cements. Bosn J Basic Med Sci 13(3): 197-202.

Shammaa I, Ngan P, Kim H, Kao E, Gladwin M, Gunel E and Brown C (1999). Comparison of bracket debonding force between two conventional resin adhesives and a resin-reinforced glass ionomer cement: an in vitro and in vivo study. Angle Orthod 69(5): 463-469.

Sideridou I D, Karabela M M and Vouvoudi E (2008). Volumetric dimensional changes of dental light-cured dimethacrylate resins after sorption of water or ethanol. Dent Mater 24(8): 1131-1136.

Sidhu S K and Schmalz G (2001). The biocompatibility of glass-ionomer cement materials. A status report for the American Journal of Dentistry. Am J Dent 14(6): 387-396.

Sidhu S K and Watson T F (1995). Resin-modified glass ionomer materials. A status report for the American Journal of Dentistry. Am J Dent 8(1): 59-67.

Sidhu S K and Watson T F (1998). Interfacial characteristics of resin-modified glass-ionomer materials: a study on fluid permeability using confocal fluorescence microscopy. J Dent Res 77(9): 1749-1759.

Simmons J J (1983). The miracle mixture. Glass ionomer and alloy powder. Tex Dent J 100(10): 6-12.

Sindel J, Frankenberger R, Kramer N and Petschelt A (1999). Crack formation of all-ceramic crowns dependent on different core build-up and luting materials. J Dent 27(3): 175-181.

Small I C, Watson T F, Chadwick A V and Sidhu S K (1998). Water sorption in resin-modified glass-ionomer cements: an in vitro comparison with other materials. Biomaterials 19(6): 545-550.

Smith D C (1998). Development of glass-ionomer cement systems. Biomaterials 19(6): 467-478.

Snyder M D, Lang B R and Razzoog M E (2003). The efficacy of luting all-ceramic crowns with resin-modified glass ionomer cement. J Am Dent Assoc 134(5): 609-612.

Souza P P C, Aranha A M F, Hebling J, Giro E M A and Costa C A d S (2006). In vitro cytotoxicity and in vivo biocompatibility of contemporary resin-modified glass-ionomer cements. Dent Mater 22(9): 838-844.

Stafford G D and Braden M (1968). Water Absorption of Some Denture Base Polymers. Journal of Dental Research 47(2): 341.

Stanislawski L, Daniau X, Lauti A and Goldberg M (1999). Factors responsible for pulp cell cytotoxicity induced by resin-modified glass ionomer cements. J Biomed Mater Res 48(3): 277-288.

Stansbury J W, Trujillo-Lemon M, Lu H, Ding X, Lin Y and Ge J (2005). Conversion-dependent shrinkage stress and strain in dental resins and composites. Dent Mater 21(1): 56-67.

Stepanian S G, Reva I D, Radchenko E D and Sheina G G (1996). Infrared spectra of benzoic acid monomers and dimers in argon matrix. Vibrational Spectroscopy 11(2): 123-133.

Sun J, Weng Y, Song F and Xie D (2011). In-Vitro Cellular Responses of Human Dental Primary Cells to Dental Filling Restoratives. Journal of Biomaterials and Nanobiotechnology 2: 267-280.

Sunico-Segarra M and Segarra A (2014). A Practical Clinical Guide to Resin Cements. New York: Springer.

Szep S, Kunkel A, Ronge K and Heidemann D (2002). Cytotoxicity of modern dentin adhesives--in vitro testing on gingival fibroblasts. J Biomed Mater Res 63(1): 53-60.

Tam L E, McComb D and Pulver F (1991). Physical properties of proprietary light-cured lining materials. Oper Dent 16(6): 210-217.

Tay F R, Gwinnett J A and Wei S H (1996). Micromorphological spectrum from overdrying to overwetting acid-conditioned dentin in water-free acetone-based, single-bottle primer/adhesives. Dent Mater 12(4): 236-244.

ten Cate J M and van Duinen R N (1995). Hypermineralization of dentinal lesions adjacent to glass-ionomer cement restorations. J Dent Res 74(6): 1266-1271.

Thomas A G and Muniandy K (1987). Absorption and desorption of water in rubbers. Polymer 28(3): 408-415.

Thomas N L and Windle A H (1982). A theory of case II diffusion. Polymer 23(4): 529-542.

Thornton J B, Retief D H and Bradley E L (1986). Fluoride release from and tensile bond strength of Ketac-fil and ketac-silver to enamel and dentin. Dent Mater 2(6): 241-245.

Toledano M, Osorio R, Osorio E, Fuentes V, Prati C and Garcia-Godoy F (2003). Sorption and solubility of resin-based restorative dental materials. J Dent 31(1): 43-50.

Tolidis K, Nobecourt A and Randall R C (1998). Effect of a resin-modified glass ionomer liner on volumetric polymerization shrinkage of various composites. Dent Mater 14(6): 417-423.

Trumpaite-Vanagiene R, Bukelskiene V, Aleksejuniene J, Puriene A, Baltriukiene D and Rutkunas V (2015). Cytotoxicity of commonly used luting cements -An in vitro study. Dent Mater J 34(3): 294-301.

Uno S, Finger W J and Fritz U (1996). Long-term mechanical characteristics of resin-modified glass ionomer restorative materials. Dent Mater 12(1): 64-69.

Uzzaman M A, Shimada Y, Seki Y and Tagami J (2005). Pulpal response to a hybrid composite resin inlay bonded with a newly developed resin-modified glass ionomer luting cement. Dent Mater J 24(2): 178-186.

Valanezhad A, Odatsu T, Udoh K, Shiraishi T, Sawase T and Watanabe I (2016). Modification of resin modified glass ionomer cement by addition of bioactive glass nanoparticles. J Mater Sci Mater Med 27(1): 3.

van Dijken J W (2000). Direct resin composite inlays/onlays: an 11 year follow-up. J Dent 28(5): 299-306.

Van Landuyt K L, Nawrot T, Geebelen B, De Munck J, Snauwaert J, Yoshihara K, Scheers H, Godderis L, Hoet P and Van Meerbeek B (2011). How much do resin-based dental materials release? A meta-analytical approach. Dent Mater 27(8): 723-747.

Van Nieuwenhuysen J P, D'Hoore W, Carvalho J and Qvist V (2003). Long-term evaluation of extensive restorations in permanent teeth. J Dent 31(6): 395-405.

Vande Vannet B M and Hanssens J L (2007). Cytotoxicity of two bonding adhesives assessed by three-dimensional cell culture. Angle Orthod 77(4): 716-722.

Wan Q, Rumpf D, Schricker S R, Mariotti A and Culbertson B M (2001). Influence of hyperbranched multi-methacrylates for dental neat resins on proliferation of human gingival fibroblasts. Biomacromolecules 2(1): 217-222.

Wanachottrakul N, Chotigeat W and Kedjarune-Leggat U (2014). Effect of novel chitosan-fluoroaluminosilicate resin modified glass ionomer cement supplemented with translationally controlled tumor protein on pulp cells. J Mater Sci Mater Med 25(4): 1077-1085.

Wang L, D'Alpino P H, Lopes L G and Pereira J C (2003). Mechanical properties of dental restorative materials: relative contribution of laboratory tests. J Appl Oral Sci 11(3): 162-167.

Watanabe F, Powers J M and Lorey R E (1988). In vitro bonding of prosthodontic adhesives to dental alloys. J Dent Res 67(2): 479-483.

Watts D C and Cash A J (1991). Determination of polymerization shrinkage kinetics in visible-light-cured materials: methods development. Dent Mater 7(4): 281-287.

Watts D C and Hindi A A (1999). Intrinsic 'soft-start' polymerisation shrinkage-kinetics in an acrylate-based resin-composite. Dent Mater 15(1): 39-45.

Watts D C and Marouf A S (2000). Optimal specimen geometry in bonded-disk shrinkage-strain measurements on light-cured biomaterials. Dent Mater 16(6): 447-451.

Willershausen B, Schafer D, Pistorius A, Schulze R and Mann W (1999). Influence of resin-based restoration materials on cytotoxicity in gingival fibroblasts. Eur J Med Res 4(4): 149-155.

Williams D F (1987). Definitions in biomaterials: proceedings of a consensus conference of the European Society for Biomaterials, Chester, England: Elsevier,

Wilson A, Crisp S, Prosser H J, Lewis B G and Merson S A (1980). Aluminosilicate glasses for polyelectrolyte cements. Industrial and Engineering Chemistry Product Research Development. 19: 263-270.

Wilson A and Nicholson J W (1993). Acid-Base Cements: Their Biomedical and Industrial Applications Cambridge: Cambridge University Press.

Wilson A D (1990). Resin-modified glass-ionomer cements. Int J Prosthodont 3(5): 425-429.

Wilson A D, Crisp S and Abel G (1977). Characterization of glass-ionomer cements 4. Effect of molecular weight on physical properties. Journal of Dentistry 5(2): 117-120.

Wilson A D, Groffman D M and Kuhn A T (1985). The release of fluoride and other chemical species from a glass-ionomer cement. Biomaterials 6(6): 431-433.

Wilson A D, Hill R G, Warrens C P and Lewis B G (1989). The influence of polyacid molecular weight on some properties of glass-ionomer cements. J Dent Res 68(2): 89-94.

Wilson A D and Kent B E (1972). A new translucent cement for dentistry. The glass ionomer cement. Br Dent J 132(4): 133-135.

Wilson A D and McLean J W (1988). Glass-ionomer cement. Michigan: Quintessence Pub. Co.

Wilson A D and Nicholson J W (2005). Acid-Base Cements: Their Biomedical and Industrial Applications. Cambridge: Cambridge University Press.

Wilson A D, Paddon J M and Crisp S (1979). The hydration of dental cements. J Dent Res 58(3): 1065-1071.

Wilson A D and Prosser H J (1982). Biocompatibility of the glass ionomer cement. J Dent Assoc S Afr 37(12): 872-879.

Wilson A D, Prosser H J and Powis D M (1983). Mechanism of adhesion of polyelectrolyte cements to hydroxyapatite. J Dent Res 62(5): 590-592.

Xie D, Brantley W A, Culbertson B M and Wang G (2000). Mechanical properties and microstructures of glass-ionomer cements. Dent Mater 16(2): 129-138.

Xie D, Chung I L D, Wu W and Mays J (2004). Synthesis and evaluation of HEMA-free glass–ionomer cements for dental applications. Dent Mater 20(5): 470-478.

Xu J, Stangel I, Butler I S and Gilson D F (1997). An FT-Raman spectroscopic investigation of dentin and collagen surfaces modified by 2-hydroxyethylmethacrylate. J Dent Res 76(1): 596-601.

Yamazaki T, Schricker S R, Brantley W A, Culbertson B M and Johnston W (2006). Viscoelastic behavior and fracture toughness of six glass-ionomer cements. J Prosthet Dent 96(4): 266-272.

Yan Y L, Kim Y K, Kim K H and Kwon T Y (2010). Changes in degree of conversion and microhardness of dental resin cements. Oper Dent 35(2): 203-210.

Yap A and Lee C M (1997). Water sorption and solubility of resin-modified polyalkenoate cements. J Oral Rehabil 24(4): 310-314.

Yap A U J (1996). Resin-modified glass ionomer cements: a comparison of water sorption characteristics. Biomaterials 17(19): 1897-1900.

Yelamanchili A and Darvell B W (2008). Network competition in a resin-modified glass-ionomer cement. Dent Mater 24(8): 1065-1069.

Yoon T H, Lee Y K, Lim B S and Kim C W (2002). Degree of polymerization of resin composites by different light sources. J Oral Rehabil 29(12): 1165-1173.

Yoshii E (1997). Cytotoxic effects of acrylates and methacrylates: relationships of monomer structures and cytotoxicity. J Biomed Mater Res 37(4): 517-524.

Young A M (2002). FTIR investigation of polymerisation and polyacid neutralisation kinetics in resin-modified glass-ionomer dental cements. Biomaterials 23(15): 3289-3295.

Young A M, Rafeeka S A and Howlett J A (2004). FTIR investigation of monomer polymerisation and polyacid neutralisation kinetics and mechanisms in various aesthetic dental restorative materials. Biomaterials 25(5): 823-833.

Young A M, Sherpa A, Pearson G, Schottlander B and Waters D N (2000). Use of Raman spectroscopy in the characterisation of the acid-base reaction in glass-ionomer cements. Biomaterials 21(19): 1971-1979.

Yourtee D M, Smith R E, Russo K A, Burmaster S, Cannon J M, Eick J D and Kostoryz E L (2001). The stability of methacrylate biomaterials when enzyme challenged: kinetic and systematic evaluations. J Biomed Mater Res 57(4): 522-531.

Zach L and Cohen G (1965). Pulp Response to Externally Applied Heat. Oral Surg Oral Med Oral Pathol 19: 515-530.

Zhang L, Tang T, Zhang Z L, Liang B, Wang X M and Fu B P (2013). Improvement of enamel bond strengths for conventional and resin-modified glass ionomers: acid-etching vs. conditioning. J Zhejiang Univ Sci B 14(11): 1013-1024.

Zimmerli B, Strub M, Jeger F, Stadler O and Lussi A (2010). Composite materials: composition, properties and clinical applications. A literature review. Schweiz Monatsschr Zahnmed 120(11): 972-986.

APPENDICES

9.1 *Appendix 1: Excluded Compositions*

Table 9.1 show the sixteen compositions that were excluded from this project due to phase separation:

Table 9.1 Sixteen compositions excluded from project due to phase separation including the compositions number and % weight of each component.

Composition Number	Water %	PAA %	Tartaric acid %	UDMA %	THFM %	HPM %	HEMA %	Ethyl acetate %
9	35	30	5	0	29	0	0	1
10	35	30	5	0	20.3	0	8.7	1
11	35	30	5	0	14.5	14.5	0	1
12	30	30	5	5	30	0	0	0
13	30	30	5	5	21	0	9	0
14	30	30	5	5	15	0	15	0
15	30	30	5	5	15	0	15	0
16	30	30	5	5	9	0	21	0
17	30	30	5	5	0	30	0	0
18	30	30	5	5	9	21	0	0
19	30	30	5	5	14.5	0	14.5	1
20	30	30	5	5	8.7	20.3	0	1
21	30	30	5	4	31	0	0	0
22	35	30	5	0	29	0	0	1
23	35	30	5	0	14.5	14.5	0	1
24	30	30	5	4	15.5	15.5	0	0

9.2 *Appendix 2: Published Manuscript*

DENTAL MATERIALS XXX (2016) XXX–XXX

Available online at www.sciencedirect.com

ScienceDirect

journal homepage: www.intl.elsevierhealth.com/journals/dema

Development of experimental resin modified glass ionomer cements (RMGICs) with reduced water uptake and dimensional change

Amani Agha, Sandra Parker, Mangala P. Patel*

Oral Growth and Development, (Dental Physical Sciences), Institute of Dentistry, Barts and the London School of Medicine and Dentistry, Queen Mary, University of London, London, United Kingdom

ARTICLE INFO

Article history:
Received 23 July 2015
Received in revised form
20 December 2015
Accepted 10 March 2016
Available online xxx

Keywords:
Resin modified glass ionomer
Water uptake
Monomer
Desorption
Diffusion coefficient
Solubility
2-Hydroxyethyl methacrylate
Tetrahydrofurfuryl methacrylate

ABSTRACT

Objective. To investigate water uptake, desorption, diffusion coefficient, solubility and dimensional changes of four experimental RMGICs in deionized water (DW) and artificial saliva (AS), and compare with two commercial RMGICs and control home liquids based on the two commercial materials used.

Methods. Two commercial RMGICs, RelyX Luting (RX, 3M ESPE) and Fuji Plus (FP, GC), two control home liquids and four new liquid compositions (F1, F2, R1, R2) comprising different percentages of the monomer THFM (tetrahydrofurfuryl-methacrylate) with the original monomer HEMA (2-hydroxyethyl-methacrylate) were used in this study. Home and experimental liquids were mixed with the corresponding commercial powder. Disk-shaped specimens (16 mm diameter 1 mm thickness) were immersed in DW/AS at 37 C ($n = 6$) and weighed at regular time intervals. Percentage weight change with time was recorded. At 24 weeks, disks were desorbed in an oven at 37 C to minimum weight.

Results. All new compositions showed lower water uptake and dimensional (volume) changes than the commercial products in both DW and AS. On desorption, FP showed higher weight loss compared to materials in the same group in both solutions ($p < 0.0001$), with the exception of F2 in DW ($p = 0.283$). RX had higher weight loss compared to R1 and R2 in DW and AS ($p < 0.0001$). Fickian diffusion was confirmed for all materials immersed in DW and AS.

Significance. The experimental compositions in this study have shown promising results when tested in both DW and AS with lower water uptakes and volume changes than commercial materials. This may lead to wider applications than current commercial materials.

* *Corresponding author at*: Dental Physical Sciences, (Oral Growth and Development), Francis Bancroft Building, (2nd Floor), Queen Mary, University of London, Mile End Road, London E1 4NS, United Kingdom. Tel.: +44 020 7882 5966; fax: +44 020 7882 7979.
E-mail address: amany_ma@hotmail.com (A. Agha).

http://dx.doi.org/10.1016/j.dental.2016.03.004
0109-5641/

Please cite this article in press as: Agha A, et al. Development of experimental resin modified glass ionomer cements (RMGICs) with reduced water uptake and dimensional change. Dent Mater (2016), http://dx.doi.org/10.1016/j.dental.2016.03.004

1. Introduction

Glass ionomer cements (GICs) were introduced by Wilson and Kent in 1972 [1] and were first called glass polyalkenoate cements containing a degradable glass and a polymeric acid (poly(alkenoic acid)), e.g. poly(acrylic acid) [2]. The term GIC has been adopted by clinicians although it does not describe accurately their chemical composition [2]. GIC (also called conventional GIC) is best defined by McLean [2] as 'a cement that consists of basic glass and an acidic polymer, which sets by an acid–base reaction between these components'.

Conventional GICs possess many advantages such as good chemical adhesion to tooth substance [3], fluoride release and caries inhibition [4], do not undergo polymerization shrinkage nor produce an exotherm during setting [3,5,6]. However, a number of limitations are associated with GICs as they are more susceptible to wear and abrasion, they possess low flexure strength and low modulus of elasticity, resulting in them being brittle and more 'prone to fracture' [7,8]. Another disadvantage of GICs is their moisture sensitivity especially during the setting reaction and more importantly within the first 24 h of application (maturation phase) [9]. If water is lost, then the setting reaction will be disrupted and this will subsequently affect the cement's physical and mechanical properties [10].

Different approaches have been suggested and tested to overcome GIC's weaknesses. One proposal included preparation of novel glasses with the addition of 'dispersed-phases of crystallites'. These materials included the addition of large amounts of reinforcing crystals, e.g. corundum (Al_2O_3), rutile (TiO_2), baddeleyite (ZrO_2) and tielite (Al_2TiO_5) [11]. These modifications showed improved flexural strength compared to conventional GIC, but with the other problems, e.g. sensitivity to moisture remaining the same [12].

A second suggestion was incorporation of different fibers (alumina, glass, carbon and silica) in the cement powder to enhance the flexural strength. However, in order to enhance the strength efficiently, the fibers needed to be added in large quantities, which adversely affected the handling properties [12].

Addition of metal fibers to conventional GIC was patented by Sced and Wilson [13]. The benefit of this material is the increased flexural strength of the set cement. Simmons [14] introduced the 'miracle mixture' in 1983, which involved the addition of amalgam alloy powder to the cement. Although these new compositions resulted in a set cement with improved flexural strength and abrasion resistance, they lacked in esthetics and they had lower bond strengths to enamel and dentin [15] than conventional GICs, which led to more micro-leakage [16]. Modifying the particle size and distribution of the GIC glass powder was found to improve mechanical properties and reduce the early sensitivity to moisture, but the esthetics and the translucency of the set cement were compromised [17,18].

All the above compositions and improvements did not solve two important problems associated with conventional GIC, sensitivity to moisture and 'lack of command cure' [19]. In order to solve these problems, the incorporation of a resin system into the GIC cement was introduced, to provide a material that incorporates the advantages of a resin (e.g. improved strength) with the improved properties of GICs [20]. This was first mentioned in a patent application in 1988 [21] and it was introduced as a new development by Mitra in 1989 [22]. Since then these cements have been further developed into a range of what we now know as resin modified glass ionomer cements (RMGICs). This type of cement incorporates two setting mechanisms: the conventional acid–base reaction and polymerization of the resin monomer, where polymerization can be either light or chemically activated [23]. These materials have the same composition as conventional GICs, with the incorporation of poly(acrylic acid) or co-polymer of poly(acrylic acid) and other alkenoic acids, but the difference in RMGIC is the addition of a polymerizable resin monomer, commonly 2-hydroxyethyl methacrylate (HEMA). HEMA also works as a 'co-solvent' in order to keep all the components in one phase [20,24].

HEMA, as a hydrophilic monomer, plays an important role in the water uptake of RMGIC from the oral environment. A 'mild hydrogel' behavior has been associated with these cements [25]. According to literature, hydrogels based on HEMA monomer are linked with high water uptake, which was reported to reach 80% by mass [26]. Consequently, a higher amount of HEMA in the material correlated to higher water sorption [27] and associated swelling of the RMGIC resin matrix [28,29]. Different problems, e.g. plasticization and weakening of the cement have been linked to the water uptake of RMGICs [30,31]. Cattani-Lorente et al. [32] reported that RMGIC samples immersed in water, or in a humid environment for 24 h to three months, showed lower physical properties (flexure strength and hardness) compared to those stored in dry conditions; therefore, they correlated the decrease in the strength to the water uptake of RMGICs [32]. A decrease in compressive and flexure strength following immersion in distilled water for 24 h and 150 days was also reported by Piwowarczyk and Lauer [33].

The aforementioned weaknesses of RMGICs have been attributed to the high water uptake of the RMGIC and this is reported to be correlated with the HEMA monomer [34–36] due to its hydrophilic nature. With increased water sorption (e.g. in a clinical situation, where the restoration is not coated), the polymer matrix tends to be more 'flexible' and the physical properties of the material are adversely affected [37]. The release of residual unreacted HEMA from the material has reduced biocompatibility where HEMA has been associated with both apoptosis and cell necrosis. The effects on cells were tested in vitro and the damage was seen in the cells that were exposed to the monomer [38]. As an attempt to overcome the cytotoxicity of the material, Xie et al. [39] introduced HEMA free RMGIC where they replaced HEMA with acrylate and methacrylate derivatives of amino acids. The authors [39] reported that the new cement demonstrated improved mechanical properties compared to commercial products but did not seem to demonstrate the water uptake behavior of the new cement.

One of the possible alternative monomers to be used in RMGICs is tetrahydrofurfuryl methacrylate (THFM). THFM is a heterocyclic, hydrophobic monomer that has been patented for different potential biomedical applications such as temporary crown and bridge materials [40], fluoride releasing biomaterials [41], and as a tissue repair material [42]. This

Please cite this article in press as: Agha A, et al. Development of experimental resin modified glass ionomer cements (RMGICs) with reduced water uptake and dimensional change. Dent Mater (2016), http://dx.doi.org/10.1016/j.dental.2016.03.004

monomer was also mentioned in patents concerning RMGICs [43,44]. Mitra [43] included it in the description and as one of the various choices that could be used in RMGICs, but did not include any examples or evidence of utilizing or testing the monomer. Anstice et al. [44] included several examples of using THFM in RMGIC but without reporting on water uptake or desorption data. Moreover, they utilized THFM with different percentages of other monomers, and replaced all the HEMA in the cement.

THFM was studied with poly(ethyl methacrylate) (PEM), forming a low shrinkage, room temperature polymerizing system [45–47]. The molar volume of THFM itself is high compared to methyl methacrylate (MMA), and this contributes to its low polymerization shrinkage [45]. This characteristic was advantageous for potentially improving the fit of hearing aids [47].

Materials comprising room-temperature polymerizing PEM/THFM presented with a low polymerization exotherm and adequate mechanical properties for potential clinical use [45,46,48,49]. Earlier water uptake data from distilled water for this system was reported to be ~34% over two years, which was reduced to <3% in solutions like artificial saliva (AS) and phosphate buffered saline (PBS) [50,51]. The mechanism of the water absorption process is reported to be in two stages; an initial Fickian stage until the matrix is saturated (<3%), followed by a second stage involving clusters/droplets being formed at hydrophilic/water soluble sites (e.g. clustering of the furfuryl rings or droplets formed around water soluble additives or impurities [51–53], indicating that the water uptake process is osmotically driven. On replacing part of the THFM monomer with HEMA (50:50) in the PEM/THFM room temperature polymerizing system resulted in an increased polymerization exotherm. Also its water absorption behavior was modified, due to suppression of the secondary uptake process (clustering) in the PEM/THFM system [54], and this was accompanied with increased diffusion coefficients.

Hence, the aims/objectives of this study were to:

Develop experimental RMGIC liquids by replacing the monomer HEMA partially with different percentages of THFM, but using them with the powder of commercial products.

Investigate water uptake, desorption, solubility and dimensional (volume) changes of commercial, home and experimental RMGICs.

2. Materials and methods

2.1. Materials

Two chemically cured RMGICs were included in this study, namely Fuji Plus (GC Corporation, Tokyo, Japan) and RelyX Luting (3M ESPE, St Paul, MN, USA). The two cements were supplied as separate powder and liquid components. The powder in both cements contained fluoroalumino-silicate glass and a redox system consisting of potassium persulfate and ascorbic acid capable of initiating polymerization chemically in the absence of light. The liquid in the two materials consisted mainly of water, acrylic acid, 2-hydroxyethyl methacrylate (HEMA) and tartaric acid (Table 1).

Two additional control (home) liquids were prepared in house based on the commercial liquids as given in the manufacturer's safety data sheets (MSDS). Since it was not possible to determine the exact compositions of each product from the manufacturers, different percentages were tried and tested to match the commercial liquids. Home liquids were formulated and characterized using Fourier Transform Infrared Spectroscopy (FTIR) and compared with the commercial liquids. The final compositions of the home liquids are presented in Table 2. Commercial and home liquids were stored in a cool dry place between 4 and 6 °C.

Four experimental liquid formulations were prepared, two based on each of the commercial products (RX, FP), where HEMA was replaced with either 70%/30% THFM/HEMA in F2 and R2 or 50%/50% THFM/HEMA in F1 and R1. Attempts were made to replace all the HEMA in the liquid composition with 100% THFM but, as THFM is a hydrophobic monomer, it showed phase separation on mixing with water; thus there was a need for the THFM to be combined with HEMA to avoid this separation.

Table 1 – Components of commercial materials (FP – Fuji Plus and RX – RelyX Luting) with CAS number, percentage of components and manufacturers recommended mixing ratio.

RMGIC	Composition	CAS number	Percentage of components (by weight)	Powder: liquid mixing ratio
FP powder	Fluoroalumino-silicate glass	Not listed	95–100	2
FP liquid	Distilled water	7732-18-5	20–30	1
	Poly(acrylic acid)	9003-01-4	20–30	
	HEMA	868-77-9	25–35	
	Urethanedimethacrylate (UDMA)	72869-86-4	<10	
	Tartaric acid	87-69-4	5–7	
RX powder	Fluoroalumino-silicate glass	Not listed	>98	1.6
	Potassium persulfate	7727-21-1	≤0.2	
RX liquid	Water	7732-18-5	30–40	1
	Copolymer of acrylic and itaconic acids	25948-33-8	30–40	
	HEMA	868-77-9	25–35	
	Ethyl acetate	141-78-6	<2	
	Tartaric acid	Not listed	Not listed	

Please cite this article in press as: Agha A, et al. Development of experimental resin modified glass ionomer cements (RMGICs) with reduced water uptake and dimensional change. Dent Mater (2016), http://dx.doi.org/10.1016/j.dental.2016.03.004

Table 2 – Liquid compositions of the two in-house materials with the corresponding CAS number and percentage of each component.

RMGIC	Composition	CAS number	Percentage of components (by weight)
FP in-house liquid	Distilled water	7732-18-5	30
	Poly(acrylic acid)	9003-01-4	30
	HEMA	868-77-9	31
	Urethanedimethacrylate (UDMA)	72869-86-4	4
	Tartaric acid	87-69-4	5
RX in-house liquid	Water	7732-18-5	35
	Poly(acrylic acid)	9003-01-4	30
	HEMA	868-77-9	29
	Ethyl acetate	141-78-6	1
	Tartaric acid	87-69-4	5

2.2. *Immersion media*

Deionized water (DW) and artificial saliva (AS) were used as immersion media. AS used was Orthano Saliva supplied by A.S. Pharma Ltd., UK. (components are given in Table 3; pH of AS was 6.5).

2.3. *Methods*

2.3.1. *Sample preparation*

Twelve discs were prepared for each material, six immersed in DW and six in AS. Mixing and preparing the samples was performed according to the manufacturer's instructions and the manufacturers recommended powder: liquid mixing ratio by weight (2:1 g:g for FP group and 1.6:1 for RX group) (Table 1). The components were mixed on a glass slab with a stainless-steel spatula at room temperature. Two discs were prepared at a time using polytetrafluoroethylene (PTFE) molds with internal dimensions of 16 mm ± 0.1 mm diameter and 1.0 ± 0.1 mm depth. The molds were placed on a glass microscope slide covered with an acetate sheet and were slightly over filled with the mixed materials; another acetate sheet and glass microscope slide was placed on top of the material while applying pressure manually to remove excess material. This assembly was clamped together with a bulldog clip in order to keep the samples in place and eliminate entrapment of air bubbles. Samples were left to set in an oven (Carbolite, Camlab, Cambridge, UK) at 37 ± 1 °C for 1 h. Following removal from the oven and molds, each specimen underwent visual examination to check for internal porosities or defects and any with porosities or imperfections were discarded. Samples were finished by hand using dry silicon carbide abrasive paper P600 (Buehler, IL, USA) to remove any irregularities on the periphery of each disk and the debris was blown away with a dust blower. Any samples with porosities or imperfections were discarded.

Table 3 – Artificial saliva (AS) components and their amount in g/100 ml (pH = 6.5).

Component	Amount (g/100 ml)
Mucin gastric	3.5
Xylitol	2.0
Methyl parahydroxybenzoate	0.1
E.D.T.A.-disodium	0.05
Menate pipertae aetheroteum	0.005
Spearmint oil	0.005
Benzalkonium chloride	0.002
Sodium fluoride	0.00042
Na^+	0.08
K^+	0.07
Ca^{2+}	0.025
Mg^{2-}	0.015
HPO_4^{2-}	0.022
Cl^-	0.12

2.3.2. *Water uptake*

Following 1 h from the start of mixing, samples were weighed on an electronic balance (Explorer, Ohaus Europe GmbH, Nänikon, Switzerland) to an accuracy of ±0.0001 g. Each sample was then immersed in individual numbered screw top bottles filled with 100 ml of DW or AS at 37 °C. At regular time intervals following immersion, samples were removed from the bottles, blotted on blotting paper to remove excess water and weighed. Care was taken so the whole process did not take more than 20–30 s to avoid water loss. Several readings were taken on the first day and then at regular time intervals thereafter up to 24 weeks.

At time 't', the percentage weight change was calculated for each specimen using Eq. (1).

$$\text{Weight change (\%)} = \left(\frac{W_t - W_0}{W_0}\right) \times 100 \quad (1)$$

where W_t is the weight at time t; W_0 is the weight before immersion in solution. The mean weight change (%) and standard deviation (SD) was calculated then plotted against time$^{1/2}$ (seconds) in order to create the weight change profile for each material.

2.3.3. *Desorption, solubility and diffusion coefficient*

After 24 weeks, samples were removed from the solutions, blotted, weighed and then transferred to an oven (Carbolite, Camlab, Cambridge, UK) maintained at 37 ± 1 °C. Again, they were weighed at regular time intervals, as for water uptake, until a constant minimum weight was reached (W_d).

The percentage weight loss after desorption was also calculated using Eq. (1) but replacing W_t with W_d and then, as for water uptake, plotted against time$^{1/2}$ (seconds).

Please cite this article in press as: Agha A, et al. Development of experimental resin modified glass ionomer cements (RMGICs) with reduced water uptake and dimensional change. Dent Mater (2016), http://dx.doi.org/10.1016/j.dental.2016.03.004

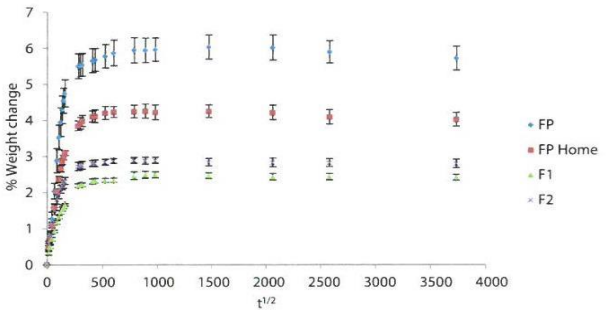

Fig. 1 – Water uptake (weight change) of commercial, home and experimental FP group materials in DW at 24 weeks immersion.

The solubility of the material was calculated by subtracting the weight after desorption (W_d) from the initial specimen weight (W_0) (Eq. (2)). This is equivalent to the total mass of components leached from the material.

$$\text{Solubility (\%)} = \left(\frac{W_0 - W_d}{W_0}\right) \times 100 \quad (2)$$

The water absorption/desorption data were plotted as M_t/M_∞ against time$^{1/2}$ (seconds$^{1/2}$) to obtain the slope, which was then used to calculate the diffusion coefficients for the water uptake (Dabs) and desorption (Ddes) processes, using Eq. (3) [55]:

$$D = \frac{s^2\pi l^2}{4} \quad (3)$$

where l = half thickness; s = slope of graph; M_t = the mass uptake at time (t); M_∞ = the mass uptake at equilibrium.

2.3.4. *Dimensional changes*

Prior to immersion, two measurements were taken of the diameter, at right angles to each other using digital micrometer (Mitutoyo, RS Components Ltd., Northants, UK) to an accuracy of 0.001 mm. Thickness was measured at the center and at four equally spaced points on the circumference. These measurements were repeated after one week, three weeks and at the final reading time (at 24 weeks).

In order to calculate the volume changes of the specimens, the following equation was used:

$$\text{Volume} : \pi r^2 h \quad (4)$$

where r is the radius and h is the mean thickness of each specimen [56].

2.3.5. *Statistical methods*

Where appropriate, data were analyzed using one way ANOVA followed by post hoc Tukey test at significance level of $p = 0.05$ using SPSS (IBM SPSS statistics version 22) under the assumptions of normally distributed measurements using Shapiro–Wilk test ($p < 0.05$) and equal variances between groups using Levene's test.

3. Results

Percentage mean weight change during uptake was plotted against $t^{1/2}$ and Figs. 1 and 2a are representatives of these results for FP and RX groups respectively (both in DW). Uptake in AS showed similar trends to DW, Fig. 2b is weight change of RX in AS.

All experimental compositions showed statistically significant lower water uptake (weight changes) compared to their commercial counterparts in both DW and AS. FP showed a maximum weight change 6% (±0.43%) in DW and 6.11% (±0.08%) in AS, while the values for compositions F1 and F2 ranged from 2.49% (±0.09%) to 2.89% (±0.08) in DW and 2.14% (±0.08%) to 3.19% (±0.35) in AS. A statistically significant reduction in the water uptake was also shown for RX experimental compositions in both DW and AS compared to both commercial and home materials. Although samples in AS did not appear to equilibrate, they were removed from AS at 24 weeks immersion (similarly to the samples immersed in DW). As a result, diffusion coefficient values for water uptake in AS could not be calculated.

Figs. 3 and 4 show the mean weight loss on desorption against $t^{1/2}$ in seconds in AS for commercial, home and experimental FP and RX materials respectively. Desorption of samples immersed in DW showed similar trends compared to the ones immersed in AS.

All materials (commercial, home and experimental compositions in both FP and RX groups) appeared to have reached apparent equilibrium, within a week ($t^{1/2} \approx 777$), during desorption, after immersion in both DW and AS. In the RX group, RX home presented significantly higher weight loss in DW (12.49 ± 0.49%) ($p < 0.0001$) followed by commercial (11.74 ± 0.26%) ($p < 0.0001$) then R2 (10.98 ± 0.24%) ($p \leq 0.02$) (HEMA 70%, THFM 30%) and finally R1 (10.46 ± 0.16%) ($p \leq 0.02$) (50% HEMA, 50% THFM) with the lowest weight loss. FP commercial and F2 weight losses were not significantly different (8.95 ± 0.27%, 8.58 ± 0.08% respectively) ($p = 0.283$) but FP showed higher values compared to F1 (8.22 ± 0.13%) and home FP (8.33 ± 0.18%) ($p \leq 0.004$). In AS, FP showed higher weight loss results compared to all other compositions ($p < 0.0001$), while RX had similar weight loss compared to the home material ($p = 1$), but higher than R1 and R2 ($p < 0.0001$).

Please cite this article in press as: Agha A, et al. Development of experimental resin modified glass ionomer cements (RMGICs) with reduced water uptake and dimensional change. Dent Mater (2016), http://dx.doi.org/10.1016/j.dental.2016.03.004

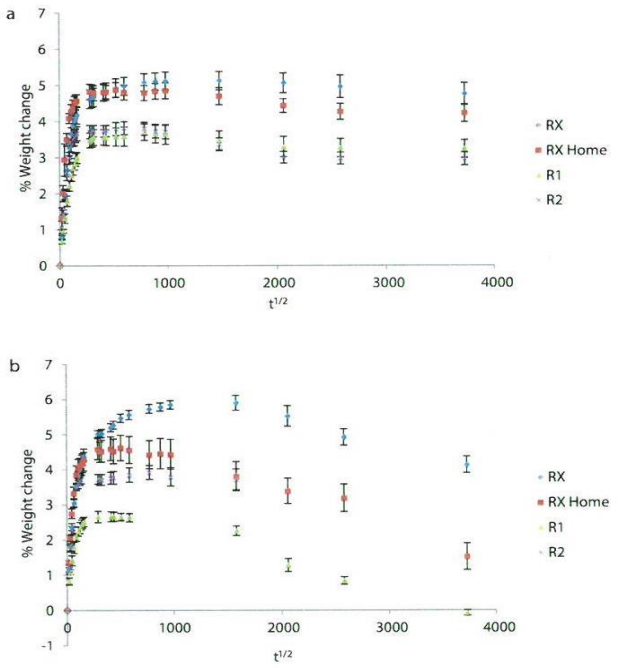

Fig. 2 – Water uptake (weight change) of commercial, home and experimental RX group materials in DW (a) and AS (b) at 24 weeks immersion.

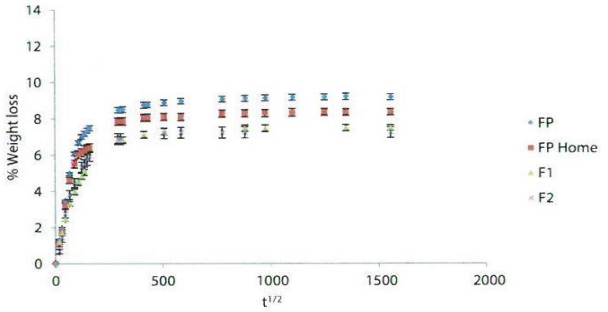

Fig. 3 – Percentage weight loss of commercial, home and experimental FP group materials following immersion in AS.

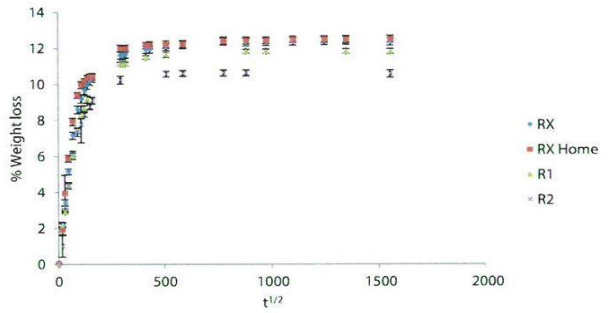

Fig. 4 – Percentage weight loss of commercial, home and experimental RX group materials following immersion in AS.

Please cite this article in press as: Agha A, et al. Development of experimental resin modified glass ionomer cements (RMGICs) with reduced water uptake and dimensional change. Dent Mater (2016), http://dx.doi.org/10.1016/j.dental.2016.03.004

Table 4 – Diffusion coefficients for absorption (Dabs), desorption (Ddes) and solubility % (SD) in both DW and AS for commercial, home and experimental materials. Similar superscript letters indicate no significant difference between materials at $p > 0.05$.

	Dabs ($m^2 s^{-1}$) DW	Ddes ($m^2 s^{-1}$) DW	Ddes ($m^2 s^{-1}$) AS	Solubility in DW % (SD)	Solubility in AS % (SD)
FP	5.84×10^{-12}	4.12×10^{-11}	1.24×10^{-11}	3.72 (0.14)	4.73 (0.15)^b
FP Home	7.72×10^{-12}	1.091×10^{-11}	1.17×10^{-11}	4.58 (0.15)	5.46 (0.43)
F1	5.72×10^{-12}	1.19×10^{-11}	1.12×10^{-11}	6.04 (0.15)^c	7.01 (0.28)^a
F2	1.44×10^{-11}	1.84×10^{-11}	0.88×10^{-11}	6.1 (0.14)^c	4.31 (0.09)^b
RX	1.92×10^{-11}	3.86×10^{-11}	2.22×10^{-11}	7.53 (0.31)^b	8.74 (0.06)
RX Home	5.1×10^{-11}	2.67×10^{-11}	1.62×10^{-11}	8.56 (0.2)^a	11.18 (0.36)
R1	1.32×10^{-11}	1.62×10^{-11}	1.48×10^{-11}	7.54 (0.22)^b	11.89 (0.16)
R2	0.958×10^{-11}	1.97×10^{-11}	0.96×10^{-11}	8.49 (0.24)^a	7.27 (0.19)^a

RMGICs (commercial, home and experimental) exhibited a linear uptake and desorption process when plotted against $t^{1/2}$, therefore both processes were diffusion controlled. Although the diffusion in AS followed Fick's law, the samples did not show any sign of equilibrium following 24 weeks of immersion (Fig. 2b), therefore, the Dabs values could not be calculated for absorption in AS. Dabs in DW, Ddes in DW and AS and solubility are shown in Table 4. Similar to commercial and home materials, FP experimental group showed slower diffusion during both water uptake and desorption processes compared to the RX group. Also, diffusion was slower for the water uptake process in the FP group compared to desorption. FP solubility results in DW were significantly lower than experimental materials (F1 and 2) ($p < 0.0001$), while in RX group R1 did not show any significant difference to the commercial material ($p = 1$). All FP formulations presented significantly lower solubility in DW compared to the RX group ($p < 0.0001$). This was also true for samples immersed in AS with the exception of F1 were there was no significant difference compared to R2 ($p = 0.607$), but it was lower than the remaining RX group ($p < 0.0001$). Composition F2 in AS did not show any significant difference compared to commercial FP ($p = 0.089$), however R2 showed significantly lower solubility compared to commercial RX ($p < 0.0001$) (Table 4).

Figs. 5 and 6 show dimensional (volume) changes of samples following immersion in DW and AS after 1, 3 and 24 weeks. All experimental materials in DW and AS presented significantly lower volume increase compared to home and

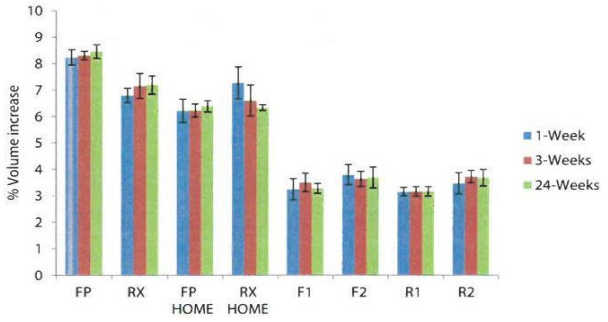

Fig. 5 – Volume increase (%) of all commercial, home and experimental samples immersed in DW after 1, 3 and 24 weeks.

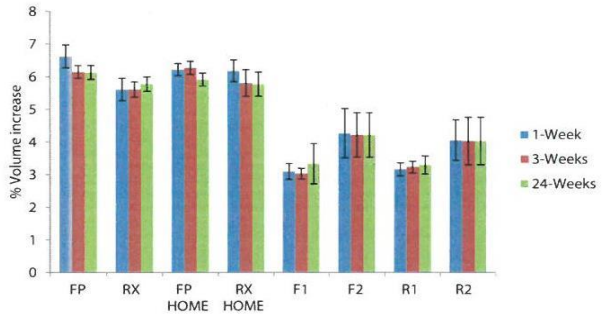

Fig. 6 – Volume increase (%) of all commercial, home and experimental samples immersed in AS at 1, 3 and 24 weeks.

Please cite this article in press as: Agha A, et al. Development of experimental resin modified glass ionomer cements (RMGICs) with reduced water uptake and dimensional change. Dent Mater (2016), http://dx.doi.org/10.1016/j.dental.2016.03.004

commercial materials ($p < 0.0001$). FP commercial in DW exhibited a significantly higher volume increase compared to all other materials at all-time points ($p < 0.0001$). In AS, commercial and home materials did not show any significant difference in dimensional change at 3 ($p \leq 1$) and 24 weeks ($p \leq 0.991$), however RX had a significantly lower volume increase at one week of immersion compared to FP ($p = 0.004$), but it was similar to the other two home materials ($p \leq 0.316$).

4. Discussion

This study focused on developing new experimental RMGICS with lower water uptake compared to the current commercial materials. Moreover, the choice of monomers to replace HEMA in the commercial products was based on selecting a monomer that is known for its low water uptake and good biocompatibility [57]. Four different experimental compositions were formulated and tested; two were based on FP and the other two on RX formulations. Two further home liquids were prepared as controls.

The experimental liquid compositions were formulated following data provided by the manufacturer in the MSDS. Although theoretically accurate, manufacturers are not required to mention the exact composition and other details. Therefore, FT-IR was performed on (i) the commercial liquids in order to identify their precise composition, and (ii) home and experimental liquids to ensure similarity.

The ISO 4049:2009 standards concerning resin based materials include desiccation of samples prior to immersion in water [58]. Conventional GICs contain water in their structure which is divided between 'loosely bound' and 'tightly bound' water to metal cations and poly(acrylic acid) chain [8,59,60]; with time, more loosely bound water converts to tightly bound. Conversely, when this cement is placed in the oral environment, the loosely bound water evaporates and this procedure jeopardizes the setting of GIC as water is one of the essential parts of the setting reaction therefore a protective varnish is applied [23]. A pilot study was conducted before commencing this study to determine the most suitable water uptake experimental method to follow. As a result of this study, the method that did not include desiccation of samples was deemed to be more clinically relevant as samples tested according to ISO 4049:2009 demonstrated higher water uptake values than immersion without desiccation. Moreover, with the ISO 4049:2009 standard method, higher uptake values are obtained in DW and AS, as a result of desiccation, and this therefore does not mimic the oral environment's situation. Also, the loosely bound water in the GIC structure was evaporated rapidly through desiccation and subsequently the uptake value was an exaggeration of what would happen clinically as the water uptake in this case was a combination of the evaporated water and the actual water uptake value. Additionally, water evaporated during the initial 24 h required for setting of GIC, might cause cracks and voids within the cement matrix. This may then contribute to an increase in the amount of water diffusing through the voids.

Immersion fluids (100 ml per sample) were not changed throughout the course of the experiment, since saturation was not expected, as a result of released monomers, or other components from the samples. This amount was 10× higher than that recommended by ISO 4049:2009.

The resin matrix in RMGIC is responsible for the material's water uptake, and thus it is expected that different percentages of the monomer (e.g. HEMA) would lead to different levels of water uptake [61]. Water uptake values were not statistically significant between the two home materials (controls) in both DW and AS, despite the higher powder liquid ratio in FP. This can be explained by the fact that, although FP Home and RX Home contained similar amounts of HEMA, FP compositions included an additional monomer, urethane dimethacrylate (UDMA), and therefore, in the final cement the resin content was similar. Although UDMA is more hydrophobic than HEMA, the hydroxyl (OH^-) and urethane ($NHCOO^-$) groups in poly-UDMA play a role in the water uptake of this polymer through acquired hydrogen bonds with water [62]. However, commercial FP exhibited significantly higher water uptake compared to RX; this difference might be a result of the different acid used in RX (copolymer of acrylic and itaconic acids). Itaconic acid which contains two carboxyl groups might demonstrate an increase in the crosslinking potential of the set cement [63], therefore the set cement might exhibit less water uptake since the uptake is negatively correlated with crosslinking density [64].

As shown in Figs. 1 and 2(a and b), all experimental compositions presented with lower water uptake (weight changes) compared to their commercial and home counterparts. This reduction in water uptake can be correlated to the replacement of HEMA with THFM in the experimental compositions, which agrees with published literature concerning this monomer and its lower water uptake compared to HEMA [50,54].

Solubility reflects the amount of residuals leaching out from the system. All FP formulations presented with significantly lower solubility in DW and AS compared to the RX group, with the exception of F1, which did not present any significant difference compared to R2; but it was still lower than all other RX compositions. This may be due to the difference in compositions of each material, with FP containing UDMA and HEMA while RX contained only HEMA as a monomer. Additional cross-linking may occur between HEMA and UDMA, UDMA and THFM and thus the amount of residual, unconverted HEMA or THFM would be lower in the FP formulations compared to RX; this will consequently decrease the amount of residuals released and hence the solubility of the material. All solubility results (in the range of 2–10%) are consistent with those published in the literature [56].

The diffusion coefficients for the FP group (all formulations) were high for the uptake process compared to those obtained for the desorption process. This indicates that water diffused faster out of the matrix during the desorption process compared to slowly diffusing into the matrix during the uptake process. This is in agreement with literature on polymers [49,65], due to the fact that the desorption process includes only evaporation of water compared to the water uptake process that involves water absorption, other components leaching out of the material and, in some cases, clustering and droplet formation in areas that contain 'water soluble components' [66,67]. A small difference was observed between Dabs and Ddes in the RX group and this indicates that

Please cite this article in press as: Agha A, et al. Development of experimental resin modified glass ionomer cements (RMGICs) with reduced water uptake and dimensional change. Dent Mater (2016), http://dx.doi.org/10.1016/j.dental.2016.03.004

diffusion was concentration dependent for both processes. Water uptake process in DW was Fickian for all materials (FP and RX groups) and this was in agreement with Kanchanavasita et al. [56] and Nicholson [68]. However, different diffusion coefficient values have been reported and therefore they could not be correlated with this study. This could be due to the differences in the methods used and the commercial materials that were tested. Water uptake has been also reported to follow Fickian diffusion in biomaterials containing HEMA as a monomer [69–71] or poly(THFM-co-HEMA) [72,73]. All materials immersed in AS showed Fickian diffusion for the uptake and desorption processes but values could not be calculated for the uptake process as samples did not seem to equilibrate after 24 weeks of immersion. This can be explained by the fact that AS contains water and other components that could be diffusing in and out of the sample. Droplets are formed within the sample due to the presence of soluble components within it [67]. After reaching a maximum weight change some of the components that diffused into the samples, and those that were not bound to any chemical groups, diffused out again thus accounting for the weight loss due to a chemical potential gradient [74].

All experimental materials showed lower dimensional changes compared to the commercial and control products. While the expansion of RMGIC can be beneficial to compensate the material's polymerization shrinkage [56], this dimensional change may cause problems for restored teeth causing stress on tooth tissues. It may also cause, as described earlier, fracture of the weak ceramic structure where RMGIC is used as luting cement. Therefore, decreasing the dimensional changes of commercial RMGIC is highly desirable and all experimental materials presented with lower weight change following immersion in DW and AS.

5. Conclusion

Decreasing water uptake and expansion of commercially available RMGIC materials is highly desirable since they may result in expansion stresses in both teeth and restorations; hence they are unsuitable to bond glass ceramic restorations as a result of possible fracture. Experimental compositions in this study have shown promising results with lower water uptake and dimensional changes than commercial materials when immersed in DW and AS. This may lead to a wider range of applications than commercially available products.

Acknowledgment

The authors are grateful to Dr. Pete Tomlins for his help and advice on the statistical analyses carried out in this paper.

REFERENCES

[1] Wilson AD, Kent BE. A new translucent cement for dentistry. The glass ionomer cement. Br Dent J 1972;132:133–5.
[2] McLean JW. Evolution of glass-ionomer cements: a personal view. J Esthet Dent 1994;6:195–206.
[3] Wilson AD, McLean JW. Glass-ionomer cement. Michigan: Quintessence Pub. Co.; 1988.
[4] Mount GJ. Glass ionomer cements and future research. Am J Dent 1994;7:286–92.
[5] Brook IM, Hatton PV. Glass-ionomers: bioactive implant materials. Biomaterials 1998;19:565–71.
[6] Sidhu SK, Watson TF. Resin-modified glass ionomer materials. A status report for the American Journal of Dentistry. Am J Dent 1995;8:59–67.
[7] Cho SY, Cheng AC. A review of glass ionomer restorations in the primary dentition. J Can Dent Assoc 1999;65:491–5.
[8] Lohbauer U. Dental glass ionomer cements as permanent filling materials? – Properties, limitations and future trends. Materials 2009;3:76–96.
[9] Nicholson JW, Czarnecka B. Kinetic studies of water uptake and loss in glass-ionomer cements. J Mater Sci Mater Med 2008;19:1723–7.
[10] Nicholson JW, Czarnecka B. Kinetic studies of the effect of varnish on water loss by glass-ionomer cements. Dent Mater 2007;23:1549–52.
[11] Prosser HJ, Powis DR, Wilson AD. Glass-ionomer cements of improved flexural strength. J Dent Res 1986;65:146–8.
[12] Moshaverinia A, Roohpour N, Chee WWL, Schricker SR. A review of powder modifications in conventional glass-ionomer dental cements. J Mater Chem 2011;21:1319–28.
[13] Sced I, Wilson A. Hardenable compositions; 1980.
[14] Simmons JJ. The miracle mixture. Glass ionomer and alloy powder. Tex Dent J 1983;100:6–12.
[15] Thornton JB, Retief DH, Bradley EL. Fluoride release from and tensile bond strength of Ketac-fil and ketac-silver to enamel and dentin. Dent Mater 1986;2:241–5.
[16] Robbins JW, Cooley RL. Microleakage of Ketac-Silver in the tunnel preparation. Oper Dent 1988;13:8–11.
[17] Croll T. Alternatives to silver amalgam and resin composite in pediatric dentistry. Quintessence Int 1998;29:697–703.
[18] Leirskar J, Nordbø H, Mount GJ, Ngo H. The influence of resin coating on the shear punch strength of a high strength auto-cure glass ionomer. Dent Mater 2003;19:87–91.
[19] Rao A. Principles and practice of pedodontics. second ed. London: Jaypee Brothers Medical Publishers (P) Ltd.; 2008.
[20] Mathis RS, Ferracane JL. Properties of a glass-ionomer/resin-composite hybrid material. Dent Mater 1989;5:355–8.
[21] Antonucci JM, McKinney JE, Stansbury JW. Resin modified glass ionomer dental cement; 1988.
[22] Mitra SB. Photocurable ionomer cement systems; 1989.
[23] Wilson AD, Nicholson JW. Acid–base cements: their biomedical and industrial applications. Cambridge: Cambridge University Press; 2005.
[24] Nicholson JW, Anstice HM. The physical-chemistry of light-curable glass-ionomers. J Mater Sci Mater Med 1994;5:119–22.
[25] Nicholson JW, Anstice HM. The physical chemistry of light-curable glass-ionomers. J Mater Sci Mater Med 1994;5:119–22.
[26] Pedley DG, Skelly PJ, Tighe BJ. Hydrogels in biomedical applications. Brit Polym J 1980;12:99–110.
[27] Yap AUJ, Lee CM. Water sorption and solubility of resin-modified polyalkenoate cements. J Oral Rehabil 1997;24:310–4.
[28] Oysaed H, Ruyter IE. Composites for use in posterior teeth: mechanical properties tested under dry and wet conditions. J Biomed Mater Res 1986;20:261–71.
[29] Braden M, Causton EE, Clarke RL. Diffusion of water in composite filling materials. J Dent Res 1976;55:730–2.
[30] Pastila P, Lassila LV, Jokinen M, Vuorinen J, Vallittu PK, Mantyla T. Effect of short-term water storage on the elastic

Please cite this article in press as: Agha A, et al. Development of experimental resin modified glass ionomer cements (RMGICs) with reduced water uptake and dimensional change. Dent Mater (2016), http://dx.doi.org/10.1016/j.dental.2016.03.004

properties of some dental restorative materials–A resonant ultrasound spectroscopy study. Dent Mater 2007;23:878–84.
[31] Malacarne J, Carvalho RM, de Goes MF, Svizero N, Pashley DH, Tay FR, et al. Water sorption/solubility of dental adhesive resins. Dent Mater 2006;22:973–80.
[32] Cattani-Lorente MA, Dupuis V, Payan J, Moya F, Meyer JM. Effect of water on the physical properties of resin-modified glass ionomer cements. Dent Mater 1999;15:71–8.
[33] Piwowarczyk A, Lauer HC. Mechanical properties of luting cements after water storage. Oper Dent 2003;28:535–42.
[34] Yap AUJ. Resin-modified glass ionomer cements: a comparison of water sorption characteristics. Biomaterials 1996;17:1897–900.
[35] Meyer JM, Cattani-Lorente MA, Dupuis V. Compomers: between glass-ionomer cements and composites. Biomaterials 1998;19:529–39.
[36] Karaoglanoglu S, Akgul N, Ozdabak HN, Akgul HM. Effectiveness of surface protection for glass-ionomer, resin-modified glass-ionomer and polyacid-modified composite resins. Dent Mater 2009;28:96–101.
[37] Anstice HM, Nicholson JW. Studies on the structure of light-cured glass-ionomer cements. J Mater Sci Mater Med 1992;3:447–51.
[38] Becher R, Kopperud HM, Al RH, Samuelsen JT, Morisbak E, Dahlman HJ, et al. Pattern of cell death after in vitro exposure to GDMA, TEGDMA, HEMA and two compomer extracts. Dent Mater 2006;22:630–40.
[39] Xie D, Chung ILD, Wu W, Mays J. Synthesis and evaluation of HEMA-free glass–ionomer cements for dental applications. Dent Mater 2004;20:470–8.
[40] Ibsen R, Glace W. Provisional crown-and-bridge resin; 1981.
[41] Braden M, Patel MP, Pearson GJ. Fluoride releasing biomaterials; 1998.
[42] Braden M, Downes S, Patel MP, Davy KWM. The use of biomaterials for tissue repair; 1993.
[43] Mitra SB, Mitra S. Universal water-based medical and dental cement; 1996.
[44] Anstice HM, Kanchanavasita W, Pearson GJ, Schottlander BD, Sherpa AL. Polymerizable cement compositions; 2001.
[45] Patel MP, Braden M, Davy KW. Polymerization shrinkage of methacrylate esters. Biomaterials 1987;8:53–6.
[46] Patel MP, Braden M. Heterocyclic methacrylates for clinical applications. II. Room temperature polymerizing systems for potential clinical use. Biomaterials 1991;12:649–52.
[47] Bhusate M, Braden M. Low shrinkage polymer/monomer mixtures for biomedical use; 1983.
[48] Patel MP, Braden M. Heterocyclic methacrylates for clinical applications. I. Mechanical properties. Biomaterials 1991;12:645–8.
[49] Patel MP, Braden M. Heterocyclic methacrylates for clinical applications. III. Water absorption characteristics. Biomaterials 1991;12:653–7.
[50] Sawtell RM, Downes S, Patel MP, Clarke RL, Braden M. Heterocyclic methacrylates for clinical applications-further studies of water sorption. J Mater Sci Mater Med 1997;8:667–74.
[51] Riggs PD, Braden M, Tilbrook DA, Swai H, Clarke RL, Patel MP. The water uptake of poly(tetrahydrofurfuryl methacrylate). Biomaterials 1999;20:435–41.
[52] Thomas AG, Muniandy K. Absorption and desorption of water in rubbers. Polymer 1987;28:408–15.
[53] Patel MP, Swai H, Davy KW, Braden M. Water sorption behaviour of polymeric systems based on tetrahydrofurfuryl methacrylate. J Mater Sci Mater Med 1999;10:147–51.
[54] Patel MP, Johnstone MB, Hughes FJ, Braden M. The effect of two hydrophilic monomers on the water uptake of a heterocyclic methacrylate system. Biomaterials 2001;22:81–6.
[55] Crank J. The Mathematics of Diffusion. second ed. Oxford: Clarendon Press; 1979.
[56] Kanchanavasita W, Anstice HM, Pearson GJ. Water sorption characteristics of resin-modified glass-ionomer cements. Biomaterials 1997;18:343–9.
[57] Pearson GJ, Picton DC, Braden M, Longman C. The effects of two temporary crown materials on the dental pulp of monkeys (*Macaca fascicularis*). Int Endod J 1986;19:121–4.
[58] International Standardization Organization. ISO 4049:2009. Dentistry-polymer-based restorative materials. Geneva: ISO; 2009.
[59] Crisp S, Lewis BG, Wilson AD. Glass ionomer cements: chemistry of erosion. J Dent Res 1976;55:1032–41.
[60] Wilson AD, Paddon JM, Crisp S. The hydration of dental cements. J Dent Res 1979;58:1065–71.
[61] Li Y, Swartz ML, Phillips RW, Moore BK, Roberts TA. Effect of filler content and size on properties of composites. J Dent Res 1985;64:1396–401.
[62] Sideridou ID, Karabela MM, Vouvoudi E. Volumetric dimensional changes of dental light-cured dimethacrylate resins after sorption of water or ethanol. Dent Mater 2008;24:1131–6.
[63] Crisp S, Kent BE, Lewis BG, Ferner AJ, Wilson AD. Glass-ionomer cement formulations. II. The synthesis of novel polycarobxylic acids. J Dent Res 1980;59:1055–63.
[64] Cefaly DF, Wang L, de Mello LL, dos Santos JL, dos Santos JR, Lauris JR. Water sorption of resin-modified glass-ionomer cements photoactivated with LED. Braz Oral Res 2006;20:342–6.
[65] Barrie JA. Water in polymers. In: Crank J, Park GS, editors. Diffusion in polymers. First ed. New York: Academic Press Inc.; 1968. p. 259–313.
[66] Nazhat SN, Parker S, Patel MP, Braden M. Isoprene-styrene copolymer elastomer and tetrahydrofurfuryl methacrylate mixtures for soft prosthetic applications. Biomaterials 2001;22:2411–6.
[67] Parker S, Braden M. Water absorption of methacrylate soft lining materials. Biomaterials 1989;10:91–5.
[68] Nicholson JW. The physics of water sorption by resin-modified glass-ionomer dental cements. J Mater Sci Mater Med 1997;8:691–5.
[69] Hill DJT, Lim MCH, Whittaker AK. Water diffusion in hydroxyethyl methacrylate (HEMA)-based hydrogels formed by (-radiolysis. Polym Int 1999;48:1046–52.
[70] Sideridou ID, Papanastasiou GE. Water sorption kinetics in light-cured poly-HEMA and poly(HEMA-co-TEGDMA); determination of the self-diffusion coefficient by new iterative methods. J Appl Polym Sci 2007;106:2380–90.
[71] Gehrke SH, Biren D, Hopkins JJ. Evidence for Fickian water transport in initially glassy poly(2-hydroxyethyl methacrylate). J Biomater Sci Polym Ed 1994;6:375–90.
[72] Ghi PY, Hill DJT, Maillet D, Whittaker AK. N.m.r. imaging of the diffusion of water into poly(tetrahydrofurfuryl methacrylate-co-hydroxyethyl methacrylate). Polymer 1997;38:3985–9.
[73] Ghi P, Hill DJT, Whittaker AK. Water sorption by poly(tetrahydrofurfuryl methacrylate-co-2-hydroxyethyl methacrylate). I. A mass-uptake study. J Polym Sci, B: Polym Phys 2000;38:1939–46.
[74] Riggs PD, Parker S, Braden M, Kalachandra S. Development of novel elastomer/methacrylate monomer soft lining materials. J Mater Sci Mater Med 2001;12:359–64.

Please cite this article in press as: Agha A, et al. Development of experimental resin modified glass ionomer cements (RMGICs) with reduced water uptake and dimensional change. Dent Mater (2016), http://dx.doi.org/10.1016/j.dental.2016.03.004